Évaluation de la pénétration cutanée des ingrédients de systèmes dispersés : utilisation combinée des cellules de diffusion et de la microscopie confocale Raman

Matthias Förster

N° d'ordre 340 – 2010 Année 2010

THESE DE L'UNIVERSITE DE LYON

Délivrée par

L'UNIVERSITE CLAUDE BERNARD LYON 1

ECOLE DOCTORALE INTERDISCIPLINAIRE SCIENCES-SANTE

DIPLOME DE DOCTORAT

(arrêté du 7 août 2006)

soutenue publiquement le 21. Décembre 2010

par

Monsieur FÖRSTER MATTHIAS

Evaluation de la pénétration cutanée des ingrédients de systèmes dispersés : utilisation combinée des cellules de diffusion et de la microscopie confocale Raman

JURY : Madame BRIANÇON Stephanie (Directeur de thèse)

Madame BOLZINGER Marie-Alexandrine (Co-directeur de thèse)

Madame BAILLET-GUFFROY Arlette (Rapporteur)

Madame MARTI-MESTRES Gilberte (Rapporteur)

Monsieur FESSI Hatem (Président du jury)

Monsieur HUMBERT Philippe (Rapporteur)

Monsieur DEMARNE Frédéric (Examinateur)

Monsieur JOSSE Denis (Examinateur)

Sommaire

Introduction

L'objet de ce travail est l'étude de la pénétration d'actifs cosmétiques modèles dans la peau et l'influence des différents ingrédients de la formule choisie sur leur passage. Les principaux axes d'investigation ont concerné l'influence des propriétés physicochimiques des actifs et de la formulation sur les mécanismes de pénétration, le devenir des actifs et les éventuelles modifications structurelles de la peau engendrées par les formulations.

Les actifs étudiés sont des ingrédients cosmétiques choisis de manière à prendre en compte les sites d'action au sein du tissu cutané, ciblés classiquement par les actifs cosmétiques.

Dans ce travail de thèse, la première partie est un travail de veille bibliographique destiné à dégager les règles de formulation, si elles existent, qui permettent de moduler le passage percutané d'actifs. Cela concerne aussi bien la structure chimique des ingrédients ou des actifs utilisés et leurs propriétés physicochimiques, que la forme galénique, dans laquelle ils sont formulés.

Le but de cette recherche est de pouvoir définir les actifs, les formulations et les paramètres de pénétration qui vont être étudiés dans la partie expérimentale. Le Chapitre 1 donne une introduction sur la peau, sa structure et ses fonctions. Il explique la théorie de la pénétration fondée sur des lois de diffusion. Cette partie introduit les études de pénétration en fonction de plusieurs actifs et des différents types de formulations. Il ressort de ce travail que l'influence de la forme galénique, lorsqu'elle est étudiée, est corrélée à la pénétration de l'actif depuis la formule uniquement. Il est difficile d'établir des règles générales, parce que chaque étude est menée dans des conditions différentes et correspond à cas particulier. Inversement, les modèles de pénétration cutanée sont centrés sur les propriétés physicochimiques des molécules candidates à la pénétration cutanée et non sur la formulation qui est rarement considérée [1-4].

De ce fait, il est extrêmement difficile de déterminer quel composant de la formulation a un impact réel sur la pénétration percutanée. De plus, les travaux n'étudient que rarement les impacts de la structure d'un ingrédient ou de ses propriétés sur le passage de l'actif. Le passage d'un actif n'est jamais considéré en relation avec son environnement immédiat puisque les études de pénétration permettent d'évaluer le passage de l'actif et non de l'actif et des excipients environnants dans le même temps. Telles sont les raisons pour lesquelles les objectifs de la thèse se sont concentrés sur des formulations simples : des formulations de type « émulsion » et « solution de tensioactifs » ont été choisies pour étudier la pénétration percutanée *in vitro* par une méthode standard, la méthode des cellules de Franz ou en mode statique ou en mode dynamique (cellule à flux continu). Deux actifs modèles ont été choisis dans ce travail, un actif hydrophile (logP=-0,07) et un actif lipophile (logP=7,62), afin de pouvoir étudier en premier lieu les aspects cinétiques de la pénétration en fonction :

- de la structure chimique de différents tensioactifs non ioniques de type esters. Les tensioactifs diffèrent par la longueur de leur chaînes hydrophile et lipophile et donc par leur HLB;
- des phases huileuses qui se distinguent par leur polarité;
- de la nature des actifs, un lipophile et un hydrophile qui diffèrent par leur logP.

Dans un deuxième temps, l'aspect mécanistique du passage a été étudié en relation avec les interactions potentielles entre les ingrédients et la peau. En effet, dans la littérature, l'effet promoteur d'absorption de certains composants est bien décrit. Ces composés modifient l'organisation structurelle des lipides cutanés et sont capables de fluidifier les lipides facilitant ainsi la pénétration des actifs. La microspectroscopie confocale Raman (MCR) a été choisie pour étudier qualitativement la pénétration des composants des formulations et leurs effets sur la barrière cutanée [5]. Le Chapitre 2 introduit cette nouvelle méthode avec laquelle il est possible de faire non seulement le suivi des actifs dans la peau de façon non invasive mais aussi de suivre certains ingrédients dont l'eau et l'huile. De surcroît, cette méthode permet de mesurer l'influence de la formulation sur la barrière cutanée, sur l'hydratation

cutanée et enfin de mesurer l'épaisseur du *stratum corneum*. Un article de revue est actuellement soumis dans Eur. J. Dermatol.

Dans ce travail de thèse, nous avons appliqué cette méthode dans différentes voies.

Le Chapitre 3 décrit les méthodes mises au point. La première utilisation de la MCR a consisté à se servir de la mesure de la teneur en eau pour nous assurer de la parfaite séparation du *stratum corneum* des couches viables de la peau. Cette mise au point méthodologique fait l'objet du Chapitre 4 et d'une publication acceptée dans Skin Physiol. Pharmacol. En effet dans la méthode d'absorption cutanée en cellule de Franz, la quantification de la substance active dans chaque couche cutanée permet d'établir le profil quantitatif de la pénétration cutanée pour un actif considéré. Une parfaite séparation des compartiments cutanés (*stratum corneum*, épiderme et derme) permet d'obtenir un profil de distribution précis de l'actif considéré. Ce point est particulièrement important avec la pénétration des actifs lipophiles comme le rétinol qui ne traverse pas la peau pour s'accumuler dans le liquide récepteur mais qui se distribue dans les compartiments cutanés. Afin d'évaluer des différences assez fines, une quantification la plus précise possible du rétinol dans les différentes couches de la peau (*stratum corneum*, épiderme et derme) est nécessaire. Pour la séparation, trois méthodes classiques sont utilisées, avec leurs avantages et leurs inconvénients : la méthode du tape stripping, la méthode utilisant de la colle cynaoacrylique et enfin la trypsine. Dans le Chapitre 4, la pertinence de ces méthodes pour assurer la séparation franche et nette du *stratum corneum* de l'épiderme viable est évaluée à l'aide de coupes histologiques et de la MCR. La discussion de ce chapitre repose sur la qualité de séparation du *stratum corneum* grâce à chacune des trois méthodes et sur la discussion de la capacité de la MCR à remplacer les méthodes histologiques.

Le Chapitre 5 rapporte l'étude de l'influence des composants des formulations sur la pénétration percutanée du rétinol en utilisant des ingrédients modèles (eau deuterée et dodécane deuteré) susceptibles d'être suivis en MCR. Les formulations utilisées sont des

émulsions simples et leurs solutions de tensioactifs correspondantes. La distribution quantitative de l'actif dans la peau est mesurée grâce à une étude parallèle menée en cellule de Franz. Pour pouvoir expliquer les différents comportements de pénétration observés par rapport aux différentes formulations, des études par MCR ont été ajoutées. Dans ce chapitre, la possibilité de suivre les composants des formulations dans la peau et de mesurer l'influence de la formulation sur l'organisation de la couche lipidique du *stratum corneum* et, par conséquent, l'influence sur la barrière de la peau a été démontrée.

Les formulations utilisées dans le Chapitre 6 sont plus proches des formulations cosmétiques réelles que des formulations modèles du Chapitre 5 notamment concernant le choix de la phase huileuse. Ce chapitre traite de l'influence de la chaîne carbonée des tensioactifs non ioniques, question peu étudiée dans la littérature [6-11], et de l'influence de la polarité des huiles sur la pénétration percutanée de la caféine et du rétinol. La deuxième problématique soulevée dans ce chapitre est la question de la localisation de l'actif dans la dispersion utilisée.

Le dernier chapitre « discussion générale » remet en contexte les cinq chapitres précédents, spécialement les chapitres expérimentaux 3 à 6 et donne donc une conclusion générale sur la thèse et sur les points intéressants qui devraient être traités dans le futur.

Partie A Bibliographie

Chapitre 1 L'absorption percutanée des actifs cosmétiques

La fonction principale de la peau est de protéger l'intérieur du corps, très riche en eau, contre l'environnement extérieur. La fonction barrière du *stratum corneum* a été démontrée dans les années 40 [12]. Cette couche fine est constituée de cellules mortes (en général entre 15 et 20 couches) et de cornéocytes qui contiennent principalement des kératines, protéine fibreuse très résistante et qui sont enserrés dans une matrice complexe de lipides organisés. Il s'agit donc d'une couche lipophile, au contraire des couches suivantes (épiderme et derme) qui elles, sont hydrophiles.

Un actif peut traverser le *stratum corneum* selon deux principales voies de passage, hors annexes: la voie intercellulaire et la voie intracellulaire (transcellulaire) (Figure 1-1). La voie la plus commune est la perméation intercellulaire [13] et, par conséquent, la barrière principale est la matrice lipidique [14,15]. Des études ont montré que la fonction barrière ne dépendait pas seulement de la composition du *stratum corneum* mais aussi de son organisation structurale [16].

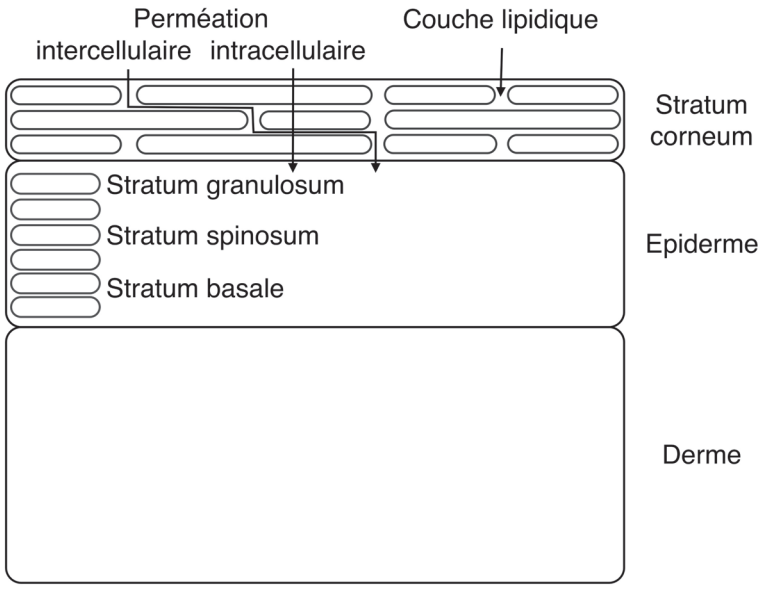

Figure 1-1 : Représentation des voies de passage cutanées

Les lipides du *stratum corneum* s'organisent en multicouches et s'intercalent en un film continu parallèlement aux parois cellulaires des cornéocytes. Ces couches lipidiques se superposent et établissent un réseau fonctionnel avec une organisation selon un schéma répétitif. Ils se positionnent selon deux phases lamellaires cristallines qui coexistent au sein même du *stratum corneum* et se différencient par leur période. La première phase représente une courte période (SP pour small periodicity) tandis que la deuxième phase représente une période longue (LP pour long periodicity). Leur période est de 6 nm ou 13 nm.

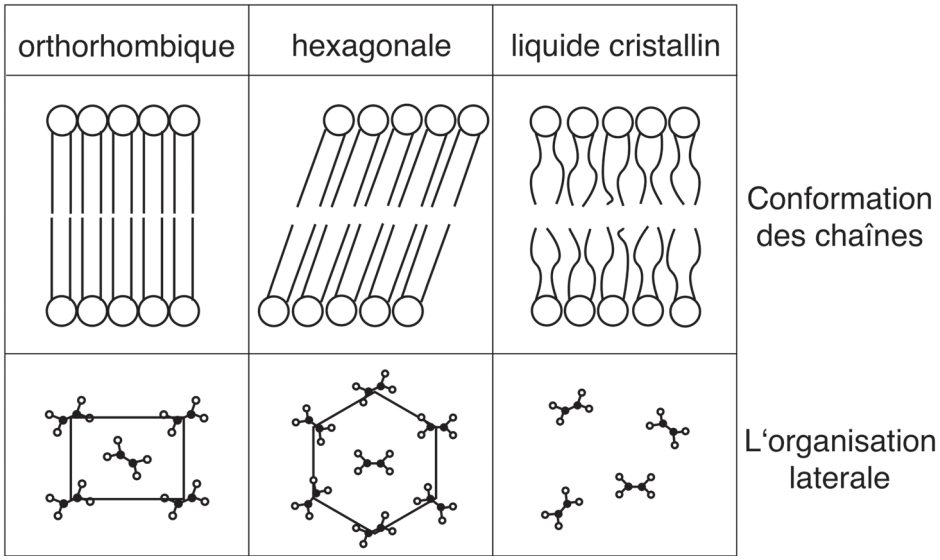

Figure 1-2 : L'organisation des lipides du *stratum corneum*. Schéma de la conformation des chaînes et de l'organisation latérale des chaines dans une phase orthorhombique, hexagonale et cristalline liquide.

En plus de l'organisation lamellaire, les lipides s'organisent latéralement avec des degrés de densité plus ou moins importants à l'intérieur des phases lamellaires selon trois schémas possibles du plus désordonné au plus ordonné (Figure 1-2) [17] :

- Orthorhombique

  Lorsque les lipides s'organisent en phases orthorhombiques chacun se positionne par rapport à l'autre selon un angle de 60°. Cette organisation particulière qui permet un empilement assez resserré des lipides renforce l'imperméabilité du ciment lipidique et interviendrait dans la fonction barrière de la peau.

- Hexagonale

  Les phases hexagonales sont légèrement moins denses que les phases orthorhombiques et proviendraient de l'impact des lipides des glandes sébacées sur les lipides du ciment intercornéocytaire qu'ils pénètrent en surface. Ils agiraient soient en formant eux-mêmes des phases hexagonales soit en favorisant le passage de phases orthorhombiques compactes en phases hexagonales moins denses. On parle alors de fluidification des lipides dans les couches les plus superficielles de la couche cornée.

- Liquide cristallin

  D'après Boncheva *et al.* [17] et Bouwstra *et al.* [18] les lipides peuvent également se présenter sous une forme liquide fluide. Cette organisation serait en accord avec le modèle LP ainsi qu'avec les séquences larges/étroites/larges observées en microscopie électronique. Ce modèle est cependant contredit par Rodriguez *et al.* [19] pour qui les lipides n'ont que les deux organisations décrites précédemment.

Plusieurs études biophysiques font l'hypothèse d'une coexistence entre les domaines de phase cristalline liquide et les domaines des phases solides ou cristallines gélifiées dans la membrane du *stratum corneum* [16-18,20-25]. Ces conditions provoquent de légères diffusions latérales à la température physiologique. Cinq concepts ont été proposés pour représenter cette organisation des lipides du ciment intercornéocytaire.

Le « stacked monolayer model » de Swartzendruber en 1989, le « mosaic fluid model » de Forslind en 1994, « le sandwich model » de Bouwstra, le « single gel phase model de Norlén en 2001 et la « asymetric bilayer model de McIntosh en 2003. A l'intérieur de ces modèles, les lipides sont positionnés de façon plus ou moins ordonnée dans des structures cristallines ou liquides se succédant les unes aux autres par superposition ou alternance. Il n'y a pas de consensus actuellement décrivant un schéma unique de l'organisation des lipides au sein de ciment cornéocytaire. Cependant si la structure orthorhombique prédomine les auteurs

s'accordent [18] pour indiquer que la perméabilité cutanée est faible. Ainsi, comprendre la structure physique de la membrane est essentiel pour comprendre la fonction barrière et les mécanismes de désorganisation de la barrière causée par l'application topique des produits. Ces mécanismes sont à la base de certaines stratégies utilisées en formulation pour augmenter la pénétration cutanée des actifs, comme l'utilisation de promoteurs d'absorption, de systèmes dispersés, de particules, etc.

La pénétration percutanée est une méthode biopharmaceutique qui évalue l'absorption cutanée d'un principe actif ou d'une substance cosmétique dans une forme galénique. La méthode la plus utilisée pour l'apprécier et la méthode de diffusion en cellules de Franz (Figure 1-3).

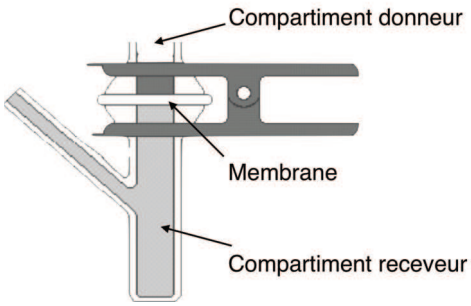

Figure 1-3: Représentation de la Cellule de Franz.

Dans cette méthode une cellule de diffusion est utilisée. Elle comprend deux compartiments : le compartiment donneur séparé du compartiment receveur par la peau. Le compartiment donneur reçoit la formulation contenant l'actif et des prélèvements successifs dans le compartiment receveur permettent d'établir au cours du temps le profil cinétique de passage. En fin d'expérience, la quantité d'actif qui n'a pas pénétré dans la peau est mesurée ainsi que la distribution dans les assises cutanées (*stratum corneum*, épiderme et derme) et la quantité présente dans le compartiment récepteur. Ces données permettent d'établir un bilan massique, un profil de distribution et de calculer un certain nombre de paramètres.

La pénétration est définie par un ensemble de paramètres dont le coefficient de perméabilité défini par l'équation suivante :

$$P = \frac{K_{octanol/eau} D}{L}$$

Equation 1-1 : Définition du coefficient de perméabilité

avec P, le coefficient de perméabilité (pénétration) en unité de vitesse ($m.s^{-1}$), $K_{octanol/eau}$, le coefficient de partage octanol/eau, D, le coefficient de diffusion ($m^2.s^{-1}$) et L, la longueur du chemin de diffusion de la molécule qui pénètre (m) [26]. Il est difficile de mesurer le coefficient de perméabilité expérimentalement dans la mesure où P et D sont deux inconnues reliées par la même équation. Il existe plusieurs estimations empiriques pour calculer ce coefficient de perméabilité, rassemblées sous terme relation quantitative structure perméabilité (QSPRs) [27,28]. Le calcul le plus connu, et le plus simple, qui est très largement utilisé est obtenu grâce à une relation mathématique établie de façon empirique par Potts et Guy à la suite d'une étude portant sur la perméabilité de différentes substances chimiques, comme les corticoïdes, de logP compris entre -3 et +6 et de masses moléculaires variées (entre 18 et >750) dans la peau [14] :

$$\log P = 0,71 \log K_{oct/eau} - 0,0061 M_r - 6,3$$

Equation 1-2 : Définition de logP après Potts et Guy [14]

avec M, la masse molaire en g/mol de l'actif.

La diffusion d'une substance dans la peau est décrite par la première loi de Fick [29] (Equation 1-3).

$$J = -D \frac{\partial C}{\partial x}$$

Equation 1-3 : Première loi de Fick.

Avec J le flux en $g.m^{-2}.s^{-1}$, D le coefficient de diffusion en $m^2.s^{-1}$ et dC/dx le gradient de concentration sur la distance x de la membrane. Pour quantifier la pénétration d'un actif dans

la peau, le flux est calculé en évaluant la concentration d'actif qui atteint au cours du temps le compartiment récepteur de la cellule de Franz une fois l'état stationnaire atteint. Cet état est obtenu en se plaçant en condition de saturation dans le compartiment donneur (concentration élevée de la substance active dans le compartiment donneur et considérée constante) et au contraire en très faible concentration (considérée nulle) dans le compartiment récepteur (« sink conditions »). Dans ces conditions, le coefficient de perméabilité devient :

$$P = \frac{J_{SS}}{C_f}$$

Equation 1-4 : Coefficient de perméabilité dans des conditions « sink »

avec J_{ss}, le flux en $g.m^{-2}.s^{-1}$ à l'état stationnaire et C_f (g/m^3), représente la concentration de la substance dans la formulation quand les conditions de saturation sont appliquées.

Les propriétés physicochimiques (M_w, volume moléculaire, polarité) de l'actif déterminent le profil de pénétration. Quand un actif n'a pas les propriétés idéales, par exemple une masse moléculaire trop élevé [30], des études de formulation deviennent indispensables. En accord avec la loi de Fick, deux possibilités existent pour favoriser la pénétration. Premièrement, la formulation peut changer la nature de la fonction barrière de la peau et, deuxièmement, la formulation peut optimiser le comportement de l'actif dans le système galénique et donc, influencer les coefficients de diffusion et de partage.

La barrière de la peau peut être modifiée par l'hydratation et par une désorganisation/fluidification des lipides. L'hydratation a deux effets qui permettent une augmentation de la pénétration percutanée des actifs hydrophiles [31] et lipophiles [32]. Premièrement, la solubilité de l'actif dans la peau est modifiée, ce qui provoque une variation du coefficient de partage et, deuxièmement, le *stratum corneum* gonfle et ouvre sa structure ce qui augmente la pénétration [33,34].

Le coefficient de diffusion d'un actif peut être influencé par le désordre ou fluidification de la structure lipidique du *stratum corneum* [6]. Dans les années 90, ces effets ont été montrés avec les promoteurs d'absorption tels que le DMSO, les alcools, l'Azone®, les terpènes, les acides gras et les tensioactifs [35],[36-44].

Le système galénique peut influencer les propriétés de solubilité de l'actif, ainsi que le coefficient de partage. L'utilisation de prodrogues peut par exemple être envisagée pour faciliter le transport de molécules possédant un coefficient de partage défavorable [45]. La modification chimique temporaire de la molécule permet d'améliorer son passage de la barrière cutanée, la molécule active originelle est ensuite libérée par hydrolyse ce qui permet d'optimiser la solubilité de l'actif dans l'épiderme. La complexation est une autre possibilité pour modifier la solubilité des actifs dans les couches hydrophiles de la peau [46] et pour stabiliser un actif [47] dans la formulation. Les cyclodextrines par exemple peuvent être utilisées pour incorporer un actif lipophile tout en conservant une solubilité aqueuse [48].

Les microémulsions sont des dispersions constituées d'eau, huile et de tensioactif qui forment des solutions transparentes, isotropes et stables d'un point de vue thermodynamique [49]. Il a été montré que les microémulsions augmentaient la pénétration percutanée d'actifs hydrophiles et lipophiles en comparaison avec des émulsions, hydrogels ou liposomes [50-52]. Cet effet est lié à leurs excellentes propriétés solubilisantes, à l'activité thermodynamique de l'actif dans la formulation et partiellement à l'effet promoteur qui dépend de leur composition en huiles et tensioactifs.

Cette première publication est un article de revue publié dans European Jounal of Dermatology, qui donne une vue globale de plusieurs aspects de la pénétration percutanée des actifs. Dans la littérature, il existe de nombreuses études qui traitent de l'influence de la structure de la peau et ses propriétés sur la pénétration d'un actif et les paramètres cinétiques. Au début de cet article, l'effet barrière de la peau est expliqué et discuté en fonction de la structure des lipides cutanés essentiellement. Ensuite, les principaux modèles

mathématiques sont détaillés, qui caractérisent les cinétiques de pénétration en tenant compte des propriétés physicochimiques de l'actif. La dernière partie de cette publication prend en considération les nouveaux développements galéniques qui permettent de modifier la pénétration percutanée par des formulations qui influencent le coefficient de partage de l'actif entre la formulation et la peau ou qui modifient la structure du *stratum corneum*.

Les faits marquants :

- La peau est séparée en deux parties, la partie lipophile, le stratum corneum, et la partie hydrophile, l'épiderme et derme.
- La barrière de la peau est essentiellement constituée par la couche lipidique du stratum corneum, qui contrôle la pénétration intercellulaire.
- Les expériences de pénétration percutanée doivent être menées en conditions « sink » et le flux à l'état stationnaire doit être considéré pour pouvoir appliquer la première loi de Fick.
- Pour pouvoir étudier l'effet de chaque composant de la formulation, des émulsions simples vont être formulées.
- L'influence des composants de la formulation sur la pénétration d'un actif et sur les modifications apportées à la couche lipidique, la barrière, vont être étudiées simultanément pour tenter de corréler les résultats.

Förster et al. Topical delivery of cosmetics and drugs. Molecular aspects of percutaneous absorption and delivery. Eur J Dermatol (2009) vol. 19 (4) pp. 309-23

Topical delivery of cosmetics and drugs. Molecular aspects of percutaneous absorption and delivery

Matthias Förster, Marie-Alexandrine Bolzinger, Hatem Fessi, Stephanie Briançon

Université de Lyon, F-69008 Lyon, France;

Université Lyon 1, ISPB, Faculté de Pharmacie

CNRS, UMR 5007, LAGEP, F-69622, Villeurbanne, France

Percutaneous penetration/permeation is a useful tool for obtaining qualitative and/or quantitative information on the amount of a drug, a cosmetic substance, or any chemical that may enter a skin compart- ment or the systemic circulation of the human body for pharmaceutical or cosmetic purposes, or for toxicological studies. In the latter case, the extent entering can then be taken into consideration in order to calculate the margin of safety using the NOAEL (No Observed Adverse Effect Level) of an appropriate repeated dose toxicity study with the respective substance. This paper is a short overview of vari- ous aspects of skin penetration/permeation of drugs or cosmetic agents. The literature reports numerous studies on skin structure and skin properties influencing drug/cosmetic agent permeation profiles and kinetic parameters. The extensive research concerning the skin structure for determining the key parameters of the penetration/permeation process is therefore described first. Mathematical models of the skin absorption process for a drug are then discussed. Finally new developments in pharmaceutical and cosmetic fields to enhance drug permeation or to modify the stratum corneum structure are considered.

Key words: Fick's diffusion laws, penetration enhancement, skin barrier, stratum corneum, nanoparticles

Topical delivery is, and has been for many thousands of years, a route of cosmetic and drug delivery. In this review we are speaking about modern medical cosmetology, which is part of modern dermatology[1]. In the cosmetic field the active substance must reach a skin compartment to exert its effect because the skin is itself the target. Conversely, in the pharmaceutical field using patch systems the skin is often the main barrier to cross in order to deliver hormones and analgesics to the systemic circulation[2]. The transdermal route of administration avoids hepatic first-pass metabolism and allows sustained drug release into the systemic circulation. A drug applied in a vehicle on the skin surface penetrates into the skin by a passive mechanism according to Fick's Laws depending on its molar mass and physicochemical properties. In the case of large molecules such as proteins, active mechanisms such as electroporation or iontophoresis have been developed to overcome the barrier. This review focuses on passive diffusion through skin (the more common process) but some examples of active diffusion will also be considered.

In both cosmetic and drug delivery, despite the high potential of the skin, extensive work has been done to develop new carrier systems because of the high barrier function of the outermost layer of the skin, the *stratum corneum*. Actually the skin is a heterogeneous membrane; lipophilic on its surface and hydrophilic in its deeper layers. The *stratum corneum* is a highly resistant barrier which limits the penetration of drugs into the skin because its structure contributes to its function both as a barrier to water loss and as a barrier against the external environment. The skin's barrier function is therefore important in considering both the transdermal delivery of drugs and in making a risk assessment following dermal exposure to chemicals. The major challenge for dermal or transdermal delivery is to 'tune' the vehicle in which the drug is entrapped in order to reach its

target site *i.e.* the skin surface, the skin compartments or the systemic circulation.

Today it is even possible to build three dimensional skin equivalent models by *in vitro* tissue engineering which are more and more complete and similar to the physiological skin[3]. Auxenfans *et al.* showed that their models can be used for better understanding the mechanisms of action of active substances and to test the innocuity as well as the efficacy of finished products.

In both pharmaceutical and cosmetic fields, new strategies have therefore been developed to provide an increase in drug penetration and of skin targeting without inducing skin damage. The optimum development of a drug delivery system for the topical route requires percutaneous absorption studies in order to establish the extent of drug repartitioning in the skin in relation to its formulation. Percutaneous absorption describes the entering of a drug into the skin from a drug-loaded formulation. This penetration is called permeation if the drug reaches the systemic circulation. The percutaneous absorption of a broad range of drugs has been extensively reported in the literature allowing the development of predictive models consistent with the transport mechanisms. The degree of penetration and/or permeation depends not only on the drug itself but also on the vehicle in which it is formulated and on the interaction between the vehicle and the skin.

This review follows the pattern: a) a consideration and discussion of skin barrier function in relation to skin structure; b) a description of the modelling of the drug permeation process relating the physicochemical properties of drugs to a mathematical model and c) a consideration of strategies to enhance or slow down skin permeation. Throughout this review the word "drug" is applied both to pharmaceutical drugs and to cosmetic agents. For each case considered it will be stated whether it is a cosmetic or a pharmaceutical example.

Skin barrier function

The role of the *stratum corneum*

The development of a water-resistant skin keeping water in and exogenous substances out is a necessary evolution for living on our earth[4]. The principal function of the skin is to protect the inner body that is rich in water against a dry environment. The role of the *stratum corneum* as a performing barrier was first established in the 40s[5,6] when researchers abraded layers of cells from the abdominal skin of anaesthetized surgical patients with sandpaper while monitoring water loss through the skin. With the removal of the lowest layers of the *stratum corneum* they observed a major increase in water flux.

The *stratum corneum* represents the outermost part of the skin and is the main skin barrier. The horny layer consists of dead cells (in general 15 to 20 layers) named corneocytes. The corneocytes are filled with keratins and embedded in a complex matrix of organized lipid bilayers. The *stratum corneum* is lipophilic and contains 13% of water.

The hydrophilic properties of skin increase from the surface as its depth increases. The viable epidermis, represented by respectively the *stratum granulosum*, the *stratum spinosum* and the *stratum germinativum*, is significantly hydrophilic (>50%). In the dermis the water content reaches 70%, favouring hydrophilic drug uptake. Therefore research interest is focused on the *stratum corneum* lipid matrix and on water diffusion through it. Knowing the structure and properties of this compartment at the molecular level is essential for studying drug penetration through the *stratum corneum* and for the development of new dermal drug delivery systems. This barrier is lipophilic and therefore imposes drug limitations on the type of permeant that can cross it.

Therefore, depending on the lipophilic or hydrophilic properties of a drug, it will accumulate in the *stratum corneum* (lipophilic substances), or stay on the surface (very hydrophilic drugs) or cross the skin (amphiphilic drugs). The molar mass and the volume of active agent entering the skin are also of some significance.

The intercellular route and the role of the lipid matrix

The *stratum corneum* consists of two components: non-living cells rich in proteins and intercellular lipid domains[7,8]. Proteins represent 75-80% of the content of the *stratum corneum* (based on the dry mass of the *stratum corneum*)

while lipids make up between 5 and 15%[9].The composition of the remaining 5-10% of the *stratum corneum* still needs elucidating[10,11].

By means of thin layer chromatography the composition of the lipids was determined as an equimolar mixture of (i) nine ceramide types (40-50 % of dry mass)[12], (ii) cholesterol (25 wt%), (iii) free fatty acids (10-15 wt%) and, (iv) about 5% of other lipids such as cholesterol sulphate, cholesterol esters and glucosyl ceramides[13]. The composition and structural details of the different ceramides in pigs, mice and human skin were first determined in the 80s[14-16] and in a more detailed way in more recent years[12,17-20].

The lipid arrangement displays a continuous lamellar structure of alternating lipid and aqueous regions, which most effectively hinders the diffusion of both non-polar and polar substances[21]. The first characterization results concerning the structure of the lamellar lipid regions were published in the 50s and 60s using X-ray diffraction and indicated a tube-like organization[22,23]. Using electron microscope and freeze fracture techniques it was shown that the lipids are in a lamellar organization[7,24-26] localized in the intercellular regions of the *stratum corneum*. However the lipid membrane was not visible with a standard electron microscope. This bilayer arrangement constitutes a tortuous diffusion pathway for molecules in the *stratum corneum* and so is involved in its barrier function[27]. The corneocyte membrane, known as a cornified cell envelope, is composed of a very compact cross-linked protein structure, the corneodesmosome, and reinforces the barrier function[28].

Three main routes have been identified in the *stratum corneum*: Pathway 1 - the intercellular route (see Figure 1); Pathway 2 - the intracellular (transcellular) route crossing through successive bilayers and dead cells and Pathway 3 - the route *via* skin appendages *i.e.* hair follicles and sweat glands which form shunt pathways through the intact epidermis. Pathway 3 is usually considered of little significance as only 0.1% of the total human skin is occupied by skin appendages[29]. Pathway 2 is the most direct route but requires transport through densely packed keratin-filled corneocytes followed by multiple transfers between the corneocytes and the lipid-filled intercellular areas. A drug passing through this pathway should therefore encounter significant resistance to permeation.

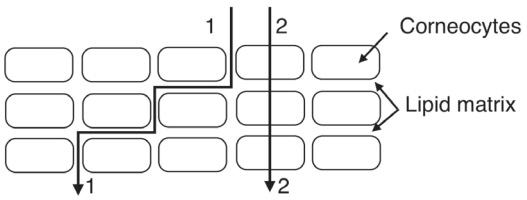

Figure 1: Different penetration pathways in the epidermis and especially through the *stratum corneum* (Pathway 1: transcellular way, Pathway 2: intercellular way)

The more common of the two main routes for drug permeation is by intercellular passage between the corneocytes[30]. This was confirmed *in vitro* by Simonetti and Meuwissen who showed that the penetration pathway of a dye (Nile Red in PEG, PG and DMSO vehicles[31] and FI-DHPE, a fluorescent probe, in liposomes[32]) is principally by traversing the intercellular region in the *stratum corneum*. The principal barrier to permeation of drugs is therefore the lipid matrix, which constitutes the intercellular pathway. The barrier effects of lipid bilayers have been known since the 50s. Several studies have shown that a modification of the lipid composition by solvent extraction dramatically increases water permeability[33-36]. For this reason lipid regions are considered to be the major barrier of the skin[37,38]. These studies were confirmed and extended by Yardley *et al.*[39]. Wertz *et al.* wrote a historical review of lipid research up to the 90s[40].

Understanding the physical structure of a membrane is essential for understanding both its barrier function and the disruption mechanism for that barrier caused by topical applied products and, additionally, for the understanding of several skin diseases.

Recently it has been shown that this epidermal barrier depends not only on the composition of the *stratum corneum* but also on its structural organization[41-43]. Furthermore its structure is linked to its composition and therefore a small change in the composition of its lipids might have an enormous effect on their physical organization in the liquid crystalline state[44].

More recently still, very detailed studies of lipid organization have been carried out in a synthetic *stratum corneum* lipid mixture[45,46]. The conclusion, therefore, from research studies is that the structure of the lipids depends primarily on cholesterol and on the fatty acids that they

contain. Fatty acids play an important role in the formation of the lamellar phase because they are one of the principal lipid groups in the *stratum corneum*. Cholesterol is an omnipresent membrane lipid, and the second component in terms of quantity, in the *stratum corneum* (25% of lipid mass). It can either increase the fluidity of membrane domains or make them more rigid depending on the physical properties of the other lipids and on the relative proportion of cholesterol compared to the other components. The role of cholesterol in the epidermal barrier is probably to provide a degree of fluidity in what would otherwise be a rigid, possibly brittle, membrane system. This may be necessary for the pliability of the skin[47]. More detailed information on the lipid phase structure can be found in the work of Wertz[47] and Bouwstra[48].

All free fatty acid chains and amide-linked fatty acids in ceramides are non-branched and have no double bonds. All ceramides and free fatty acids in the *stratum corneum* are arranged in a bar-like form or a cylindrical form. These structures allow the formation of highly ordered gel phase membrane domains. These gel phase domains are less fluid and so less permeable than typical biological membranes which are dominated by liquid crystalline phospholipid domains. In contrast to the phospholipids, ceramides cannot form bilayers on their own. Instead they form ordered structures by interaction with other skin lipids.

Several biophysical studies of the structure of the *stratum corneum* assume the presence and coexistence of liquid crystalline phase domains and of solid or gellified crystalline phase domains in the membrane of the *stratum corneum*. These conclusions imply low lateral diffusion properties at physiological temperatures. This concept introduced by Forslind[49] was presented as a 'mosaic domain' model. Two other models were also suggested for explaining the unique properties of the *stratum corneum*. Bouwstra presented a model for the existence of fluid phases in the lamellae, which is called the 'sandwich model'[50] and Norlen introduced a 'single gel phase' model[51] that was, he felt, more consistent with the described properties of the *stratum corneum*. A review giving more details on this research area has been written by Bouwstra[52].

Percutaneous absorption

A broad range of formulations can be applied to the skin. For topical delivery the most commonly used formulations are emulsions, which are dispersions of oil droplets in water (o/w emulsions; see Figure 2) or, conversely, dispersions of water droplets in an oily phase (w/o emulsions) stabilized by surfactants. The drug could therefore be entrapped in dispersed droplets or solved in the continuous phase depending on its affinity for oil or water. Emulsions have been extensively studied as dermal or transdermal vehicles and it has been known for a long time that their ability to solubilize both hydrophilic and lipophilic substances favours drug absorption, which is often higher from emulsions than from solutions[53]. Moreover by changing the polarity of the oil phase, the emulsion viscosity, the droplet size or the type of emulsion used, *i.e.* o/w or w/o or even multiple w/o/w or o/w/o, it has been shown that skin penetration of a drug can be modulated[54-57]. No consensus exists in the literature in relation to permeation enhancement from o/w or w/o emulsions because frequently the studied formulations using percutaneous experiment do not have the same compositions and the drugs used have very different physicochemical properties. Under such conditions general rules cannot be formulated. Few research teams have studied the influence of similar formulations loaded with the same drug at the same concentration and then, even more rarely, for the topical route. In this context attention should be drawn to the research carried out by Marti, Seiller and Grossiord because these workers performed percutaneous experiments on different types of emulsions having the same composition and under controlled operating conditions (finite or infinite doses…). In the study carried out by Ferreira[58] three emulsions (o/w, w/o and w/o/w) containing water, paraffin oil and the same combination of surfactants, were formulated and loaded with 0.5% of metronidazole (logP = -0.15) or glucose (logP = -2.2). For glucose, the more hydrophilic substance of the two, after 24h of exposure, skin absorption from the o/w emulsion was 4-fold higher than from a w/o emulsion, and 2.8-fold higher compared to the w/o/w emulsion which was therefore intermediate in effect. These results were confirmed by Youenang Piemi *et al.*[55] in 1998 when using an infinite dose. For metronidazole (log P=-0.15) the results were close to the previous ones with a skin absorption of 55% to

69% of applied dose depending on emulsion type but in this research a slightly better absorption from the w/o emulsion was noted. The authors explained their results in terms of the occlusive properties of w/o emulsions[58]. Water evaporation of the formulation after application (in finite dose) should also be taken into consideration because it may change the drug concentration on the skin surface while the structure remaining on the skin after evaporation could be dependent on the emulsion type. Taking advantage of their compartmental structure, emulsions and, especially multiple emulsions, can be considered as reservoirs for an active drug modulating its release. Multiple emulsions allow drug-controlled release when the substance is entrapped in the inner core of water droplets in the w/o/w emulsion[55] or conversely in the oily internal droplets of an o/w/o emulsion[54,55,57,58].

Recently sophisticated formulation strategies have been described in the literature using, for example, liposomes, nanoparticles or microemulsions, in order to enhance drug penetration or to target a particular skin layer. Examples are provided in paragraph 4.

The mechanisms by which a drug leaves its formulation and penetrates the skin are explained in next paragraphs.

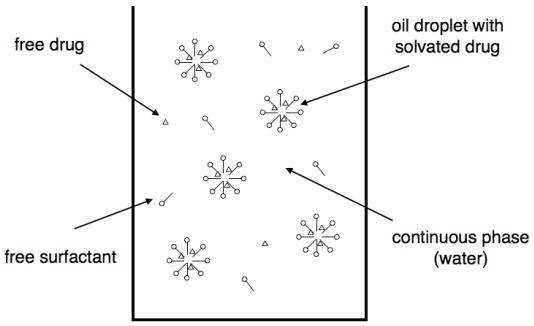

Figure 2: Microscopic scheme of an o/w emulsion

The partition coefficient

Partition is the term applied to the distribution of a substance between two adjacent but different phases at equilibrium.

Consider a drug formulated in a complex vehicle such as an emulsion, which is applied directly onto the skin. The first contact that the product makes with the skin is with the outermost skin layer, the *stratum corneum*. The drug therefore has to be absorbed into the *stratum corneum* from the product. The first critical step determining the skin absorption level of a drug from a topical delivery (for example, from a cream) is partition. Two partitions are involved. The first is partitioning of the drug between two emulsion phases (oil and water) and the second is partitioning of it between the skin and the formulation. Partition between the skin and the formulation is described by the (*stratum corneum*/formulation) partition coefficient, K_m, for the molecules of the penetrating ingredient. This partition coefficient is defined as:

$$K_m = \frac{C_{penetrant} \text{ in stratum corneum}}{C_{penetrant} \text{ in formulation}}$$

Equation 1: The partition coefficient where $C_{penetrant}$ is a measure of the solvated amount of the particles of the penetrating ingredient.

Equation 1 shows that the partitioning of a drug into the *stratum corneum* is enhanced when the drug has a higher affinity for the *stratum corneum* than for the formulation. Lipophilic drugs have a greater affinity for the *stratum corneum* and therefore tend to accumulate in this layer. The partition coefficient $K_{oct/water}$ of a drug between octan-1-ol and water (or rather the logarithm of this value, log $K_{oct/water}$) is used in pharmaceutics as an *in vitro* model for the partition coefficient given in Equation 1[59,60]. It is considered a good model, representative of the heterogeneous nature of the *stratum corneum*.

To enhance the partitioning of a drug the most common way is to change its solubility in the formulation. Changing the solubility or the concentration of dissolved drug in the *stratum corneum* is rather difficult. The concentration in the *stratum corneum* can only be increased if the drug leaves the *stratum corneum* and diffuses into the deeper skin layers.

The permeability coefficient

Partition is therefore influenced by diffusion and so both factors (partition and diffusion) are important in determining skin penetration (skin permeability). They are combined in the permeability coefficient P:

$$P = \frac{K_{oct/water} D}{L}$$

Equation 2: The permeability coefficient.

where P is the permeability coefficient with units of velocity ($m.s^{-1}$), $K_{oct/water}$ the octanol/water partition coefficient, D the diffusion coefficient ($m^2.s^{-1}$) and L the length of the diffusion pathway

of the penetrating molecule (m). The exact diffusion pathway of a drug in the skin cannot be determined. In general, the skin thickness is measured and its value is assumed to be the same as the length of the diffusion pathway, L61. However its value could be quite different if the intercellular route (pathway 1 in Figure 1) through the SC structure was followed.

The determination of the permeability coefficient is rather difficult. Theoretical relationships have been developed taking into consideration only the two reliable parameters: the octan-1-ol/water partition coefficient and the relative molecular mass, M_r[37]. These theoretical relationships were first published in the late 80s and early 90s and are based on empirical values. Potts and Guy were amongst the first workers who developed a mathematical relationship:[37]

$$\log P = 0.71 \log K_{oct/water} - 0.0061 M_r - 6.3$$

Equation 3: Empirical log P calculation from Potts according to Guy[37]

These estimations of skin permeation coefficients are sometimes known as quantitative structure–permeability relationships (QSPeRs or QSPRs). Recent overviews of QSPeRs for permeation into human skin from water have been reported in the literature[62-66].

Fick's Diffusion Laws

The simplest way to model the process of skin transport is to consider the skin as a membrane through which the drug has to pass. The diffusion of the compound through the skin is described by Fick's First Law[67]

$$J = -D\frac{\partial C}{\partial x}$$

Equation 4: Fick's First Law.

This law says that the flux (mass.m^{-2}.s^{-1}), which is the rate of transfer per unit area of a compound at a given time and position is proportional to the differential concentration change ∂C over the differential distance ∂x. The negative sign indicates that the flow is in the direction of decreasing thermodynamic activity (coefficient of activity multiplied by mole fraction), which can often be represented by concentration. To describe the concentration within a membrane, Fick's First Law is combined with the differential mass balance existing in a membrane making several assumptions: the compound is not metabolized, it does not bind with the membrane and its diffusion coefficient does not vary with position or composition[67]. The result is called Fick's Second Law.

$$\frac{\partial C}{\partial t} = D\frac{\partial^2 C}{\partial x^2}$$

Equation 5: Fick's Second Law.

The individual layers of the skin can be treated as pseudo-homogeneous membranes and so Fick's First Law can be applied to diffusion processes in these layers[68].

The flux at steady state (*i.e.* when the flux is constant) is given by:

$$J_{SS} = \frac{D(C_1 - C_2)}{L}$$

Equation 6: Expression of the flux at steady state.

where L is the length of the diffusion pathway of the penetrating molecules (layer thickness) (m), C_1 and C_2 are the mass concentrations (kg.m^{-3}) of the penetrant in the membrane at the two faces (at x = 0 and x = L) and D is the diffusion coefficient (m^2.s^{-1}) (Figure 3).

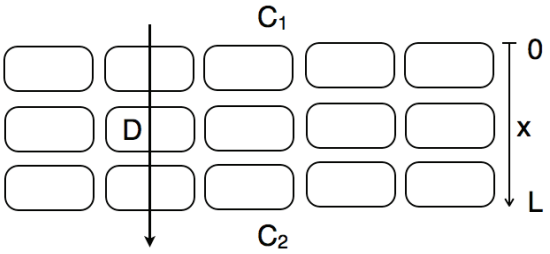

Figure 3: Schematic illustration of the variables related to skin layers.

Sink conditions will mean that the concentration at x = L is zero or very small (C_2 = 0). In addition, the concentration of penetrant at x = 0 is in local equilibrium with the concentration of penetrant in the formulation (C_1=$K_m C_f$ in which K_m is the pseudo-homogeneous partition, or distribution coefficient defined by Equation 1 and C_f the concentration in the formulation). Under these conditions Equation 6 becomes:

$$J_{SS} = \frac{D \cdot K_m \cdot C_f}{L}$$

Equation 7: Flux at steady state under sink conditions

Comparing Equation 7 with Equation 1 and

replacing $K_{oct/water}$ by K_m gives Equation 8, an alternative expression for the dermal permeability coefficient, P ($m.s^{-1}$)[29].

$$P = \frac{J_{SS}}{C_f}$$

Equation 8: Dermal permeability coefficient

where J_{ss} is the steady-state flux of the solute and C_f represents the concentration of the penetrant in the formulation or vehicle when sink conditions apply.

A practical example

A practical example of a classical penetration study is given below. Bolzinger *et al.*69 followed *in vitro*, using the Franz cell method70, the permeation of a model substance, caffeine, formulated in a gel, an emulsion (o/w) and a microemulsion. Caffeine is a somewhat hydrophilic drug, which penetrates well through the skin and has been extensively studied. In this example the authors followed OECD guidance71, which describes the methodology to assess drug permeation study for risk assessment determination and is based on the Franz cell diffusion method70. Basically in the Franz cell method, diffusion cells are divided in two parts. One is called the donor chamber and is filled with a known amount of a formulation. The second one is called the receiver or receptor chamber and is separated from the donor chamber by the skin. The receptor chamber is filled with a solution in which the studied substance under study is soluble. A few aliquots are analysed for caffeine content at specific times during the experiment and the cumulative amount of caffeine is then plotted against time. Bolzinger *et al.* thus followed the variation in caffeine permeation in the receptor fluid with time.

Figure 4 shows graphs comparing different formulation systems (a microemulsion, an emulsion and a gel).

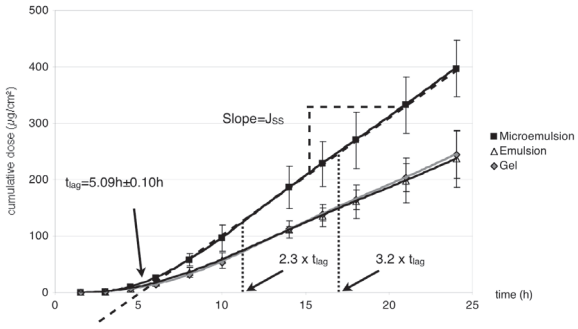

Figure 4: Permeation of caffeine (µg/cm²) across the skin (with hypodermis) as a function of time (n=6); adapted from[69]

These graphs show a diffusion lag time followed by a linear increase. Extrapolation of the linear section to meet the x-axis gives the lag time and the slope yields the pseudo steady-state flux J_{SS}. The dermal permeability coefficient can be calculated using Equation 8 where C_f is the concentration of the drug in the donor compartment. The lag time reflects a complex sequence of events including the release of the drug from its vehicle, the reorganization of the skin barrier and the diffusion of the drug through this time-varying medium. The time required for the permeation rate across a membrane to reach 95% of its steady-state value is approximately 2.3 times the lag time rising to 99% of the steady state value after approximately 3.2 times the lag time[72,73].

A problem concerning skin delivery arises from the existence of two parameters that influence the permeability in contrasting ways. In general, firstly, and in accordance with Fick's First Law, the flux increases when the concentration of the drug in the formulation increases (Equation 7). This can be achieved by increasing the drug solubility in the formulation. Secondly the flux will also be increased if P is greater *i.e.* the relative solubility of the drug in the *stratum corneum* is greater than the solubility of the drug in the formulation. The relative contributions of the velocity of absorption (flux J) and the amount of absorbed active substance cannot be separated as the two parameters have been combined into one equation (Equation 7). The problem therefore remains. Finding the right compromise in each case is the only way to solve this problem. To do so successfully it is necessary to understand as much as possible about each of the parameters which influence the solubility of the active ingredient in the skin and in the formulation.

In the experiment described below, the authors

used a constant caffeine concentration. The highest flux obtained with the microemulsion system is probably due to the higher amphiphilic character of the microemulsion system and the high amount of surfactants present which are able to modify the skin barrier. This will be discussed in the next section.

Penetration enhancement techniques

The physicochemical properties of an active ingredient, which determine its penetration profile, include molar mass, molecular size, the hydrophilic-lipophilic balance, the distribution of polar and nonpolar parts in the molecule and the extent of the ionized state. These factors play a large part in determining the solubility and the partition coefficient of the ingredient and have been extensively studied in recent decades. In the search for a compromise to overcome the problem mentioned in the previous section it has been found that molecules which exhibit intermediate partition coefficients (log $P_{octanol/water}$ values between 1 and 3) are sufficiently soluble in the lipid domains of the *stratum corneum* to permit diffusion through those domains while still having a sufficiently hydrophilic nature to be soluble in the formulation and to allow partitioning into the viable tissue of the epidermis. The molar mass and the molecular size of an ingredient affect the diffusion coefficient and the melting point and therefore relates to the solubility, so optimal permeability is reached with low molar mass[37] (ideally equivalent to less than 500 Da[74]). This latter restriction limits the available choices especially when using proteins and peptides[75].

For optimising transdermal delivery of drugs with a molar mass bigger than 500 Da active mechanisms have to be used. In electroporation high voltage impulses are applied during short time intervals to create temporary pores on the skin. The driving force for drug permeation is either ion repulsion or electro-osmosis. Sonophoresis uses low frequency ultrasonic energy to disrupt lipid packing in the *stratum corneum* creating aqueous pores, which improve drug delivery76,77. Other methods include (i) local thermal treatments78,79, (ii) the possibility of mechanical perforation of the *stratum corneum* by high-velocity particles (the so-called ballistic method)79 and (iii) the use of a micro-needles array, the effects of which include temporary loosening of the barrier properties until the *stratum corneum* is restored to its usual state by the normal turnover cycle80-82. Iontophoresis is an electrically assisted method where the drug has to be used in an ionic form. By applying an external electrical field to the skin the active ingredient will be accelerated and as a result of electromigration and electro-osmotic forces it will be transported into the skin layers. This method is used for proteins and peptides, for example in insulin delivery in diabetes therapy. Insulin is negatively charged and has a relative molar mass of 6000 Da. A number of fundamental *in vitro* studies have investigated the effect of iontophoretic parameters on insulin delivery[83-88] while pharmacodynamic studies have demonstrated the physiological effect of iontophoretically delivered insulin on blood glucose levels in a variety of small animals, usually mice, rats or rabbits[85,89,90]. Kari[91] used cathodal iontophoresis with currents ranging from 0.2 to 0.8 mA (patch area 6.2 cm^2) applied for 2 h in delivering insulin to alloxan-diabetic rabbits. The results showed that blood glucose levels decreased as serum insulin concentrations increased. Doubling the iontophoretic current from 0.2 to 0.4 mA produced a 3-fold increase in the serum insulin concentration but a further increase to 0.8 mA had no additional effect. This result was attributed to the generation of hydroxide ions at the electrode surface, which compete in the carrying of the current in the cathodal compartment[91].

When a drug does not have near-ideal physicochemical properties, formulation studies (passive skin penetration enhancement) become necessary. Formulation is the key to successful topical delivery. As previously mentioned, and in accordance with Fick's First Law, there are two possibilities of penetration enhancement. Firstly the formulation can change the skin barrier and can therefore influence the Fick's parameters (diffusion coefficient and partition coefficient). Secondly the formulation can optimize the drug behaviour in the galenic system and therefore also influences the Fick's parameters.

Modification of the skin barrier

A modification of the skin barrier influences both the partition coefficient and the diffusion coefficient. Both the structure and the function of the *stratum corneum* have also been considered. The literature indicates the two main aspects in reducing skin barrier capability

to be hydration and lipid fluidization. A review of penetration enhancement techniques made by Benson[92] will be summarized and extended in the following sections. There are also many excellent reviews[93-96] that consider methods for promoting skin penetration.

Hydration

Using water is the safest method for increasing skin penetration of hydrophilic[97] and lipophilic permeants[98]. An increase in water content has two effects. Firstly it can alter the solubility of an ingredient and thereby modify the partition coefficient as indicated in Equation 1. Secondly the *stratum corneum* may swell and open its structure leading to an increase in penetration. For example the diffusion coefficient of alcohols in hydrated skin is 10 times higher than in dry skin[68,99]. This effect can be obtained by occlusion with plastic film (patch systems[100]) and with long-chain alkanes, oils and waxes as components of ointments and water-in-oil emulsions that prevent transepidermal water loss as well as with oil-in-water emulsions that moisturize the skin.

Fluhr *et al.* explain in their review[101] the importance of the hydration of the *stratum corneum* for normal functioning of the biochemical and biophysical processes in the skin. It has been shown that water acts as a plasticizer for both the corneocyte proteins and the intercellular medium[102]. In dry skin or even in diseases with reduced *stratum corneum* hydration, *e.g.* ichthyosis vulgaris and winter xerosis[103], the formation of the rigid cornified envelope (CE) of the corneocytes (corneodesmolysis) is impaired due to the level and activity of transglutaminase (a key enzyme in the cross-linking of CE proteins)[104]. Skin xerosis in patients with end-stage renal disease correlates with reduced levels of endogenous glycerol in the *stratum corneum*[105]. Thus glycerol plays an important role in sustaining skin hydration. It was confirmed by Breternitz *et al.* that glycerol exerts its hydrating effect not only on healthy skin but also on subjects with diseased skin, primarily characterized by xerosis and skin barrier impairment[106]. Glycerol has an action on aquaporin-3, a homologous water-transporting protein in many mammalian epithelial, endothelial and other cell types[107]. The effect of glycerol on hydration in the entire *stratum corneum* was obtained by *in vivo* Raman microspectroscopy. Chrit *et al.* revealed an increase in water content and so an increase in skin moisture after application of a glycerol-based cream, which is the most widely used hydrating agent. [108].

Barichello *et al.*[109] studied the transdermal delivery of isosorbide-5-nitrate (ISN) on rat abdominal skin *in vitro* from firstly liposomal systems and secondly from the drug solution used as control. In both cases studies were carried out using 5% glycerol and without glycerol. The authors showed that the amount of ISN permeated through rat abdominal skin from a liposomal formulation containing 5% glycerol was significantly higher when compared with the amount of ISN permeated from the other formulations ($p<0.001$). No significant difference in the permeated ISN mean values was noticed among the other tested formulations. The authors explained that the enhancement effect of glycerol might be due to an increase in *stratum corneum* hydration.

Lipid disruption/fluidization by chemical penetration enhancers

The diffusion coefficient of a drug, estimated from Equation 6, can be influenced by disordering or by fluidizing the lipid structure of the *stratum corneum*. Enhancers like azone, DMSO, alcohols, fatty acids and terpenes form microcavities within the lipid bilayers and increase the free volume fraction; they can even penetrate into and mix with the lipids. Octadecanoic acids (oleic acids) and terpenes can create permeable pores that provide less resistance to polar molecules. These effects have been demonstrated in the 90s using different analytical methods[110-118].

Surfactants, DMSO, decylmethylsulphoxide and urea can also interact with keratin in the corneocytes119. The resulting increase in diffusion coefficient is caused by binding with keratin filaments after the chemicals have penetrated into the intercellular matrix of the *stratum corneum*. This results in a disruption of order within the corneocytes. However in many studies it has been shown that there is a close relationship between permeation enhancement and lipid bilayer fluidization and that the lipid lamella of the *stratum corneum* is the main site of action[7,26,41,120].

Kim *et al.* used a pore-forming peptide (magainin) under co-enhancement by NLS-ethanol (N-lauroyl sarcosine) to increase skin permeability. They showed a 47-fold increase in

penetration of magainin into the *stratum corneum*, by NLS-ethanol enhancement. The magainin also increased *stratum corneum* lipid disruption (and especially so in ceramides and cholesterol) and skin permeability. They presented this study as a novel concept, using a first chemical enhancer (NLS-ethanol) to increase penetration of a second chemical enhancer (magainin) into the skin in order to synergistically increase skin permeability of a model drug (fluorescein in their study)[121].

Formulation based enhancement

Formulation-based optimizing has an influence on the solubility properties of a drug and on its partition coefficient. But the formulation itself can also influence both the *stratum corneum* and the solubility of the drug as in encapsulation techniques.

Prodrug

A prodrug is a drug derivative with better solubility and transport properties in the *stratum corneum* than the parent drug; its use may be helpful for drugs with unfavourable partition coefficients[122]. Application of this technique is mainly in pharmaceutics. When the derivative has reached the viable epidermis the parent drug will be released by hydrolysis *via* esterases thus optimizing solubility in the aqueous epidermis. Saab et. al increased the intrinsic poor permeability of very polar 6-mercaptopurine up to 240 times using S[6]-acyloxymethyl and 9-dialkylaminomethyl promoieties[123]. More recently the same research group also increased the permeability (P) of 5-fluorouracil, a polar drug with reasonable skin permeability, up to 25 times using N-acyl derivatives[124,125].

Prodrugs are also used to place charged drugs under the skin. A charge-neutralized complex is formed by adding an oppositely charged species to the charged drug so that the drug can diffuse into the aqueous viable epidermis where the charged parent drug is released by dissociation126-128. In each reported case the permeability increase obtained was only two to three-fold. But recently Sarveija *et al.* reported a 16-fold increase in the steady-state flux of ibuprofen ion pairs across a lipophilic membrane[129].

Eutectic systems

It has been stated that a lower melting point for a drug influences positively the solubility and the penetration into the *stratum corneum*. This can be achieved using a prodrug (see 4.2.1) or by a eutectic system. The latter is a mixture of two components in a certain ratio, each of which affects the crystallizing of the other. The freezing point of each component in the mixture is reduced by the presence of the other and the solid, which crystallizes at the eutectic temperature, has the same composition as the original mixture. Eutectic systems can be found in both cosmetic and pharmaceutical fields.

A good example is EMLA® (AstraZeneca) cream. This is a formulation consisting of a eutectic mixture of the local anaesthetics lignocaine (m.p. 68°C) and prilocaine (m.p. 16°C), applied under an occlusive film as the free bases. Together they provide a more effective local anaesthetic effect and consequently prevent the pain associated with needle insertion. The mixture is a 1:1 eutectic mixture (eutectic temperature 18 °C) formulated as an oil-in-water emulsion which maximizes the thermodynamic activity of each component[130]. There are several eutectic systems containing a penetration enhancer as the second component, for example: ibuprofen with terpenes[131], menthol[132] and methyl nicotinate[133], lignocaine with menthol[134] and propranolol with fatty acids[135].

Complexation in cyclodextrins

Complexation is another possibility for modifying the aqueous solubility and drug stability in a formulation. In this context cyclodextrins (CDs) have the greatest pharmaceutical relevance but they have also been used in cosmetic research work. CDs are a group of cyclic oligosaccharides derived from starch and are composed of 6, 7 or 8 dextrose molecules in a cylinder-shaped structure and named respectively -, - and -cyclodextrin. The central cavity of each molecule is hydrophobic while the surrounding walls are hydrophilic. These hydrophobic cavities form inclusion complexes with many hydrophobic drugs. Complexation can considerably increase both the solubility and bioavailability of a drug[136]. Figure 5 shows a molecule of -cyclodextrin.

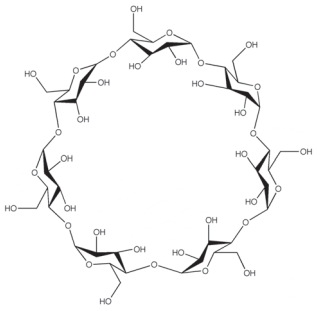

Figure 5: Representation of a -cyclodextrin molecule

In cosmetic applications complexation has improved the photostability of sunscreens[137,138] but its influence on penetration behaviour is a compromise. There is an increasing effect due to better solubility[139-141] but a decreasing effect resulting from using molecules with large relative molar masses (equivalent to more than 1000 Da)[129,142,143].

A recent trend is the use of modified cyclodextrin molecules. The most commonly used is hydroxypropylbeta-cyclodextrin (HP-b-CD). It is able to form hydrophilic inclusion complexes with many lipophilic compounds in aqueous solution, which can enhance the aqueous solubilities of lipophilic drugs without changing their intrinsic abilities to permeate lipophilic membranes. An interesting example is sunscreen delivery onto a skin surface. Simeoni *et al.* have investigated the penetration of oxybenzone, a lipophilic sunscreen agent, on human skin, from HP-b-CD and from SBE-b-CD, a sulfobutylether-b-cyclodextrin142,144. The authors showed that SBE-b-CD had the greater solubilizing activity on oxybenzone, a highly lipophilic sunscreen, (a 1049-fold increase) when compared with the use of HP-b-CD (a 540-fold increase). The sunscreen penetration to the deeper living layers of the skin was remarkably decreased (1.0% and 2.0% of applied dose for epidermis and dermis respectively) compared with the unbound OMC formulation used as control and with OMC loaded HP-b-CD (~5%). This result is interesting because this type of carrier can promote the solubilizing and photostabilizing properties of sunscreen agents while staying on top of the skin where they are intended to act[144].

Even with modified complexes, conflicting results have been found in the literature concerning their effect to promote or decrease skin penetration of drugs. But there still remain the problems of their molar mass and their limited capacity to penetrate into the skin[145].

Chemical potential

Another possible modification is to change the chemical potential of a formulation through the use of saturated and supersaturated solutions. Supersaturated solutions have the highest thermodynamic activity and these solutions show the maximum skin penetration rate. This can be explained using Fick's First Law (Equation 4). It was mentioned earlier that thermodynamic activities can often replace concentration terms. The expression summarizing Fick's First Law can be rewritten in terms of activities in the following way.

$$J = \frac{\alpha D}{\gamma L}$$

Equation 9: Fick's first law expressed in terms of activities

where α is the thermodynamic activity of the drug in the formulation and is the apparent activity coefficient in the membrane. The dependence of the flux on thermodynamic activity rather than concentration has been demonstrated by Twist and Zatz[146,147].

Moser[148] has shown the enhancement effect of supersaturated formulations using a lipophilic model compound (a lavendustin derivative, LAP) passing through excised pig skin *in vitro*. He has also drawn attention to the supersaturation effect, by replacing in Equation 7 the partition coefficient with the relationship given in Equation 1, so that Equation 7 now becomes:

$$J_{SS} = \frac{C_f}{C_{S,f}} \cdot \frac{D \cdot C_{S,SC}}{L}$$

Equation 10: Flux at steady state under sink conditions related to the degree of drug saturation in the formulation.

where C_f / $C_{S,f}$ is the degree of drug saturation in the formulation. When this latter term is equal to 1 the formulation is saturated and if it is bigger than 1 it is supersaturated. Cf is the drug concentration dissolved in the formulation, $CS,_{SC}$ is the solubility of the drug in the barrier (*stratum corneum*) and $C_{S,f}$ the solubility of the drug in the formulation. Supersaturated solutions can be produced by evaporation of solvent or by a co-solvent technique. This involves mixing two solvents chosen so that the drug is significantly more soluble in one solvent than the other. This supersaturation technique can only be used in certain instances. One of the major drawbacks of this method is that the

thermodynamic instability of the supersaturated solutions leads to crystallization of the drug and hence to a decrease of the drug flux.

Use of Microemulsions

During the last decades microemulsions have been more and more frequently studied. Microemulsions have small emulsion-like structures and are transparent, optically isotropic and thermodynamic stable[149]. Microemulsions are commonly systems of oil, water and surfactants of low viscosity. Three microstructures exist (o/w, w/o and bicontinuous) and the size domain is typically in the range of 10-100nm. Due to their high solubilization properties and to their improved drug delivery properties microemulsions offer several advantages for cosmetic and pharmaceutical delivery. However as yet no pharmaceutical microemulsions suitable for the dermal administration route have been launched on the market. In the cosmetic field microemulsions suffer from their appearance because they look like water or oil solutions but since they have been shown to enhance dermal and transdermal many *in vivo* and *in vitro* studies on microemulsion formulations have been reported (see, for example, reviews written by Kreilgaard, Heuschkel, and Kogan)[150-152]. The mechanisms by which microemulsions enhance drug delivery were explored by Delgado-Charro[153] and Kreilgaard[154]. Delgado-Charro *et al.* studied a widely used combination of non-ionic surfactants, ethyl oleate as oil, sucrose as hydrophilic model drug and water. They varied the microemulsion microstructure (o/w or w/o) and the water to oil ratio. Despite the high amount of surfactant (25% to 44%) necessary to obtain single-phase microemulsions, a major drawback of these systems, no erythema or loss of skin barrier function (measured as Trans Epidermal Water Loss in $g.h^{-1}.m^{-2}$) was noticed on the forearms of 6 human volunteers after 3 hours exposure under occlusion of their coemulsions. The enhancement of drug permeation (one order of magnitude compared to an aqueous solution) from microemulsions tested on hairless mouse skin *in vitro* for 9h was firstly attributed to the high surfactant percentage necessary to obtain them. But since Delgado-Charro et al. did not notice any increase in TEWL values after application on human volunteers under occlusion over the 3h period and they suggested other possibilities including the different partitioning processes between droplets, continuous phase and skin, and the different relative activities of the drug in these fractions. Diffusion of microemulsion components may also disturb the *stratum corneum* arrangement and reduce or modify the skin barrier function leading to increased penetration. It is also possible that the formulation can also extract some horny layer components. More recently Kreilgaard *et al.* studied the delivery of prilocaine hydrochloride and lidocaine from seven microemulsions using throughout the same surfactant combination but differing in the amounts of each component used[150]. These authors found considerable variation in the mean transdermal flux with microemulsion composition. However, the microemulsions increased the transdermal flux of lidocaine up to at least four times compared with a conventional oil-in-water emulsion (Xylocain® 5% cream), and that of prilocaine hydrochloride by almost 10 times compared with a hydrogel (Xylocain® 2% gel).

Moreover the authors compared the *in vitro* permeation of microemulsions to EMLA® cream, a eutectic mixture of lidocaine and prilocaine (2.5%). A superior transdermal permeation coefficient of lidocaine was obtained with EMLA compared with microemulsions, which contained between 9 and 27% of lidocaine (saturated conditions in the different microemulsions studied). The authors explained this result by the eutectic composition, which exhibits a unique thermodynamic activity in the formulation. Nevertheless the microemulsion containing 9.1% of lidocaine exhibited an average transdermal flux 50% larger. This could be explained by a larger 4-fold concentration gradient in the microemulsion.

It can be concluded from this study that the drug delivery potential of microemulsions is greatly dependent on the internal structure/fractional composition of the phases.

A correlation between transdermal drug fluxes and their self-diffusion coefficients determined by spin echo NMR spectroscopy has been found. This result has been explained by the increased solubility of the drugs (lidocaine showed a 28-62% increase in solubility and prilocaine hydrochloride an increase of 24-40%), which appeared to be dependent on the drug mobility in the individual vehicles. This result has been supported by other earlier studies[155,156].

Nanoparticles

Nanoparticles (NPs) can be of polymeric or lipidic type and in the form of nanospheres or nanocapsules[157]. The structural configuration of nanoparticles varies greatly depending on the ingredients (polymers, monomers, lipids etc) and the manufacturing methods employed (polymerisation, precipitation, homogenisation, hot melt, membrane etc.)[158,159]. Nanoparticles are highly suitable systems for dermal application (both cosmetic and pharmaceutical). They improve protection of unstable active ingredients, may ensure a controlled release of active ingredients and may enhance penetration into the skin. The nanoparticles offer a number of advantages over other available carrier systems. In addition to their very small size, their stability and their very high specific area, which facilitates surface adsorption, they offer a targeted release of active ingredients and enhanced penetration of the encapsulated actives. In addition the nanocarriers provide a certain level of cutaneous penetration since their size can be less than that of the cutaneous pores. Moreover, they can accumulate in cutaneous appendices. Finally, from a technological point of view, nanoparticles can be easily worked into emulsions.

Lipid nanoparticles

Solid lipid nanoparticles (SLNs) and nanostructured lipid carriers (NLCs) are composed of physiological and biodegradable lipids. SLNs consist of pure solid lipid while NLCs are made of a solid matrix entrapping liquid lipid compartments[160,161].

SLNs possess some advantages when compared with liposomes (which are also lipid carriers but without a solid structure) and emulsions, *e.g.* protection against chemical degradation of a drug and the modulating capacity of active compound release.

The main disadvantage of SLNs are that during storage the drug entrapped is expulsed due to a change in lipid conformation to a lower energy crystal state. This transformation from polymorphic to a more stable crystalline form stops any guest molecules from being included in the structure.

To overcome this problem NLCs were developed. In these nanocarriers solid and liquid lipids are mixed in such a combination that the particles solidify upon cooling but do not recrystallize, remaining in an amorphous state. This allows the drug to be accommodated in the particles for a longer time and so will increase the drug loading capacity of the systems[162].

Through the use of solid lipid nanoparticles an occlusive film can be formed on the skin leading to an increase in skin hydration. However, SLNs have a high surfactant content that causes fast penetration in and through the skin. Often there is no depositing effect in the skin layers and thus they are of interest for fast transdermal delivery of actives[163-166]. Wissing *et al.* showed a 31% increase in skin hydration after applying an SLN-enriched cream to skin for four weeks[167]. In a recent study Küchler *et al.* compared dendritic core-multishell (CMS) nanotransporters (20-30 nm) and SLNs (150-170 nm) loaded with Nile red168. They found that SLNs enhanced pig skin penetration 3.8 fold in the *stratum corneum* and 6.3-fold in the epidermis compared with a reference cream. The potential for CMS use is greater since increased penetrations of 8-fold and 13-fold were obtained; these results can be attributed to the smaller size of CMS transporters.

Jenning *et al.* studied intensively *in vitro* penetration with lipid nanoparticles loaded with retinol. They compared the flux of retinol from a lipid particle dispersion with the flux of retinol from an o/w nanoemulsion. The flux of retinol from the nanoemulsion system remained unchanged during 24h but due to increased order and increased expulsion of drug the flux from nanoparticle dispersion increased[169,170].

Lombardi *et al.*[171] studied the skin penetration profiles of SLNs, NLCs and nanoemulsions (NEs) by using the lipophilic dye Nile red as a model agent. Nile red was incorporated into the lipid matrix or the covering tensed shell. The Nile red concentrations were followed by image analysis of vertical sections of pig skin treated with dye-loaded nanoparticular dispersions and an o/w cream. Using SLN dispersions dye penetration increased about fourfold over the uptake using a cream. The use of NLCs was less effective (<3-fold increase) and penetration appeared to be even further reduced when applying NEs. In contrast to previous studies with glucocorticoids attached to the surfaces of SLNs, no targeting effect was detected. Therefore drug targeting appears to be more closely related to the mode

of interaction of drug and particle than to penetration enhancement[171].

Polymeric nanocarriers

Polymeric nanocarriers are prepared from natural or synthetic polymers [172-174]. Natural polymers, such as protein and polysaccharides, gelatin, chitosan, and hyaluronic acid, have not been widely used since they vary in purity and often their preparative processes can lead to drug degradation. The most widely used polymers are synthetic polymers such as polyalkylcyanoacrylates175, poly(lactic acid), poly(glycolic acid) or their copolymers, poly(lactide-co-glycolide)176. The last two mentioned polymers are well known for their biocompatibility and their resorbability through natural pathways. Their degradation and drug release rates can be regulated according to the polymer composition (monomers proportions and linkages)[177,178]. Poly(D,L-lactide-co-glycolide) (PLGA) has been studied for different therapeutic applications such as sustained drug release, in vaccines, and in gene delivery[176,179-181].

Microencapsulation in such polymers has been extensively applied in the field of protein delivery. The major research challenges in protein delivery include the stabilization of proteins in delivery devices and the design of appropriate protein carriers in order to overcome biological barriers. Moreover a long lasting immune response could be induced by such systems. For vaccine delivery the immunogenic components must be efficiently delivered in the appropriate compartments of the immune system and especially in the dendritic cells (DCs). Biodegradable polymers such as PLGA are good candidates because they do not induce a strong or durable immune response against themselves. Moreover they are efficiently degraded into non-toxic metabolites[182]. The most important parameters regarding the immune responses are the size of the particles[183] and their surface properties. Using nucleic acids it has been shown that positively charged particles facilitate association with them and, similarly, with negatively charged protein antigens, *via* ionic cross-linking with the particles.

Particle charge is also an important parameter for enhanced delivery *in vivo*. Kohli *et al.* have reported that efficient permeation on pig skin was obtained with negatively charged particles ranging in size between 50 and 500 nm[184]. Despite these advances there is little information concerning biological interactions between DCs and particulate carrier systems[182].

PLGA microparticles have also been described as vehicles for topical drug delivery of rhodamine and acyclovir, providing a reservoir system for release in the basal epidermis[180,185].

Alvarez-Román *et al.* reported the visualization of skin penetration of nanoparticulate carriers by confocal laser scanning microscopy (CLSM)[186]. In this study, CLSM was used to visualize the distribution of non-biodegradable, fluorescent, polystyrene nanoparticles (diameters 20 and 200 nm) across porcine skin. The surface images revealed that polystyrene nanoparticles and, in particular, the smaller particles, accumulated preferentially in follicular openings, and that this distribution increased in a time-dependent manner. In all cases, the progression of nanoparticules into the skin was impeded by the *stratum corneum*. The accumulation of such particles in the epidermis is of interest in anti-solar studies. Some research has been focused on the skin delivery of UV filters from polymeric nanoparticles because these substances must accumulate on the skin surface and penetrate as little as possible into the viable skin. Alvarez-Román *et al.*[187] reported epidermal targeting of octylmethoxycinnamate (OMC) poly-ε-caprolactone nanoparticles. OMC-loaded nanoparticles resulted in better photoprotection thus promoting a partial protection against erythema. These authors suggested that the extent of crystallinity in a polymer may contribute to reflection and scattering of UV radiation on its own thus leading to partial photoprotection[188,189]. Later, Jimenez *et al.*, who studied the permeation of octylmethoxycinnamate (OMC) from OMC-loaded poly-ε-caprolactone nanoparticles using the Franz cell method in our laboratory, showed quantitatively that the penetration % of OMC in the skin was three to four times lower than from a conventional emulsion and was clearly impeded by the *stratum corneum*, confirming the results of Alvarez-Román *et al.*. Despite the apparent advantages of polymeric nanoparticles compared with other drug delivery systems, they appear to have been comparatively little studied for drug delivery to the skin.

Liposomes and Analogue Vehicles

Liposomes are colloidal carriers formed as concentric biomolecular layers. The most

common ingredient of their membrane composition is phosphatidylcholine although many other potential ingredients have been evaluated190. It was stated earlier that liposomes either penetrate the *stratum corneum* to some extent and then interact with the skin lipids to release their drug or that their components alone enter the *stratum corneum*. The encapsulation of drugs in vesicles has been used in a large number of studies. A variety of encapsulating systems such as liposomes, transfersomes® and ethosomes has been used. Mezei and Gulasekharam were the first to employ liposomes as skin drug delivery systems. They showed that skin delivery of triamcinolone acetonide was four to five times greater from a liposomal lotion than from an ointment containing the same drug concentration191. A series of studies reflected the localising effects of liposomes and highlighted the dependence of 'deposition efficiency" on the lipid composition and method of preparation[192]. For example, Egbaria *et al.*[193] compared conventional liposomal formulations made using phospholipids with liposomes made from "skin lipids", each containing IFN (interferon). The authors found that liposomes increased the IFN deposition in the *stratum corneum* (~46% for "skin lipid liposomes" compared with ~52% for conventional liposomes). No IFN was recovered in the receptor fluid indicating that liposomes provided a localising effect due to improved accumulation in the *stratum corneum*.

Whilst researchers were reporting mainly localised or, rarely, transdermal effects of liposomes, Cevc and Blume[194] claimed that certain types of lipid vesicles (ultradeformable vesicles) can penetrate intact into the deeper layers of the skin and may progress far enough to reach the systemic circulation, but to do so they must be applied under non-occlusive conditions[192].

Transfersomes® (IDEA AG, Munich, Germany) contain 10-25% surfactant (sodium cholate) and 3-10% ethanol. Such compositions confer ultradeformability to the transfersomes® allowing them to squeeze through channels in the *stratum corneum* that are less than one-tenth the diameter of the transfersomes® themselves (up to 500 nm). Cevc *et al.* suggested that the driving force for penetration into the skin is the transdermal gradient caused by the difference in water content between a relatively dehydrated skin surface (approximately 20% water) and an aqueous viable epidermis (close to 100% water)[195-198]. Extraordinary claims have been made for the penetration enhancement ability of transfersomes®, such as skin transport of 50-80% of the applied dose of transfersome®-associated insulin[199].

Ethosomes are liposomes with a high ethanol content. The alcohol fluidizes the ethosomal lipids and *stratum corneum* bilayer lipids thus allowing better penetration[200,201]. Dayan *et al.* have compared the flux of trihexyphenidyl hydrochloride (THP HCl) from THP ethosomes and liposomes. Their results indicated that the flux of THP through nude mouse skin from THP ethosomes was, respectively, 87, 51 and 4.5 times higher than from liposomes, phosphate buffer solution and hydroethanolic solution ($p<0.01$)[202].

Conclusion

The skin, and especially the *stratum corneum*, provides the outermost barrier for topical applications. The study of the *stratum corneum* structure is essential for understanding the barrier function of the skin. Recently there has been much progress in this area as a result of improvement in analytical methods. Further understanding of this barrier and the finding of a general mathematical model are challenges for further research.

At the same time research is taking place on galenic formulations for topical application to skin. This is currently an exciting and fast moving area. There are numerous formulation parameters and formulation systems, which influence percutaneous penetration. In this review the newest examples have been given and discussed. But the effects of these systems on the skin still cannot be completely explained. The study of microemulsions and nanoparticles is an on-going area of research seeking to optimize and explore their effects. Even after thousands of years the development of new strategies guarantees that topical delivery remains an area of considerable interest.

Acknowledgement-

We thank Robin Hillman for his helpful comments and critically reading the manuscript.

The financial support of Gattefossé France is greatly appreciated.

Abbreviation index

α (-)thermodynamic activity of a drug in a formulation
CE cornified envelope
CDs cyclodextrins
CLSM confocal laser scanning microscope
$C_{penetrant}$ (mass.m^{-3}) dissolved mass of the penetrating molecule per cubic metre of solution
D [m^2.s^{-1}] diffusion coefficient
DCs dendritic cells
DMSO dimethyl sulfoxide
EMLA® eutectic mixture of local anaesthetic
FI-DHPE fluorescein-dihydropalmitoylphosphatidylethanolamine
γ [-] effective activity coefficient in the membrane
HCl hydrochloride
IPM isopropyl myristate
ISN isosorbide-5-nitrate
J [mass.m^{-2}.s^{-1}] flux of a compound
J_{ss} flux at steady state
Km [-] partition coefficient of a penetrant
Koct/water [-] octan-1-ol/water partition coefficient of a drug
K_p [m.s^{-1}] permeability coefficient
L [m] length of the diffusion pathway
Mr average molar mass
NEs nanoemulsions
NLCs nanolipid structured carriers
NOAEL no observed adverse effect leve
INPs nanoparticles
OMC octyl methoxycinnamate
PEG polyethane-1,2-diol (polyethylenglycol)
PG polyglycerol
PLGA poly(D,L-lactide-co-glycolide)
SC *stratum corneum*
SLNs solid lipid nanoparticles
TEWL trans epidermal water loss
TG transglutaminase
UV ultraviolet
wt% weight percentage

References

1 Kerscher M, Williams S, Dubertret L. Cosmetic dermatology and skin care. *Eur J Dermatol* 2007; 17: 180-2.
2 Padula C, Nicoli S, Aversa V, Colombo P, Falson F, Pirot F, Santi P. Bioadhesive film for dermal and transdermal drug delivery. *Eur J Dermatol* 2007; 17: 309-12.
3 Auxenfans C, Fradette J, Lequeux C, Germain L, Kinikoglu B, Bechetoille N, Braye F, Auger FA, Damour O. Evolution of three dimensional skin equivalent models reconstructed in vitro by tissue engineering. *Eur J Dermatol* 2008; 1.
4 Attenborough D. Life on earth: A natural history. *Little, Brown* 1979: 319.
5 Windsor T, Burch GE. Rate of insensible perspiration (diffusion of water) locally through living and through dead human skin. *Arch Intern Med* 1944; 74: 428–44.
6 Blank IH. Further observations on factors which influence the water content of the stratum corneum. *J Invest Dermatol* 1953; 21: 259-71.
7 Elias PM, Friend DS. The permeability barrier in mammalian epidermis. *J Cell Biol* 1975; 65: 180-91.
8 Elias PM. Epidermal lipids, barrier function, and desquamation. *J Invest Dermatol* 1983; 80 Suppl: 44s-9s.
9 Gray GM, Yardley HJ. Lipid compositions of cells isolated from pig, human, and rat epidermis. *J Lipid Res* 1975; 16: 434-40.
10 Wilkes GL, Brown IA, Wildnauer RH. The biomechanical properties of skin. *CRC Crit Rev Bioeng* 1973; 1: 453-95.
11 Kalasinsky VF, Johnson FB, Ferwerda R. Fourier transform infrared and raman microspectroscopy of materials in tissue. *Cell Mol Biol (Noisy-le-Grand)* 1998; 44: 141-4.
12 Ponec M, Weerheim A, Lankhorst P, Wertz P. New acylceramide in native and reconstructed epidermis. *J Invest Dermatol* 2003; 120: 581-8.
13 Law S, Wertz P, Swartzendruber DC, Squier CA. Regional variation in content, composition and organization of porcine epithelial barrier lipids revealed by thin-layer chromatography and transmission electron microscopy. *Arch Oral Biol* 1995; 40: 1085-91.
14 Wertz PW, Downing DT. Ceramides of pig epidermis: Structure determination. *J Lipid Res* 1983; 24: 759-65.
15 Long SA, Wertz PW, Strauss JS, Downing DT. Human stratum corneum polar lipids and desquamation. *Arch Dermatol Res* 1985; 277: 284-7.
16 Madison KC, Swartzendruber DC, Wertz PW, Downing DT. Sphingolipid metabolism in organotypic mouse keratinocyte cultures. *J Invest Dermatol* 1990; 95: 657-64.
17 Robson KJ, Stewart ME, Michelsen S, Lazo ND, Downing DT. 6-hydroxy-4-

sphingenine in human epidermal ceramides. *J Lipid Res* 1994; 35: 2060-8.
18 Doering T, Holleran WM, Potratz A, Vielhaber G, Elias PM, Suzuki K, Sandhoff K. Sphingolipid activator proteins are required for epidermal permeability barrier formation. *J Biol Chem* 1999; 274: 11038-45.
19 Stewart ME, Downing DT. A new 6-hydroxy-4-sphingenine-containing ceramide in human skin. *J Lipid Res* 1999; 40: 1434-9.
20 Hamanaka S, Hara M, Nishio H, Otsuka F, Suzuki A, Uchida Y. Human epidermal glucosylceramides are major precursors of stratum corneum ceramides. *J Invest Dermatol* 2002; 119: 416-23.
21 Kessner D, Kiselev M, Dante S, Hauß T, Lersch P, Wartewig S, Neubert R. Arrangement of ceramide [eos] in a stratum corneum lipid model matrix: New aspects revealed by neutron diffraction studies. *Eur Biophys J* 2008; 37: 989-99.
22 Swanbeck G, Thyresson N. A study of the state of aggregation of the lipids in normal and psoriatic horny layer. *Acta Derm Venereol* 1962; 42: 445-7.
23 Swanbeck G, Thyresson N. An x-ray diffraction study of scales from different dermatoses. *Acta Derm Venereol* 1961; 41: 289-96.
24 Breathnach AS. Aspects of epidermal ultrastructure. *J Invest Dermatol* 1975; 65: 2-15.
25 Breathnach AS, Goodman T, Stolinski C, Gross M. Freeze-fracture replication of cells of stratum corneum of human epidermis. *J Anat* 1973; 114: 65-81.
26 Elias PM, McNutt NS, Friend DS. Membrane alterations during cornification of mammalian squamous epithelia: A freeze-fracture, tracer, and thin-section study. *Anat Rec* 1977; 189: 577-94.
27 Guy RH, Hadgraft J. Physicochemical aspects of percutaneous penetration and its enhancement. *Pharm Res* 1988; 5: 753-8.
28 Kalinin AE, Kajava AV, Steinert PM. Epithelial barrier function: Assembly and structural features of the cornified cell envelope. *Bioessays* 2002; 24: 789-800.
29 Singh S, Singh J. Transdermal drug delivery by passive diffusion and iontophoresis: A review. *Med Res Rev* 1993; 13: 569-621.
30 Talreja P, Kleene NK, Pickens WL, Wang TF, Kasting GB. Visualization of the lipid barrier and measurement of lipid pathlength in human stratum corneum. *AAPS PharmSci* 2001; 3: E13.
31 Simonetti O, Hoogstraate AJ, Bialik W, Kempenaar JA, Schrijvers AH, Boddé HE, Ponec M. Visualization of diffusion pathways across the stratum corneum of native and in-vitro-reconstructed epidermis by confocal laser scanning microscopy. *Arch Dermatol Res* 1995; 287: 465-73.
32 Meuwissen ME, Janssen J, Cullander C, Junginger HE, Bouwstra JA. A cross-section device to improve visualization of fluorescent probe penetration into the skin by confocal laser scanning microscopy. *Pharm Res* 1998; 15: 352-6.
33 Berenson GS, Burch GE. Studies of diffusion of water through dead human skin; the effect of different environmental states and of chemical alterations of the epidermis. *Am J Trop Med Hyg* 1951; 31: 842-53.
34 Onken HD, Moyer CA. The water barrier in human epidermis. Physical and chemical nature. *Arch Dermatol* 1963; 87: 584-90.
35 Matoltsy AG, Downes AM, Sweeney TM. Studies of the epidermal water barrier. Ii. Investigation of the chemical nature of the water barrier. *J Invest Dermatol* 1968; 50: 19-26.
36 Sweeney TM, Downing DT. The role of lipids in the epidermal barrier to water diffusion. *J Invest Dermatol* 1970; 55: 135-40.
37 Potts RO, Guy RH. Predicting skin permeability. *Pharm Res* 1992; 9: 663-9.
38 Yamashita F, Hashida M. Mechanistic and empirical modeling of skin permeation of drugs. *Adv Drug Deliv Rev* 2003; 55: 1185-99.
39 Yardley HJ, Summerly R. Lipid composition and metabolism in normal and diseased epidermis. *Pharmacol Ther* 1981; 13: 357-83.
40 Wertz P, van den Bergh B. The physical, chemical and functional properties of lipids in the skin and other biological barriers. *Chem Phys Lipids* 1998; 91: 85-96.
41 Potts RO, Francoeur ML. The influence of stratum corneum morphology on water permeability. *J Invest Dermatol* 1991; 96: 495-9.
42 Swartzendruber DC, Wertz PW, Kitko DJ, Madison KC, Downing DT. Molecular models of the intercellular lipid lamellae in mammalian stratum corneum. *J Invest Dermatol* 1989; 92: 251-7.
43 Swartzendruber DC. Studies of epidermal lipids using electron microscopy. *Semin Dermatol* 1992; 11: 157-61.
44 Israelachvili JN. *Intermolecular and surface forces*. Academic Press 1991: 1-450.
45 De Jager M, Groenink W, i Guivernau BR, Andersson E, Angelova N, Ponec M, Bouwstra JA. A novel in vitro percutaneous penetration model: Evaluation of barrier properties with p-aminobenzoic acid and two of

its derivatives. *Pharm Res* 2006; 23: 951-60.
46 De Jager M, Groenink W, van der Spek J, Janmaat C, Gooris G, Ponec M, Bouwstra JA. Preparation and characterization of a stratum corneum substitute for in vitro percutaneous penetration studies. *Biochim Biophys Acta* 2006; 1758: 636-44.
47 Wertz PW. Lipids and barrier function of the skin. *Acta Derm Venereol Suppl (Stockh)* 2000; 208: 7-11.
48 Bouwstra JA. *Structure of stratum corneum lipid layers and interactions with lipid liposomes*. In: Cosmetic Lipids and the Skin Barrier. New York: Informa Health Care, 2002: 37-73.
49 Forslind B. A domain mosaic model of the skin barrier. *Acta Derm Venereol* 1994; 74: 1-6.
50 Bouwstra JA, Dubbelaar FE, Gooris GS, Ponec M. The lipid organisation in the skin barrier. *Acta Derm Venereol Suppl (Stockh)* 2000; 208: 23-30.
51 Norlén L. Skin barrier structure and function: The single gel phase model. *J Invest Dermatol* 2001; 117: 830-6.
52 Bouwstra JA, Honeywell-Nguyen PL, Gooris GS, Ponec M. Structure of the skin barrier and its modulation by vesicular formulations. *Prog Lipid Res* 2003; 42: 1-36.
53 Izquierdo P, Wiechers J, Escribano E, Garcia-Celma MJ, Tadros T, Esquena J, Dederen J, Solans C. A study on the influence of emulsion droplet size on the skin penetration of tetracaine. *Skin Pharmacol* 2007; 20: 263-70.
54 Laugel C, Rafidison P, Potard G, Aguadisch L, Baillet A. Modulated release of triterpenic compounds from a o/w/o multiple emulsion formulated with dimethicones: Infrared spectrophotometric and differential calorimetric approaches. *J Control Release* 2000; 63: 7-17.
55 Youenang Piemi MP, de Luca M, Grossiord JL. Transdermal delivery of glucose through hairless rat skin in vitro: Effect of multiple and simple emulsions. *Int J Pharm* 1998; 171: 207-15.
56 Lalor CB, Flynn GL, Weiner N. Formulation factors affecting release of drug from topical formulations. 1. Effect of emulsion type upon in vitro delivery of ethyl p-aminobenzoate. *J Pharm Sci* 1994; 83: 1525-8.
57 Laugel C, Baillet A, Ferrier D, Grossiord JL, Marty JP. Incorporation of triterpenic derivatives within an o/w/o multiple emulsion: Structure and release studies. *Int J Cosmet Sci* 1998; 20: 183-91.
58 Ferreira LAM, Doucet J, Seiller M, Grossiord JL. In vitro percutaneous absorption of metronidazole and glucose: Comparison of o/w, w/o/w and w/o systems. *Int J Pharm* 1995; 121: 169-79.
59 El Tayar N, Tsai RS, Testa B, Carrupt PA, Hansch C, Leo A. Percutaneous penetration of drugs: A quantitative structure-permeability relationship study. *J Pharm Sci* 1991; 80: 744-9.
60 Roberts MS, Pugh WJ, Hadgraft J. Epidermal permeability: Penetrant structure relationships. 2. The effect of h-bonding groups in penetrants on their diffusion through the stratum corneum. *Int J Pharm* 1996; 132: 23-32.
61 Marti-Mestres G, Mestres JP, Bres J, Martin S, Ramos J, Vian L. The "In vitro" Percutaneous penetration of three antioxidant compounds. *Int J Pharm* 2007; 331: 139-44.
62 Moss GP, Dearden JC, Patel H, Cronin MT. Quantitative structure-permeability relationships (qsprs) for percutaneous absorption. *Toxicol In Vitro* 2002; 16: 299-317.
63 Vecchia BE, Bunge AL. *Skin absorption databases and predictive equations*. In: Transdermal Drug Delivery. Informa Health Care, 2002: 57-141.
64 Walker JD, Rodford R, Patlewicz G. Quantitative structure-activity relationships for predicting percutaneous absorption rates. *Environ Toxicol Chem* 2003; 22: 1870-84.
65 Fitzpatrick D, Corish J, Hayes B. Modelling skin permeability in risk assessment--the future. *Chemosphere* 2004; 55: 1309-14.
66 Geinoz S, Guy RH, Testa B, Carrupt PA. Quantitative structure-permeation relationships (qspers) to predict skin permeation: A critical evaluation. *Pharm Res* 2004; 21: 83-92.
67 Crank J. *The mathematics of diffusion*. Oxford University Press, 1979: 1-414.
68 Scheuplein RJ, Blank IH. Permeability of the skin. *Physiol Rev* 1971; 51: 702-47.
69 Bolzinger MA, Briançon S, Pelletier J, Fessi H, Chevalier Y. Percutaneous release of caffeine from microemulsion, emulsion and gel dosage forms. *Eur J Pharm Biopharm* 2008; 68: 446-51.
70 Franz TJ. Percutaneous absorption. On the relevance of in vitro data. *J Invest Dermatol* 1975; 64: 190-5.
71 OECD. Skin absorption: In vitro method. *OECD Guideline for the testing of chemicals* 2004: 1-8.
72 Barry BW. *Dermatological Formulations: Percutaneous Absorption.* Informa Health Care, 1983: 1-480.
73 Bunge AL, Cleek RL. A new method for estimating dermal absorption from chemical exposure: 2. Effect of molecular weight and

octanol-water partitioning. *Pharm Res* 1995; 12: 88-95.
74 Bos JD, Meinardi MMHM. The 500 dalton rule for the skin penetration of chemical compounds and drugs. *Exp Dermatol* 2000; 9: 165-9.
75 Hennino A, Marty JP, Nicolas J. Pénétration des allergènes protéiques par voie cutanée. *Rev Fr Allerg Immunol Clin* 2005; 45: 50-3.
76 Boucaud A. Trends in the use of ultrasound-mediated transdermal drug delivery. *Drug Discov Today* 2004; 9: 827-8.
77 Tezel A, Dokka S, Kelly S, Hardee GE, Mitragotri S. Topical delivery of anti-sense oligonucleotides using low-frequency sonophoresis. *Pharm Res* 2004; 21: 2219-25.
78 Cevc G. Lipid vesicles and other colloids as drug carriers on the skin. *Adv Drug Deliv Rev* 2004; 56: 675-711.
79 Barry BW. *Penetration enhancer classification*. In: Smith EW, Maibach HI, Percutaneous Penetration Enhancers. 2nd ed. CRC Press, 2006: 1-16.
80 Prausnitz MR. Microneedles for transdermal drug delivery. *Adv Drug Deliv Rev* 2004; 56: 581-7.
81 Martanto W, Davis SP, Holiday NR, Wang J, Gill HS, Prausnitz MR. Transdermal delivery of insulin using microneedles in vivo. *Pharm Res* 2004; 21: 947-52.
82 Cormier M, Johnson B, Ameri M, Nyam K, Libiran L. Transdermal delivery of desmopressin using a coated microneedle array patch system. *J Control Release* 2004; 97: 503-11.
83 Langkjaer L, Brange J, Grodsky GM, Guy RH. Iontophoresis of monomeric insulin analogues in vitro: Effects of insulin charge and skin pretreatment. *J Control Release* 1998; 51: 47-56.
84 Banga AK, Chien YW. Characterization of in vitro transdermal iontophoretic delivery of insulin. *Drug Dev Ind Pharm* 1993; 19: 2069-87.
85 Chien YW, Siddiqui O, Sun Y, Shi WM, Liu JC. Transdermal iontophoretic delivery of therapeutic peptides/proteins. I: Insulin. *Ann N Y Acad Sci* 1987; 507: 32-51.
86 Pillai O, Borkute SD, Sivaprasad N, Panchagnula R. Transdermal iontophoresis of insulin. Ii. Physicochemical considerations. *Int J Pharm* 2003; 254: 271-80.
87 Pillai O, Panchagnula R. Transdermal iontophoresis of insulin. V. Effect of terpenes. *J Control Release* 2003; 88: 287-96.
88 Pillai O, Kumar N, Dey CS, Borkute, Sivaprasad N, Panchagnula R. Transdermal iontophoresis of insulin: Iii. Influence of electronic parameters. *Methods Find Exp Clin Pharmacol* 2004; 26: 399-408.
89 Kanikkannan N, Singh J, Ramarao P. Transdermal iontophoretic delivery of bovine insulin and monomeric human insulin analogue. *J Control Release* 1999; 59: 99-105.
90 Siddiqui O, Sun Y, Liu JC, Chien YW. Facilitated transdermal transport of insulin. *J Pharm Sci* 1987; 76: 341-5.
91 Kari B. Control of blood glucose levels in alloxan-diabetic rabbits by iontophoresis of insulin. *Diabetes* 1986; 35: 217-21.
92 Benson HA. Transdermal drug delivery: Penetration enhancement techniques. *Curr Drug Deliv* 2005; 2: 23-33.
93 Barry BW. Novel mechanisms and devices to enable successful transdermal drug delivery. *Eur J Pharm Sci* 2001; 14: 101-14.
94 Asbill CS, El-Kattan AF, Michniak BB. Enhancement of transdermal drug delivery: Chemical and physical approaches. *Crit Rev Ther Drug Carrier Syst* 2000; 17: 621-58.
95 Hadgraft J. Passive enhancement strategies in topical and transdermal drug delivery. *Int J Pharm* 1999; 184: 1-6.
96 Walters KA, Hadgraft J. *Skin Penetration Enhancement*. Informa Health Care, 1993: 1-440.
97 Behl CR, Flynn GL, Kurihara T, Harper N, Smith W, Higuchi WI, Ho NF, Pierson CL. Hydration and percutaneous absorption: I. Influence of hydration on alkanol permeation through hairless mouse skin. *J Invest Dermatol* 1980; 75: 346-52.
98 McKenzie AW, Stoughton RB. Methods for comparing percutaneous absorption of steroids. *Arch Dermatol* 1966; 86: 608–10.
99 Scheuplein RJ, Blank IH. Mechanism of percutaneous absorption. Iv. Penetration of nonelectrolytes (alcohols) from aqueous solutions and from pure liquids. *J Invest Dermatol* 1973; 60: 286-96.
100 Agner T, Serup J. Time course of occlusive effects on skin evaluated by measurement of transepidermal water loss (tewl). Including patch tests with sodium lauryl sulphate and water. *Contact Derm* 1993; 28: 6-9.
101 Fluhr JW, Darlenski R, Surber C. Glycerol and the skin: Holistic approach to its origin and functions. *Br J Dermatol* 2008; 159: 23-34.
102 Rawlings AV. Sources and role of stratum corneum hydration. *Skin Barrier* 2006: 399–425.
103 Rawlings AV. Trends in stratum corneum research and the management of dry skin conditions. *Int J Cosmet Sci* 2003; 25: 63-95.

104 Candi E, Schmidt R, Melino G. The cornified envelope: A model of cell death in the skin. *Nat Rev Mol Cell Biol* 2005; 6: 328.
105 Yosipovitch G, Duque MI, Patel TS, Ishiuji Y, Guzman-Sanchez DA, Dawn AG, Freedman BI, Chan YH, Crumrine D, Elias PM. Skin barrier structure and function and their relationship to pruritus in end-stage renal disease. *Nephrol Dial Transplant* 2007; 22: 3268-72.
106 Breternitz M, Kowatzki D, Langenauer M, Elsner P, Fluhr JW. Placebo-controlled, double-blind, randomized, prospective study of a glycerol-based emollient on eczematous skin in atopic dermatitis: Biophysical and clinical evaluation. *Skin Pharmacol Physiol* 2008; 21: 39-45.
107 Hara-Chikuma M, Verkman AS. Aquaporin-3 functions as a glycerol transporter in mammalian skin. *Biol Cell* 2005; 97: 479-86.
108 Chrit L, Bastien P, Sockalingum G, Batisse D, Leroy F, Manfait M, Hadjur C. An in vivo randomized study of human skin moisturization by a new confocal raman fiber-optic microprobe: Assessment of a glycerol-based hydration cream. *Skin Pharmacol Physiol* 2006; 19: 207-15.
109 Barichello J, Yamakawa N, Kisyuku M, Handa H, Shibata T, Ishida T, Kiwada H. Combined effect of liposomalization and addition of glycerol on the transdermal delivery of isosorbide 5-nitrate in rat skin. *Int J Pharm* 2008; 357: 199-205.
110 Yamane MA, Williams AC, Barry BW. Terpene penetration enhancers in propylene glycol/water co-solvent systems: Effectiveness and mechanism of action. *J Pharm Pharmacol* 1995; 47: 978-89.
111 Francoeur ML, Golden GM, Potts RO. Oleic acid: Its effects on stratum corneum in relation to (trans)dermal drug delivery. *Pharm Res* 1990; 7: 621-7.
112 Rehfeld SJ, Plachy WZ, Hou SY, Elias PM. Localization of lipid microdomains and thermal phenomena in murine stratum corneum and isolated membrane complexes: An electron spin resonance study. *J Invest Dermatol* 1990; 95: 217-23.
113 Cornwell PA, Barry BW, Bouwstra JA, Gooris GS. Modes of action of terpene penetration enhancers in human skin; differential scanning calorimetry, small-angle x-ray diffraction and enhancer uptake studies. *Int J Pharm* 1996; 127: 9-26.
114 Ogiso T, Iwaki M, Bechako K, Tsutsumi Y. Enhancement of percutaneous absorption by laurocapram. *J Pharm Sci* 1992; 81: 762-7.
115 Ongpipattanakul B, Burnette RR, Potts RO, Francoeur ML. Evidence that oleic acid exists in a separate phase within stratum corneum lipids. *Pharm Res* 1991; 8: 350-4.
116 Anigbogu ANC, Williams AC, Barry BW, Edwards HGM. Fourier transform raman spectroscopy of interactions between the penetration enhancer dimethyl sulfoxide and human stratum corneum. *Int J Pharm* 1995; 125: 265-82.
117 Bouwstra JA, Peschier LJC, Brussee J, Bodde HE. Effect of n-alkyl-azocycloheptan-2-ones including azone on the thermal behaviour of human stratum corneum. *Int J Pharm* 1989; 52: 47-54.
118 Bouwstra JA, Gooris GS, van der Spek JA, Bras W. Structural investigations of human stratum corneum by small-angle x-ray scattering. *J Invest Dermatol* 1991; 97: 1005-12.
119 Walters KA, Walker M, Olejnik O. Non-ionic surfactant effects on hairless mouse skin permeability characteristics. *J Pharm Pharmacol* 1988; 40: 525-9.
120 Nemanic MK, Elias PM. In situ precipitation: A novel cytochemical technique for visualization of permeability pathways in mammalian stratum corneum. *J Histochem Cytochem* 1980; 28: 573-8.
121 Kim YC, Ludovice PJ, Prausnitz MR. Transdermal delivery enhanced by magainin pore-forming peptide. *J Control Release* 2007; 122: 375-83.
122 Sloan KB, Wasdo S. Designing for topical delivery: Prodrugs can make the difference. *Med Res Rev* 2003; 23: 763-93.
123 Saab AN, Sloan KB, Beall HD, Villaneuva R. Effect of aminomethyl (n-mannich base) derivatization on the ability of s6-acetyloxymethyl-6-mercaptopurine prodrug to deliver 6-mercaptopurine through hairless mouse skin. *J Pharm Sci* 1990; 79: 1099-104.
124 Beall HD, Sloan KB. Topical delivery of 5-fluorouracil (5-fu) by 3-alkylcarbonyl-5-fu prodrugs. *Int J Pharm* 2001; 217: 127-37.
125 Beall HD, Sloan KB. Topical delivery of 5-fluorouracil (5-fu) by 1,3-bisalkylcarbonyl-5-fu prodrugs. *Int J Pharm* 2002; 231: 43-9.
126 Megwa SA, Cross SE, Whitehouse MW, Benson HA, Roberts MS. Effect of ion pairing with alkylamines on the in-vitro dermal penetration and local tissue disposition of salicylates. *J Pharm Pharmacol* 2000; 52: 929-40.
127 Megwa SA, Cross SE, Benson HA, Roberts MS. Ion-pair formation as a strategy to enhance topical delivery of salicylic acid. *J Pharm Pharmacol* 2000; 52: 919-28.

128 Valenta C, Siman U, Kratzel M, Hadgraft J. The dermal delivery of lignocaine: Influence of ion pairing. *Int J Pharm* 2000; 197: 77-85.
129 Sarveiya V, Templeton JF, Benson HA. Ion-pairs of ibuprofen: Increased membrane diffusion. *J Pharm Pharmacol* 2004; 56: 717-24.
130 Ehrenström Reiz GM, Reiz SL. Emla--a eutectic mixture of local anaesthetics for topical anaesthesia. *Acta Anaesthesiol Scand* 1982; 26: 596-8.
131 Stott PW, Williams AC, Barry BW. Transdermal delivery from eutectic systems: Enhanced permeation of a model drug, ibuprofen. *J Control Release* 1998; 50: 297-308.
132 Yong CS, Jung SH, Rhee JD, Choi HG, Lee BJ, Kim DC, Choi YW, Kim CK. Improved solubility and in vitro dissolution of ibuprofen from poloxamer gel using eutectic mixture with menthol. *Drug Deliv* 2003; 10: 179-83.
133 Woolfson AD, Malcolm RK, Campbell K, Jones DS, Russell JA. Rheological, mechanical and membrane penetration properties of novel dual drug systems for percutaneous delivery. *J Control Release* 2000; 67: 395-408.
134 Kang L, Jun HW, McCall JW. Physicochemical studies of lidocaine-menthol binary systems for enhanced membrane transport. *Int J Pharm* 2000; 206: 35-42.
135 Stott PW, Williams AC, Barry BW. Mechanistic study into the enhanced transdermal permeation of a model beta-blocker, propranolol, by fatty acids: A melting point depression effect. *Int J Pharm* 2001; 219: 161-76.
136 Del Valle EMM. Cyclodextrins and their uses: A review. *Process Biochemistry* 2004; 39: 1033-46.
137 Scalia S, Villani S, Scatturin A, Vandelli MA. Complexation of the sunscreen agent, butyl-methoxydibenzoylmethane, with hydroxypropyl-β-cyclodextrin. *Int J Pharm* 1998; 175: 205-13.
138 Scalia S, Villani S, Casolari A. Inclusion complexation of the sunscreen agent 2-ethylhexyl-p-dimethylaminobenzoate with hydroxypropyl-beta-cyclodextrin: Effect on photostability. *J Pharm Pharmacol* 1999; 51: 1367-74.
139 Vollmer U, Müller BW, Peeters J, Mesens J, Wilffert B, Peters T. A study of the percutaneous absorption-enhancing effects of cyclodextrin derivatives in rats. *J Pharm Pharmacol* 1994; 46: 19-22.
140 Legendre JY, Rault I, Petit A, Luijten W. Effects of β-cyclodextrins on skin: Implications for the transdermal delivery of piribedil and a novel cognition enhancing-drug, s-9977. *Eur J Pharm Sci* 1995; 3: 311-22.
141 Loftsson T, Brewster ME. Pharmaceutical applications of cyclodextrins. 1. Drug solubilization and stabilization. *J Pharm Sci* 1996; 85: 1017-25.
142 Simeoni S, Scalia S, Benson HA. Influence of cyclodextrins on in vitro human skin absorption of the sunscreen, butyl-methoxydibenzoylmethane. *Int J Pharm* 2004; 280: 163-71.
143 Williams AC, Shatri SR, Barry BW. Transdermal permeation modulation by cyclodextrins: A mechanistic study. *Pharm Dev Technol* 1998; 3: 283-96.
144 Simeoni S, Scalia S, Tursilli R, Benson H. Influence of cyclodextrin complexation on the in vitro human skin penetration and retention of the sunscreen agent, oxybenzone. *J Incl Phenom Macrocycl Chem* 2006; 54: 275-82.
145 Cal K, Centkowska K. Use of cyclodextrins in topical formulations: Practical aspects. *Eur J Pharm Biopharm* 2008; 68: 467-78.
146 Twist JN, Zatz JL. Characterization of solvent enhanced permeation through a skin model membrane. *J Soc Cosmet Chem* 1988; 39: 324.
147 Twist JN, Zatz JL. Membrane-solvent-solute interaction in a model permeation system. *J Pharm Sci* 1988; 77: 536-40.
148 Moser K, Kriwet K, Kalia YN, Guy RH. Enhanced skin permeation of a lipophilic drug using supersaturated formulations. *J Control Release* 2001; 73: 245-53.
149 Danielsson I, Lindman B. The definition of microemulsion. *Colloids Surf* 1981; 3: 391-2.
150 Kreilgaard M. Influence of microemulsions on cutaneous drug delivery. *Adv Drug Deliv Rev* 2002; 54 Suppl 1: S77-98.
151 Heuschkel S, Goebel A, Neubert RH. Microemulsions--modern colloidal carrier for dermal and transdermal drug delivery. *J Pharm Sci* 2008; 97: 603-31.
152 Kogan A, Garti N. Microemulsions as transdermal drug delivery vehicles. *Adv Colloid Interface Sci* 2006; 123-126: 369-85.
153 Delgado-Charro MB, Iglesias-Vilas G, Blanco-Méndez J, López-Quintela AM, Marty J, Guy RH. Delivery of a hydrophilic solute through the skin from novel microemulsion systems. *Eur J Pharm Biopharm* 1997; 43: 37-42.
154 Kreilgaard M, Pedersen EJ, Jaroszewski JW. Nmr characterisation and transdermal drug delivery potential of microemulsion systems. *J Control Release* 2000; 69: 421-33.
155 Kriwet K, Müller-Goymann CC. Diclofenac release from phospholipid drug

systems and permeation through excised human stratum. *Int J Pharm* 1995; 125: 231–42.
156 Osborne DW, Ward AJ, O'Neill KJ. Microemulsions as topical drug delivery vehicles: In-vitro transdermal studies of a model hydrophilic drug. *J Pharm Pharmacol* 1991; 43: 450-4.
157 Rawat M, Singh D, Saraf S, Saraf S. Nanocarriers: Promising vehicle for bioactive drugs. *Biol Pharm Bull* 2006; 29: 1790-8.
158 Moinard-Chécot D, Chevalier Y, Briançon S, Beney L, Fessi H. Mechanism of nanocapsules formation by the emulsion-diffusion process. *J Colloid Interface Sci* 2008; 317: 458-68.
159 Moinard-Chécot D, Chevalier Y, Briançon S, Fessi H, Guinebretière S. Nanoparticles for drug delivery: Review of the formulation and process difficulties illustrated by the emulsion-diffusion process. *J Nanosci Nanotechnol* 2006; 6: 2664-81.
160 Müller RH, Radtke M, Wissing SA. Solid lipid nanoparticles (sln) and nanostructured lipid carriers (nlc) in cosmetic and dermatological preparations. *Adv Drug Deliv Rev* 2002; 54 Suppl 1: S131-55.
161 Schäfer-Korting M, Mehnert W, Korting HC. Lipid nanoparticles for improved topical application of drugs for skin diseases. *Adv Drug Deliv Rev* 2007; 59: 427-43.
162 Souto EB, Wissing SA, Barbosa CM, Müller RH. Development of a controlled release formulation based on sln and nlc for topical clotrimazole delivery. *Int J Pharm* 2004; 278: 71-7.
163 Santos Maia C, Mehnert W, Schaller M, Korting HC, Gysler A, Haberland A, Schäfer-Korting M. Drug targeting by solid lipid nanoparticles for dermal use. *J Drug Target* 2002; 10: 489-95.
164 Dingler A, Blum RP, Niehus H, Müller RH, Gohla S. Solid lipid nanoparticles (sln/lipopearls)--a pharmaceutical and cosmetic carrier for the application of vitamin e in dermal products. *J Microencapsul* 1999; 16: 751-67.
165 Mei Z, Chen H, Weng T, Yang Y, Yang X. Solid lipid nanoparticle and microemulsion for topical delivery of triptolide. *Eur J Pharm Biopharm* 2003; 56: 189-96.
166 Wissing SA, Müller RH. Solid lipid nanoparticles as carrier for sunscreens: In vitro release and in vivo skin penetration. *J Control Release* 2002; 81: 225-33.
167 Wissing SA, Müller RH. Cosmetic applications for solid lipid nanoparticles (sln). *Int J Pharm* 2003; 254: 65-8.
168 Küchler S, Radowski MR, Blaschke T, Dathe M, Plendl J, Haag R, Schäfer-Korting M, Kramer KD. Nanoparticles for skin penetration enhancement - a comparison of a dendritic core-multishell-nanotransporter and solid lipid nanoparticles. *Eur J Pharm Biopharm* 2008; 18: 289-94.
169 Jenning V, Schäfer-Korting M, Gohla S. Vitamin a-loaded solid lipid nanoparticles for topical use: Drug release properties. *J Control Release* 2000; 66: 115-26.
170 Jenning V, Gohla SH. Encapsulation of retinoids in solid lipid nanoparticles (sln). *J Microencapsul* 2001; 18: 149-58.
171 Lombardi Borgia S, Regehly M, Sivaramakrishnan R, Mehnert W, Korting HC, Danker K, Röder B, Kramer KD, Schäfer-Korting M. Lipid nanoparticles for skin penetration enhancement-correlation to drug localization within the particle matrix as determined by fluorescence and parelectric spectroscopy. *J Control Release* 2005; 110: 151-63.
172 Uhrich KE, Cannizzaro SM, Langer RS, Shakesheff KM. Polymeric systems for controlled drug release. *Chem Rev* 1999; 99: 3181-98.
173 Duncan R. The dawning era of polymer therapeutics. *Nat Rev Drug Discov* 2003; 2: 347-60.
174 Brigger I, Dubernet C, Couvreur P. Nanoparticles in cancer therapy and diagnosis. *Adv Drug Deliv Rev* 2002; 54: 631-51.
175 Vauthier C, Dubernet C, Fattal E, Pinto-Alphandary H, Couvreur P. Poly(alkylcyanoacrylates) as biodegradable materials for biomedical applications. *Adv Drug Deliv Rev* 2003; 55: 519-48.
176 Panyam J, Labhasetwar V. Biodegradable nanoparticles for drug and gene delivery to cells and tissue. *Adv Drug Deliv Rev* 2003; 55: 329-47.
177 Hans ML, Lowman AM. Biodegradable nanoparticles for drug delivery and targeting. *Curr Opin Solid St M* 2002; 4: 319-27.
178 Brannon-Peppas L. Recent advances on the use of biodegradable microparticles and nanoparticles in controlled drug delivery. *Int J Pharm* 1995; 116: 1-9.
179 Yoo HS, Oh JE, Lee KH, Park TG. Biodegradable nanoparticles containing doxorubicin-plga conjugate for sustained release. *Pharm Res* 1999; 16: 1114-8.
180 de Jalón EG, Blanco-Prieto MJ, Ygartua P. Plga microparticles: Possible vehicles for topical drug delivery. *Int J Pharm* 2001; 226: 181-4.
181 Rolland A, Wagner N, Chatelus A,

Shroot B, Schaefer H. Site-specific drug delivery to pilosebaceous structures using polymeric microspheres. *Pharm Res* 1993; 10: 1738-44.
182 McCullough KC, Summerfield A. Targeting the porcine immune system-particulate vaccines in the 21st century. *Dev Comp Immunol* 2008; 33: 394-409.
183 Vila A, Sánchez A, Evora C, Soriano I, McCallion O, Alonso MJ. Pla-peg particles as nasal protein carriers: The influence of the particle size. *Int J Pharm* 2005; 292: 43-52.
184 Kohli AK, Alpar HO. Potential use of nanoparticles for transcutaneous vaccine delivery: Effect of particle size and charge. *Int J Pharm* 2004; 275: 13-7.
185 de Jalón EG, Blanco-Príeto MJ, Ygartua P, Santoyo S. Topical application of acyclovir-loaded microparticles: Quantification of the drug in porcine skin layers. *J Control Release* 2001; 75: 191-7.
186 Alvarez-Román R, Naik A, Kalia YN, Fessi H, Guy RH. Visualization of skin penetration using confocal laser scanning microscopy. *Eur J Pharm Biopharm* 2004; 58: 301-16.
187 Alvarez-Román R, Barré G, Guy RH, Fessi H. Biodegradable polymer nanocapsules containing a sunscreen agent: Preparation and photoprotection. *Eur J Pharm Biopharm* 2001; 52: 191-5.
188 Jiménez MM, Pelletier J, Bobin MF, Martini MC. Influence of encapsulation on the in vitro percutaneous absorption of octyl methoxycinnamate. *Int J Pharm* 2004; 272: 45-55.
189 Alvarez-Román R, Naik A, Kalia YN, Guy RH, Fessi H. Enhancement of topical delivery from biodegradable nanoparticles. *Pharm Res* 2004; 21: 1818-25.
190 Touitou E, Junginger HE, Weiner ND, Nagai T, Mezei M. Liposomes as carriers for topical and transdermal delivery. *J Pharm Sci* 1994; 83: 1189-203.
191 Mezei M, Gulasekharam V. Liposomes--a selective drug delivery system for the topical route of administration. Lotion dosage form. *Life Sci* 1980; 26: 1473-7.
192 El Maghraby GM, Barry BW, Williams AC. Liposomes and skin: From drug delivery to model membranes. *Eur J Pharm Sci* 2008; 34: 203-22.
193 Egbaria K, Ramachandran C, Kittayanond D, Weiner N. Topical delivery of liposomally encapsulated interferon evaluated by in vitro diffusion studies. *Antimicrob Agents Chemother* 1990; 34: 107-10.
194 Cevc G, Blume G. Lipid vesicles penetrate into intact skin owing to the transdermal osmotic gradients and hydration force. *Biochim Biophys Acta* 1992; 1104: 226-32.
195 Blume G, Cevc G, Crommelin MD, Bakker-Woudenberg IA, Kluft C, Storm G. Specific targeting with poly(ethylene glycol)-modified liposomes: Coupling of homing devices to the ends of the polymeric chains combines effective target binding with long circulation times. *Biochim Biophys Acta* 1993; 1149: 180-4.
196 Cevc G, Gebauer D, Stieber J, Schätzlein A, Blume G. Ultraflexible vesicles, transfersomes, have an extremely low pore penetration resistance and transport therapeutic amounts of insulin across the intact mammalian skin. *Biochim Biophys Acta* 1998; 1368: 201-15.
197 Cevc G, Blume G. New, highly efficient formulation of diclofenac for the topical, transdermal administration in ultradeformable drug carriers, transfersomes. *Biochim Biophys Acta* 2001; 1514: 191-205.
198 Cevc G, Blume G. Biological activity and characteristics of triamcinolone-acetonide formulated with the self-regulating drug carriers, transfersomes. *Biochim Biophys Acta* 2003; 1614: 156-64.
199 Cevc G, Schätzlein A, Blume G. Transdermal drug carriers: Basic properties, optimization and transfer efficiency in the case of epicutaneously applied peptides. *J Control Release* 1995; 36: 3-16.
200 Touitou E, Godin B, Dayan N, Weiss C, Piliponsky A, Levi-Schaffer F. Intracellular delivery mediated by an ethosomal carrier. *Biomaterials* 2001; 22: 3053-9.
201 Touitou E, Dayan N, Bergelson L, Godin B, Eliaz M. Ethosomes - novel vesicular carriers for enhanced delivery: Characterization and skin penetration properties. *J Control Release* 2000; 65: 403-18.
202 Dayan N, Touitou E. Carriers for skin delivery of trihexyphenidyl hcl: Ethosomes vs. Liposomes. *Biomaterials* 2000; 21: 1879-85.

Chapitre 2 Application de la microspectroscopie confocale Raman aux études de biopharmacie cutanée

La relation structure cutanée/fonction barrière du *stratum corneum* a été traitée dans le Chapitre 1 et des exemples sur la modification de la pénétration percutanée des actifs cosmétiques et pharmaceutiques par un impact sur la barrière de la peau ou sur le coefficient de partage entre la formulation et la peau ont été donnés. La revue de la littérature montre qu'à ce jour, il n'existe pas beaucoup d'études décrivant conjointement la pénétration percutanée d'une formulation et l'influence potentielle de la formulation sur la barrière cutanée. Ce manque est généralement dû aux limitations des méthodes analytiques. La spectroscopie est une méthode non-invasive basée sur l'absorption infrarouge ou sur la diffusion Raman. La microscopie infrarouge est limitée en résolution spatiale à cause de la longueur d'onde infrarouge élevée et de la faible profondeur de pénétration dans des milieux biologiques. La diffusion Raman permet d'obtenir une résolution spatiale bien meilleure avec des longueurs d'onde d'excitation plus faibles [53].

La microspectroscopie confocale Raman (MCR) est une technique intéressante qui permet d'étudier *in vitro* et *in vivo* des tissus biologiques et des échantillons de peau, grâce à son caractère non invasif. La MCR peut servir dans les études physiologie cutanée pour obtenir des informations sur la composition moléculaire et la structure de la peau, par exemple sa teneur en eau, son humidité relative et les modifications éventuelles de son effet barrière.

Avec cette méthode, il est possible de mesurer la teneur en eau et donc l'hydratation de la peau en utilisant les pics entre 2500 cm^{-1} et 4000 cm^{-1} (Figure 2-1) [54-57].

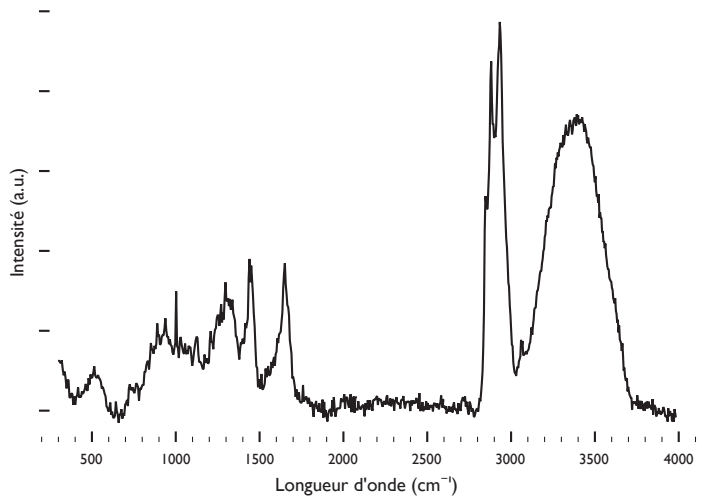

Figure 2-1 : Spectre Raman d'une peau porcine non traitée.

Grâce à la différence du pourcentage d'eau dans le *stratum corneum* (13 %) et l'épiderme viable sous jacent (50 à 70 %), l'épaisseur du *stratum corneum* peut être mesurée indirectement par l'évolution de la concentration en eau selon la profondeur dans la peau (Figure 2-2) [58-61].

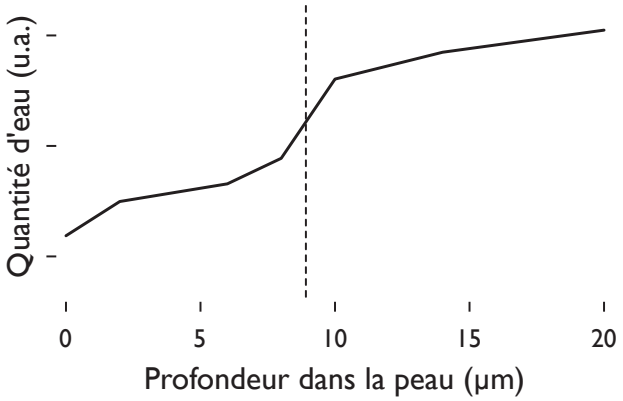

Figure 2-2 : Quantité d'eau endogène en fonction de la profondeur du stratum corneum, indiquant la limite du *stratum corneum* vers 9 µm dans cet exemple.

Des informations sur la composition et la structure de la barrière percutanée peuvent être obtenues par analyses des spectres et plus particulièrement des pics correspondant aux protéines et lipides entre 500-1800 cm^{-1} et 2500-3200 cm^{-1} (Figure 2-1) [62-64].

Le paramètre S_{lat} est utilisé pour caractériser l'organisation des lipides du *stratum corneum*. Ce paramètre a été introduit par Gaber *et al.* [65] et met les intensités des deux pics à 2850 (vibration symétrique de CH_2) et 2880 cm^{-1} (vibration asymétrique de CH_2) en relation.

$$S_{lat} = \frac{(I_{2880} / I_{2850} - 0,7)}{1,5}$$

Equation 2-1 : Paramètre d'interaction latéral après Gaber *et al.* [65]

S_{lat} est un paramètre d'ordre qui exprime le degré d'interaction latérale des lipides, il indique un degré d'organisation des chaines alkyles des lipides. Il est normalisé à 1 pour l'hexadécane solide (état cristallin) et pour l'hexadécane liquide (état liquide). Le pic à 2880 cm^{-1} est sensible aux interactions intra- et interchaînes. L'intensité du pic diminue si le désordre intramoléculaire de la chaine augmente (*trans*-gauche C-C bond isomérisation). 50 % de l'intensité relative de ce pic est influencée par le rotamères *trans*-gauche. Les interactions latérales entre les chaines influencent les 50 % restant de l'intensité du pic à 2880 cm^{-1} et ces variations sont utilisées pour calculer le paramètre S_{lat}.

Avec la MCR il est aussi possible de suivre des actifs dans la peau. Qualitativement, il faut que les substances présentent des pics uniques qui n'interfèrent pas avec ceux de la peau, comme par exemple le rétinol [58,59,66,67] ou la caféine [68,69], le DMSO [70] et le Metronidazole [71]. Si une substance ne montre pas de pic caractéristique dans le spectre, une alternative est de lui substituer un homologue deutéré avec un décalage de pics [72,73]. Les études quantitatives sont plus rares. L'étalonnage ne peut se faire dans la peau qui est trop complexe et doit être remplacée par des milieux modèles. Jusqu'à aujourd'hui, des méthodes étalonnées standardisées pour la peau n'existent pas. Caspers *et al.* utilisent un mélange de protéines pour simuler le milieu protéinique de la peau et quantifier l'eau endogène [74,75].

La MCR permet aujourd'hui d'ouvrir de nouvelles perspectives. Un grand progrès dans l'utilisation de cette technologie permet de plus en plus d'utiliser cette méthode analytique dans des laboratoires non spécialistes.

La publication présente une revue générale sur le niveau de développement de cette technologie et montre comment la diffusion Raman apparaît de plus en plus pour des applications sur la peau. Les principes de la spectroscopie Raman sont présentés. Dans une deuxième partie, des exemples de nouveaux développements d'applications dans la recherche dermatologique *in vivo* et *in vitro* sont donnés. A la fin de la publication, des prévisions sur des développements futurs et, plus concrètement, des détails de l'application de la microscopie Raman en diffusion stimulée sont donnés.

Les faits marquants :

- La microspectroscopie confocale Raman permet d'obtenir des informations sur la structure de la peau et la pénétration des actifs simultanément.
- Pour pouvoir suivre les composants de la formulation, chaque composant doit avoir un pic caractéristique dans le spectre Raman.
- Le paramètre latéral d'interaction est choisi dans un premier temps pour cette thèse comme information sur l'organisation des lipides du *stratum corneum*.

Confocal Raman Microspectroscopy of the skin

Matthias, Förster [1, 2, 3]; Marie-Alexandrine, Bolzinger [2, 3]; Bruno Reynard [4], Stephanie Briançon [2, 3]

1 Gattefossé SAS, St Priest, France

2 Université de Lyon F-69008, Lyon, France; Université Lyon 1, Institut des Sciences Pharmaceutiques et Biologiques, Laboratoire de Dermopharmacie et Cosmétologie, F-69008, Lyon, France;

3 Laboratoire d'Automatique et de Génie des Procédés (LAGEP), UMR CNRS 5007, F-69622, Villeurbanne, France

4 Université de Lyon F 69007, Lyon, France; Université Lyon 1, Laboratoire des Sciences de la Terre UMR 5570 CNRS, ENS de Lyon, Lyon, France

Confocal Raman spectroscopy is a technique with considerable potential for the non-invasive study of biological tissues and skin samples *in vitro* or *in vivo*. It can be used to study skin physiology and possible pathological conditions and to obtain data about molecular composition and structure of skin, for example, water content, moisturization, and changes in the skin barrier function can all be observed. In-depth measurements also allow biopharmaceutical studies, such as analyzing the rate of penetration of a drug and of biochemical changes that may be induced by an applied formulation.

Confocal Raman microspectroscopy is now at such a stage of refinement that it opens up new vistas. The big leap forward in ease of use enables this technology to be used as an analytical method by more and more non-specialist laboratories. This review gives an overview of the state of the art of this technology by presenting an update to the principles of Raman spectroscopy and then looking at examples of new developments *in vivo* and *in vitro* applications.

Key words: Confocal Raman Microspectroscopy, *in vitro*, *in vivo*, Penetration rate, Skin barrier

Introduction

Skin is an inhomogeneous membrane constituting an efficient barrier against the external environment. In the cosmetic field active substances have to reach a skin compartment to exert their effect because the skin is itself the target. In the pharmaceutical field the whole skin is often the main barrier to cross in order to deliver hormones and analgesics to the systemic circulation. Biopharmaceutical studies are necessary to evaluate drug absorption in skin layers and the permeation of drugs through skin. Enhancing drug transport through skin can be achieved by optimal formulation to allow drug availability. Formulation can influence the skin barrier [1] by modifying the *stratum corneum* water content or by modifying the lipid bilayers. Investigation of these skin barrier changes and of drug tracking in the skin requires the use of various analytical methods which should be ideally non-invasive.

To screen drugs or active substances in skin layers non-invasively Fourier transformed infrared spectroscopy (FT-IR) and confocal microscopy can be used. Using confocal microscopy it is possible to follow the penetration of a drug after chemical modification by, for example, tagging the drug with probes such as fluorescent molecules. Such probes can affect the intracellular drug dynamics by modification of the molar mass of the drug and so interfere with the biological activities of the molecules in the sample [2]. In molecular imaging methods employing radiation, such as positron emission tomography and single photon emission computed tomography, spatial resolution is only accurate to the order of a millimetre [3]: thus, microscopic analysis of intracellular drug dynamics is difficult.

In this context, and in contrast, vibrational spectroscopies based on infrared absorption and Raman scattering have been used as label-free methods as a result of the characteristic frequencies associated with specific chemical bonds.

Vibrational techniques have been widely employed in situ to characterize drugs in the pharmaceutical field. However, infrared

microscopy has limited spatial resolution because of its long infrared wavelengths and its low depth of penetration into biological specimens as a result of strong water absorption. Spontaneous Raman scattering overcomes the problems associated with long excitation wavelengths. In pharmaceutical analysis vibrational spectroscopy has been used for several decades. During the 1990s Raman spectroscopy moved out of the shadow of IR spectroscopy as a result of the development of stable diode lasers, fiber-optic sample probes, compact optical designs, high-quantum-efficiency detectors, and personal computers with fast electronics and associated data acquisition and analysis. These advantages provide for real time, multicomponent chemical analysis and allow use of Raman spectroscopy for process monitoring and control. The main areas of application in pharmaceutical analysis are in identification of raw materials; quantitative determination of active substances in different formulations; supporting polymorphic screenings (polymorphs have different solubility rates thereby impacting the effective dosing); and in monitoring the scaling-up of a chemical development process (as process steps are modified and refined to ascertain whether the same form of the same chemical is being produced or not). [4,5].

In dermatological research and in skin science the ability to measure molecular, structural and compositional information of a sample non-destructively is a valuable tool. Raman spectroscopy coupled with confocal microscopy is a new method that is very promising in following drug penetration into the skin in both vivo and *in vitro* skin samples provided that the drug itself is associated with characteristic Raman bands. Confocal Raman microspectroscopy is a new technique based on spontaneous Raman scattering that is now established in pharmaceutical and cosmetical fields allowing the tracking of a drug and in exploring the possibility of skin modification induced by formulation ingredients.

This review explains firstly how Raman scattering arises from the use of skin samples and in the second part details applications in dermatological research. Lastly, this review provides an overview of likely future developments and of the possible advantages and applications of stimulated Raman scattering microscopy.

Theory of Raman spectroscopy

Raman effect

Raman and Krishnan [6] first reported the Raman effect in 1928. When a sample is irradiated with an intense beam of monochromatic radiation (e.g. from a laser) of frequency, most of the radiation is transmitted by the sample. A very small fraction of the incident radiation (1 photon in 10^4) is elastically scattered (Rayleigh scattering). The wavenumber of the Rayleigh scattering is the same as that of the incident radiation ($\omega+\Omega$). In addition, an even smaller quantity (1 photon of 10^8) is scattered inelastically resulting in wavenumbers different from that of the incident radiation (shifted frequency). These photons can be observed, the inelastic scattering being termed Raman scattering. The differences in wavenumber are derived from the excitation of vibrational and rotational levels of the electronic ground state of the molecules. This causes an energy loss of the incident radiation and if the shift is to longer wavelength as compared with the Rayleigh line, it is known as a Stokes shift ($\omega+\Omega->\omega$). When the molecules under consideration are in excited vibrational levels before the interaction with the laser source, anti-Stokes lines can be observed ($\omega->\omega+\Omega$). At room temperature, these anti-Stokes lines are weaker than the Stokes lines (Figure 1).

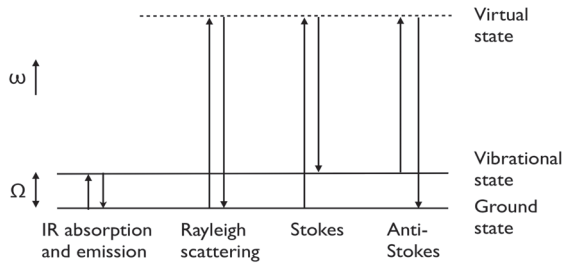

Figure 1: Schematic representation of energy transition in IR and Raman spectroscopy

In a similar way to infrared (IR) spectroscopy, Raman spectroscopy can deliver information about the vibrational and rotational states of molecules and crystals. Both methods are complementary and differ in the interactions of the incident radiation with the compound. The requirement for vibrational activity in Raman spectra is not a change in dipole moment as it is in IR spectra, but a change in the polarizability of the molecule. It is therefore possible to obtain

spectral information from a molecule containing, say, a C=C homonuclear double bond using Raman spectroscopy which is not possible by IR spectroscopy [7].

Vibrational spectra of biological specimens contain a multitude of molecular signatures that can be used for identifying biochemical constituents in tissue. Fourier transform infrared absorption (FT-IR) microscopy is limited by low spatial resolution due to the long wavelength of infrared light and by its low depth of penetration into biological specimens as a result of strong water absorption.

Confocal Raman microspectroscopy can selectively probe any given XYZ-location in a sample with spatial resolution in the micron range. It is best done using dispersive Raman spectroscopy with short wavelengths. In confocal Raman microspectroscopy, laser light from the probe-head is focused onto a diffraction limited spot in the sample by the microscope objective. The backscattered Raman signal is refocused onto a small confocal aperture that acts as a spatial filter, passing the Raman signal excited at the beam waist, but eliminating Raman produced at other points above and below the beam waist. The filtered Raman signal then returns to the spectrometer where it is dispersed onto a CCD (charge couple device) camera to produce a spectrum similar to that shown in Figure 2 for a pig skin sample.

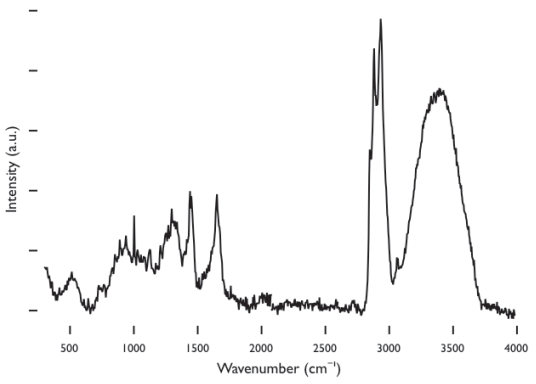

Figure 2: Raman spectra of porcine skin at the surface, baseline corrected

The identification of peaks in the resulting spectra can be complex. In literature there are many listings of Raman frequencies and their assignments [8-11]. The Raman frequency assignments of the major vibrational modes for the *stratum corneum* of mammalian skin are given in Table 1.

Raman frequency (cm^{-1})	Assignment
526	υ(SS)
600	ρ(H)
623	υ(CS)
644	υ(CS); amide 4
746	$\rho(CH_2)$ in phase
827	δ(CCH) aliphatic
850	δ(CCH) aromatic
883	$\rho(CH_2)$; υ(CC); υ(CN)
931	$\rho(CH_3)$ terminal; υ(CC) α-helix
956	$\rho(CH_3)$; δ(CCH) alkenic
1002	υ(CC) aromatic ring
1031	υ(CC) skeletal *cis* conformation
1062	υ(CC) skeletal *trans* conformation
1082	υ(CC) skeletal random conformation
1126	υ(CC) skeletal *trans* conformation
1155	υ(CC); δ(COH)
1172	υ(CC)
1244	$\delta(CH_2)$ wagging; υ(CN) amide 3 disordered
1274	υ(CN) and δ(NH) amide 3 α-helix
1296	$\delta(CH_2)$
1336	not assigned
1385	$\delta(CH_3)$ symmetric
1421	$\delta(CH_3)$
1438	$\delta(CH_2)$ scissoring
1552	δ(NH) and υ(CN) amide 2
1585	υ(C=C) alkenic
1602	not assigned

1652	υ(C=O) amide I α-helix
1743	υ(C=O) amide I lipid
1768	υ(COO)
2723	υ(CH) aliphatic
2852	$\upsilon(CH_2)$ symmetric
2883	$\upsilon(CH_2)$ asymmetric
2931	$\upsilon(CH_3)$ symmetric
2958	$\upsilon(CH_3)$ asymmetric
3060	υ(CH) alkenic
3280	υ(OH) of H_2O

Table 1: Raman assignments of the major vibrational modes for *stratum corneum*. δ = deformation; υ= stretch; ρ = rock

Advantages and limits of CRM

In dermatological research and in skin science the ability to measure molecular, structural and compositional information of a sample non-destructively is a valuable tool and makes Raman spectroscopy combined with a confocal optical system an unusually attractive method for such measurements. The non-invasive character of the method means that after measuring *in vitro* a skin sample, the sample can be used for other analytical tests: a major advantage in *in vivo* studies. Another advantage is the coupling of Raman spectroscopy with a confocal microscope, this enables the possibilities of making an axial screening into the sample in both *in vivo* and *in vitro* studies. These screening steps can be combined with an automatic focus to enable the measurements to be made automatically. To carry out these Raman assays no sample preparation is required which simplifies study design and shortens the time taken to obtain experimental results.

However, confocal Raman microspectroscopy also has some drawbacks, such as the cost of the necessary equipment. A major technical problem for Raman measurements lies in the high level of biological tissue fluorescence overlaying the Raman bands [12]. However, this can be avoided by fitting algorithms in the process of spectra interpretation or by shifting the laser wavelength to NIR (>800 nm) region. But if excitation intensities are too high, they may thermally decompose the sample and so the technique will became destructive and also not suitable for *in vivo* measurements.

Following one special substance in the skin via confocal Raman microspectroscopy demands a characteristic, unique peak in the measured Raman spectra. This point limits the 'normal' confocal Raman microspectroscopy and so not all pharmaceutical substances can be analyzed.

The main sampling difficulties arising from *in vivo* and *in vitro* conditions result from body and skin sample movements, heart beat disturbances and laser heating effects, which all affect the laser focal point as reported by Chrit [10]. However, nowadays the laser heating effects are usually negligible due to the low laser power used at the sample level. Caspers avoided the defocusing interferences due to movements by a window placed between the lens and the sample [13]. Chrit wanted to avoid interference of Raman features generated by the window material itself and to limit refractive index effects induced by an additional interface, which might affect the spatial and namely axial resolution. To avoid large motions and therefore defocusing interferences the measurement device can be stabilized by using an inverted set-up. The part of the body being investigated is pressed against a holder, in which a small hole has been drilled in order to make measurements. This set-up is currently commercialized by River Diagnostics in the model 3510 SCA. Differences in the refractive index between air and skin and, especially, between the different layers of skin, induce a deviation of the light beam; this gives an incorrect estimation of the depth value, a problem which also exists in the inverted setup. This problem has been studied and described by many groups [14-20] and in a study by Xiao *et al.*; using multilayered systems constituted with polymer films with refractive indices close to those of human skin, it was shown that the resulting errors in measurements lead to an underestimation of the depth value by 15–20% [21].

In the applications, which follow, examples of the limits of confocal Raman microspectroscopy and solutions to overcome them are to be considered. It will be shown that CRM can give, at the same time, short and non-invasive measurements which provide information about skin hydration, drug content and skin structure.

Applications

Depending on the strategy chosen, a drug could be formulated to stay on top of the skin, to penetrate into a specific layer or to traverse the skin. In the last case two approaches have been proposed [1]: the first one is a formulation-based enhancement and the second one depends on the modification of the skin barrier using a chemical penetration enhancer and/or lipid disruption/fluidization. Using confocal Raman microspectroscopy numerous analytical studies related to these enhancements have been analyzed for the first time not only *in vivo* but also *in vitro*. Additionally further questions related to these studies such as drug penetration; rate of penetration of topically applied materials; residence time of applied materials in the skin; metabolic or chemical changes that an applied material may undergo once in the skin; biochemical effects that may be induced by the presence of an active compound in the skin and the appearance in the skin of materials delivered to the body, can all be studied. Changes in skin barrier function, swelling of the *stratum corneum* and moisturizing can also be observed. In the first part of the next section biopharmaceutical studies will be detailed and in the second part studies related to the modification of the skin barrier will be presented.

Determination of substances

A number of different substances can be tracked using confocal Raman microspectroscopy. They can be drugs such as caffeine or retinol, or a penetration enhancer such as dimethyl sulphoxide, DMSO, or formulation components such as water. Table 2 gives a summary of such substances together with the wavenumber of the characteristic peak and a reference for each of them.

Substance	Wavenumber (cm^{-1})	Assignment	Source
DMSO	671, 701 130/1048	(CSC) (S=O)	[22]
Caffeine	555, 556	(O=C-N)	[23], [24] own work
Iminosulfuranes	670		[25]
Retinol	1550-1650	(C=C)	[26-29], own work
Metronidazole	1191, 1369	(C=N)	[30]
ODPABA, OMC, OCS, DBM, BZ3	Depending on solvent		[31]
Parsol MCX, 1789, Eusolex 232	1580-1680		[32]
Heavy water	2500	(O-H)	Own work
D-(26)-dodecane	2099	(C-D)	Own work
1-ethyloxycarbonyl-5-fluorouracil and 5-fluorouracil	866 and 637		[33]
DPPC-d_{62} and P-d_{31}OPC, DMPC-d_{54}	2000–2200	(C-D)	[34], [35]

Table 2: Summary of the characteristic Raman wavenumbers of pharmaceutical and cosmetic substances

Active substances

Retinol

Retinol (Vitamin A) is a well-known active that has applications in cosmetic and medical fields. The biological role of retinol and the products of its metabolism have been reviewed by Perlmann [36].

Failloux *et al.* studied topical delivery of retinol *in vitro* using Raman micospectroscopy in conjunction with a Franz cell to measure penetration and diffusion rates [26]. They compared penetration and diffusion of retinol into the epidermis when retinol was introduced in either an oil in water (o/w) emulsion or in

encapsulated form. Both the Franz cell and the Raman experiments showed that retinol is released more slowly from its formulation when in its encapsulated form. In line with this, the Franz cell experiments showed that the residence time of retinol in the skin was increased for an encapsulated formulation. The Raman data showed that retinol in encapsulated form is absorbed more quickly into the skin than is retinol in an oil in water emulsion formulation.

In vivo studies of retinol penetration affected by penetration enhancers were carried out by Mélot *et al.* [27] on volar forearms. They tested four formulations: one of them being trans-retinol in propylene glycol (PG)/ethanol, with PG being a well-known and efficient penetration enhancer. The other three formulations were based on 0.3% *trans*-retinol in caprylic/capric acid triglyceride (MYRITOL 318), a commonly used oil in skin creams, but in two of them a specific penetration enhancer was added. One of the latter contained a lipid extractor, octoxynol-9 (Triton X 100), whereas the other contained a lipid fluidizer, oleic acid. Each solution was applied once to a forearm and measurements were performed up to 6 h after treatment. Remarkable differences in the delivery of *trans*-retinol between formulations with and without penetration enhancer were observed. In addition, the type of penetration enhancer used was also shown to influence delivery. When using oleic acid, a lipid fluidizer, an improved delivery of trans-retinol in the skin could be detected. This result was associated with a phase separation of *stratum corneum* lipids causing a pathway for retinol penetration. This study demonstrated that confocal Raman microspectroscopy could show *in vivo* the efficacy of certain formulations and the influence on drug delivery of ingredients such as penetration enhancers.

Metronidazole

Tfayly *et al.* showed that it was possible to track, *in vitro*, metronidazole, a drug produced by Galderma as a therapeutic agent for rosacea treatment in real time. They used full thickness human skin, obtained from plastic surgery [30] but also compared excised human skin to a reconstructed skin model [37]. After 1 h diffusion, metronidazole, applied as a transcutol solution, was present under the skin surface and was detected down to 20 µm. One hour later, metronidazole was detected, mainly between 14 and 34 µm. Furthermore, confocal Raman microspectroscopy allowed the authors to relate skin penetration results to structural changes in the *stratum corneum*: they showed that lipid organization was altered by the formulation. It should be noted that metronidazole was applied in solution in transcutol, which itself is a well-known penetration enhancer. To complement their study they added a spectral database to index the vibrational peaks and bands of the well-known reconstructed epidermis model, the Episkin®. The authors compared the Episkin model with a natural epidermis and put forward several spectral differences associated with molecular and structural differences between the skin and the reconstructed model.

UV filters

In vitro Raman studies of UV filter compounds used in commercial sun protection formulations have been reported in the literature for some time [31,38]. Beyere *et al.* presented Raman spectra of 5 common sunscreen agents in 10 solvents, providing a useful set of reference spectra: octyl *N,N*-dimethyl-*p*-aminobenzoic acid (ODPABA), octyl *p*-methoxycinnamate (OMC, also know as Parsol MCX®), octyl salicylate (OCS), dibenzoylmethane (DBM) and oxybenzone (BZ3) [31].

Percutaneous absorption of UV filters has been evaluated *in vitro* by classical methods in several formulations [39,40] [41,42]. It is an important issue for safety and efficacy reasons to ensure that UV filters do not penetrate through deeper skin layers and so reach the bloodstream [43]. CRM could allow tracking of the filter through skin without any further development of it as an analytical method being required.

The first real time *in vivo* kinetic measurements of sunscreen active absorption in the *stratum corneum* were presented by van der Pol and Caspers [32]. They applied to a 5x5 cm^2 surface of an inner forearm 5 µL of a standard sunscreen sample (P3: High SPF standard, Bayer Standard C202/101) containing UV-A and B absorbers Parsol MCX, butyl methoxydibenzoylmethane (Parsol 1789) and phenylbenzimidazole sulfonic acid (Eusolex 232). Measurements were made for 5 minutes at 20 s time intervals. The UV blockers were found to penetrate very easily into the *stratum corneum*. After ~1.5 minutes the product could be detected at a depth of 10 micrometers and reached a maximum after

about 3 min; the concentration of the UV blocker then started to decrease, indicating that the product in the sample on the skin surface had been depleted, while axial and/or lateral diffusion continued to move the UV blocker away from the measurement location.

To assess the efficacy of sunscreen products Egawa *et al.* developed a new *in vivo* method using CRM [44,45]. The level of *trans*-urocanic acid was followed in the *stratum corneum* as an indicator of UV exposure as this induces an isomerisation of uronic acid from a *trans*- to a *cis*- conformation. This non-invasive monitoring allows conclusions to be made concerning the efficacy of a sunscreen if the decrease of *trans*-uroanic acid is hindered after formulation application.

Lipid uptake

Although many oils are commonly used in topical formulations, their fates after application have not been extensively studied. Their moisturization potential is also well-known, but quantification of this effect is difficult using classical methods based on skin electrical conductivity due to their lipophilic nature. Raman microspectroscopy provides an alternative method to measure, at the molecular level, lipid uptake and water profile and thus to evaluate lipid penetration and skin occlusion.

Stamaras *et al.* [46] tested *in vivo* the efficacy of paraffin oil (mineral oil) and two vegetable oils (jojoba oil, sweet almond oil) in terms of skin penetration and occlusion on adult and infant skin. Petrolatum was used as a positive control. The paraffin oil and the vegetable oils penetrated the top layers of the *stratum corneum* with similar concentration profiles, a result that was confirmed both for adult and infant skin. The three oils tested demonstrated modest SC swelling (10-20%) compared to moderate swelling (40-60%) for petrolatum. There was no statistical difference between the paraffin oil and vegetable oils in terms of skin penetration and skin occlusion. Finally it was concluded that *in vivo* confocal Raman microspectroscopy is a sensitive and specific enough method, able to measure both lipid uptake and skin occlusion through *stratum corneum* swelling.

Penetration Enhancers

An effective penetration enhancer could exert its action by one or more of a number of different ways: i) it may increase the diffusion coefficient of the drug in the stratum corneum (i.e. disrupt the barrier nature of the stratum corneum); ii) it may act to increase the effective concentration of the drug in the vehicle (for example acting as an anti-solvent); iii) it could affect drug partitioning between the formulation and the stratum corneum (by altering the solvent nature of the skin membrane to favor partitioning into the tissue) or, iv) less likely, by decreasing the skin thickness (by providing a drug permeation 'shortcut' as opposed to a normally more tortuous and so longer pathway).

Many chemical enhancers including Azone, terpenes and DMSO (at concentrations above 50%), have been shown to increase the diffusion coefficient by disordering the lipids in the *stratum corneum* [47-49]. Some enhancers, such as DMSO at concentrations above 40%, propylene glycol and Transcutol, have been found to increase the partitioning of drugs into the skin [9,47,48].

DMSO

The distribution of DMSO, a common penetration enhancer used as a cosolvent in a vehicle [50,51], was monitored *in vivo* in the *stratum corneum* of palmar skin by Caspers at various depths after application of a finite dose. Most of the dose permeated through the *stratum corneum* within 20 min. Surprisingly however, some DMSO remained within the tissue for hours and a small fraction was still detected after 3 days [22]. There was evidence for some interactions between DMSO and water, and probably other skin polar moieties. However the majority of DMSO molecules passed rapidly through the *stratum corneum*. In this study the quantities of DMSO applied were small and there was no evidence of *stratum corneum* component modification.

Iminosulfurances

A novel group of chemical penetration enhancers, the iminosulfuranes, was studied by Song *et al.* on human cadaver skin. The results showed penetration of the enhancer into the *stratum corneum* to a depth of ≈20 µm, with a maximum at 5-10 µm depth from the skin surface. They also showed that the enhancer remained primarily in the *stratum corneum* without significant penetration into the viable epidermis [25] suggesting that it was bound to proteins and/or lipids in the *stratum corneum* as previously observed with DMSO (Casper *et al.*

[22]).

Formulation based penetration enhancement

In a cited review [1] the use of formulation based penetration enhancements via a prodrug and via encapsulation were discussed. Zhang *et al.* [33] overcame the skin barrier by using a prodrug form of an active therapeutic agent to enhance transdermal delivery. They used 1-ethyloxycarbonyl-5-fluorouracil that, once in the epidermis, can be converted to 5-fluorouracil, an important systemic antitumor drug. They used confocal Raman microscopy on intact pigskin biopsies treated with a prodrug, and were able to image the spatial distribution of both prodrug and drug in the SC and viable epidermis, thereby providing information about permeation and metabolism. Although drug and prodrug were chemically quite similar, Raman sensitivity was sufficient to distinguish between their spectra.

Mendelsohn and his group studied the strategy required to improve transport rates into skin by encapsulation of drugs in lipid vesicles using confocal Raman microscopy *in vitro* on pig skin [34,35]. They monitored the permeation of chain perdeuterated 1,2-dimyristoylphosphatidylcholine (DMPC-d_{54}), 1,2-dipalmitoylphosphatidylcholine (DPPC-d_{62}) and 1-palmitoyl-d_{31}, 2-oleoylphosphatidylcholine (P-d_{31}OPC) vesicles into pigskin. The permeation of the gel phase DPPC-d_{62} was limited to approximately 5-15 µm, whereas the liquid-crystalline phase P-d_{31}OPC permeated to substantially greater depths (35-100 µm), at times ranging up to 24 h after application. In addition, the state of the P-d_{31}OPC (intact vesicles or molecularly dispersed with skin constituents) was evaluated from the spatial dependence of the deuteriopalmitate chain conformational order. Upon permeation, the chains became more ordered. The use of deuterated products in these experiments produced Raman bands due to CD stretching vibrations in the 2000-2200 cm^{-1} region, where other Raman bands are sparse. This enabled a clear differentiation between the deuterated exogenous components and intrinsic skin constituents, allowing the penetration process to be mapped. CRM provided, at the same time, data about drug location in the skin; an eventual alteration of skin structure via *stratum corneum* lipid organization and skin protein structure; and, finally, changes in drug and/or vehicle physical state during permeation. Combining these sets of data is helpful in elucidating drug permeation pathways.

Determination of cutaneous physiology

Determination of skin water content and of natural moisturizing factor (NMF)

Skin water content

Water is known to play an important role in *stratum corneum* barrier function. Determination of *stratum corneum* water content can be achieved via several indirect techniques; the most common is *in vivo* measurement of TransEpidermalWaterLoss (TEWL). However TEWL gives a mean value for skin water content with no data about the water concentration profile through skin layers [52]. Using confocal Raman microspectroscopy it is possible to monitor the gradual increase in water concentration with depth penetration in the skin.

To determine water concentration in the skin the use of the spectral region from 2500 to 3800 cm^{-1} is essential [52]. The water content in tissue can be determined from the ratio of Raman intensities of the OH stretch vibration of water at 3390 cm^{-1} and the CH_3 stretch of protein at 2935 cm^{-1} [53-55]. For this the ratio of the integrated intensities of water (3350 – 3550 cm^{-1}) and protein (2910 – 2965 cm^{-1}) must be used in order to maximize the signal-to-noise ratio and avoid overlap of the water signal with the NH vibration of protein at 3329 cm^{-1} [13,56] (Figure 3). Further information about the water concentration in the skin can be received from the deconvolution of the amide I band; this also enhances the hidden vibration of the water bending mode around 1642 cm^{-1} which is assigned to the deformation of the O-H bond of water. The intensity of this band is clearly linked to the hydration of the *stratum corneum* of the anatomical site [10].

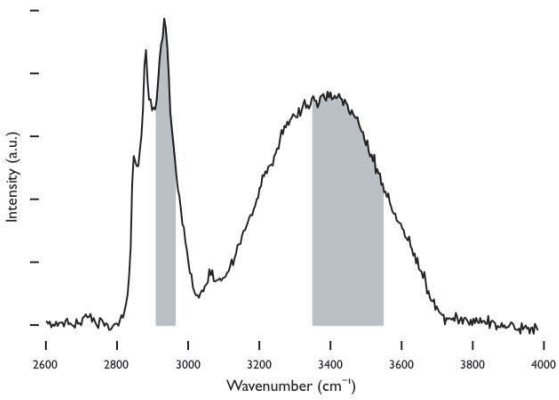

Figure 3: Corrected upper wavenumber portion of the spectral baseline of porcine skin with highlighted OH stretching of water (3390 cm^{-1}) and CH_3 stretch of protein (2935 cm^{-1}) for estimating the water content of the skin.

For quantitative water measurements a calibration is necessary. Caspers *et al.* [13,52] demonstrated a calibration method based on prepared solutions of proteins such as bovine serum albumin, pepsin, lysozyme and urease to replace the keratin of the cells. Recently Wu and Polefka [57] equilibrated extracted (via trypsinization) pigskin *stratum corneum* at different relative humidities (0, 11, 32, 75 and 100 %) and subsequently cut the skins in half. For one half the absolute water concentration in the *stratum corneum* was determined by Karl Fischer's titration method [58] while the other half was analyzed according to the Raman method of Caspers. The correlation proved good with an R^2 of 0.989. For water concentration above 30 mass-% the Raman method was more reliable than the Karl Fischer method.

Natural moisturizing factor (NMF)

Hydration of the *stratum corneum*, which is exposed to a relatively dry environment, is maintained by NMF. NMF is a highly hygroscopic, water-soluble mixture of amino acids, derivatives of amino acids and specific salts which is found exclusively in the *stratum corneum* [59] where it is produced in the lower part by enzymatic degradation of the protein filaggrin [60,61].

Caspers established a semi-quantitative method for measuring NMF via confocal Raman microspectroscopy [13,62]. A set of Raman spectra of the dominant constituents of NMF in solution, pyrrolidone carboxylic acid (PCA), arginine (Arg), ornithine (Orn), citrulline (Cit), serine (Ser), proline (Pro), glycine (Gly), histidine (His) and alanine (Ala), is required [63] [60,64,65]. A spectrum of washed and delipidized skin was also obtained *in vitro* to achieve a semi-quantitative analysis of skin NMF constituents. All of these data were used in monitoring the evolution of *in vivo* skin spectra through *stratum corneum* depth. Comparing the experimental spectra with model data allowed the authors to determine the semi-quantitative concentrations of NMF constituents and the development of these concentrations in the skin. Significant molecular changes were observed in the *stratum corneum* between the surface of the skin and 10 µm depth and especially so for certain sweat constituents (lactate and urea). NMF constituents increased in the *stratum corneum* up to 20 µm, were quite constant between 20 and 50 µm and then decreased sharply to near 0 at 70 µm.

Applications can be found in the measurement of skin moisturizing and NMF content after topical application on a skin surface, in skin hydration/dehydration quantification and evaluation of treatments and also for classifying different skin types and skin ages. Summarized examples are given in Table 3.

Author	Experimental design	Year	Reference
Caspers *et al.*	*In vivo*, moisturizing with wet towels.	2000	[52]
Chrit *et al.*	Studying moisturizing cream containing glycerol *in vivo*.	2006	[66]
Crowther *et al.*	*In vivo* studying of cosmetic moisturizers containing niacinamide on *stratum corneum* thickness.	2008	[67]
Wu and Polefka	Lotion, commercial soap bar, non-	2008	[57]

	emollient shower gel, emollient-containing shower gel *in vitro* on pigskin		
Egawa *et al.*	*In vivo* study of water content depending on skin temperature.	2009	[68]
Nikolovski	Comparing *in vivo* infant and adult skin water penetration and NMF content by applying wet towels.	2008	[69]
Nakagawa	*In vivo* evaluation of ageing by water content in skin.	2009	[70]
Egawa	Age dependency of forearm *stratum corneum* thickness before and after hydration via wet cotton patch.	2007	[71]

Table 3: Summary of skin hydration studies measuring, via confocal Raman microspectroscopy, skin water, NMF content and *stratum corneum* thickness.

Skin moisturizing/hydration

Caspers simply moisturized *in vivo* forearm skin for 45 minutes with a wet bandage, which was covered with Parafilm and observed a dramatic change in the resulting water depth concentration profile: the concentration increase was from 20 to 30 mass-% for untreated skin and 50 mass-% to 60 mass-% after moisturizing [52].

Chrit *et al.* studied *in vivo* the short-term efficacy of a moisturizing cream. They compared an emollient without hydrating agent and a cream containing 3% glycerol. After treatment for one hour they measured a significantly higher water concentration between 0 and 20 µm with the glycerol-based cream [66].

Crowther *et al.* presented an *in vivo* 14-volunteer study of forearm skin in a cumulative treatment over 3 weeks (2 weeks treatment and one week regression) with cosmetic moisturizers. The moisturizing effect was evaluated from three *stratum corneum* properties: thickness, total water content, and water concentration as a function of depth. All water profiles followed a sigmoidal curve, varying from 20-30% at the skin surface to 60-70% at the *stratum corneum* epidermis junction. Changes in the shape of the water profile curves were observed only with one formulation containing nicacinamide and then only after two week of treatment. This difference still remained after one week regression. Total water content was calculated from the area under the water concentration profiles for the entire thickness of the *stratum corneum*. During the treatment the thickness of the *stratum corneum* changed and this was taken into account. Skin hydration confocal Raman microspectroscopy results were compared to classical capacitance measurements (corneometry). The results did not correlate as an increase in corneometer values was observed for all treatments. This was attributed to the presence of glycerol, which has a high dielectric constant, in the formulations [67]. This example shows the limited nature of electrical measurements and increases the interest in confocal Raman microspectroscopy as a more sensitive and depth resolving method.

Wu and Polefka [57] used confocal Raman microspectrocopy on isolated pigskin *stratum corneum* to analyse the water content after several treatments and compared these results with classical Karl Fischer water analysis. They showed that CRM results correlated very well with Karl Fisher titrations. There was also correlation with conductance measurements using a skin surface hygrometer (Skicon®). However, CRM appears to be a more powerful method as a result of its ability to provide in-depth measurements rapidly and non-invasively. CRM has also been used to compare the influence on skin of different skin care/cleansing products: lotion, commercial soap bars, non-emollient shower gel and emollient-containing

shower gel. The results were as expected. The water content on the skin treated with lotion was significantly higher than the non-treated control. Syndet bar-treated skin had a significantly higher water content than soap-based bar-treated sites. Emollient shower gel-treated skin was significantly more hydrated than non-emollient shower gel-treated skin. This study demonstrated the value of CRM in a study of skin moisturization and in the evaluation of the hydration potential of skin care products.

Egawa *et al.* addressed the effects of season and *stratum corneum* temperature on the distribution of water in the skin. They measured *in vivo* the *stratum corneum* water content after applying, externally, water or steam to the forearms of healthy volunteers. Water content in the *stratum corneum* increased with increasing water-application duration. Warming the skin during water application increased the water penetration amount, depth, and water-holding time in the outermost part of the skin (0-8 µm) [45,68]. Furthermore, application of water in the form of steam also increased the water content in the upper parts of the *stratum corneum*. Thanks to confocal Raman microspectroscopy, a correlation could be established between skin water profiles and cutaneous sensations. Increasing water content in the upper parts of the *stratum corneum* was associated with hydration sensations whereas increasing water content in the deeper *stratum corneum* parts corresponded to resilient and water penetration feelings.

Skin water distribution for different skin types

Water holding and water transport properties of infant skin (3-12 months) were compared to adult skin (14-73 years) by Nikolovski [69]. After application of a wet-soaked paper towel for 10 seconds the infant skin showed a rapid increase of 5% to 10% by mass of water in the outer 10 µm of the skin. In contrast no significant exogenous water absorption was found in adult skin. In addition the amounts of NMF constituents were compared and were reported lower for infants.

Nakagawa *et al.* [70] showed that dermal water content could also be measured using CRM. They adjusted the exposure time and the depth increments according to the skin depth to keep a high signal to noise ratio and obtained reliable results. Nakagawa *et al.* concluded that the water content in the dermis may be a useful parameter for evaluation of ageing after comparing the water profiles of an older group (30 subjects, average age: 64 years) and a younger group (30 subjects, average age: 27.8 years) of Japanese volunteers. They observed no differences in water concentration profiles in either the *stratum corneum* or the epidermis. However, the water content in the upper dermis was found significantly lower for the younger group, as had already been reported using ex vivo conditions and other measurement methods [72-74]. Nagawa *et al.* justified these results by arguing that the dermis of the older group was mechanically more worn and therefore contained more damaged areas such as voids, which may become filled with water.

Egawa et al also observed changes in the apparent thicknesses of the *stratum corneum* (SCATs), as the depth where water content reaches an almost constant value, after hydration. The volar forearm skin was hydrated with a wet cotton patch and measurements were done after 15, 50 and 90 minutes of hydration. A swelling of *stratum corneum* was observed with a thickness increase of 4%, 40% and 95% respectively.

Determination of *stratum corneum* thickness

The thickness of the stratum corneum cannot be measured directly by confocal Raman spectroscopy. But it is known [1] that the water content increases from 13 % in the *stratum corneum* to > 50 % in the viable epidermis. The water content can be measured at different depths under the skin surface. By plotting the water content (determined from the ratio of the integrated intensities of water (3350 – 3550 cm^{-1}) to the integrated intensities of protein) (2910 – 2965 cm^{-1}) against the corresponding measured depth, an increase in gradient can be observed (Figure 4). The corresponding depth at which this increase occurs indicates the approximate limit of the *stratum corneum*.

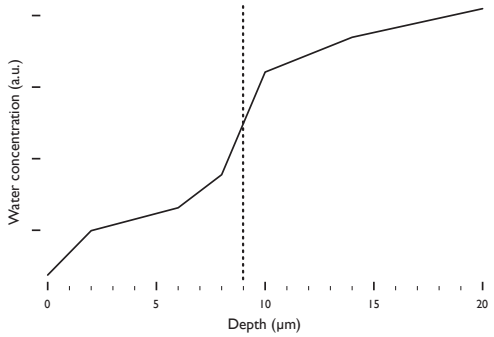

Figure 4: Measured water concentration versus depth. The dotted vertical line indicates the approximate *stratum corneum*-epidermis interface.

A number of groups have published estimates of *stratum corneum* thicknesses, on the basis of confocal Raman measurements and their corresponding water depth concentration profiles some of which were included in the examples given in section 3.2.3 of this review when discussing water distribution. Crowther *et al.* studied water depth concentration profiles at different body sites [67]. They proposed a model of the profiles using a sigmoid-like function (the Weibull function). One of the parameters used in securing the best fit between experimental results and a model is the location of the steepest gradient; this is indicative of the *stratum corneum* thickness (it is not the thickness itself). The *stratum corneum* thicknesses obtained from water profiles were compared with values obtained directly by Optical Coherence Tomography (OCT). A strong correlation was obtained between the thicknesses derived from the two techniques; this validated the use of water concentration profiles from confocal Raman microspectroscopy. Furthermore, confocal Raman microspectroscopy was shown to be significantly more sensitive in measurements of thin *stratum corneum* (under 15 µm). This makes discrimination possible between several anatomic sites all having thin skin (leg, cheek, forearm) in a more successful way than using OCT.

Pudney *et al.* calculated the approximate location of the *stratum corneum* – epidermis boundary from water concentration profiles and from concentration profiles of the component of the natural moisturizing factor (NMF) recorded at the same location [27,28].

Egawa *et al.* arrived at the location of the *stratum corneum* – epidermis boundary by calculating the depth at which the first derivative of the water concentration profile was almost zero and termed this the *stratum corneum* apparent thickness (SCAT) [71]. This SCAT value includes the upper part of the *stratum granulosum* in addition to the *stratum corneum*. It was deduced by Egawa *et al.* from the water concentration profile obtained by CRM, SCAT corresponding to the thickness at which water content reaches a plateau. For forearm samples the SCAT values tended to be higher for older skin but for cheek samples no age dependence was found. This site variation had already been observed by others using both *in vivo* and *in vitro* methods. However if we consider only one particular body site, whatever it is, the absolute values for *stratum corneum* thickness reported in the literature are different according to the measurement method used [75,76].

Van der Pol *et al.* proposed a method for fitting of the water profiles, on the basis of diffusion of water through the *stratum corneum* – epidermis bilayer [77]. The bilayer is thought of as two homogeneous media with two different (but constant) water diffusion coefficients. The water flux is also considered constant. Under these conditions it follows from Fick's first law of diffusion that the water concentration gradients must be linear in both media. The experimental water depth concentration profile is then a simple model with two linear functions (one in the *stratum corneum* and the other in the epidermis). This model is further improved by including an optical point spread function (a Gaussian function with a full width at half maximum of 5 µm), to account for the spatial resolution of the confocal Raman technique. The only variables for this model are therefore the position of the discontinuity at the interface of the *stratum corneum* and the epidermis and the slopes of the water concentration gradients in the two media. The method is now automated and implemented in routine moisturization efficacy studies on human study group subjects [78].

Protein structure

Protein structure can be observed by differences in amide I (1600 to 1700 cm^{-1}) and amide 3 (1240 to 1300 cm^{-1}) regions characteristic of keratin, the major protein of *stratum corneum*, which predominantly adopts an alpha-helical conformation [8]. Alpha helix conformation featured mostly at 1653 cm^{-1}, -sheet conformation at 1666 cm^{-1} and random coil

configuration at 1660 cm^{-1} [79]. Zhang studied the influence of two solvents, DMSO and chloroform/methanol, on the conformations of keratin. These two solvents are commonly used in dermatological research for studies of permeation enhancement and for extracting lipids from *stratum corneum* [80]. They were shown to induce large reversible alterations (alpha-helix to beta-sheet) in the secondary structure of keratin. Further information can be obtained in the region of 730 – 1170 cm^{-1} [8-10,21,81], which also reveals the lamellar organization of lipids as. The bands 1060, 1087, 1125 and 1296 cm^{-1} are characteristic of ceramides (major lipids component of the *stratum corneum*).

Determination of lipid alkyl chain order

The degree of alkyl chain order is given by the lateral interaction parameters S_{lat} and S_{trans} [82]. The 2880 cm^{-1} band is sensitive to intrachain and interchain interactions. The integrated intensity and peak height of the band decrease as intramolecular chain disorder (*trans*-gauche C-C bond isomerization) increases. About 50% of the relative intensity of this band is influenced by *trans*-gauche rotomer content. Lateral packing interactions between chains contributes to the other 50% of the intensity of the 2880 cm^{-1} band. Lesser interactions result in lower intensity. Apart from transitions in crystal packing, there is relatively little change observed in the 2850 cm^{-1} band in lipid transitions. Therefore the peak height ratio I_{2880}/I_{2850} is used to monitor the change in the peak height of the 2880 cm^{-1} band. S_{lat} is a Raman order parameter that was designed to provide a quantitative estimate of the degree of lateral interaction. Thus, it indicates the packing order of the lipidic alkyl chains. This ratio, I_{2880}/I_{2850}, is normalized to 1 for solid hexadecane (crystalline state) and 0 for hexadecane liquid (liquid state). S_{lat} parameter is calculated as follows: $S_{lat} = (I_{2880}/I_{2850} - 0.7)/1.5$ [82].

Bands at 1064 and 1133 cm^{-1} are assigned to the B_{1g} and A_g vibrational modes of all *trans*- chain segments) [83]. When lipids are very ordered, these two *trans* bands are relatively large. When hydrocarbon chains are disordered, the relative intensity of the *trans* bands decreases, and a band near 1080 cm^{-1} due to gauche rotations arises. S_{trans} is a Raman order parameter that can be used to estimate the percentage of *trans* rotomers in a hydrocarbon. S_{trans} is based on the intensity ratio at 1133and 1064cm−1. It is normalized to 1 for solid hexadecane and 0 for hexadecane liquid via $S_{trans} = (I_{1133}/I_{1064})/1.77$. S_{total}, the total order of a sample, is the sum of S_{lat} and S_{trans}.

The determination of lipid alkyl chain order, which is expressed by S_{lat}, can be used to explain the mechanism of penetration enhancement. DMSO and oleic acid, two well-known enhancers induced skin penetration enhancement by a mechanism involving *stratum corneum* lipid fluidization from a gel to a liquid crystalline conformational change in the skin lipids [84 9,85]. Anigbogu *et al.* showed that DMSO penetrated into the SC and altered both the keratin conformation from a-helix to b-sheets and the lipid bilayer from a *trans*-gel to a gauche *trans*- liquid crystalline phase. Furthermore, these transformations were concentration dependent. The keratin conformation was altered even at low DMSO concentrations (20% for example) but lipid changes occurred at higher concentrations (around 70%). This concentration dependence can be related to the penetration enhancement power of DMSO, which is generally only observed at high concentrations. These structural modifications involve an enhancement of skin permeability and therefore of penetration by drugs and actives. This conclusion concerning an enhancement mechanism could lead to improvements in pharmaceutical and cosmetic formulations.

Oshima showed that Raman spectroscopy could be used as a diagnostic tool for the detection of meibomian gland dysfunction by measuring the composition, conformation, and amount of meibum lipid on lid margins when studying meibomian gland dysfunction in samples from patients of 19 years and 80 years [86].

Beattie used confocal Raman microspectroscopy for analyses of vitamin E, its oxidation products, and its metabolites as well as for analyzing pulmonary surfactant (bovine lung extract surfactant) in cells and in fixed lung tissue sections. In addition it could be used for analysing main structural membrane lipids, such as cholesterol, ceramide (Cer[NS] and phosphatidyl-choline (PC), thus accounting for over 50% of the phospholipid fraction [87,88].

Outlook

In Raman microscopy, the skin can be scanned in planar but also in axial directions. Raman spectra are obtained from each measurement position in

a sample, and the distribution of intensity of Raman scattering is used to construct an image of a molecular distribution. In the examples above typical Raman microscopes are used where the laser light is focused onto a sample so as to obtain Raman scattering. In studies involving a formulation topically applied to skin and the effect that it has, it has to be guaranteed that the particular substance for which the Raman specta is being observed is distributed homogeneously in or on the skin in order to produce valid results. For obtaining information from a bigger area than the cross section of the focal spot, the sample area has to be scanned while obtaining the Raman spectra in order to construct Raman images. However, with typical Raman microscopy, it takes several seconds to obtain Raman spectra from each point in the observation area because the efficiency of Raman scattering is low, which makes the observation of living specimens or large surfaces difficult.

Spontaneous Raman scattering microscopy, while having higher spatial resolution than IR spectroscopy due to its shorter excitation wavelengths, is insensitive compared to IR and often has limited imaging speed. Coherent anti-Stokes Raman scattering (CARS) microscopy offers higher sensitivity than spontaneous Raman microscopy [89,90]. However, a CARS spectrum is different from a corresponding spontaneous Raman spectrum as a result of having a non-resonant background, which complicates spectral assignments, causes difficulties in image interpretation, and limits detection sensitivity [91].

Very recently development of stimulated Raman scattering microscopy (SRS) has begun to overcome the challenges posed by the difficulties.

SRS is analogous [92] to the well-known phenomenon of stimulated emission [93] and was fist observed in 1962 [94,95]. Since then it has been used in many spectroscopic studies.

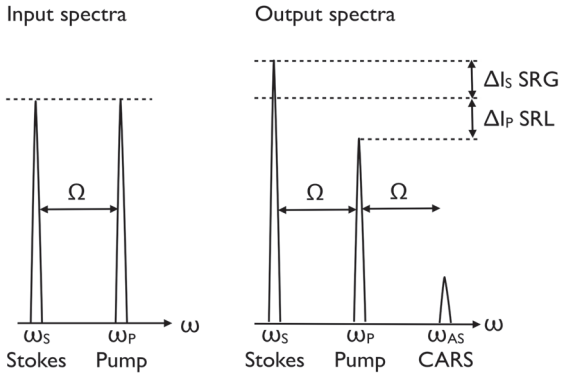

Figure 5: Input and output spectra of SRS. SRS leads to an intensity increase in the Stokes beam (SRG) and an intensity decrease in the pump beam (SRL). Also shown (not to scale) is the CARS signal generated at the anti-Stokes frequency ω_{AS}.

In spontaneous Raman scattering, one laser beam at a frequency ω_P illuminates the sample (called the pump beam) and the signal is generated at the Stokes and anti-Stokes frequencies, ω_S and ω_{AS}, respectively, due to inelastic scattering. SRS requires the spatial and temporal superpositioning of two laser beams (ω_P and ω_S) with a frequency difference ($\Delta\omega=\omega_P-\omega_S$) matching that of a molecular vibration (Ω). When this condition is fulfilled, photons from the pump beam are depleted (stimulated Raman loss ΔI_S) leading to an increase of the number of photons in the Stokes beam (stimulated Raman gain I_P). Detecting this modulation in either beam provides image contrast based on the vibration. But when $\Delta\omega$ does not match any vibrational resonances, SRL and SRG cannot occur. Therefore, unlike CARS, SRL and SRG do not exhibit a non-resonant background Figure 5 [96,97]. Recently demonstrated for biological imaging by Freudiger *et al.* [98] and Nandakumar [99], SRS alleviates some of the key difficulties associated with CARS microscopy and spectroscopy. Firstly, the signal intensity is linear with respect to the intensity of both excitation lasers and also to the concentration of Raman active molecules within the focal volume so allowing simple quantitative analysis. Secondly, there is no non-resonant background and the signal follows the Raman spectrum, increasing the image contrast and removing the distorted line shape present in a CARS spectrum. Finally, the spatial resolution of SRS can be expressed in terms of the point spread function of the imaging system, allowing image deconvolution in a similar manner to fluorescence microscopy [100] and in stark contrast to CARS microscopy [101]. The great potential of SRS for tissue imaging has been described in the paper by Freudiger *et al.* where the authors showed the imaging capabilities of

SRS on fresh mouse tissue with different Raman lines (lipids, DMSO, retinoic acid). The authors also demonstrated the technique's ability to observe the distribution of retinoic acid, a drug used for treating skin disorders, in tissues. First efforts towards *in vivo* spectral imaging have been published by the Feld group on human breast tissue [102]. However as Bégin has reported the SRS technique is not yet sufficiently developed for *in vivo* applications because, currently, it is limited by the lack of availability of sufficiently rapid tunable light sources. As technology evolves further, applications to *in vivo* spectral imaging are likely to become more important [103].

Abbreviations

Ala alanine
Arg arginne
BZ3 oxybenzone
CARS Coherent anti-Stokes Raman scattering
CCD Charge couple device
Cer[NS] Ceramide non-hydroxy fatty acid sphingosin
Cit citrulline
CRM confocal Raman microspectroscopy
DBM dibenzoylmethane
DMPC-d_{54} dipalmitoylphosphatidylcholine
DMSO Dimethyl sulfoxide
DPPC-d_{62} 1,2-dipalmitoylphosphatidylcholine
FT-IR Fourier transform infrared
Gly glycine
His histidine
IR Infrared
NMF natural moisturizing factor
OCS octyl salicylate
OCT Optical Coherence Tomography
ODPABA octyl *N,N*-dimethyl-*p*-aminobenzoic acid
OMC octyl *p*-methoxycinnamate
Orn ornithine
SC stratum corneum
SCAT *stratum corneum* apparent thickness
Ser serine
SRS Spontaneous Raman scattering microscopy
TEWL Trans epidermal water loss
PC phosphatidyl-choline
PCA pyrrolidone carboxylic acid
P-d_{31}OPC 1-palmitoyl-d_{31}, 2-oleoylphosphatidylcholine
PG Propylenglycol
Pro proline

Acknowledgments

We thank Gattefossé SAS for their financial support for this work and Robin Hillman for insightful discussion and editing of the manuscript.

References

1. Förster M, Bolzinger M-A, Fessi H, Briançon S 2009. Topical delivery of cosmetics and drugs. Molecular aspects of percutaneous absorption and delivery. Eur J Dermatol 19(4):309-323.
2. Baker M 2010. Laser tricks without labels. Nat Methods 7(4):261-266.
3. Rudin M, Weissleder R 2003. Molecular imaging in drug discovery and development. Nat Rev Drug Discov 2(2):123-131.
4. Farquharson S, Smith W, Carangelo R 1999. Industrial Raman: providing easy, immediate, cost-effective chemical analysis anywhere. Proc SPIE 14(3859):14-23.
5. Vankeirsbilck T, Vercauteren A, Baeyens W, Van der Weken G, Verpoort F, Vergote G, Remon J 2002. Applications of Raman spectroscopy in pharmaceutical analysis. Trends Analyt Chem 21(12):869-877.
6. Raman C, Krishnan K 1928. A new type of secondary radiation. Nature 121:501-502.
7. Koningstein JA 1971. Introduction to the theory of the Raman effect. Boston, D Reidel Publishing Company 3(3).
8. Barry BW, Edwards H, Williams A 1992. Fourier transform Raman and infrared vibrational study of human skin: assignment of spectral bands. J Raman Spectrosc 23:641-645.
9. Anigbogu A, Williams A, Barry BW, Edwards H 1995. Fourier transform Raman spectroscopy of interactions between the penetration enhancer dimethyl sulfoxide and human stratum corneum. Int J Pharm 125:265-282.
10. Chrit L, Hadjur C, Morel S, Sockalingum G, Lebourdon G, Leroy F, Manfait M 2005. In vivo chemical investigation of human skin using a confocal Raman fiber optic microprobe. J Biomed Opt 10(4):0440071-04400711.
11. Edwards H, Farwell D, Williams A, Barry BW 1993. Raman spectroscopic studies of the skins of the Sahara sand viper, the carpet python and the American black rat snake. Spectrochim Acta 7(49A):913-999.
12. Wartewig S, Neubert RHH 2005. Pharmaceutical applications of Mid-IR and Raman spectroscopy. Adv Drug Deliv Rev 57(8):1144-1170.

13. Caspers PJ, Lucassen GW, Carter EA, Bruining HA, Puppels GJ 2001. In vivo confocal Raman microspectroscopy of the skin: noninvasive determination of molecular concentration profiles. J Invest Dermatol 116(3):434-442.
14. Baldwin K, Batchelder D 2001. Confocal Raman microspectroscopy through a planar interface. Appl Spectrosc 55(5):517-524.
15. Bruneel J, Lassegues J, Sourisseau C 2002. In-depth analyses by confocal Raman microspectrometry: experimental features and modeling of the refraction effects. J Raman Spectrosc 33(10):815-828.
16. Everall N 2004. Depth profiling with confocal Raman microscopy, part II. Spectroscopy 19(11):16-25.
17. Everall N 2004. Depth profining with confocal Raman microscopy, part I. Spectroscopy 19(10):22-27.
18. Everall N 2000. Confocal Raman microscopy: Why the depth resolution and spatial accuracy can be much worse than you think. Appl Spectrosc 54(10):1515-1520.
19. Everall N 2000. Modeling and measuring the effect of refraction on the depth resolution of confocal Raman microscopy. Appl Spectrosc 54(6):773-782.
20. Gotter B, Faubel W, Neubert RHH 2010. FTIR microscopy and confocal Raman microscopy for studying lateral drug diffusion from a semisolid formulation. Eur J Pharm Biopharm 74(74):14-20.
21. Xiao C, Flach CR, Marcott C, Mendelsohn R 2004. Uncertainties in depth determination and comparison of multivariate with univariate analysis in confocal Raman studies of a laminated polymer and skin. Appl Spectrosc 58(4):382-389.
22. Caspers PJ, Williams AC, Carter EA, Edwards HGM, Barry BW, Bruining HA, Puppels GJ 2002. Monitoring the penetration enhancer dimethyl sulfoxide in human stratum corneum in vivo by confocal Raman spectroscopy. Pharm Res 19(10):1577-1580.
23. Baranska M, Proniewicz L 2008. Raman mapping of caffeine alkaloid. Vib Spectrosc (48):153-157.
24. Edwards H, Farwell D, Oliveira L, Alia J 2005. FT-Raman spectroscopic studies of guarana and some extracts. Anal Chim Acta (532):177-186.
25. Song Y, Xiao C, Mendelsohn R, Zheng T, Strekowski L, Michniak B 2005. Investigation of iminosulfuranes as novel transdermal penetration enhancers: enhancement activity and cytotoxicity. Pharm Res 22(11):1918-1925.
26. Failloux N, Baron M-H, Abdul-Malak N, Perrier E 2004. Contribution of encapsulation on the biodisponibility of retinol. Int J Cosmet Sci 26(2):71-77.
27. Mélot M, Pudney PDA, Williamson A-M, Caspers PJ, Van Der Pol A, Puppels GJ 2009. Studying the effectiveness of penetration enhancers to deliver retinol through the stratum cornum by in vivo confocal Raman spectroscopy. J Control Release 138(1):32-39.
28. Pudney PDA, Mélot M, Caspers PJ, Van Der Pol A, Puppels GJ 2007. An in vivo confocal Raman study of the delivery of trans-retinol to the skin. Appl Spectrosc 61(8):804-811.
29. Failloux N, Bonnet I, Perrier E 2004. Effects of light, oxygen and concentration on vitamin A1. J Raman Spectrosc 2(35):140-147.
30. Tfayli A, Piot O, Pitre F, Manfait M 2007. Follow-up of drug permeation through excised human skin with confocal Raman microspectroscopy. Eur Biophys J 36(8):1049-1058.
31. Beyere L, Yarasi S 2003. Solvent effects on sunscreen active ingredients using Raman spectroscopy. J Raman Spectrosc (34):743-750.
32. van der Pol A, Caspers PJ 2006. Penetration of UV blockers monitored in vivo by confocal Raman microspectroscopy. Perspectives in Percutaneous Penetration Conference, la Grande Motte, France (10A):105.
33. Zhang G, Moore DJ, Sloan KB, Flach CR, Mendelsohn R 2007. Imaging the prodrug-to-drug transformation of a 5-fluorouracil derivative in skin by confocal Raman microscopy. J Invest Dermatol 127(5):1205-1209.
34. Xiao C, Moore DJ, Rerek ME, Flach CR, Mendelsohn R 2005. Feasibility of tracking phospholipid permeation into skin using infrared and Raman microscopic imaging. J Invest Dermatol 124(3):622-632.
35. Xiao C, Moore D, Flach C, Mendelsohn R 2005. Permeation of dimyristoylphosphatidylcholine into skin-Structural and spatial information from IR and Raman microscopic imaging. Vib Spectrosc 38(38):151-158.
36. Perlmann T 2002. Retinoid metabolism: a balancing act. Nat Genet 31(1):7-8.
37. Tfayli A, Piot O, Draux F, Pitre F, Manfait M 2007. Molecular characterization of reconstructed skin model by Raman microspectroscopy: comparison with excised human skin. Biopolymers 87(4):261-274.
38. Asher S 1984. Ultraviolet resonance Raman spectrometry for detection and

speciation of trace polycyclic armoatic hydrocarbons. Anal Chem 56(56):720-724.
39. Godwin DA, Kim N-H, Felton LA 2002. Influence of Transcutol CG on the skin accumulation and transdermal permeation of ultraviolet absorbers. Eur J Pharm Biopharm 53(1):23-27.
40. Montenegro L, Paolino D, Puglisi G 2004. Effects of silicone emulsifiers on in vitro skin permeation of sunscreens from cosmetic emulsions. J Cosmet Sci 55(6):509-518.
41. Calderilla-Fajardo SB, Cázares-Delgadillo J, Villalobos-García R, Quintanar-Guerrero D, Ganem-Quintanar A, Robles R 2006. Influence of sucrose esters on the in vivo percutaneous penetration of octyl methoxycinnamate formulated in nanocapsules, nanoemulsion, and emulsion. Drug Dev Ind Pharm 32(1):107-113.
42. Klinubol P, Asawanonda P, Wanichwecharungruang SP 2008. Transdermal penetration of UV filters. Skin Pharmacol Physiol 21(1):23-29.
43. Weiss-Angeli V, Bourgeois S, Pelletier J, Guterres SS, Fessi H, Bolzinger M-A 2010. Development of an original method to study drug release from polymeric nanocapsules in the skin. J Pharm Pharmacol 62(62):35-45.
44. Egawa M, Nomura J, Iwaki H 2010. The evaluation of the amount of cis- and trans-urocanic acid in the stratum corneum by Raman spectroscopy. Photochem Photobiol Sci 9(5):730-733.
45. Egawa M, Iwaki H 2008. In vivo evaluation of the protective capacity of sunscreen by monitoring urocanic acid isomer in the stratum corneum using Raman spectroscopy. Skin Res Technol 14(4):410-417.
46. Stamatas GN, de Sterke J, Hauser M, von Stetten O, van der Pol A 2008. Lipid uptake and skin occlusion following topical application of oils on adult and infant skin. J Dermatol Sci 50(2):135-142.
47. Harrison JE, Watkinson AC, Green DM, Hadgraft J, Brain K 1996. The relative effect of Azone and Transcutol on permeant diffusivity and solubility in human stratum corneum. Pharm Res 13(4):542-546.
48. Hadgraft J 2001. Skin, the final frontier. Int J Pharm 224(1-2):1-18.
49. Moser K, Kriwet K, Naik A, Kalia YN, Guy RH 2001. Passive skin penetration enhancement and its quantification in vitro. Eur J Pharm Biopharm 52(2):103-112.
50. Williams AC, Barry BW 2004. Penetration enhancers. Adv Drug Deliv Rev 56(5):603-618.
51. Songkro S 2009. An overview of skin penetration enhancers: penetration enhancing activity, skin irritation potential and mechanism of action. Songklanakarin J Sci Technol 3(31):299-321.
52. Caspers P, Lucassen G, Bruining H, Puppels G 2000. Automated depth-scanning confocal Raman microspectrometer for rapid in vivo determination of water concentration profiles in human skin. J Raman Spectrosc 31(31):813-818.
53. Huizinga A, Bot AC, de Mul FF, Vrensen GF, Greve J 1989. Local variation in absolute water content of human and rabbit eye lenses measured by Raman microspectroscopy. Exp Eye Res 48(4):487-496.
54. Bauer NJ, Wicksted JP, Jongsma FH, March WF, Hendrikse F, Motamedi M 1998. Noninvasive assessment of the hydration gradient across the cornea using confocal Raman spectroscopy. Invest Ophthalmol Vis Sci 39(5):831-835.
55. Samanta S, Walrafen G 1978. Raman intensities and interactions in aqueous lysozyme solutions. J Chem Phys 68(7):3313-3315.
56. Leikin S, Parsegian VA, Yang W, Walrafen GE 1997. Raman spectral evidence for hydration forces between collagen triple helices. Proc Natl Acad Sci USA 94(21):11312-11317.
57. Wu J, Polefka TG 2008. Confocal Raman microspectroscopy of stratum corneum: a pre-clinical validation study. Int J Cosmet Sci 30(1):47-56.
58. Houston TE, Poore MW 1995. The application of the Karl Fischer oven for the determination of water in consumer products. J Air Waste Mgt Assoc 46(46):990-992.
59. Rawlings AV, Scott IR, Harding CR, Bowser PA 1994. Stratum corneum moisturization at the molecular level. J Invest Dermatol 103(5):731-741.
60. Scott IR, Harding CR, Barrett JG 1982. Histidine-rich protein of the keratohyalin granules. Source of the free amino acids, urocanic acid and pyrrolidone carboxylic acid in the stratum corneum. Biochim Biophys Acta 719(1):110-117.
61. Haydock PV, Dale BA 1990. Filaggrin, an intermediate filament-associated protein: structural and functional implications from the sequence of a cDNA from rat. DNA Cell Biol 9(4):251-261.
62. Caspers PJ, Lucassen GW, Puppels GJ 2003. Combined in vivo confocal Raman spectroscopy and confocal microscopy of human skin. Biophys J 85(1):572-580.

63. Tabachnick J, LaBadie JH 1970. Studies on the biochemistry of epidermis. IV. The free amino acids, ammonia, urea, and pyrrolidone carboxylic acid content of conventional and germ-free albino guina pig epidermia. J Invest Dermatol 54(1):24-31.
64. Pratzel H, Fries P 1977. Modification of relative amount of free amino acids in the stratum corneum of human epidermis by special factors of the environment. I. The influence of UV-irradiation (author's transl). Arch Dermatol Res 259(2):157-160.
65. Koyama J, Horii I, Kawasaki K, Nakayama Y, Morikawa Y, Mitsui T, Kumagai H 1984. Free amino acids of stratum corneum as a biochemical marker to evaluate dry skin. J Soc Cosmet Chem 35(4):183-195.
66. Chrit L, Bastien P, Sockalingum GD, Batisse D, Leroy F, Manfait M, Hadjur C 2006. An in vivo Randomized Study of Human Skin Moisturization by a New Confocal Raman Fiber-Optic Microprobe: Assessment of a Glycerol-Based Hydration Cream. Skin Pharmacol Physiol 19(4):207-215.
67. Crowther JM, Sieg A, Blenkiron P, Marcott C, Matts PJ, Kaczvinsky JR, Rawlings AV 2008. Measuring the effects of topical moisturizers on changes in stratum corneum thickness, water gradients and hydration in vivo. Br J Dermatol 159(3):567-577.
68. Egawa M, Kajikawa T 2009. Changes in the depth profile of water in the stratum corneum treated with water. Skin Res Technol 15(15):242-249.
69. Nikolovski J, Stamatas GN, Kollias N, Wiegand BC 2008. Barrier function and water-holding and transport properties of infant stratum corneum are different from adult and continue to develop through the first year of life. J Invest Dermatol 128(7):1728-1736.
70. Nakagawa N, Matsumoto M, Sakai S 2009. In vivo measurement of the water content in the dermis by confocal Raman spectroscopy. Skin Res Technol 16(2):137-141.
71. Egawa M, Hirao T, Takahashi M 2007. In vivo estimation of stratum corneum thickness from water concentration profiles obtained with Raman spectroscopy. Acta Derm Venereol 87(1):4-8.
72. Kligman AM 1979. Perspectives and problems in cutaneous gerontology. J Invest Dermatol 73(1):39-46.
73. Pearce RH, Grimmer BJ 1972. Age and the chemical constitution of normal human dermis. J Invest Dermatol 58(6):347-361.
74. Gniadecka M, Nielsen OF, Wessel S, Heidenheim M, Christensen DH, Wulf HC 1998. Water and protein structure in photoaged and chronically aged skin. J Invest Dermatol 111(6):1129-1133.
75. Sandby-Møller J, Poulsen T, Wulf HC 2003. Epidermal thickness at different body sites: relationship to age, gender, pigmentation, blood content, skin type and smoking habits. Acta Derm Venereol 83(6):410-413.
76. Huzaira M, Rius F, Rajadhyaksha M, Anderson RR, González S 2001. Topographic variations in normal skin, as viewed by in vivo reflectance confocal microscopy. J Invest Dermatol 116(6):846-852.
77. van der Pol A, de Sterke J, Caspers PJ 2007. Modeling and interpretation of water concentration gradients in the stratum corneum as measured by confocal Raman microspectroscopy. Int J Cosmet Sci 3(29):235.
78. Bielfeldt S, Schoder V, Ely U, van der Pol A 2009. Assessment of Human Stratum Corneum Thickness and its Barrier Properties by In-Vivo Confocal Raman Spectroscopy. IFSCC Magazine 1(12):9-15.
79. Williams A, Edwards H 1994. Raman Spectra of Human Keratotic Biopolymers; Skin, Callus, Hair and Nail. J Raman Spectrosc 25(1):95-98.
80. Zhang G, Moore DJ, Flach CR, Mendelsohn R 2007. Vibrational microscopy and imaging of skin: from single cells to intact tissue. Anal Bioanal Chem 387(5):1591-1599.
81. Rodríguez-Casado A, Moore SD, Prevelige PE, Thomas GJ 2001. Structure of bacteriophage P22 portal protein in relation to assembly: investigation by Raman spectroscopy. Biochemistry 40(45):13583-13591.
82. Gaber BP, Peticolas WL 1977. On the quantitative interpretation of biomembrane structure by Raman spectroscopy. Biochim Biophys Acta 465(2):260-274.
83. Pilgram GS, Van Pelt AM, Spies F, Bouwstra JA, Koerten HK 1998. Cryo-electron diffraction as a tool to study local variations in the lipid organization of human stratum corneum. J Microsc 189(Pt 1):71-78.
84. Naik A, Pechtold L, Potts R, Guy R 1995. Mechanism of oleic acid-induced skin penetration enhancement in vivo in humans. J Control Release 37:299-306.
85. Kwak S, Lafleur M 2009. Effect of dimethyl sulfoxide on the phase behavior of model stratum corneum lipid mixtures. Chem Phys Lipids 161(1):11-21.
86. Oshima Y, Sato H, Zaghloul A, Foulks GN, Yappert MC, Borchman D 2009.

Characterization of human meibum lipid using raman spectroscopy. Curr Eye Res 34(10):824-835.
87. Beattie JR, Schock BC 2009. Identifying the spatial distribution of vitamin E, pulmonary surfactant and membrane lipids in cells and tissue by confocal Raman microscopy. Methods Mol Biol 579:513-535.
88. Beattie JR, Maguire C, Gilchrist S, Barrett LJ, Cross CE, Possmayer F, Ennis M, Elborn JS, Curry WJ, McGarvey JJ, Schock BC 2007. The use of Raman microscopy to determine and localize vitamin E in biological samples. FASEB J 21(3):766-776.
89. Evans C, Xie X 2008. Coherent anti-Stokes Raman scattering microscopy: chemical imaging for biology and medicine. Annual Reviews 1:883-909.
90. Zumbusch A, Holtom G, Xie X 1999. Three-dimensional vibrational imaging by coherent anti-Stokes Raman scattering. Phys Rev Lett 82(20):4142-4145.
91. Ozeki Y, Dake F, Kajiyama Si, Fukui K, Itoh K 2009. Analysis and experimental assessment of the sensitivity of stimulated Raman scattering microscopy. Opt Express 17(5):3651-3658.
92. Bloembergen N 1967. The stimulated Raman effect. Am J Phys 35(11):989-1023.
93. Einstein A 1917. On the quantum theory of radiation. Phys Z 18:121-128.
94. Woodbury EJ, Ng WK 1962. Ruby laser operation in the near IR. Proc Ire 50(11):2367.
95. Eckhardt G, Hellwarth R, McClung F, Schwarz S, Weiner D 1962. Stimulated Raman scattering from organic liquids. Phys Rev Lett 9(11):455-457.
96. Levenson M 1984. Introduction to nonlinear laser spectroscopy. J Opt Soc Am B 1(3):409-410.
97. Gratton E, Digman M 2009. One photon up, one photon down. Nat Biotechnol 27(2):147-148.
98. Freudiger CW, Min W, Saar BG, Lu S, Holtom GR, He C, Tsai JC, Kang JX, Xie XS 2008. Label-free biomedical imaging with high sensitivity by stimulated Raman scattering microscopy. Science 322(5909):1857-1861.
99. Nandakumar P, Kovalev A, Volkmer A 2009. Vibrational imaging based on stimulated Raman scattering microscopy. New J Phys 11(11):1-9.
100. Potma E, de Boeij W 2000. Nonlinear coherent four-wave mixing in optical microscopy. J Opt Soc Am 17(10):1678-1684.
101. Hagmar J, Brackmann C, Gustavsson T, Enejder A 2008. Image analysis in nonlinear microscopy. J Opt Soc Am A Opt Image Sci Vis 25(9):2195-2206.
102. Shafer-Peltier K, Haka A 2002. Raman microspectroscopic model of human breast tissue: implications for breast cancer diagnosis in vivo. J Raman Spectrosc 33:552-563.
103. Bégin S, Bélanger E, Laffray S, Vallée R, Côté D 2009. In vivo optical monitoring of tissue pathologies and diseases with vibrational contrast. J Biophotonics 2(11):632-642.

Partie B Expérimentale

Introduction

Après l'étude détaillée de la bibliographie, le but de cette thèse est de développer des méthodes pour pouvoir étudier la pénétration percutanée quantitativement et qualitativement et expliquer l'impact d'une formulation sur la pénétration percutanée. Ces méthodes sont :

- La méthode de diffusion en cellules à flux continu pour étudier les profils de diffusion de la caféine à travers la peau au cours du temps sans perturber le système.

- La méthode de cellule de diffusion statique associée à une technique de séparation des assises cutanées afin d'établir la distribution du rétinol dans les couches cutanées.

- La MCR sur explants de peaux en collaboration avec le Laboratoire des Sciences de la terre (UMR CNRS 5570, Université Lyon 1, ENS).

Les actifs choisis pour cette thèse sont la caféine, un actif hydrophile, et le rétinol, un actif lipophile. Pour pouvoir étudier la pénétration et la perméation de ces deux actifs, la cellule de Franz est utilisée. La polarité des deux actifs caractérisée par leur logP respectif explique que la caféine (logP=-0,07) traverse toute la peau et s'accumule dans le liquide récepteur avec un pourcentage inférieur à 5 % de la dose appliquée dans les couches cutanées (calculer depuis nos publis) contrairement au rétinol (logP=7,62) qui s'accumule dans l'épiderme et derme [76,77].

Dans un premier temps, une méthode analytique en flux continu a été mise au point pour pouvoir observer la cinétique de diffusion de la caféine depuis le compartiment donneur de la cellule à flux continu dans le liquide récepteur mimant le compartiment sanguin.

Dans un deuxième temps; une méthode plus précise que celle de tape stripping a due être développée pour séparer le *stratum corneum* de l'épiderme et derme. En raison des faibles

différences attendues pour la pénétration du rétinol dans les couches cutanées en fonction de la formulation, une quantification précise du rétinol dans le *stratum corneum*, compartiment lipophile où il s'accumule, était nécessaire.

Enfin, la microspectroscopie Raman a été mise en place pour utiliser sa capacité à évaluer :

- L'homogénéité de l'explant cutané une fois le *stratum corneum* éliminé, homogénéité appréciée par la teneur en eau de l'explant.
- Le suivi du rétinol et des ingrédients de la formule dans la peau. La faisabilité de la méthode a été appréciée avec une formulation modèle contenant des ingrédients « modèles », l'huile de dodécane deuterée et de l'eau deuterée , pour ensuite s'approcher des formulations cosmétiques avec des huiles classiques telles que le butylene glycol cocoate, l'octyldodecyl myristate et l'huile de paraffine.
- La modification de l'organisation des lipides cutanés, apprécié par le paramètre S_{lat}.

Le chapitre 3 décrit les méthodes mises au point et les chapitres 4 à 6 les principaux résultats obtenus.

Chapitre 3 Méthodologie

Dans ce chapitre la mise au point des expériences est décrite afin d'expliquer le cheminement qui a conduit aux choix des formulations étudiées, à leur procédés de fabrication et aux contrôles effectués afin de les retenir pour les études de pénétration ou non.

3.1 La pénétration cutanée : aspects méthodologiques

3.1.1 La méthode statique

Cette méthode a été appliquée pour l'ensemble des formulations contenant du rétinol.

La peau sépare les deux compartiments de la cellule de Franz [78]. La formulation est appliquée sur le *stratum corneum* sur la peau au niveau du compartiment donneur de la cellule. Le compartiment dermique fait face au liquide récepteur placé dans le compartiment inférieur encore appelé, compartiment receveur (Figure 1-3).

La peau de porc dans les cellules de Franz utilisées pendant la thèse a une surface de 2,54 cm^2. Le liquide récepteur utilisé est un tampon phosphate (PBS 0,01 M pH=7,2) (Sigma). Ce liquide est sous agitation magnétique. Les cellules sont posées dans un bain marie à 37°C pour maintenir la température de la peau dans les cellules à 32 ± 1°C [79].

Après une séparation des différentes couches de la peau (*stratum corneum*, épiderme et derme) le rétinol est extrait avec du méthanol contenant 0,5 % de α-tocopherol acétate à 100 % après deux extractions itératives.

La quantité de rétinol dans chaque couche est mésurée par CLHP. Pour pouvoir faire un bilan massique total de la pénétration percutanée, la formulation restante sur la peau a été injectée de même dans la CLHP et donc quantitfiée. La quantité de rétinol dans ce dépôt restant (proche à 100% de la masse appliquée) est très grande par rapport à la quantité de rétinol penetrée. Ce grand rapport, ajouté aux contraintes pratiques liées au procédé de dilution (vaporization du solvent) provoque une erreur dans la quantité de rétinol. Cela peut donner un

bilan massique de rétinol supérieur à 100%. Pour évaluer la pénétration des formulations, les quantités de rétinol dans les differents couches de la peau sont déterminées. En maintenant contantes les procédures de manipulations et les limites statistiques de signification de $p \leq 0,05$, les comparaisons sont justifiées et correctes.

Les échantillons ont été analysés par chromatographie liquide avec une colonne reverse. Le CLHP de Waters (St Quentin en Yvelines, France) est composé d'un injecteur Waters 717, d'une pompe Waters 600 pompe, d'une colonne en phase inverse XTerra®MS C18 (3,9 mm × 150 mm, 5 µm) et d'une photodiode Array Waters 2996. Le détecteur UV travaille à 325 nm longueur d'onde. La phase mobile est un mélange méthanol/eau (85:15) avec un débit de 1 ml/min et 25°C qui donne une temps de rétention de 8,8 min pour le rétinol. Le volume d'injection est 20 µl. La courbe de calibration pour les analyses quantitatives est linéaire jusqu'à 84,73 µg/g et la limite de détection pour rétinol est de 491 pg.

Pour mesurer la cinétique de pénétration, plusieurs méthodes ont été envisagées. Dans un premier temps, une analyse par prélèvement du liquide récepteur à intervalles de temps réguliers et un dosage de la concentration de l'actif par HPLC ont été envisagés. L'inconvénient de cette méthode est que les prélèvements réguliers interrompus durant la nuit peuvent perturber le phénomène de diffusion et engendrer des erreurs.

3.1.2 La méthode dynamique à flux continu

Pour ce travail, un système en flux continu a été installé. Les cellules dynamiques se caractérisent par un renouvellement ininterrompu de la phase réceptrice dans le compartiment receveur. Ainsi grâce à l'utilisation d'une pompe, les opérations de remplissage et de dosage sont effectuées automatiquement et en continu. Ce type de cellule simule mieux l'effet de la circulation sanguine [80]. Le système fonctionne en « circuit fermé » c'est-à-dire que le prélèvement du liquide récepteur, une fois la mesure faite, est redirigé vers ce même milieu récepteur. Une épure du système est illustrée Figure 3-1. Plusieurs auteurs ont montré l'intérêt de cette cellule dynamique qui mime de façon plus précise la perfusion du système

capillaire cutané. Cependant les flux d'actifs peuvent varier fortement en fonction de certains paramètres de la méthode. A titre d'exemple, le débit du liquide récepteur peut influer sur le flux d'actif. Un débit minimal est nécessaire pour assurer un mélange efficace mais il doit être contrôlé pour une bonne reproductibilité de la méthode. Ainsi Crutcher *et al.* [81] mais aussi Bronaugh *et al.* [80] ont observé des variations des flux en fonction du débit appliqué. Généralement les flux augmentent avec l'augmentation du débit de liquide récepteur ainsi que Córdoba-Diaz *et al.* [82] l'ont observé avec le kétoprofène.

Ainsi nous allons détailler les choix méthodologiques pris dans ce travail.

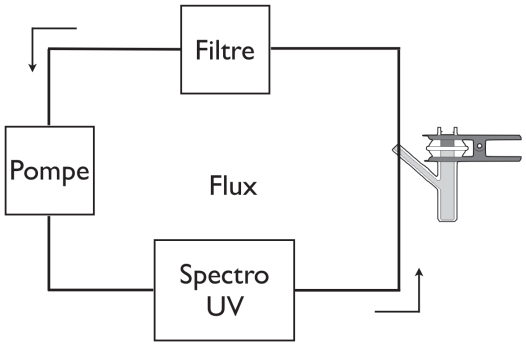

Figure 3-1: Système à flux continu avec méthode de dosage en spectrophotométrie UV

Le spectrophotomètre utilisé est fourni par Shimadzu, il s'agit du modèle UV-1800 qui permet de mesurer 6 cuvettes en même temps et garantit une application de la loi de Beer-Lambert jusqu'à une absorbance de 3,5 [83]. Pour la caféine l'absorption est mesurée tous les 15 min à la longueur d'onde de 271 nm. La vitesse, avec laquelle le liquide récepteur est pompé dans la cuvette, est paramétrée de telle sorte que le volume de la cuvette soit renouvelé toutes les 15 minutes.

Les cuvettes spécifiques pour travailler en flux continu sont fournies par Hellma avec une longueur de chemin optique de 0,2 cm (170-QS). Cette longueur de chemin optique a été choisie afin de garantir que la saturation du détecteur UV n'est jamais atteinte même en fin d'expérience (24 h) quand la concentration du liquide récepteur est la plus élevée.

Dependant de la formulation, 1 g (solution pure et tensioactive) et 0,7 g d'émulsions sont appliqués sur la peau. Cette différence est liée au fait que les formulations ont une faible viscosité et donc peuvent être appliquées sur la peau par une pipette. Le volume appliqué est fixé à 1 mL et donc, avec les différence de densité entre les solutions tensioactives et les émulsions, la masse est différente. Le volume a été fixé constant pour permettre de garantir les mêmes conditions infinies dans toutes les mesures et donc pouvoir négliger la vaporisation de solvant dans le chambre de donneur qui est maintenu à un minimum avec le couvercle de la chambre fermé.

Le volume de liquide récepteur est fixé à 11 mL. En considérant que 100 % de la caféine appliquée pénètre dans le liquide récepteur (soit maximum 15 mg car 1 g de solution aqueuse de caféine à 1,5% en caféine a été appliquée), ce volume, correspondant à une dilution de 15 par rapport à la saturation de la caféine (2,2%), permet de garantir les conditions « sink ». La pompe tourne à une vitesse de 10 tours par minute (environ 0,07 mL/min), ce qui garantit que le volume dans les cuvettes (240 µl) est renouvelé toutes les 15 minutes.

Des essais préliminaires ont montré qu'il faut utiliser un système de pré-filtre (acétate de cellulose) (1,2 µm) suivi d'un filtre 0,2 µm. Ces pré-filtres sont nécessaires pour éviter un phénomène de diffusion lié à la présence de particule ou fragments de peau dans les cuvettes et générant une absorbance non nulle pour les solutions de blanc comme montré dans le Tableau 3-1.

Avec cette méthode, des informations sur la vitesse et la quantité de l'actif qui traverse la peau sont collectées. En plus, les paramètres de la pénétration (temps de latence, flux stationnaire et perméabilité) peuvent être déterminés. Par contre, la quantité d'actif stockée dans la peau reste inconnue, quantité qui peut être cependant mesurée par ailleurs en séparant les différentes couches cutanées en fin d'expérience. Cette technique ne permet pas

non plus d'étudier les mécanismes de passage et les modifications éventuelles de la barrière cutanée, seule la quantité permée est prise en compte.

Pour une mesure quantitative, une courbe d'étalonnage entre 0 µg/ml et 411,4 µg/mL avec 11 points a été établie. L'équation de la droite est y=0,009x+0,0362 avec un R^2 de ~0,999 (Figure 3-2).

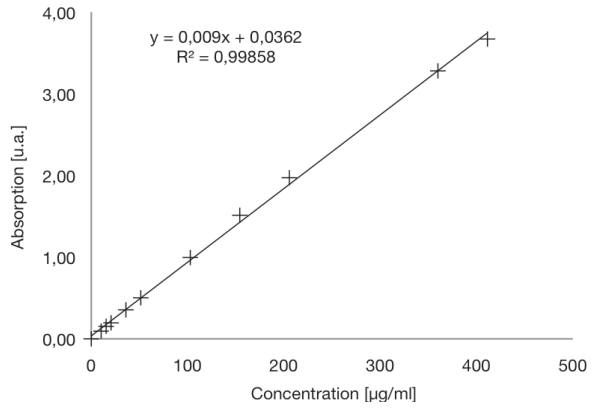

Figure 3-2: Courbe étalonnage caféine en spectrophotométrie UV

Afin de valider notre méthode de dosage analytique, la caféine a été dosée dans les liquides récepteurs à la fin de l'essai par HPLC (avec détection UV). Les résultats sont rassemblés dans le Tableau 3-1. On peut voir que les quantités de caféine déterminées par les deux techniques sont assez proches, et qu'en revanche, l'analyse des blancs montre une différence importante selon que l'on utilise l'UV ou l'HPLC. Cette différence s'explique par l'absence de préfiltres lors de ces essais préliminaires et a justifié leur utilisation systématique pour la suite des mesures.

		UV (µg)	%	HPLC (µg)	%
Blanc	**1**	38		2	
	3	45		6	
	5	90		3	
Echantillons	**2**	392	26 %	366	24 %
	4	207	14 %	183	12 %
	6	447	30 %	449	30 %

Tableau 3-1 : Détermination de la quantité de caféine ayant pénétré la peau après 21h30 et du pourcentage par rapport à la quantité appliquée : comparaison du dosage UV ou HPLC-UV

3.2 Les formulations

Les formulations doivent rester stables, c'est-à-dire ne pas présenter de séparation de phase, pendant la durée de la pénétration, donc 24 h. Pour cela la concentration en tenisoactif (3 % minimum) et le rapport eau/huile ont pu varier afin de garantir la stabilité des formules.

3.2.1 Les formulations à base de caféine

Les émulsions formulées et utilisées pour les études de pénétration cutanée sont regroupées dans le Tableau 3-2.

Plusieurs procédés de formulation ont été testés, la difficulté résidant dans l'utilisation d'un seul tensioactif pour stabiliser les émulsions. Le procédé utilisé peut être décrit de la façon suivante : toutes les solutions sont chauffées à 70°C pour garantir une solubilité des composants. Les phases huileuse et aqueuse sont mélangées à l'aide d'une défloculeuse à 3500 rpm durant 2-5 min puis l'émulsion est homogénéisée avec un rotor stator (UltraTurrax®Ika®T25 Germany) à 12000 rpm pendant 12 min et pour finir à 9000 rpm pendant 20 min.

Huile	Concentration huile	Tensioactif	Concentration du tensioactif	Concentration de caféine
BGC	20,02 %	PEG20C12	3,00 %	1,15 %
BGC	20,00 %	PEG20C18	3,00 %	1,15 %
BGC	19,99 %	PEG20C18:1	3,02 %	1,15 %
ODM	20,01 %	PEG20C8	6,00 %	1,10 %
ODM	20,01 %	PEG20C12	5,99 %	1,10 %
ODM	20,00 %	PEG20C18	3,02 %	1,15 %
ODM	20,00 %	PEG20C18:1	6,01 %	1,10 %
Paraffine liquide	20,01 %	PEG20C12	6,01 %	1,10 %
Paraffine liquide	50,00 %	PEG20C18:1	6,00 %	0,66 %

Tableau 3-2 : Compositions des émulsions à base de caféine utilisées pour la pénétration cutanée.

3.2.2 Les formulations à base de rétinol

Les émulsions formulées et utilisées pour les études de pénétration cutanée sont regroupées dans le Tableau 3-3.

Les composants huileux (BHT, tensioactifs huileux et huile) et aqueux (eau et tensioactif hydrophile) sont chauffés à 70°C pour une meilleure solubilisation puis refroidis à température ambiante. Le rétinol est ajouté dans la phase huileuse à température ambiante sous agitation magnétique afin d'éviter sa dégradation. Ensuite un procédé identique à celui utilisé pour les émulsions de caféine a été employé : mélnage à la défloculeuse à 3500 rpm durant 2-5 min puis homogénéisation avec un rotor stator (UltraTurrax® Ika®T25 Germany) à 12000 rpm pendant 12 min et pour finir à 9000 rpm pendant 20 min.

Huile	Concentration huile	Tensioactif	Concentration du tensioactif	Concentration de rétinol
BGC	19,94 %	PEG20C12	3,04 %	0,50 %
BGC	20,00 %	PEG20C18	3,05 %	0,47 %
BGC	20,18 %	PEG20C18:1	3,10 %	0,49 %
Dodécane	54,95 %	PEG6C18:1	7,09 %	0,53 %
Dodécane	54,60 %	PEG20C12	7,15 %	0,59 %
Dodécane	54,80 %	PEG20C18:1	7,96 %	0,50 %

Tableau 3-3 : Compositions des émulsions à base de rétinol.

3.3 Caractérisation des émulsions

Les émulsions ont été caractérisées par rapport à la distribution de taille et de viscosité. Ces caractéristiques ont été choisies pour pouvoir vérifier que les différents émulsions et solutions tensioactives ont des structures similaires et donc ces deux propriétés doivent être le plus proches possibles pour toutes les émulsions afin de ne pas influencer la pénétration [84 85].

La stabilité de toutes les émulsions a été vérifiée avant de les appliquer sur la peau.

3.3.1 Stabilité

Les formulations sont caractérisées spécialement par rapport à leur stabilité. Une formulation est définie comme stable, dans cette thèse, s'il n'y a pas de séparation visible de phase à 32°C, la température de la peau dans les cellules de Franz, et à température ambiante pendant le temps de mesure, 24h. Arrivés à ce point, il faut rappeler que cette thèse étudie des formulations expérimentales et non pas commerciales et donc une stabilité minimale pendant la durée de l'expérience est nécessaire et suffisiant.

Bien évidemment, la stabilité de certaines formulations est légèrement supérieure à 24h, mais toutes les formulations ont été formulées juste avant leur application sur la peau.

3.3.2 Sens de l'émulsion

Le type d'émulsion est analysé par la méthode de dilution et par des mesures de résistivité. Une gouttelette d'émulsion est dissoute très rapidement quand elle est posée sur une surface d'eau, montrant de cette manière que l'eau est la phase continue de l'émulsion. La résistivité de l'émulsion (mesurée avec un conductivimètre DT-830 B) est très grande (>2000 kΩ.cm) et égale à la résistivité de l'eau mesurée dans les mêmes conditions. Ce résultat montre, une fois de plus, que l'eau est la phase continue.

3.3.3 Taille des gouttes de l'émulsion

La distribution de tailles des gouttelettes des émulsions est mesurée par diffusion de la lumière aux petits angles avec le MasterSizer® 2000 (Malvern Instruments Ltd, UK). Les indices de réfraction utilisés pour le traitement des données brutes sont 1,332 pour l'eau et 1,460 pour les gouttelettes d'émulsion.

La taille moyenne et l'indice de polydispersité des gouttelettes de rétinol dispersées dans la solution tensioactive sont mesurés par diffusion dynamique de la lumière utilisant le NanoZS® (Malvern Instruments Ltd, UK).

Les résultats montrent que les tailles des gouttlettes étaient similaires pour toutes les emulsions utilisées. Les tailles des « gouttelettes » dans les solutions tensioactives varient beaucoup. Cet effet est lié au fait que la concentration de tensioactif utilisé a été fixée à la même concentration que celle utilisée dans les émulsions correspondantes (3% ou dans certains cas 6%). Cette concentration est beaucoup plus importante que la concentraiton micilleaire critique et donc il n'y a pas de micelles qui se créent dans ces solutions tensioactives mais des aglomérats de tensioactif, ce qui rend impossible l'interprétation des résultats de diffusion dynamique.

3.3.4 Viscosité de l'émulsion

La viscosité des émulsions est mesurée à 20°C avec un viscosimètre de type Couette TV-e 05 (Lamy, France) équipé d'un système mobile MS-BV 100 qui tourne à 600 rpm. La viscosité était similaire pour toutes les formulations utilisées.

3.4 La mise au point de la MCR

Le principe de la confocalité est basé sur l'observation d'un volume de mesure limité obtenu grâce à une petite ouverture de champ. Cette limitation du volume améliore la résolution latérale et axiale grâce à un filtrage des signaux qui interviennent dans la périphérie de la zone ciblée ou dans les régions adjacentes. Par ailleurs cela permet de diminuer la fluorescence. Ces deux avantages, la haute résolution axiale et la réduction de la fluorescence, jouent un rôle important sur l'obtention de données en Raman de haute qualité aussi bien en surface de la peau que dans les couches les plus profondes.

L'appareil est composé d'un spectromètre Raman (LabRam HR800, Horiba Jobin Yvon) et d'un microscope confocal (BXFM Olympus). L'objectif utilisé dans cette thèse est un objectif à longue distance avec un grossissement 50x (Mitutoyo) et un diaphragme de 0,42 travaillant dans l'air. La source d'excitation est un laser vert d'ion argon 514,5 nm (Spectra Physics) qui fournit 10 mW CW (constant wave) au niveau de l'échantillon. Cette source a été choisie après plusieurs essais afin d'avoir un compromis entre un signal de forte intensité et les dégradations de la peau occasionnés par une source plus puissante (rouge) ou des ouvertures de fenêtre plus importantes. Le spectromètre est équipé d'un detecteur CCD refroidi avec de l'air (Synapse, Horiba Jobin Yvon) avec une surface de détection de 1024x512 et un réseau de 600 gr/mm qui permet de couvrir la gamme spectrale de 200 à 3900 cm^{-1} en trois parties d'acquisition avec une résolution spectrale de 4 cm^{-1} qui est conservée au niveau de la région profonde. Le temps d'acquisition est de 5 s, ce qui permet des mesures rapides sur la surface et également dans des couches profondes. Une caméra vidéo intégrée dans le microscope permet de visualiser l'échantillon en réflexion et le spot laser sur l'échantillon (début du

stratum corneum). La surface de la peau n'est pas couverte avec une lame pour éviter des interférences Raman générées par le verre de la lame en contact avec la peau mais aussi pour limiter les effets de réfraction provoqués par une interface supplémentaire qui peuvent influencer la résolution spatiale et axiale, comme discuté par Chrit [63].

Pour l'évaluation de la résolution, un échantillon de silicium a été exposé au faisceau laser et le signal Raman a été enregistré. Le spectre Raman de l'échantillon a été mesuré en utilisant un objectif avec une longue distance 50X. La mesure débute à 35 µm au dessus de la surface puis progresse par pas de 2 µm en profondeur jusqu'à 35 µm sous la surface. L'intensité du pic Raman associé au mode vibrationnel de la liaison Si-Si à 520 cm^{-1} est tracée en regard de la position du faisceau du laser. La résolution axiale est déduite de la valeur du *Full Width at Half Maximum* (FWHM) ou Largeur à mi-hauteur. Dans ces conditions, la FWHM était de 11 µm avec une ouverture de fenêtre de 300 µm et de 5,6 µm avec une ouverture de 200 µm. Pour avoir un bon compromis entre l'intensité du signal et la résolution axiale, l'ouverture de fenêtre de 200 µm a été choisie avec une résolution axiale de ~6 µm (Figure 3-3a).

La différence d'indice de réfraction entre l'air et la peau, mais aussi entre les différentes couches de la peau, provoque une déviation du rayon lumineux qui donne une estimation incorrecte de la valeur de la profondeur. Ce problème a été étudié et expliqué par plusieurs groupes [86-93] et fait l'objet d'une étude récente réalisée par Xiao *et al.* En utilisant un système de multicouches composées par des films polymériques avec des indices de réfraction proches de celui de la peau humaine, les auteurs ont montré que l'erreur de mesure entraîne une sous-estimation de la valeur de 15-20%. Pour cette raison, toutes les valeurs de profondeur mesurées par le Raman devraient être corrigées théoriquement en appliquant un facteur de 15-20%. Dans cette thèse, cette correction na pas été faite parce qu'une mesure très précise de la profondeur est impossible [71]. De plus, le but de cette thèse n'est pas de mesurer de manière exacte l'épaisseur ou la profondeur mais d'évaluer la méthode comme alternative à la technique immunohistochimique d'une part, d'évaluer la distribution d'un actif lipophile dans la totalité du *stratum corneum* et la transition *stratum corneum*-épideme

d'autre part. Les mesures sur la couche lipidique ne sont pas influencées par cette sous-estimation parce qu'elles ne nécessitent pas une analyse en profondeur.

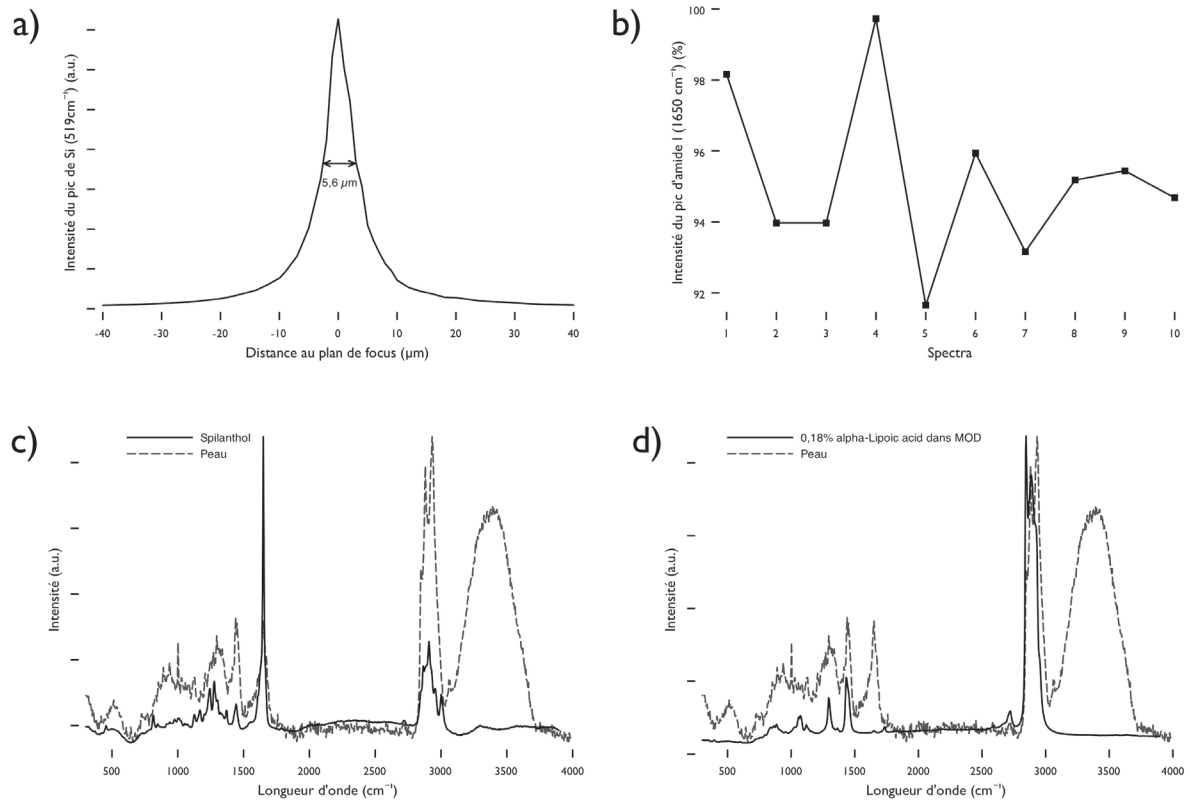

Figure 3-3 : a) Intensité du pic de la liaison Si-Si par rapport à la distance de la surface (résolution axiale); b) Reproductibilité des mesures : intensité du pic à 1650 cm^{-1} pour 10 mesures; c) Spectres Raman du spilanthol et de la peau; d) Spectres Raman du l'acide lipoïque et de la peau.

La reproductibilité des résultats a été expérimentalement vérifiée par l'enregistrement de dix spectres sur la surface de la peau. La variation d'intensité du pic à 1650 cm^{-1} était inférieure à 3 % (Figure 3-3b).

3.4.1 Choix des actifs

Pour mesurer la pénétration d'un actif, il faut avoir un actif lipophile qui se stocke dans le *stratum corneum*. Un actif hydrophile au contraire a une vitesse de pénétration trop importante pour suivre une quantité dans le *stratum corneum* en Raman. L'actif doit de plus posséder au moins un groupement chimique qui répond en Raman et dans une zone du spectre où il n'y a pas d'interférences avec les pics de la peau. Plusieurs actifs ont été testés.

Le spilanthol est un actif lipophile de Gattefossé SAS. Le pic de la liaison amide (1500 cm^{-1}) est très intense et peut être utilisé comme pic de détection (Figure 3-3c). Cependant, ce pic existe aussi dans la peau, l'interprétation du spectre de la peau traitée avec le spilanthol peut donc poser des problèmes. En raison de cette interférence et de son coût, l'actif a été écarté.

L'acide lipoïque est un principe actif pharmaceutique qui a été pressenti comme actif modèle lipophile. Les propriétés chimiques de l'acide lipoïque sont proches de celles du spilanthol. C'est un actif lipophile avec une masse molaire de 206 g/mol (spilanthol : 221 g/mol) et une solubilité 127 mg/ml (à 25°C). D'après sa structure chimique, un pic caractéristique de la liaison S-S est attendu à ~526 cm^{-1} mais en raison d'une hydrolyse, ou d'une instabilité en solution aqueuse, le spectre Raman ne montre pas de pic caractéristique (Figure 3-3d) et donc cet actif a également été abandonné.

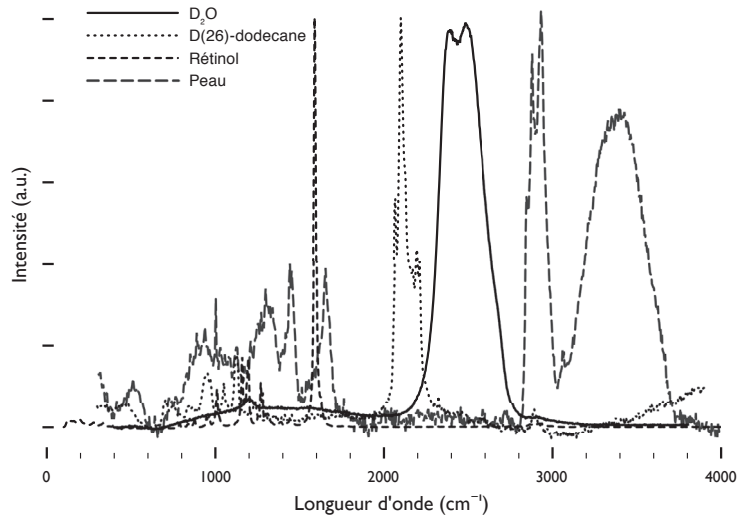

Figure 3-4 : Spectres Raman de l'eau deuterée, du dodécane deuteré, du rétinol et de la peau

Le rétinol a un pic unique à 1585 cm^{-1} (Figure 3-4). Par contre, le rétinol est sensible à la lumière et à la chaleur et s'oxyde facilement. Cette oxydation n'est pas très rapide. Pour les mesures effectuées sous 24 h, en cellule de Franz, l'actif doit être stabilisé avec du butylhydroxytoluène (BHT). Cet actif est un actif cosmétique d'intérêt et il a donc été sélectionné.

Le dodécane deuteré (D(26)-dodécane) a un pic caractéristique à 2099 cm^{-1} (Figure 3-4) qui n'interfère pas avec les pics de la peau. Cette huile permettra d'effectuer les mesures de pénétration des huiles dans des formulations modèles.

L'eau de la formulation va être remplacée par l'eau lourde pour pouvoir distinguer l'eau de la formulation de l'eau endogène. L'eau deuterée a un pic caractéristique à 2500 cm^{-1} (Figure 3-4) qui n'interfère pas avec les pics de la peau.

Chapitre 4 Évaluation des méthodes de séparation du stratum *corneum*

Dans la Partie A, il a été rappelé que la peau peut être séparée en deux grandes parties; la partie lipophile, le *stratum corneum*, et la partie hydrophile, composée de l'épiderme et du derme. De même, un rappel sur la fonction barrière de la peau, le *stratum corneum*, a été décrit. Plusieurs aspects de cette fonction barrière peuvent être étudiés, comme par exemple, la quantité d'actif présente après la pénétration percutanée ou les modifications d'organisation et de composition de la couche lipidique. Pour pouvoir étudier ces modifications, la séparation du *stratum corneum* de l'épiderme est nécessaire. La méthode la plus connue est la méthode du tape stripping décrite par Wolf en 1939 [94]. Cette méthode qui consiste à éliminer le *stratum corneum* couche après couche à l'aide d'une bande adhésive est facile à mettre en œuvre mais difficile à standardiser. Depuis les années 50, il existe des doutes sur la qualité de séparation en terme d'homogénéité et d'intégralité [95-98]. La méthode du tape stripping présente cependant l'avantage de permettre une évaluation de la quantité d'actif selon la profondeur du *stratum corneum*. D'autres méthodes existent comme la méthode d'arrachage en une seule étape grâce à la colle cyanoacrylique ou grâce à la trypsinisation. Le présent article compare et évalue les trois méthodes les plus utilisées : le tape stripping [94,99,100], le traitement par l'enzyme trypsine [101] et la biopsie pratiquée avec de la colle cyanoacrylique [102]. L'étude présentée évalue la qualité de la séparation du *stratum corneum* en fonction de la méthode utilisée et discute leurs avantages et inconvénients respectifs. L'imagerie histologique et la microspectroscopie confocale Raman sont les méthodes utilisées pour évaluer la qualité de la technique pour éliminer cette couche cutanée. Les avantages de la microspectroscopie confocale Raman ont déjà été exposés dans la Partie A. Ici, cette méthode est utilisée pour sa capacité à mesurer la quantité d'eau dans la peau. En effet, le passage du *stratum corneum* pauvre en eau (13 %) à l'épiderme viable riche en eau se traduit par un saut sur le graphe reliant la profondeur de la peau à l'intensité du pic (Figure 2-2). Si l'arrachage du *stratum corneum* est homogène et total ce saut va

disparaître de la courbe qui va s'aplanir. C'est ce que nous avons cherché à mettre en évidence en utilisant la MCR et nous avons vérifié nos résultats en les confrontant aux images des coupes histologiques effectuées après arrachage du *stratum corneum*. Cette méthode a le potentiel de pouvoir remplacer les méthodes de séparation classiques dans de nombreuses études à cause de ses diverses possibilités analytiques.

Les résultats de cette étude montrent les différentes qualités de séparations résultant de chacune des méthodes utilisées. Les faits marquants de cet article sont les suivants :

- Le tape stripping permet de séparer avec chaque strip une certaine quantité du *stratum corneum*. Cependant, cette quantité n'est pas constante et identique à chaque strip appliqué [98]. Les résultats montrent de plus que la séparation n'est pas homogène sur toute la surface et n'est pas complète même après l'application de 28 strips. Le moyen le plus simple de résoudre cette inhomogénéité est de peser chaque strip avant et après chaque arrachage et de déterminer la quantité (m) de tissu arraché par différence entre les deux masses. La profondeur dans le *stratum corneum* (x) peut alors être calculée en utilisant la formule $x=m/(A.\rho)$, avec A la surface du strip (3,8 cm^2), et ρ la densité du tissu. Une valeur pour la densité a été publiée par Anderson avec 1,2 g/cm^3 [103]. Cependant il s'agit d'une valeur moyenne, la densité variait dans ce travail entre 0,88 g/cm^3 et 1,42 g/cm^3. Le calcul de l'épaisseur par cette méthode est donc très approximatif. Afin d'évaluer cette méthode et de la comparer à la MCR, nous avons mesuré la perte insensible en eau en fonction du nombre de strip arraché et recalculé à chaque fois l'épaisseur correspondante. Les résultats sont rprésentés sur la Figure 4-1 qui montre le TEWL en fonction de la profondeur du *stratum corneum*, calculée avec une densité de 0,9 g/cm^3 (triangles), 1,2 g/cm^3 (carrés) et 1,5 g/cm^3 (cercles). Une rupture de pente est observée à la limite *stratum corneum* – épiderme, Le TEWL augmente alors très rapidement. La limite entre les deux couches cutanées peut être estimée par l'intersection des deux

droites [98]. Les épaisseurs résultantes varient de 8 µm (triangle), 10 µm (carré) à 13 µm (cercle).

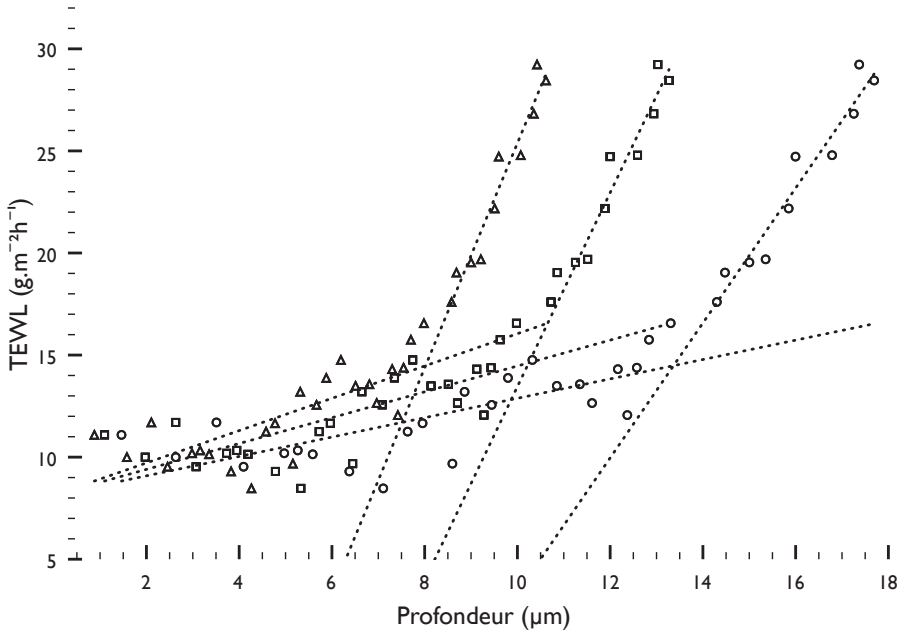

Figure 4-1 : Augmentation progressive du « transepidermal water loss (TEWL) en fonction avec la profondeur du *stratum corneum* (µm) en utilisant 0,9 (triangle), 1,2 (carré) et 1,5 (cercle) g/cm3 comme valeur de densité pour transformé la mass du *stratum corneum* arraché par tape sttipping en profondeur.

- La trypsination peut enlever le *stratum corneum* complètement et de manière homogène. Si une étude de la peau par screening n'est pas demandée, cette méthode est une bonne alternative. Par contre, une solution aqueuse est utilisée, pouvant alors perturber certaines expériences notamment celles avec des actifs hydrosolubles.

- La qualité de la séparation du *stratum corneum* avec la colle dépend du protocole utilisé. Elle dépend du nombre de strips et du temps nécessaire pour la polymérisation de la colle. Il a été démontré qu'avec l'application de trois strips et un temps de polymérisation de 2-3 min environ un tiers du *stratum corneum* reste sur la peau. En revanche, deux strips et un temps de polymérisation de 15 min donnent des résultats

bien meilleurs avec une séparation homogène et totale du *stratum corneum*. Cette méthode est donc une bonne alternative à la méthode de trypsination.

Premièrement, cette étude montre de manière visuelle les différentes qualités de séparation du *stratum corneum* de la peau. Dans l'ensemble de la thèse, la pénétration percutanée d'actifs et en particulier celle du rétinol est étudiée et pour pouvoir évaluer quantitativement le rétinol dans le *stratum corneum,* la biopsie par la colle cyanoacrylique a été choisie pour réaliser la séparation totale du *stratum corneum* de la peau. La comparaison entre les coupes histologiques et la MCR a montré que l'homogénéité de la teneur en eau sur la surface de l'explant mesurée grâce à la MCR est fidèle aux coupes histologiques. Cette technique est adaptée pour évaluer rapidement que la totalité du *stratum corneum* est éliminée.

Dans la suite du travail cet outil analytique est utilisé conjointement à la méthode des cellules de Franz pour apprécier la distribution des ingrédients de la formulation dans le *stratum corneum* et pour étudier l'impact des ingrédients sur la structure des lipides.

Les faits marquants :

- La biopsie pratiquée avec la colle cyanoacrylique en appliquant 2 strips et un temps de polymérisation de 15 min a été choisie pour enlever le *stratum corneum* de l'épiderme dans la suite de ce travail.
- La MCR a été mise au point et utilisée dans cette partie pour apprécier la qualité d'élimination du *stratum corneum* par différentes méthodes d'arrachage.

Förster et al. Confocal Raman microspectroscopy for evaluating the stratum corneum skin removal of 3 standard methods. Skin pharmacol physiol. vol. 24 pp. 103-12

Confocal Raman microspectroscopy for evaluating the *stratum corneum* skin removal of 3 standard methods

M. Förster [a, b, c], MA. Bolzinger [b, c], MR. Rovere [d], O. Damour [d], G. Montagnac[e], S. Briançon [b, c]

[a] Gattefossé SAS, St Priest, France

[b] Université Lyon 1, Institut des Sciences Pharmaceutiques et Biologiques, Laboratoire de Dermopharmacie et Cosmétologie, Lyon, France;

[c] Laboratoire d'Automatique et de Génie des Procédés (LAGEP), UMR CNRS 5007, Villeurbanne, France

[d] Université Lyon 1, Laboratoire des Substituts Cutanés (LSC) CNRS UPR-412, Lyon

[e] Laboratoire des Sciences de la Terre, Université de Lyon France, UMR 5570 CNRS, ENS de Lyon, France

Key words: *Stratum corneum* removal, Confocal Raman microspectroscopy, Tape stripping, Cyanoacrylate skin surface biopsy, Trypsinization

Background/Aims:
Stratum corneum (*SC*) removal is needed in biopharmaceutical studies or in evaluating the barrier function. The most common technique is the tape stripping method. However it results in neither a homogeneous nor a complete removal.

Methods:
The removal qualities of tape stripping, cyanoacrylate skin surface biopsy and trypsinization were estimated *in vitro via* histological imaging and confocal Raman microspectroscopy (CRM) and compared. In addition the potential of the non-invasive CRM as a replacement method is discussed.

Results:
Comparison between the three methods showed, as expected, that the tape stripping method did not result in a uniform removal over the whole surface even after 28 strips. The trypsinization and cyanoacrylate skin surface biopsies allowed a complete and uniform removal of the *SC* after defining a standard protocol (2 cyanoacrylate strips with a polymerization time of 15 min).

Conclusion:
The feasibility of CRM to control the *SC* removal was demonstrated *in vitro*. Tape stripping is a simple method, but it is influenced by many extrinsic factors and axial drug quantification is difficult. With trypsinization and cyanoacrylate methods the entire *SC* is removed so that quantification over the whole *SC* is possible but not an axial drug screening.

.

In biopharmaceutical studies the methodology of tape stripping to remove the *stratum corneum* (*SC*) has been commonplace for many decades [1], optimized by Pinkus [2] and Lorincz [3]. This method is simple, inexpensive and minimally invasive and can be used to investigate percutaneous penetration and disposition of topically applied drug *in vivo* [4-7], *in vitro* [8-14] on humans [9, 14, 15] and laboratory animals, e.g., pigs [8-12, 14], rats [16], guinea pigs [17] and mice [18]. It is also used to disturb and even disrupt skin barrier function [4], to collect *SC* lipids samples [19] and to measure the *SC* mass and thickness [20-22].

Doubts about this method were raised in the 50s by Hunter [23] who reported that alternating the direction of stripping allowed removal with fewer total strips. These early observations showed that a strict and standardized protocol is essential for cross-study data comparison.

The FDA guideline recommends 10 tape strips after topical application of a substance. Weerheim and Ponec [19] reported that the average number of tape strips *in vivo* could be 18-20 strips. The amount of *SC* removed by a single adhesive tape strip depends on several extrinsic factors such as the type of adhesive tape [24], the force of removal from the skin [25], the duration of pressure onto the skin [26] and the nature of the topically applied substances [22]. Moreover, various intrinsic parameters such as the anatomical site [15], the age [7] and the season [27] also influence the amount of removed *SC* on each tape. In addition, the number of cell layers [28] and corneocytes [29], the thickness of the *SC* [21] and the composition and amount of lipids [30] all vary depending on the anatomical site. A review discussing these critical parameters in detail was written by Lademann in 2009 [31].

Tape stripping remains an accepted method for removal of the *SC* if the used protocol is given and adapted to the aim of the investigation.

One alternative for a complete separation of the *SC* without tape stripping is to use enzyme treatment with trypsin. This method was discussed in the 60s by Kligmann *et al.* [32]. The method is well established and used for various purposes [33-35] and to quantify active amounts in percutaneous penetration studies [36, 37].

The use of a cyanoacrylate strip, introduced in 1971 by Marks and Dawber [38] as the so-called "skin surface biopsy", is an established method for examination of the horny layer by obtaining a thin sheet of *SC* with a rapidly polymerizing cyanoacrylate adhesive. This method is also used to quantify the amount of an active substance [39, 40] and to study the *SC* lipids by thermal or quantitative methods [41-43]. The cyanoacrylate skin surface biopsy is rapid and easy to standardize but it must be noticed that this method removes an unknown amount of corneocytes and the follicular casts. For this reason a distinction between transepidermal and transfollicular routes of percutaneous absorption is not possible [44]. In the literature there is differing information concerning the number of strips necessary to remove all the *SC*.

Whatever the method, it is crucial to ensure the complete and uniform removal of the *SC*. For that purpose TEWL recordings were performed but they are not sensitive. Histological images are necessary but are time-consuming. In this context, the confocal Raman microspectroscopy (CRM) is a more recent method established in the last 10 years. This non-invasive method enables an analysis of skin molecular composition as a function of distance to the skin surface both *in vitro* and *in vivo*.

Apart from many applications in dermatological research it is also used in hydration studies by measuring the water content as a function of depth and indirectly for measuring the thickness of the *SC* [45-48]. The present investigation surveys *in vitro* the most commonly used methods for *SC* separation: tape stripping method, trypsinization and the skin surface biopsy. Removal quality is assessed using visual histological imaging and, for the first time, by CRM. Suitability of the different removal methods is discussed by presenting the main advantages and disadvantages. The discussion covers the main application areas and investigations of the whole *SC* and/or across the *SC* depth. The CRM was firstly used for investigation of the separation quality but it is also considered in the discussion as a non-invasive replacement method for the more or less invasive separation methods.

Material and Methods

Materials

Full-thickness pig skin (pietrain) was obtained from young animals killed at the Laboratoire de Physiologie, Université Lyon 1, France. The skin was taken from the flank, was washed and excised, the subcutaneous fatty tissue was then carefully removed and the tissue was stored flat at −20°C until use but not longer than 4 months. All experiments on excised porcine skin were from the same donor animal and were performed according to the recent guidelines [49].

Tape Stripping

The *SC* of thawed skins was removed by applying a D-Squame® adhesive tapes (diameter 22 mm, surface 3.8 cm^2, Monaderm, Monaco) for 10 seconds using a 500 g mass. The tape was then quickly stripped off. Samples were prepared in triplicate using both 9 and 28 strips of tape.

Trypsinization

The trypsinization was carried out using a 0.0016

wt-% trypsin (Sigma-Aldrich) in phosphate buffered saline (PBS) buffer pH 7.2 during 2-3 hours at 40°C. The *SC* was separated with a no. 11 surgical blade after rinsing off the skin surface with PBS [32].

Skin surface biopsy method

For the skin surface biopsy method a microscope slide (76 x 26 mm; Roth, Karlsruhe, Germany) was coated with cyanoacrylate resin (Loctite Super Glue-3 from Henkel France) and applied on the *SC* for a defined polymerization times of 3 min and 15 min respectively. Removing the slide detached the *SC* [40]. The skins were stripped 3 times for a polymerization time of 2 minutes and twice for a 15 minutes polymerization period.

Confocal Raman microscope studies

The experimental device includes a Raman spectrograph (LabRam HR800, Horiba Jobin Yvon) and a confocal microscope probe (BXFM Olympus). The objective used in this experiment had a long working distance of magnitude 50x (Mitutoyo) with a numerical aperture of 0.42, operating in air. The excitation source was a green 514.5 nm argon ion laser (Spectra Physics) delivering about 10 mW CW at sample level. The spectrograph was equipped with an air-cooled CCD detector (Synapse, Horiba Jobin Yvon), with a chip size of 1024 x 512, and a 600 gr/mm grating, which allowed the covering of the large spectral range from 200 to 3900 cm^{-1} in three windows acquisitions with a spectral resolution of about 4 cm^{-1}, which was conserved at deeper regions. The acquisition time was about 5 s, which enabled to perform rapid measurements at the surface as well as in deeper layers. A color video camera integrated within the microscope probe enabled the user to visualize the sample in reflection and the attenuated laser spot focused on the sample (beginning of the *SC*). The surface of the skin was not covered with a window to avoid interferences of Raman features generated by the window material itself in contact with the skin, but also to limit the refraction index effects induced by an additional interface, which might affect the spatial and namely axial resolution as discussed by Chrit [50].

The axial resolution, which was a critical achievement for our measurements, was determined by plotting the intensity of the Raman peak associated to the Si-Si vibrational mode of silicon at 520 cm^{-1} against the position of the laser focus. The axial resolution was inferred from the full width at half maximum (FWHM) of this response curve with about 5.6 µm with a confocal opening aperture of 200 µm.

The difference of the refractive index between the air and the skin, but also between the different skin layers, induce a deviation of the light beam which gives an incorrect estimate of the depth value. This problem was studied and described by many groups [51-58] and a recent study by Xiao et al., using multilayered systems constituted with polymers films with refractive indexes close to those of the human skin, showed that the error in the measurement lead to an underestimation of the depth value of 15–20% [59]. Therefore, all depth values deduced from Raman measurements should be theoretically corrected by applying a 15-20% factor.

Data reproducibility was experimentally checked by recording ten successive spectra at the skin surface, showing very slight spectral features and intensity variations of less than 3%.

Data analysis

In confocal Raman spectroscopy there are three effects, which have to be treated for a correct interpretation of the spectra. First biological samples like skin show fluorescence. To get rid of the intrinsic skin fluorescence a linear baseline was subtracted from 2600 to 3800 cm^{-1}.

The second effect is that with deeper probing into the sample the signal will get weaker [47]. This is due to the loss of light from an increase in scattering. It is not related to the loss of compound or a modification in the skin composition. This attenuation is purely a physical effect. To be able to compare the intensity of bands in the region 2500 - 3500 cm^{-1} spectra were equalized for the 2940 cm^{-1} band intensity as a reference. This band corresponds to the C-H_3 symmetric stretching protrudes outside the protein chain of keratin, the major component of the epidermis. It does not take part in strong intermolecular interactions; therefore the C-H_3 band is not modified by alterations in secondary protein structure [60]. Also the keratin has an approximately constant concentration. The spectrum of keratin is well known and is typical of a Raman spectrum of a protein. It has been comprehensively discussed in skin previously [61]. It has to be noted that no fitting

procedures were applied for the results interpretation.

The third effect is the uncertainties in the analysis depth, induced by the difference in the refractive index as described by previous works [51-58]. This correction might be considered because it could lead to an underestimation of the real depth by a factor of 15-20%. Therefore, the measured values could be corrected by adding a 15-20% to each measurement. This correction was not done in the present work because a high accuracy corrected value of the depth value is impossible [62]. Also, the aim of the research was not to measure accurately the *SC* thickness but rather to provide an alternative method for immunohistochemical techniques, evaluating the homogeneous and complete skin removal quality.

The thickness of the *SC* cannot be measured directly by confocal Raman spectroscopy. But it is well-known [63] that the water content increases from 13 % in the *SC* to > 50 % in the viable epidermis. Water content can be measured by the water to protein ratios in the *SC* which was calculated as the ratio between the Raman signal intensity of water integrated from 3350 to 3550 cm^{-1} and that of protein integrated from 2910 to 2965 cm^{-1}. These spectral ranges were chosen so as to maximize signal-to-noise ratio and to avoid overlay between the N-H vibration of protein at 3329 cm^{-1} and the water Raman signal [33, 45, 46, 48].

Water content was plotted against focal plane depth in steps of 2 µm from the skin surface to 20 µm depth for each skin sample. Each treatment was done in triplicate. It is assumed that the *SC* starts with the surface. With the color video camera, integrated within the microscope probe, the laser spot was focused on the sample surface. This subjective focus varies from one user to another with an error of ±1µm. The boundary between the *SC* and the viable epidermis is not well defined and can be difficult to define. Different estimations exist in the literature and will be discussed later on. In this work the *SC* thickness is fixed at the middle of the steepest increase of the resulted curve in the water content versus focal plane depth plot. The thickness of each sample was determined (middle of the steepest slope using 2 µm measurement steps) and the average for three samples (n=3) with the standard error of the mean was used for further comparisons. In Figure 4a a plot of an untreated skin is shown. A steep increase in the slope can be observed around 9 µm, which indicates the *SC* thickness (Figure4a). In Figure 4b the same skin sample after a *SC* removal treatment via trypsinization is shown. No significant slope can be observed between 0 and 20 µm. Figure 3a shows that with this technique the whole *SC* is removed and the zero µm in Figure 4b corresponds now to the surface of the epidermis and no water increase was noticed in the layers between 0 an 20 µm.

Fig. 1

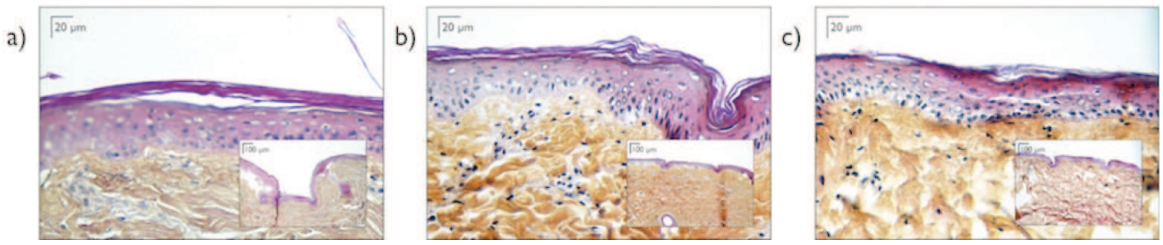

Figure 1: Histological image of a skin a) before tape stripping treatment, b) after 9 strips c) after 28 strips The large image corresponds to a magnification 40x and the smaller one shows an overview (magnification 10x).

Histological examinations

Tissues were fixed in 4% formaldehyde solution and embedded in paraffin. Cross sections of the skins, 5 mm thick, were cut and stained using hematoxylin–phloxin–saffron (HPS). Cell nuclei were stained in blue by hematoxylin, cytoplasm in pink by phloxine and extracellular matrix of connective tissue in orange/yellow by saffron. Histological images of the skin were taken with a microscope.

Results

Tape stripping technique

In Figure 1 histological photos of a skin non-stripped (a), stripped with 9 strips (b) and with

28 strips (c) are shown. The results clearly show that after 9 strips the main part of the *SC* layers still remains on the skin. Even after 28 strips parts of *SC* were still present, located particularly in wrinkles and furrows where the adhesion of the tape was less efficient.

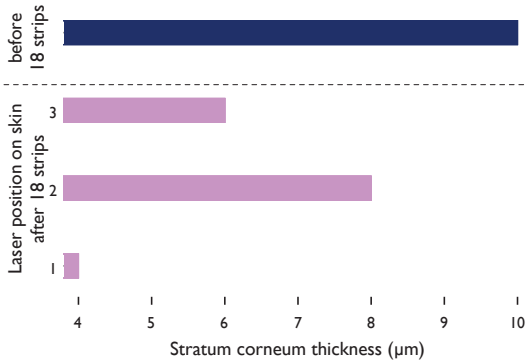

Figure 2: *SC* thickness before and after applying 18 tape strips at 3 different positions (distance from each other in micron range) on one skin sample measured by the water content using CRM.

CRM is carried out using a small laser spot and does not measure a large sample surface as does a TEWL probe (0.785 cm2). Therefore measuring the *SC* thickness at different planar positions on the skin sample surface indicates inhomogeneous removal after a tape stripping treatment. The measurement positions have distances from each other in the micron range to avoid the measurement of intrinsic inhomogeneity of the skin (skin surface relief). In Figure 2 the *SC* thickness is plotted after applying 18 strips. After the tape stripping the thickness was measured at 3 different positions. Small variations in the measurement position on the skin had a large influence on the results and also show the inhomogeneity.

For handling this inhomogeneity of tape stripping the most straightforward procedure is to weigh each strip before and after *SC* removal and to determine the amount (m) of tissue removed from the difference between the masses. The total thickness of the *SC* (x) can be calculated using the formula: x=m/(A), where A is the area of the strip (3.8 cm2), and the density of the tissue but this is inherently less accurate. An average value of 1.2 g/cm3 has been published for . However in this work the density of the *SC* varied greatly (0.88 - 1.42 g/cm3) [64]. In the present work we calculated the *SC* thickness to confirm the high impact of *SC* density using this procedure and not to determine an absolute *SC* thickness of the used samples. The strips were not dried before weighting and we followed the protocols reported in the literature [22]. We found thicknesses in the range from 8 to 13 µm for the same skin sample, depending on the chosen average density value (data not shown).

Trypsinization

Figure 3a showed that trypsinization resulted in a complete and homogenous *SC* removal over the whole surface.

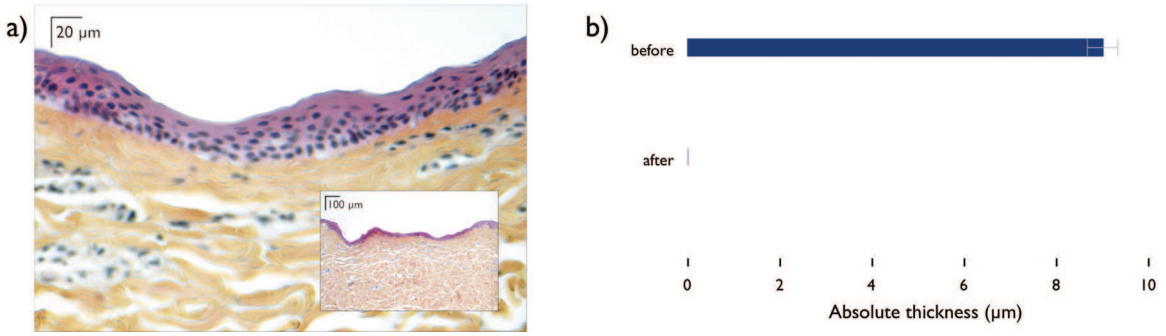

Figure 3: a) Histological image of a skin after removing the *SC* by an enzyme treatment with trypsin. The large image corresponds to a magnification 40x and the smaller one shows an overview (magnification 10x) b) *SC* thickness before (measured from 0-20 µm in 2µm steps) and after trypsinization (measured from 0-20µm in 10µm steps). The error bars represent the SEM (n=3).

The CRM measurements were taken on three samples and the *SC* thickness was determined as 9 ± 0 µm (Figure 3b). After trypsinization the *SC* thickness was insignificant (Figure 3b). On Figure 4b, CRM results show no variation in epidermal water content (over 0-20 µm) conversely to Figure 4a (untreated skin) where a continuous water content increase is observed along the *SC* depth.

Cyanoacrylate skin surface biopsy method

Because of different descriptions in the literature concerning the necessary number of strips for a

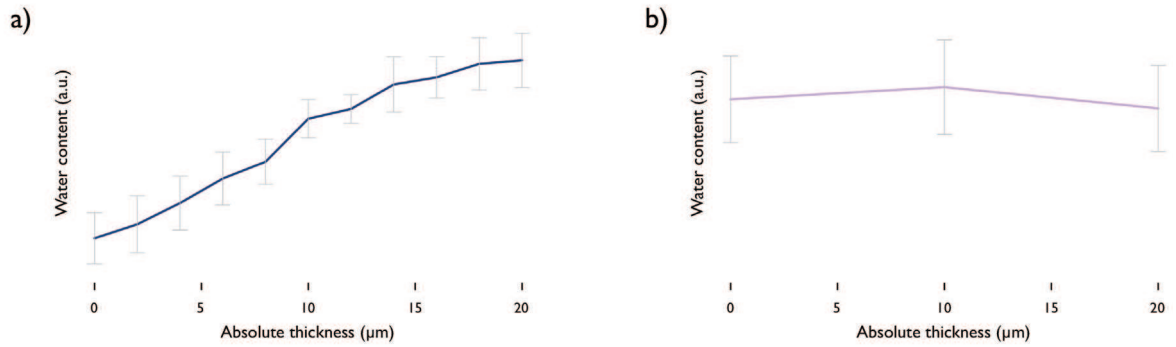

Figure 4 Water content of the *SC* measured by confocal Raman microspectroscopy a) before (measured from 0 to 20 µm in 2 µm steps) and b) after the removal of the *SC* by trypsinisation (measured from 0 to 20 µm in 10 µm steps).

total removal, two different skin surface biopsies were performed. The skin was firstly stripped 3 times with a polymerization time of 2 minutes as recommended [40, 41]. In a second assay the skin was stripped twice but with a polymerization time of 15 minutes.

The histological image Figure 5a shows that after 3 strips with a polymerization time of 2 minutes parts of the *SC* still remained on the skin. On the other hand after two strips with a polymerization time of 15 minutes the *SC* was completely removed, as Figure 5b shows.

Confocal Raman measurements gave similar results. 5 ± 1 µm of the 8 ± 1 µm *SC* remained on the skin after the treatment with 3 strips and a polymerization time of 2 minutes (Figure 6a). After a two strips protocol, an increase in water content was observed in the first 2 - 4 µm and the remaining *SC* thickness was estimated at 1 ± 1 µm (Figure 6b). Before this treatment the *SC* thickness was measured with 10 ± 1 µm.

Fig. 5

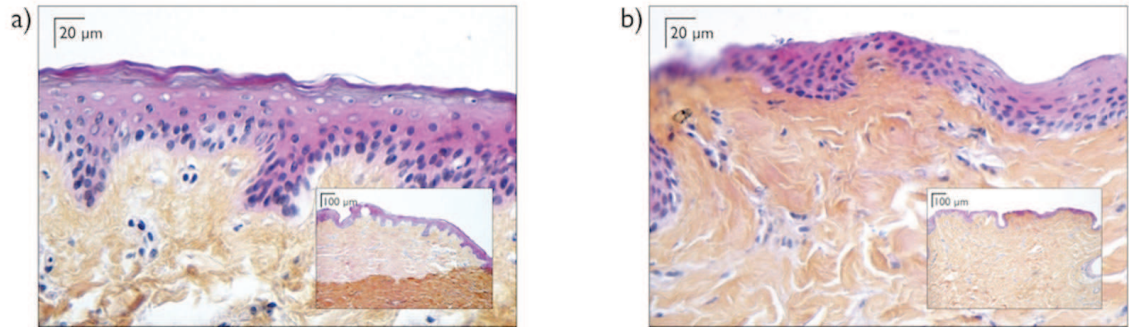

Figure 5: Histological image of a skin after removing the *SC* by a) 3 cyanoacrylate strips using a polymerization time of 2 minutes and b) 2 cyanoacrylate strips using a polymerization time of 15 minutes. The large image corresponds to a magnification 40x and the smaller one shows an overview (magnification 10x).

A summary of the removal quality of the different methods is given in Table 1.

	before treatment	after treatment
Tape Stripping	10 ± 1 µm	inhomogeneous
Trypsinization	9 ± 0.5 µm	0 µm ± 0 µm
Skin surface biopsy 3 strips 2 min	8 ± 1 µm	5 ± 1 µm
Skin surface biopsy 2 strips 15 min	10 ± 1 µm	1 ± 1 µm

Table 1: Summary of the removal qualities measured via confocal Raman microspectroscopy of tape stripping, trypsinization and cyanoacrylate skin surface biopsy using two different protocols. The errors represent the SEM (n=3).

Discussion

Histological imaging and CRM measurements were performed simultaneously to investigate the accuracy of the non-invasive Raman technique for checking the complete *SC* removal depending on the applied method (tape stripping, trypsinization and cyanoacrylate biopsies). Moreover CRM allows the estimation of *SC* thickness. A number of groups published estimations of the *SC* thickness, on the basis of confocal Raman measurements and their corresponding water depth concentration profiles [45, 47, 65]. They differ in the used fitting algorithm of the water content versus skin depth position curve (Figure 4a) and so determined slightly different *SC* thicknesses. This work compares the removed *SC* of a treated skin *in vitro*. The aim is not an exact result of the remained *SC* but a result of the complete removal quality. It was even detailed that the water content in the *SC* was measured in 2 µm steps and that the beginning of the *SC* is defined as the focus of the laser via the microscope camera. The variation of this subjective focus was determined in the range of ±1µm. As the work was focused on the comparison of different *SC* removal methods, the corrections related to the refractive index were not considered.

This work is done on skin samples *in vitro*. Instead of a constant water content in the first micrometer of the skin (*SC*) we could observe a slight increase of water content due to a drying of the skin sample but the steep slope, boundary of *SC* / viable epidermis, could always be indicated (Figure 4). These points led us concluding that the definition used for the determination of *SC* thickness is appropriate for this study and explain why histological imaging was used as a second analytical method for evaluating the removal quality.

Histological imaging and CRM measurements showed an inhomogeneous removal of *SC* by tape stripping. This has to be taken into account in the decision process as to which technique to apply in a particular case.

For instance, applying the tape strips in penetration studies for analyzing the quantity of an active substance is carried out by extraction of the *SC* adhering to the strips. The result is an average measurement over the surface area of the used tape (in this case: 3.8 cm^2) but not all the *SC* will be removed. To evaluate the drug distribution through the SC depth it is important to know exactly the measured axial depth. This

Fig. 6

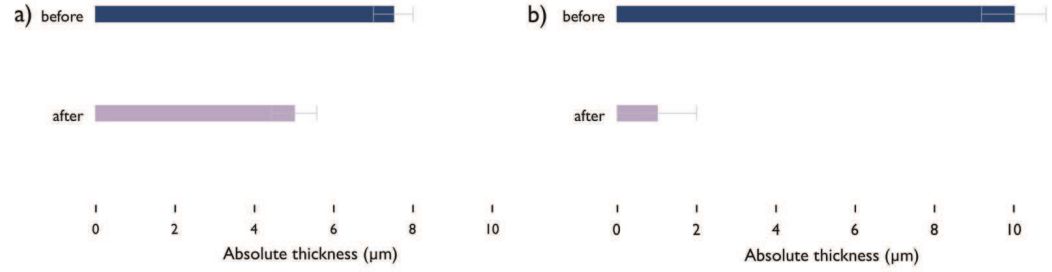

Figure 6: *SC* thickness before and after cyanoacrylate skin biopsy using a) 3 strips with a polymerization time of 2 min b) 2 strips with a polymerization time of 15 min. All points are measured from 0-20 µm in 2µm steps. The error bars represent the SEM (n=3).

can be done *via* TEWL measurements after each tape strip [17, 21]. The result also gives a surface average for the probe area (0.785 cm2) and so the influence of the planar inhomogeneity is seen to become less important. For determination of the depth the removed *SC* of each tape has to be weighted. This is not an accurate method for two reasons. Firstly the mass determination is based on the assumption that strips remove exclusively parts of the *SC*. Sebum and topically applied substances might increase the mass difference for the initial tape strips. Interstitial fluid derived after removal of several tape strips may also increase the mass difference for the strips removed from deeper parts of the skin [22]. Secondly to transform the removed *SC* mass into a depth value the precise *SC* density has to be determined because small variation in the species has an important influence on the results.

To study the influence of a treatment on the skin structure, for example on lipid organization, IR spectroscopy or X-ray diffraction measurements are commonly carried out on a small skin surface and a stripped area [35]. However results have to be interpreted with care because of the showed planar and axial variances in *SC* thickness after stripping.

SC removal by trypsinization was complete and homogeneous. With trypsinization it is possible to receive the whole *SC* in one single sheet. This is important for mechanical and thermal studies on the *SC* [33, 34]. For lipid studies and quantification of active concentration this method is an excellent alternative because the whole *SC* is removed. But firstly it has to be taken into consideration that using this method an axial screening of the *SC* is not possible and secondly that this method uses an aqueous solution of trypsin. For the quantification of water-soluble actives in biopharmaceutical studies this can be a problem because the active can be extracted from the skin into the trypsin solution. Moreover, this method can only be used for *in vitro* studies.

In a comparison with trypsinization, cyanoacrylate glue provides a dry alternative with the same removal qualities when considering a complete separation of the three main skin compartments for active quantification in order to compare different formulations. For mechanical studies this method cannot be used because the *SC* is glued to the glass slide. The same problem applies to axial screening studies which are therefore not possible using this method. But for all studies concerning quantification of substances in the *SC* (active substances, or *SC* lipids), which can be extracted from the sheet glued to the glass slide, it is an easy and quick method.

The only critical point for this method is the protocol, which has to be standardized for the laboratory and justified by histological imaging.

The comparison between histological images and CRM was in good agreement but not so for the cyanoacrylate stripping. In this latter case the histological image Figure 5b showed that after applying 2 strips with a polymerization time of 15 min no significant *SC* was observed but using CRM a *SC* thickness of 1 µm was measured (Figure 6b). These observed differences may be explained by the fact that the skin dried during the two consecutive treatments. Thus the first 2 - 4 µm of the surface was drier than the lower layers of the skin. This demonstrates the limits of the CRM in this special measurement design but it should be noticed that the applied protocol (2 strips and 15 min of polymerization) allowed a uniform and complete removal.

It should be recalled that the cyanoacrylate skin surface biopsy removed also the follicular casts. This is not the case for tape stripping. This fact is made use of in the differential stripping technique, which is a new method that combines the tape stripping method and the cyanoacrylate skin surface biopsy. This method is useful in several experimental designs. Teichmann *et al.* used it to determine the amount of topically applied substances that penetrated into hair follicles [39]. They used tape stripping for removing the part of the *SC* that contained the topically applied dye and the follicular contents were removed by cyanoacrylate skin surface biopsy.

For the depth-screening applications, CRM is an excellent alternative. It is a non-invasive, very exact method that provides small, vertical screening steps. The facilities depend on the existence of a characteristic peak in the recorded spectra from the investigated substance. Absolute qualitative mass balance is complicated in terms of its calibration but possible [66]. The use of CRM for hydration studies or *SC* thickness measurements is easy and quite accurate. Studies on lipid structures

are also possible using this method.

This leads to the overall conclusion that each method has its pros and cons but with the increasing rate of introduction of new techniques well-established methods are likely to become less significant. The future lies in direct non-invasive *in vivo* methods such as CRM.

Conflict of interest

The authors state no conflict of interest.

Acknowledgement

We thank Gattefossé SAS for their financial support of this work and Robin Hillman for insightful discussions and editing of the manuscript.

References

1 Wolf J: Die innere Struktur der Zellen des Stratum Desquamans der menschlichen Epidermis. Zeitschrift für Mikroskopisch Anatomische Forschung 1939;46:170-202.

2 Pinkus H: Examination of the epidermis by the strip method of removing horny layers. I. Observations on thickness of the horny layer, and on mitotic activity after stripping. J Invest Dermatol 1951;16:383-386.

3 Lorincz AL, Usar MC: Skin desquamating machine; a tool useful in dermatologic research. J Invest Dermatol 1957;28:275-282.

4 Benfeldt E, Serup J: Effect of barrier perturbation on cutaneous penetration of salicylic acid in hairless rats: *In vivo* pharmacokinetics using microdialysis and non-invasive quantification of barrier function. Arch Dermatol Res 1999;291:517-526.

5 Choi MJ, Maibach HI: Topical vaccination of DNA antigens: Topical delivery of DNA antigens. Skin Pharmacol Appl Skin Physiol 2003;16:271-282.

6 Jacobi U, Meykadeh N, Sterry W, Lademann J: Effect of the vehicle on the amount of *stratum corneum* removed by tape stripping. J Dtsch Dermatol Ges 2003;1:884-889.

7 Rougier A, Lotte C, Maibach HI: *In vivo* percutaneous penetration of some organic compounds related to anatomic site in humans: Predictive assessment by the stripping method. J Pharm Sci 1987;76:451-454.

8 Al Haushey L, Bolzinger MA, Bordes C, Gauvrit JY, Briançon S: Improvement of a bovine serum albumin microencapsulation process by screening design. Int J Pharm 2007;344:16-25.

9 Benech-Kieffer F, Wegrich P, Schwarzenbach R, Klecak G, Weber T, Leclaire J, Schaefer H: Percutaneous absorption of sunscreens *in vitro*: Interspecies comparison, skin models and reproducibility aspects. Skin Pharmacol Appl Skin Physiol 2000;13:324-335.

10 Bolzinger M-A, Briançon S, Pelletier J, Fessi H, Chevalier Y: Percutaneous release of caffeine from microemulsion, emulsion and gel dosage forms. Eur J Pharm Biopharm 2008;68:446-451.

11 Frelichowska J, Bolzinger M-A, Pelletier J, Valour J-P, Chevalier Y: Topical delivery of lipophilic drugs from o/w pickering emulsions. Int J Pharm 2009;371:56-63.

12 Frelichowska J, Bolzinger M-A, Valour J-P, Mouaziz H, Pelletier J, Chevalier Y: Pickering w/o emulsions: Drug release and topical delivery. Int J Pharm 2009;368:7-15.

13 Potard G, Laugel C, Schaefer H, Marty J: The stripping technique: *In vitro* absorption and penetration of five UV filters on excised fresh human skin. Skin Pharmacol Appl Skin Physiol 2000;13:336-344.

14 Wagner H, Kostka KH, Lehr CM, Schaefer UF: Interrelation of permeation and penetration parameters obtained from *in vitro* experiments with human skin and skin equivalents. J Control Release 2001;75:283-295.

15 Schwarb FP, Gabard B, Rufli T, Surber C: Percutaneous absorption of salicylic acid in man after topical administration of three different formulations. Dermatology 1999;198:44-51.

16 Dupuis D, Rougier A, Roguet R, Lotte C, Kalopissis G: *In vivo* relationship between horny layer reservoir effect and percutaneous absorption in human and rat. J Invest Dermatol 1984;82:353-356.

17 Sheth NV, McKeough MB, Spruance SL: Measurement of the *stratum corneum* drug reservoir to predict the therapeutic efficacy of topical iododeoxyuridine for herpes simplex virus infection. J Invest Dermatol 1987;89:598-602.

18 Darmstadt GL, Mao-Qiang M, Chi E, Saha SK, Ziboh VA, Black RE, Santosham M, Elias PM: Impact of topical oils on the skin barrier: Possible implications for neonatal health in developing countries. Acta Paediatr 2002;91:546-554.

19 Weerheim A, Ponec M: Determination of *stratum corneum* lipid profile by tape stripping in combination with high-performance thin-layer chromatography. Arch Dermatol Res 2001;293:191-199.

20 Kalia YN, Alberti I, Naik A, Guy RH: Assessment of topical bioavailability *in vivo*: The

importance of *stratum corneum* thickness. Skin Pharmacol Appl Skin Physiol 2001;14 Suppl 1:82-86.
21 Schwindt DA, Wilhelm KP, Maibach HI: Water diffusion characteristics of human *stratum corneum* at different anatomical sites *in vivo*. J Invest Dermatol 1998;111:385-389.
22 Weigmann H, Lademann J, Meffert H, Schaefer H, Sterry W: Determination of the horny layer profile by tape stripping in combination with optical spectroscopy in the visible range as a prerequisite to quantify percutaneous absorption. Skin Pharmacol Appl Skin Physiol 1999;12:34-45.
23 Hunter R, Pinkus H, Stelle CH: Examination of the epidermis by the strip method. III. The number of keratin cells in the human epidermis. J Invest Dermatol 1956;27:31-34.
24 Jui-Chen T, Weiner N, Flynn G, Ferry J: Properties of adhesive tapes used for *stratum corneum* stripping. Int J Pharm 1991;72:227-231.
25 Breternitz M, Flach M, Prässler J, Elsner P, Fluhr JW: Acute barrier disruption by adhesive tapes is influenced by pressure, time and anatomical location: Integrity and cohesion assessed by sequential tape stripping. A randomized, controlled study. Br J Dermatol 2007;156:231-240.
26 Reed JT, Ghadially R, Elias PM: Skin type, but neither race nor gender, influence epidermal permeability barrier function. Arch Dermatol 1995;131:1134-1138.
27 Bommannan D, Potts RO, Guy RH: Examination of *stratum corneum* barrier function *in vivo* by infrared spectroscopy. J Invest Dermatol 1990;95:403-408.
28 Ya-Xian Z, Suetake T, Tagami H: Number of cell layers of the *stratum corneum* in normal skin - relationship to the anatomical location on the body, age, sex and physical parameters. Arch Dermatol Res 1999;291:555-559.
29 Black D, Del Pozo A, Lagarde JM, Gall Y: Seasonal variability in the biophysical properties of *stratum corneum* from different anatomical sites. Skin Res Technol 2000;6:70-76.
30 Greene RS, Downing DT, Pochi PE, Strauss JS: Anatomical variation in the amount and composition of human skin surface lipid. J Invest Dermatol 1970;54:240-247.
31 Lademann J, Jacobi U, Surber C, Weigmann H-J, Fluhr JW: The tape stripping procedure--evaluation of some critical parameters. Eur J Pharm Biopharm 2009;72:317-323.
32 Kligman AM, Christophers E: Preparation of isolated scheets of human *stratum corneum*. Arch Dermatol 1963;88:702-705.
33 Wu KS, van Osdol WW, Dauskardt RH: Mechanical properties of human *stratum corneum*: Effects of temperature, hydration, and chemical treatment. Biomaterials 2006;27:785-795.
34 Van Duzee BF: Thermal analysis of human *stratum corneum*. J Invest Dermatol 1975;65:404-408.
35 Caussin J, Gooris GS, Janssens M, Bouwstra JA: Lipid organization in human and porcine *stratum corneum* differs widely, while lipid mixtures with porcine ceramides model human *stratum corneum* lipid organization very closely. Biochim Biophys Acta 2008;1778:1472-1482.
36 Downing D, Abraham W, Wegner B, Willman K: Partition of sodium dodecyl sulfate into *stratum corneum* lipid liposomes. Arch Dermatol Res 1993;285:151-157.
37 Karande P, Jain A, Arora A, Ho MJ, Mitragotri S: Synergistic effects of chemical enhancers on skin permeability: A case study of sodium lauroylsarcosinate and sorbitan monolaurate. Eur J Pharm Sci 2007;31:1-7.
38 Marks R, Dawber RP: Skin surface biopsy: An improved technique for the examination of the horny layer. Br J Dermatol 1971;84:117-123.
39 Teichmann A, Jacobi U, Ossadnik M, Richter H, Koch S, Sterry W, Lademann J: Differential stripping: Determination of the amount of topically applied substances penetrated into the hair follicles. J Invest Dermatol 2005;125:264-269.
40 Montenegro L, Ademola J, Bonina F, Maibach H: Effect of application time of betamethasone-17-valerate 0.1% cream on skin blanching and *stratum corneum* drug concentration. Int J Pharm 1996;140:51-60.
41 Imokawa G, Abe A, Jin K, Higaki Y, Kawashima M, Hidano A: Decreased level of ceramides in *stratum corneum* of atopic dermatitis: An etiologic factor in atopic dry skin? J Invest Dermatol 1991;96:523-526.
42 Röpke EM, Augustin W, Gollnick H: Improved method for studying skin lipid samples from cyanoacrylate strips by high-performance thin-layer chromatography. Skin Pharmacol 1996;9:381-387.
43 Silva CL, Nunes SCC, Eusébio MES, Sousa JJS, Pais AACC: Study of human *stratum corneum* and extracted lipids by thermomicroscopy and dsc. Chem Phys Lipids 2006;140:36-47.

44 Surber C, Schwarb F, Smith E: Tape-stripping technique. Cutan Ocul Toxicol 2001;20:461-474.
45 Crowther JM, Sieg A, Blenkiron P, Marcott C, Matts PJ, Kaczvinsky JR, Rawlings AV: Measuring the effects of topical moisturizers on changes in *stratum corneum* thickness, water gradients and hydration *in vivo*. Br J Dermatol 2008;159:567-577.
46 Caspers PJ, Lucassen GW, Carter EA, Bruining HA, Puppels GJ: *In vivo* confocal Raman microspectroscopy of the skin: Noninvasive determination of molecular concentration profiles. J Invest Dermatol 2001;116:434-442.
47 Pudney PDA, Mélot M, Caspers PJ, Van Der Pol A, Puppels GJ: An *in vivo* confocal Raman study of the delivery of trans-retinol to the skin. Appl Spectrosc 2007;61:804-811.
48 Caspers PJ, Lucassen GW, Puppels GJ: Combined *in vivo* confocal Raman spectroscopy and confocal microscopy of human skin. Biophys J 2003;85:572-580.
49 OECD: Skin absorption: *In vitro* method. OECD Guideline for the testing of chemicals 2004:1-8.
50 Chrit L, Hadjur C, Morel S, Sockalingum G, Lebourdon G, Leroy F, Manfait M: *In vivo* chemical investigation of human skin using a confocal Raman fiber optic microprobe. J Biomed Opt 2005;10:0440071-04400711.
51 Baldwin K, Batchelder D: Confocal Raman microspectroscopy through a planar interface. Appl Spectrosc 2001;55:517-524.
52 Bruneel J, Lassegues J, Sourisseau C: In-depth analyses by confocal Raman microspectrometry: Experimental features and modeling of the refraction effects. J Raman Spectrosc 2002;33:815-828.
53 Everall N: Confocal Raman microscopy: Why the depth resolution and spatial accuracy can be much worse than you think. Appl Spectrosc 2000;54:1515-1520.
54 Everall N: Modeling and measuring the effect of refraction on the depth resolution of confocal Raman microscopy. Appl Spectrosc 2000;54:773-782.
55 Everall N: Depth profining with confocal Raman microscopy, part i. Spectroscopy 2004;19:22-27.
56 Everall N: Depth profiling with confocal Raman microscopy, part ii. Spectroscopy 2004;19:16-25.
57 Gotter B, Faubel W, Neubert RHH: Optical methods for measurements of skin penetration. Skin Pharmacol 2008;21:156-165.
58 Gotter B, Faubel W, Neubert RHH: FTIR microscopy and confocal Raman microscopy for studying lateral drug diffusion from a semisolid formulation. Eur J Pharm Biopharm 2010;74:14-20.
59 Xiao C, Flach CR, Marcott C, Mendelsohn R: Uncertainties in depth determination and comparison of multivariate with univariate analysis in confocal Raman studies of a laminated polymer and skin. Appl Spectrosc 2004;58:382-389.
60 Gniadecka M, Nielsen OF, Wessel S, Heidenheim M, Christensen DH, Wulf HC: Water and protein structure in photoaged and chronically aged skin. J Invest Dermatol 1998;111:1129-1133.
61 Barry BW, Edwards H, Williams A: Fourier transform Raman and infrared vibrational study of human skin: Assignment of spectral bands. J Raman Spectrosc 1992;23:641-645.
62 Tfayli A, Piot O, Pitre F, Manfait M: Follow-up of drug permeation through excised human skin with confocal Raman microspectroscopy. Eur Biophys J 2007;36:1049-1058.
63 Förster M, Bolzinger M-A, Fessi H, Briançon S: Topical delivery of cosmetics and drugs. Molecular aspects of percutaneous absorption and delivery. Eur J Dermatol 2009;19:309-323.
64 Anderson RL, Cassidy JM: Variations in physical dimensions and chemical composition of human *stratum corneum*. J Invest Dermatol 1973;61:30-32.
65 Bielfeldt S, Schoder V, Ely U, van der Pol A: Assessment of human *stratum corneum* thickness and its barrier properties by in-vivo confocal Raman spectroscopy. IFSCC Magazine 2009;1:9-15.
66 Mélot M, Pudney PDA, Williamson A-M, Caspers PJ, Van Der Pol A, Puppels GJ: Studying the effectiveness of penetration enhancers to deliver retinol through the stratum cornum by *in vivo* confocal Raman spectroscopy. J Control Release 2009;138:32-39.

Chapitre 5 Le suivi des composants des formulations cosmétiques dans la peau avec la microspectroscopie confocale Raman

Le transport d'un actif cosmétique ou pharmaceutique dans la peau est le but le plus important des produits dermopharmaceutiques et cosmétiques. Une augmentation de la biodisponibilité de la part du véhicule peut avoir deux origines [104] : premièrement, le coefficient de partage de l'actif entre la formulation et la peau et deuxièmement, la modification physiologique de la barrière cutanée par des promoteurs chimiques pouvant modifier la structure lipidique du *stratum corneum* (appelée rupture de la barrière cutanée ou fluidification des lipides). Dans ce chapitre ces deux causes sont étudiées quantitativement et qualitativement par le suivi de la pénétration du rétinol depuis des formulations simples. Trois tensioactifs, deux hydrophiles (PEG20C12 et PEG20C18 :1) et un lipophile (PEG6C18 :1), sont utilisés à 7 % pour préparer trois émulsions de type huile (55 %) dans eau (37 %) et trois solutions de tensioactifs (utilisation du dodécane ou de l'eau comme solvant selon la solubilité des tensioactifs). L'ensemble des formules contient du rétinol (0,5 %) et BHT (0,5 %) pour stabiliser le rétinol. Avec la CLHP, la concentration de rétinol dans les différentes parties de la peau après une pénétration de 24 h a été mesurée. La MCR est utilisée pour la réalisation du suivi des différents composants des formulations (eau, huile et actif) et pour l'évaluation du paramètre d'interaction latéral des lipides, S_{lat}, permettant de connaitre la modification d'organisation des lipides (fluidification).

Le dodécane et l'eau de la formulation pénètrent dans la peau. Cependant cette pénétration n'est pas différente selon la nature des formulations et ne peut pas être corrélée à celle de l'actif. Toutes les solutions de tensioactifs ont montré une pénétration plus importante du rétinol que les émulsions correspondantes. Les mesures en MCR montrent que la fluidification des lipides la plus importante est provoquée par la solution de rétinol dans du dodécane sans tensioactif. Par contre, la pénétration du rétinol depuis cette solution n'est

quantitativement qu'en deuxième position derrière la solution de PEG6C18 :1 et qu'en troisième position comparativement à l'ensemble des formulations testées. L'étude de cette formulation montre clairement l'effet positif de la fluidification des lipides sur la pénétration du rétinol. La solution de tensioactif PEG6C18 :1 présente le pourcentage de pénétration le plus important. Cette formulation montre un effet synergique de la modification des lipides par une désorganisation et une modification du coefficient de partage du rétinol en faveur de la peau. Aucune des trois émulsions ne montre d'effet sur l'organisation de la couche lipidique. Par contre, les émulsions stabilisées avec du PEG6C18 :1 présentent une pénétration significativement plus importante. Cette augmentation de pénétration est liée à la modification du coefficient de partage.

Les solutions de tensioactif PEG20C12 et C18 :1 ne fluidifient pas les lipides de la couche lipidique comparativement à la peau non traitée. La pénétration du rétinol depuis ces deux formulations est identique mais plus faible par rapport aux formulations utilisant le tensioactif lipophile PEG6C18 :1.

Avec cette étude, l'efficacité de la MCR pour l'obtention d'informations sur la structure de la peau et la distribution de l'actif et d'autres composants de la formulation dans la peau a été évaluée. Pour la suite, il faudrait remplacer les formulations modèles comme celles avec le dodécane pour évaluer des formulations plus complexes et plus proches de celles couramment utilisées.

Les faits marquants :

- La MCR a été mise au point. La sensibilité est suffisante pour pouvoir faire des mesures significatives dans la peau.
- L'influence de l'huile (dodécane) sur la couche lipidique a été mesurée par MCR.

- La fluidification de la couche lipidique par le dodécane augmente le passage de l'actif (rétinol) dans la peau par rapport à l'émulsion aqueuse et aux solutions aqueuses de tensioactif (PEG20C12 et PEG20C18 :1) qui elles, entraînent une fluidification moindre des lipides.

- L'ajout d'un tensioactif (PEG6C18 :1) dans l'huile diminue l'influence sur la couche lipidique mais augmente, par contre, le passage de rétinol à cause, en plus, de sa capacité de modification du coefficient de partage.

- La quantité de rétinol dans le *stratum corneum* n'est pas significativement différente pour les diverses formulations, malgré les modifications de la couche lipidique observées. En revanche ces modifications entraînent une pénétration plus importante dans les couches inférieures, l'épiderme et derme,

- Il y a une distribution du rétinol dans le *stratum corneum* depuis les solutions de tensioactifs, la concentration diminue en fonction de la profondeur. Au contraire avec les émulsions, la quantité de rétinol dans le *stratum corneum* est homogène et indépendante de la profondeur.

Ingredients tracking of cosmetic formulations in the skin: a confocal Raman microscopy investigation

Matthias, Förster [1, 2, 3]; Marie-Alexandrine, Bolzinger [2, 3]; Delphine Ach [2, 3]; Gilles Montagnac [4]; Stephanie Briançon [2, 3]

[1] Gattefossé SAS, St Priest, France

[2] Université de Lyon F-69008, Lyon, France; Université Lyon 1, Institut des Sciences Pharmaceutiques et Biologiques, Laboratoire de Dermopharmacie et Cosmétologie, F-69008, Lyon, France;

[3] Laboratoire d'Automatique et de Génie des Procédés (LAGEP), UMR CNRS 5007, F-69622, Villeurbanne, France

[4] Université de Lyon F 69007, Lyon, France; Université Lyon 1, Laboratoire des Sciences de la Terre UMR 5570 CNRS, ENS de Lyon, Lyon, France

Key words: Formulation ingredient tracking, Skin, Confocal Raman microspectroscopy, Delivery, Retinol

Purpose:

Confocal Raman microspectroscopy (CRM) was used to follow the absorption of retinol, into the skin and to track the absorption of ingredients in topical applied formulations.

Method:

Three surfactants, PEG20C12, PEG20C18:1 (hydrophilic) and PEG6C18:1 (lipophilic), were used in preparing three o/w emulsions and three surfactant solutions all containing retinol. Quantitative retinol penetration studies for 24 h were carried out using Franz diffusion cells. CRM was used to follow the skin penetration of retinol, oil and water and also to study a possible modification of the lipid skin barrier in the *stratum corneum* (*SC*) using the ratio of I_{2880}/I_{2850}.

Results:

The oily surfactant solution containing PEG6C18:1 and dodecane showed the highest retinol penetration rate. This appears to be related both to the short polar head group of the surfactant and to the effect of dodecane on skin lipids. All the surfactant solutions showed a higher penetration rate compared with the corresponding emulsions. CRM measurements showed that the ratios of I_{2880}/I_{2850} were significantly modified using surfactant solutions.

Conclusions

Penetration behavior appeared to be dependent on the surfactant used in the formulation. CRM associated to the Franz cell method gives new insights on permeation of drug related to vehicle or ingredients.

Introduction

The transport of a pharmaceutical or a cosmetic active through the skin is the main goal of dermatological and cosmetical products. The delivery efficacy is always based on the penetration efficacy of actives from the formulation. The enhancement effect of vehicles on skin delivery can be achieved by two approaches (1): firstly the partition of the active from the formulation with the skin (i.e. via vehicles) and, secondly, the modification of the skin barrier by using chemical penetration enhancers which might modify the lipid structure of the skin (termed skin barrier disruption or skin lipids fluidization). The transport of drugs or cosmetic actives that are topically applied can be studied *in vitro* by the diffusion Franz cell

method. Therefore for any new formulation it is possible to determine *in vitro* whether or not an active ingredient is able to penetrate the skin barrier. *In vitro* studies also offer an interesting alternative when optimizing the composition of a formulation in order to achieve the required drug uptake across the skin. However dermatological and cosmetic products are rarely as simple as an aqueous solution and also contain many ingredients, such as surfactants, which influence the active ingredient transport across skin. Until now studies that attempted to predict skin absorption from complex formulations have been few in number; such studies are complicated in nature. (2-4). Recently Grégoire et al. have developed a model to predict the mass of a chemical absorbed into and through skin from a cosmetic or a dermatological formulation obtaining good correlations when taking into consideration the volume fraction of dispersed phase or continuous phase (5). However in their model the penetration-enhancing effects of a formulation matrix were considered to be negligible. In the current study it was decided to choose another approach to optimize active delivery to the skin. It was therefore decided to investigate active absorption and ingredient penetration into the skin by the non-invasive method of confocal Raman microspectroscopy (CRM). CRM was used in several works to study the penetration of drugs or active compounds (6-9), to investigate the influence of skin penetration enhancers (10-12) but also to evaluate skin properties and skin hydration (13, 14). Concerning the first point, several authors demonstrated the applicability of confocal Raman microscopy as a non invasive optical approach to study the delivery and the metabolism of active substances in vitro and in vivo. In some studies retinol was the model active tracked in the skin. Mélot et al, demonstrated, using CRM as analytical method, the enhanced retinol penetration in the presence of skin enhancers. Failloux et al showed a slower release of retinol from microparticles in the epidermis by CRM and an increase of its storage in epidermis (9). In some studies, researchers evaluated in the same time the active penetration but also the effect of these compounds on skin structure. For example, Zhang studied the influence of two solvents, DMSO and chloroform/methanol, on the conformations of keratin. These two solvents are commonly used in dermatological research for studies of permeation enhancement and for extracting lipids from *stratum corneum* (15). They were shown to induce large reversible alterations (alpha-helix to beta-sheet) in the secondary structure of keratin. Tfayli et al. used this method for investigating the penetration of metronidazole in transcutol through human skin in vitro. In a second step they analyzed structural modifications induced by the metronidazole on the skin by studying the changes in the spectral signature of the skin constituents (7).

Confocal Raman microspectroscopy allows simultaneous consideration of both the ingredients and the active penetration and also permits evaluation of the effects of formulation ingredients on the SC lipid bilayers arrangement.

Skin perturbation of lipid bilayers may explain skin enhancement (16) and should be examined carefully when optimizing a formulation (8, 17). CRM was used in this study to follow an active substance, retinol, delivered into the skin from simple surfactant emulsions or surfactant solutions. The surfactants were esters of polyethyleneglycol which varied in the length of both their alkyl chain (hydrophobic part) and their polyethyleneglycol (PEG) chain. It is well known that surfactants affect the permeability characteristics of several biological membranes, including skin (18, 19), and for this reason they can enhance the skin penetration of other compounds as a result of their interactions with intercellular lipids. A series of papers have shown that certain PEG alkyl ethers were effective enhancers for oral, rectal or skin delivery of insulin, heparin and ibuprofen (20-22). In this preliminary study tracking of water and an oily component (dodecane) was first demonstrated, together with the active substance retinol, from three simple o/w emulsions applied to the skin each of which was stabilized by a different surfactant PEG6C18:1, PEG20C12 or PEG12C18:1. Secondly, a comparison was made of the penetration depth for each emulsion ingredient in the *SC* compared with those from surfactant solutions formulated with the same oil (dodecane), and the same surfactant as the corresponding emulsion, in order to understand the component relationships and their different penetration behaviors using CRM. The fluidizing action of surfactants on intercellular lipids was also assessed by CRM. The extent of alkyl chain order was obtained from the ratio $\nu_{asym}CH_2/\nu_{sym}CH_2$, which is a measurement of the relative population of trans and gauche

conformers and of the degree of order of the alkyl chain. (10, 23, 24).

For a better understanding a classical *in vitro* Franz cell experiment was also carried out and classical mass balance of the penetrations into the three main skin compartments (*SC*, epidermis, dermis) was measured, as was permeation through the skin up to the receptor fluid. This work used for the first time CRM results in order to explain differences in retinol penetration behavior observed from the Franz cell experiments

Methodology

Materials

All-trans-retinol and dodecane were purchased from Sigma-Aldrich (Saint Quentin Fallavier, France), Butylhydroxytoluene (BHT) and α-tocopherol acetate were a kind gift from Jan-Dekker (Saint Germain en Laye, France) and the three different polyethyleneglycol esters (PEG6 and PEG20) with the carbon chain lengths of C12 and C18:1 were synthesized by Gattefossé SAS (Saint Priest, France) with a minimum 70 mass-% of monoesters. Oleth-20 was a gift from Croda (Trappes, France), analytical grade methanol was purchased from Carlo Erba (Milan, Italy). Deionized water of 16 $M\Omega.cm^{-1}$ resistivity was used throughout the work. D(26)-n-dodecane was purchased from Cambridge Isotope Laboratories and deuterium oxide from Sigma-Aldrich.

Full-thickness pig skin from the flanks (mean thickness ± SEM = 0.84 ± 0.02 mm) (Laboratoire de Physiologie, Université Claude Bernard Lyon 1, France) was used in the skin absorption experiments. Animals were 3 months old. The skins of three donor animals were washed and excised, the subcutaneous fatty tissue was carefully removed and the skin pieces were stored flat at -20 °C until use. The skin is considered as dead and consequently no metabolism of retinol is likely to occur during skin absorption. It is known that retinol can be converted metabolically, mainly to retinyl esters but also, to a lesser extent, to retinal or retinoic acid (25-27). The thickness of each skin piece was measured with a micrometer (Mitutoyo). TransEpidermal Water Loss (TEWL) was assessed using a Tewameter®TM300 from Courage and Khazaka, Cologne, Germany). These measurements were performed in triplicate on skin pieces just before starting the skin absorption studies. Skin samples with TEWL value higher than 15 $g.m^{-2}\ h^{-1}$ were discarded (28).

	Oily surfactant sol. PEG6C18:1	Emulsion PEG6C18:1 (o/w)	Aq. surfactant sol. PEG20C12	Emulsion PEG20C12 (o/w)	Aq. surfactant sol. PEG20C18:1	Emulsion PEG20C18:1 (o/w)
Retinol	0.52 wt%	0.53 wt%	0.47 wt%	0.50 wt%	0.49 wt%	0.51 wt%
PEG6C18:1	7.35 wt%	7.09 wt%	-	-	-	-
PEG20C12	-	-	7.07 wt%	7.15 wt%	-	-
PEG20C18:1	-	-	-	-	7.00 wt%	7.06 wt%
BHT	0.52 wt%	0.50 wt%	0.49 % wt%	0.59 wt%	0.53 wt%	0.50 wt%
Dodecane	91.61 wt%	54.95 wt%	-	54.60 wt%	-	54.80 wt%
H_2O	-	36.93 wt%	91.97 wt%	37.17 wt%	91.98 wt%	37.13 wt%
Mean diameter (nm±SD)	357.1±43.0	722±1	24.3±1.0	2075±1	17.2±0.1	2578±51
Size distribution	0.34±0.41 (PDI)	0.98±0.01 (Span)	0.80±0.03 (PDI)	0.72±0.03 (Span)	0.49±0.01 (PDI)	1.10±0.06 (Span)
Viscosity (mPa.s)	-	147	-	366	-	236

Table I: Composition of Emulsions and Surfactant Solutions for Quantitative Measurements Using the Franz Cells Method Together with the Mean Diameters of Micelles and Emulsion Droplets Based on a Spherical Model (n=3±SD) and Emulsion Viscosities

	Oily surfactant sol. PEG6C18:1	Emulsion PEG6C18:1 (o/w)	Aq. surfactant sol. PEG20C12	Emulsion PEG20C12 (o/w)	Aq. surfactant sol. PEG20C18:1	Emulsion PEG20C18:1 (o/w)
Retinol	0.51 wt%	0.50 wt%	0.52 wt%	0.38 wt%	0.49 wt%	0.46 wt%
PEG6C18:1	7.13 wt%	7.28 wt%	-	-	-	-
PEG20C12	-	-	7.04 wt%	7.2 wt%	-	-
PEG20C18:1	-	-	-	-	7.23 wt%	7.21 wt%
BHT	0.49 wt%	0.51 wt%	0.73 wt%	0.56 wt%	0.67 wt%	0.53 wt%
n-dodecane	45.73 wt%	27.50 wt%	-	27.02 wt%	-	27.37 wt%
D(26)-n-dodecane	47.96 wt%	27.75 wt%	-	27.05 wt%	-	27.78 wt%
H_2O	-	9.85 wt%	22.65 wt%	9.34 wt%	22.96 wt%	9.19 wt%
D_2O	-	27.04 wt%	69.07 wt%	28.46 wt%	68.65 wt%	27.45 wt%
Mean diameter (nm±SD)	232.9±18.6	585±9	41.0±3.0	1180±1	26.5±0.4	1915±4
Size distribution	0.08±0.03 (PDI)	131.49±21.22 (Span)	0.92±0.03 (PDI)	0.92±0.01 (Span)	0.78±0.01 (PDI)	0.86±0.04 (Span)
Viscosity (mPa.s)	-	137	-	385	-	253

Table II: Composition of Emulsions and Surfactant Solutions for CRM Measurements Together with the Mean Diameters of Micelles and Emulsion Droplets Based on a Spherical Model (n=3±SD) and Emulsion Viscosities

Formulations

Retinol saturation concentration in dodecane containing 0.50% BHT was measured: 16.67±0.660 mg/g (±SD). Its water saturation concentration was obtained from the literature: 0.06 µM (i.e. 17.2 µg/g) at pH 7.3 (29).

A retinol solution in pure dodecane containing 0.50 mass-% of BHT and 0.50 mass-% (5 mg/g) of retinol was tested in the same way as the formulations described below.

All formulations contained 0.5 mass-% of retinol. Three o/w emulsions and three surfactant solutions were prepared using three surfactants differing in their PEG Chain or alkyl chain lengths: PEG6C18:1 (HLB: 11.3) , PEG20C12 (HLB: 17.1) and PEG20C18:1 (HLB: 15.9). Their hydrophilic-lipophilic balance parameter (HLB) values were calculated in accordance with Griffin's method (30). The oil/aqueous phase ratio for emulsions was ~ 55:37 (wt:wt) for stability purposes.

The PEG6C18:1 based surfactant solution was directly prepared in dodecane because of the insolubility of this surfactant in water. Conversely PEG20C12 and PEG20C18:1 surfactant solutions were prepared in water and contained, similarly to the emulsions, retinol as the dispersed phase. Each formulation was prepared twice: the first time for skin absorption studies using the Franz cell method and the second time with deuterated ingredients D(26)-dodecane and deuterium oxide, D_2O (also known as 'heavy water'), for CRM studies. The compositions of the formulations are shown in detail in Table I and II. The batch size for each preparation was 50g and 7g for preparation with heavy water.

To prepare the emulsions, the oil and aqueous phases were mixed together with an UltraTurrax® device (Ika®T25 Germany) working at 9000 rpm for 2-5 min and then at 12000 rpm for 12 min and lastly at 9000 rpm for 20 min at room temperature. Surfactant solutions were prepared by mixing the components together using an ultrasonic bath for 15 min. The stability of retinol in formulations was investigated for 48 h at 20°C.

The retinol degradation was comprised between $8.3x10^{-4}$ $mg.g^{-1}.h^{-1}$.and 0.025 $mg.g^{-1}.h^{-1}$. All formulations were used for skin permeation studies immediately after preparation.

Physicochemical characterizations

Emulsions droplet size distributions were measured by small angle light scattering using a MasterSizer® 2000 (Malvern Instruments Ltd, UK). The refractive indices used for the "optical model" were 1.332 for water and 1.460 for the emulsion droplets. The average size and polydispersity index of retinol droplets dispersed in surfactant solutions was measured by means of dynamic light scattering using a NanoZS® instrument (Malvern Instruments Ltd, UK). The droplet mean sizes are given in Table I and II. The size distributions of the different formulations were monodisperse.

The viscosity of emulsions was measured at 20°C using a Couette rheometer TV-e 05 (Lamy, France) equipped with a mobile system MS-BV 100 rotating at 600 rpm. All emulsions were in a "liquid" state with viscosities between 137 and 385 mPa.s.

Mean size and viscosity both may influence the skin penetration (4). To avoid considering these parameters, the objective was to use emulsions with the same size and viscosity. Results presented in tables I and II show that the mean size varied from 17.2±0.1 nm to 357.1±43.0 nm for the surfactant solutions and from 585±9 nm to 2578±51 nm for emulsions and could be considered as identical for emulsions and the viscosity was not significantly different.

In vitro penetration studies

The thawed skin was mounted in two-chamber glass diffusion cells. The effective penetration area was 2.54 cm^2 and the volume of the receiver chamber was 11 cm^3. The receiver solution was composed of a phosphate buffer at pH 7.4 containing 1.5% Brij®98 (Oleth-20) and 0.1% BHT. Brij®98 and BHT were dissolved in this buffer solution at 60°C; the solution was filtered after cooling. Retinol solubility in the receptor fluid was 45 mg ml^{-1}, its stability was the same as that measured in the formulations.

The study was carried out in occlusive conditions for 24 h in static Franz cells. Freshly prepared formulations were spread uniformly on skin surfaces in the donor compartments of diffusion cells at a retinol concentration of 1900 µg/cm^2. With these quantities an infinite dose and sink conditions were ensured as recommended by OECD guidelines (28). The experiment was repeated six times for each formulation (n = 6). At the end of the study the receptor fluid was removed, filtered and analyzed by high performance liquid chromatography (HPLC). The formulation in each donor compartment was collected in a vial. The remaining formulation was absorbed by 2 filter papers, which were also collected in a vial. The skin samples were then separated into *SC*, epidermis and dermis. The *SC* was separated by the cyanoacrylate skin surface biopsy method. It has been shown in previous work (31) that this method was the most effective for the removal of the entire *SC*. For this procedure a microscope slide (76 x 26 mm; Roth, Karlsruhe, Germany) was coated with cyanoacrylate resin (Loctite® Super Glue-3 from Henkel, France) on the *SC* for a defined polymerization time of 15 min. Removing the slide detached the *SC* (32). The viable epidermis was separated from the dermis by heat treatment in water at 60°C for 45 s. After separation, the epidermis and dermis were cut into pieces with a scalpel. Retinol was extracted, and samples were filtered and analyzed by HPLC. Methanol with 0.5 wt% α-tocopherol acetate was used for the extraction of retinol via a double extraction under agitation. This extraction procedure showed a complete retinol extraction (>99%). On the third extraction no more retinol could be detected in the solvent. Skin samples and biopsy slides were immersed in extracting medium under agitation for 90 min in order to achieve full extraction. Using BHT and α-tocopherol acetate and undertaking all experiments in the dark avoided degradation of retinol under light (33-35).

HPLC analysis of retinol content

The samples were analyzed for retinol content using liquid chromatography with a reverse phase column coupled with a UV detector. The HPLC system from Waters (St Quentin en Yvelines, France) was composed of a Waters 717 injector, a Waters 600 pump, a reverse phase column XTerra®MS C18 (3.9 mm × 150 mm, 5 µm) and a Waters 2996 photodiodearray UV detector working at 325 nm wavelength. Elution with methanol/water (85:15) solvent at 1 cm^3/min flow rate and 25°C gave a retention time of 8.8 min for retinol. Injection volume was 20 µL. The calibration curve for quantitative

analysis was linear up to 85 µg.ml^{-1} and the LOD and LOQ were respectively 15 ng.ml^{-1} and 50 ng.ml^{-1}

HPLC quantitative data analysis

The mean and standard error of the mean (SEM) of n = 6 determinations were calculated. Statistical comparisons were made using the Student's t-test (two-samples assuming different variances) with the level of significance at $p \leq 0.05$.

Confocal Raman microscope studies

The experimental device included a Raman spectrograph (LabRam HR800, Horiba Jobin Yvon) and a confocal microscope probe (BXFM Olympus). The objective used in this experiment was a long working distance 50x of magnitude lens (Mitutoyo) with a numerical aperture of 0.42, operating in air. The excitation source was a green 514.5 nm argon ion laser (Spectra Physics), delivering about 10 mW CW at sample level. The spectrograph was equipped with an air-cooled CCD detector (Synapse, Horiba Jobin Yvon), and a 600-gr/mm grating, which allows the covering of the large spectral range from 200 to 3900 cm^{-1} in three shot acquisitions with a spectral resolution of about 4 cm^{-1}, which is retained at deeper regions. The acquisition time was about 5 s, which enabled rapid measurements to be made at the surface as well as in deeper layers. The surface of the skin was not covered by a window in order to avoid interferences by Raman features generated from the window material itself when in contact with skin. This also limited refractive index effects induced by an additional interface, which could affect the spatial and axial resolutions as discussed by Chrit (28). Data reproducibility was experimentally checked by recording ten successive spectra at the skin surface, which showed only very slight spectral features and intensity variations of less than 3%. The axial resolution, which was a critical factor for these measurements, was determined by plotting the intensity of the Raman peak associated with the Si-Si vibrational mode of silicon at 520 cm^{-1} against the position of the laser focus. The axial resolution was inferred from the full width at half maximum (FWHM) of this response curve with about 5.6 µm using a confocal opening aperture of 200 µm.

Data analysis

To remove the intrinsic skin fluorescence a linear baseline was subtracted. As a result of the loss of light from an increase in scattering when probing deeper into the sample, the signal becomes weaker (17). To be able to compare the intensity of bands in the region 2600 - 3900 cm^{-1} and 1500 - 300 cm^{-1} spectra were equalized for the 2940 cm^{-1} and 1450 cm^{-1} band intensities respectively. The band at 2940 cm^{-1} corresponds to the protein C-H_3 symmetric stretching band, and 1450 cm^{-1} corresponds to the δCH_2 scissoring bands of proteins and lipids in the *SC*. The C-H bands (at 1450 cm^{-1} and 2940 cm^{-1}) protrude outside the protein chain and do not take part in strong intermolecular interactions, therefore the C-H band is not modified by alterations in secondary protein structure and is used for equalization of the spectra (14, 46).

The thickness of the *SC* cannot be measured directly by CRM. But it is known (1) that the

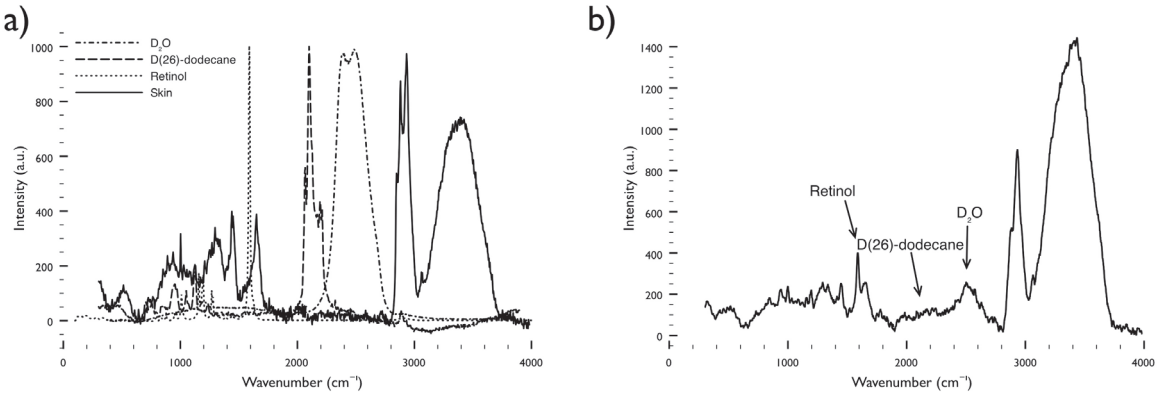

Figure 1: a) Raman spectra of an untreated skin, retinol (1,594cm^{-1}), D(26)-dodecane (2,099cm^{-1}) and heavy water (2500cm^{-1}); b) Raman spectra of a skin treated with an emulsion containing retinol, D(26)-dodecane and heavy water.

water content rises from 13% in the *SC* to >50% in the viable epidermis. To measure the water content the ratio of the C-H (around 2933 cm^{-1}) and O-H stretching bands (around 3250 cm^{-1}) was calculated as described elsewhere (13).

The D(26)-dodecane and deuterium oxide contents were measured following a similar procedure using the characteristic band at 2099 cm^{-1} with an integral area from 2075 to 2115 cm^{-1} for D(26)-dodecane and the band at 2500 cm^{-1} with an integral area from 2340 to 2680 cm^{-1} for D_2O. The retinol content was measured by dividing the intensity of the characteristic band at 1585 cm^{-1} by the intensity of the protein band at 1450 cm^{-1}. The mean and standard error of the mean (SEM) of n = 3 determinations were both calculated. Statistical comparisons were made using the Student's t-test (two-samples assuming different variances) with the level of significance at $p \leq 0.1$.

The ratio I_{2880}/I_{2850} reflects the lateral packing of lipids. The 2880 cm^{-1} band is sensitive to both intra-chain and inter-chain interactions. The integrated intensity and the peak height of the band decrease as intramolecular chain disorder (trans-gauche C-C bond isomerization) increases.

To calculate this ratio the intensities at 2850 cm^{-1} and 2880 cm^{-1} were measured. Each skin sample was measured along the *SC* at 0, 4, 6 and 8 µm and the mean was taken as the Ratio I_{2880}/I_{2850} for the skin sample.

Results

Raman characteristic peak identification

The Raman spectra of D(26)-dodecane and retinol were recorded in order to verify that their characteristic peaks do not interfere (Figure 1). The characteristic peak of D(26)-dodecane at 2099 cm^{-1} and the one for trans-retinol at 1594 cm^{-1} can readily be observed in Raman spectra. Moreover they could easily be observed in skin spectra.

In the same manner, a peak for heavy water (~2500 cm^{-1}) arising from its use in some

Depot	*SC*	Epidermis (E)	Dermis (D)	Receptor Fluid	E+D	Skin	Total
Retinol solution in dodecane; % of applied retinol per cm^2 (%/cm^2/24h)							
96.68 ±0.34	0.05 ±0.01	0.13 ±0.01	0.19 ±0.03	0.01 ±0.01	0.32 0.04	0.37 ±0.04	97.07 ±0.30
Emulsion (o/w) PEG6C18:1; % of applied retinol per cm^2 (%/cm^2/24h)							
103.42 ±0.50	0.11 ±0.01	0.15 ±0.01	0.25 ±0.03	0.00 ±0.00	0.40 ±0.05	0.51 ±0.03	103.94 ±0.51
Oily surfactant solution PEG6C18:1; % of applied retinol per cm^2 (%/cm^2/24h)							
95.77 ±2.42	0.30 ±0.05	0.22 ±0.02	0.23 ±0.01	0.05 ±0.03	0.45 ±0.00	0.75 ±0.06	96.57 ±2.36
Emulsion (o/w) PEG20C12; % of applied retinol per cm^2 (%/cm^2/24h)							
102.93 ±1.54	0.11 ±0.01	0.07 ±0.01	0.12 ±0.01	0.00 ±0.00	0.19 ±0.03	0.29 ±0.03	103.23 ±1.53
Aqueous surfactant solution PEG20C12; % of applied retinol per cm^2 (%/cm^2/24h)							
107.69 ±2.24	0.34 ±0.06	0.06 ±0.01	0.09 ±0.01	0.01 ±0.01	0.15 ±0.02	0.49 ±0.07	108.19 ±2.27
Emulsion (o/w) PEG20C18:1 % of applied retinol per cm^2 (%/cm^2/24h)							
94.15 ±2.96	0.09 ±0.01	0.05 ±0.00	0.13 ±0.01	0.01 ±0.01	0.18 ±0.04	0.28 ±0.02	94.43 ±2.97
Aqueous surfactant solution PEG20C18:1; % of applied retinol per cm^2 (%/cm^2/24h)							
105.05 ±0.80	0.30 ±0.03	0.06 ±0.00	0.05 ±0.01	0.01 ±0.01	0.11 ±0.01	0.41 ±0.04	105.47 ±0.75

Table III: Quantitative penetration results for retinol after 24h as a percentage of the applied quantity per cm^2 in different skin compartments. All results are the mean of 6 experiments (PEG6C18:1 surfactant solution n=12) and the error is the SEM.

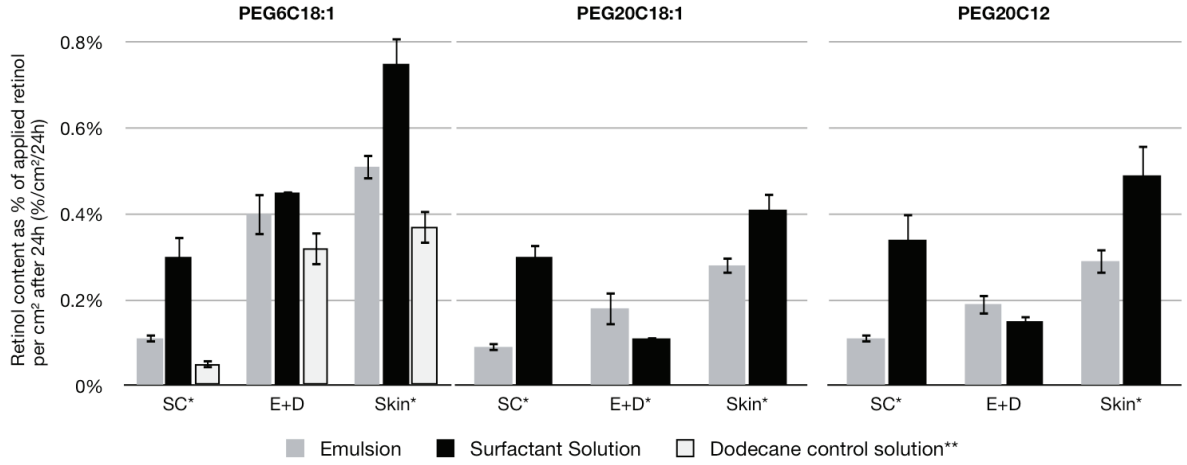

Figure 2: Retinol content given as a percentage of applied retinol per cm2 in different skin compartments (*stratum corneum* (SC), epidermis + dermis (E+D) and the whole skin) after 24 h of exposure time with a surfactant solution, Dodecane control solution (left); from emulsions with surfactants PEG6C18:1 (left), PEG20C18:1 (middle) and PEG20C12 (right). The error bars represent the SEM (n=6 and n=12 for PEG6C18:1 surfactant solution). Columns marked with a * represent a significant difference ($p \leq 0.05$) between the surfactant solution and the emulsion. ** indicate that the retinol content from the surfactant-free dodecane solution is significantly different from the PEG6 surfactant solution in the SC, E+D and skin and from the PEG6 emulsion in the SC and skin.

formulations can be observed independently of endogenous water.

Retinol penetration

The retinol content was measured after 24 h in the donor compartment (depot), *SC*, viable epidermis, dermis and in the receptor fluid. The results are given in Table III as a percentage of applied retinol par cm^2. The first result indicated that no retinol was recovered in the receptor fluid. Therefore only the retinol distribution within skin layers will be compared.

For a better understanding, a comparison will be made, firstly, of the influence of the different formulation types (emulsion and surfactant solution) and, secondly, of the influence of the different surfactants.

Comparison of vehicles

The retinol distribution according to the vehicle is illustrated in Figure 2 and Figure 3.

In Figure 2, the amounts of retinol that penetrated into the whole skin, the lipophilic *SC* (SC), and the hydrophilic part of the skin after 24 h are given as percentages of the applied dose. In Figure 3 the penetration of retinol, is shown, as determined using CRM from the use of formulations based on different vehicles.

Whole skin

Considering complete formulations, it is clear from Figure 2 that surfactant solutions promoted significantly greater retinol absorption in skin when compared with the emulsions.

The distribution of retinol in skin layers is different according to the vehicle used. The control dodecane solution loaded with retinol was compared only with the PEG6C18:1 surfactant solution because of the oily nature of its vehicle.

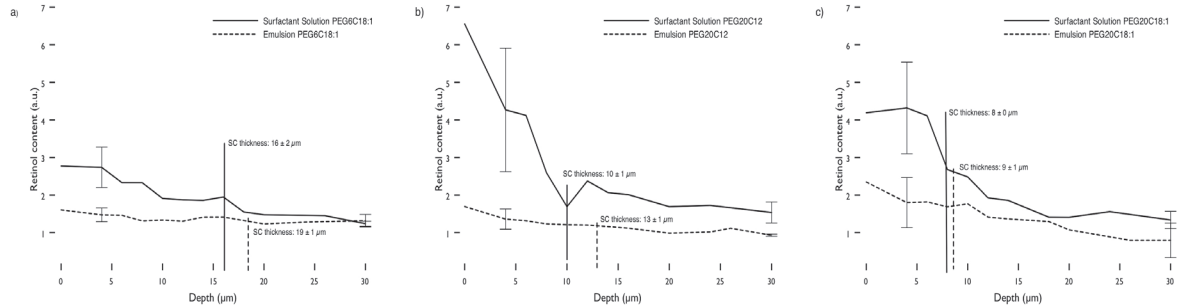

Figure 3: Relative concentration profiles of retinol in the *SC* after 24 h exposure time for an emulsion and an oily surfactant solution using PEG6C18:1 (a), PEG20C18:1 (b) and PEG20C12 (c) in the *SC* as determined by Raman spectroscopy. For better visibility the SEM (n=3) bars are given for 4 and 30 µm. For surfactant solutions the decrease from 4 to 30 µm is significant with $p \leq 0.1$. *SC* thicknesses for skin samples treated with surfactant solution were measured using 16±2 µm (PEG6C18:1), 8±0 µm (PEG20C18:1) and 10±1 µm (PEG20C12). For skins treated with emulsions *SC* thicknesses were 19±1 µm (PEG6C18:1), 9±1µm (PEG20C18:1) and 13±1 µm (PEG20C12).

Stratum corneum

As previously mentioned all emulsions (stabilized by PEG6 or PEG20) were of the oil in water type. The three surfactant solutions were different: the PEG6C18:1 surfactant solution was formulated in dodecane while the other two surfactants were formulated in water. Using the surfactant solutions the penetration of retinol in the *SC* was 0.30±0.05 %/cm2/24 h for the PEG6 (Figure 2 left), 0.30±0.03 %/cm2/24 h for the PEG20C18:1 (Figure 2 middle) and 0.34±0.06 %/cm2/24 h for the PEG20C12 (Figure 2 right). These values were significantly three times higher than for the corresponding emulsions ($p \leq 0.05$) (0.11±0.01 %/cm2/24 h for PEG6C18:1, 0.09±0.01 %/cm2/24 h for PEG20C18:1 and 0.11±0.01 %/cm2/24 h for PEG20C12). Retinol from the control dodecane solution penetrated poorly into the *SC*; (0.05±0.01 %/cm²/24 h) being twice as low as for the PEG6C18:1 (0.11±0.01 %/cm²/24h) emulsion and as much as six times lower than for the oily PEG6C18:1 surfactant solution (0.30±0.05 %/cm²/24h).

Similar results could be observed using CRM (Figure 3). It must be mentioned that no conclusions concerning the quantity of retinol in the epidermis can be made from CRM results as the measurements were only made up to 30µm, and not for the whole skin, as a consequence of technical constraints. The retinol was measured

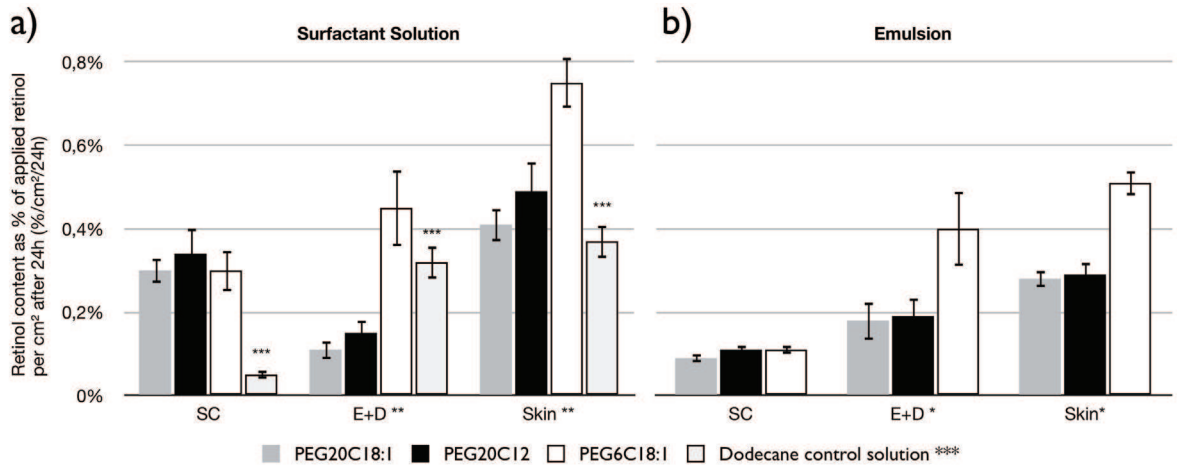

Figure 4: Retinol content given as a percentage of applied retinol per cm2 in different skin compartments *stratum corneum (SC)*, epidermis+dermis (E+D) and the whole skin after 24 h of exposure time with three different surfactant solutions using PEG20C18:1, PEG20C12 and PEG6C18:1, also including the dodecane control solution, (a), and an emulsion stabilized by the same surfactants, (b). The error bars represent the SEM (n=6 and n=12 for PEG6C18:1 surfactant solution). Columns marked with a * represent a significant difference ($p \leq 0.05$) between the PEG6C18:1 and the PEG20 solutions. ** indicates a significant difference between all surfactants, the retinol content difference between the SC and E+D of each surfactant being significant. *** indicates the retinol content from the surfactant free dodecane solution is significantly different from the PEG6C18:1 surfactant solution in the SC, E+D and skin.

from 0 µm to 30 µm under the surface which corresponded to a screening of the whole *SC* and the beginning of the viable epidermis. Significantly more retinol could be observed in the *SC* with a surfactant solution as compared to an emulsion (Table III, Figure 2 and Figure 3). A significant difference ($p \leq 0.1$) between emulsions and surfactant solutions could be observed from the retinol penetration patterns. It is clear from Figure 3 that for surfactant solutions, absorbed retinol quantities decreased significantly from 4 µm to 30 µm while a constant retinol distribution over the same range was observed for emulsions independently of the surfactant used.

Epidermis and dermis

It is interesting to notice that the amounts of retinol recovered from the *SC* were greater for emulsions than for the corresponding surfactant solutions. With the surfactant solutions (PEG20C12 and PEG20C18:1) the retinol content dropped dramatically between the SC and the hydrophilic parts of the skin (Figure 2 and Figure 3). However there was no significant difference between amounts of retinol found in the epidermis and dermis using the different formulations except for the surfactant PEG20C18:1. Emulsions formulated with PEG20C18:1 showed a significantly higher penetration of retinol in these layers than for the corresponding surfactant solutions.

Retinol from the control dodecane solution penetrated into the hydrophilic parts of the skin one third less than for the corresponding PEG6C18:1 surfactant solution.

Comparison of Surfactants

Skin absorption results related to the surfactants are reported in Figure 4.

Whole skin

The results in Figure 4 show that the highest penetration of retinol using PEG6C18 :1 formulations is independent of the vehicle. There were no significant differences between the other two surfactants.

Stratum corneum

It can be seen that the retinol amount in the *SC* is similar for the 3 emulsions used (about 0.1% /cm²/24h). Looking at the data for the surfactant solutions, retinol accumulation was found to be greater than for emulsions (0.32% /cm²/24h) but there were no differences between the three surfactants.

Only the control dodecane solution displayed a significantly lower retinol content (0.05±0.01 %/cm²/24h) in the *SC*.

Epidermis and dermis

As illustrated in Figure 4, the use of both the PEG6C18:1 surfactant solution and the corresponding emulsion showed a significantly higher retinol content in these layers than for the use of the PEG20 surfactant solution and emulsion.

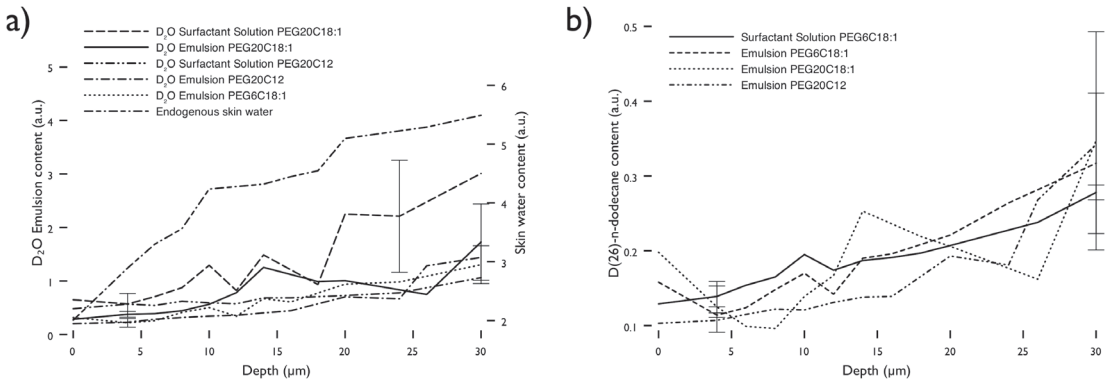

Figure 5: Relative concentration profiles in the *SC* after 24 h exposure time of D2O (a) for the three emulsions and for the two aqueous surfactant solutions using PEG20C18:1 and PEG20C12 together with the endogenous skin water for one skin sample and a comparison of the penetration patterns of D2O and of D(26)-dodecane; (b) for the three emulsions and for the oily surfactant solution with PEG6C18:1 as determined by Raman spectroscopy. For clarity the SEM (n=3) bars are given for 4 and 24 µm (surfactant solution PEG20C18:1) and 30 µm. For all formulations the increase from 4 to 24 and 30 µm is significant with $p \leq 0.1$.

The retinol content of 0.32±0.04 %/cm²/24 h from the control dodecane solution was lower than for the oily PEG6C18:1 surfactant solution but was still higher than for the aqueous PEG20 surfactant solution.

Ingredient penetration (D_2O and D(26)-dodecane penetration) by CRM

The use of CRM allows the water phase of the formulation to be tracked by replacing normal water with deuterium oxide, so-called 'heavy water', D_2O. Figure 5a represents the water content as a function of skin depth penetration. This water profile is similar to that for endogenous water. The water from the formulations penetrated into the skin and increased slowly in the *SC*, then increased more rapidly at the border between the lipophilic *SC* and the hydrophilic viable epidermis reaching values of around 8-9 µm for samples treated with PEG20C18:1, 13-14 µm for samples treated with PEG20C12 and 16-18 µm for samples treated with PEG6. The increases in the three penetration profiles are significant in the range 4 to 30 µm. For a clearer illustration of this only the SEMs for 4 µm, 24 µm and 30 µm are given. No significant differences in the water content between the five formulations could be measured (Figure 5a) nor could any correlation between the use of retinol and water penetration be established.

The dodecane also penetrated into the *SC* and the epidermis (Figure 5b) but between the four formulations no significant differences in the quantities of D(26)-dodecane that penetrated were noticed.

Lateral interaction parameter S_{lat}

Each S_{lat} value was determined in triplicate; and the values are given in Table IV.

Substance used for treating skin	Ratio I_{2880}/I_{2850}
Dodecane	1.192±0.042
Water	1.562±0.012
Emulsion (o/w)	
PEG6C18:1	1.503±0.041
PEG20C12	1.509±0.057
PEG20C18:1	1.441±0.103
Surfactant Solution	
PEG6C18:1 (oily)	1.413±0.033
PEG20C12 (aqueous)	1.779±0.037
PEG20C18:1 (aqueous)	1.546±0.023
Untreated skin (control)	1.615±0.029

Table IV: Ratio of I_{2880}/I_{2850} for Skin Samples After 24 h Treatement. All parameters were determined in triplicate. For clarity the significances are discussed in the text.

Pure dodecane (S_{lat}= 0.328±0.028), without any surfactant, influences the lateral interaction parameter significantly when compared with untreated skin (S_{lat}= 0.610±0.019) and with skin treated with water. This parameter halved in value showing the strong effect of dodecane on lipid fluidization. The oily surfactant solution of PEG6C18:1 also fluidized the lipid layer to a marked extent as indicated by a value of S_{lat}= 0.475±0.022. This is a somewhat smaller decrease than for dodecane but still significant when compared with skin treated with water and with untreated skin.

Water itself appears to have no marked influence on the value of the lateral interaction parameter when compared to untreated skin nor do the emulsions. For the aqueous surfactant solutions only the influence of the PEG20C12 gives a significantly different value when compared with the water treated skin and the untreated skin (Figure 7).

No significant differences were observed for S_{lat} values between the three emulsions. In contrast one of the S_{lat} values for the surfactant solutions was significantly different (Fig.6).

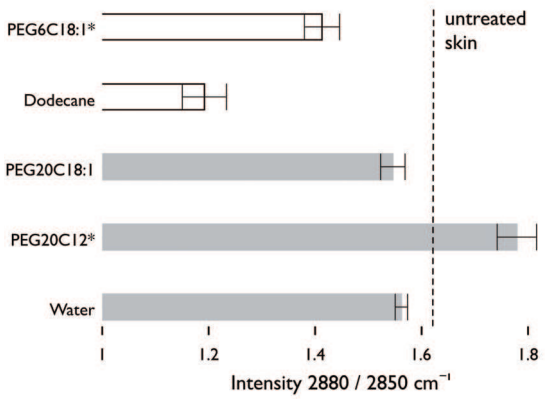

Figure 6: Ratios of I2880/I2850 for skin samples treated with dodecane, water and surfactant solutions; white indicating oily solutions and grey the aqueous solutions. The error bars represent the SEM (n=3). Columns marked with * indicate a significant difference between the ratios of the treated samples as compared with the pure solvent ($p \leq 0.05$); "PEG6C18:1" compared to "dodecane" and "PEG20C12" to "water". All skin samples treated with the surfactant solutions are between themselves significantly different; the same is true for water-treated skin compared with dodecane-treated skin.

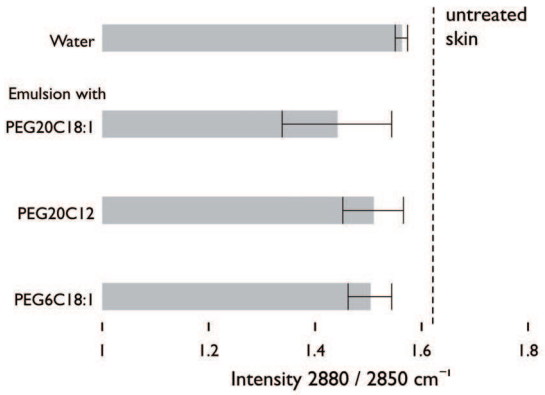

Figure 7: Ratios of I_{2880}/I_{2850} for skin samples treated with water and oil in water emulsions stabilized with PEG6C18:1, PEG20C12 and PEG20C18:1. The error bars represent the SEM (n=3). No significant differences between the ratios of I_{2880}/I_{2850} ($p \leq 0.05$) could be observed.

Discussion

This work aimed at studying the penetration behavior of the main components of retinol formulations in order to better explain the influence of ingredients on the retinol penetration. To achieve this goal the formulations may be very simple in their composition to clarify the mechanism involved.

The formulations were based on retinol, water and dodecane as the main components. Three different surfactants were chosen because these were known to affect drug distributions in skin. The surfactants differed in their alkyl chain lengths and in their PEG numbers.

Dodecane was used as the oily phase because the band from *trans*-retinol at 1594 cm^{-1} and that of D(26)-dodecane at 2099cm^{-1} can be observed simultaneously in Raman spectra (Figure 1a and 1b) without interfering with the main bands from skin.

Retinol surfactant solutions in dodecane or in water were compared with their corresponding emulsions. A retinol solution in dodecane was used as control. PEG6C18:1 was not soluble in water and consequently an oily surfactant solution was formulated in dodecane.

The model drug selected for this study was retinol, a widely used chemical for cosmetic as well as for pharmaceutical purposes. Retinol is highly lipophilic (logP=7.62 (30)) and tends to accumulate in the epidermis (20, 27). This drug is used in dermatological products as an ointment intended for skin repair. In cosmetic products, retinol is known to promote keratinocyte proliferation and to induce epidermal thickening in photo-damaged skin through its biologically active derivative, retinoic acid (22). The objective of this study was not to disclose a formulation that would provide a definite beneficial effect regarding the action of retinol, an action which is mainly located in the basal cells of epidermis and dermis (21), but to use a substance that does not penetrate deeply into the skin so as to evaluate any possible enhancing effects caused by surfactants widely used in cosmetic formulations, and to permit the simultaneous tracking of all formulation ingredients by CRM.

Retinol did not penetrate into the receptor fluid from the different formulations (Table III). This result was expected because, in general, retinol penetrates the skin very poorly (31). In earlier skin absorption studies conducted on human or porcine skin retinol was barely detectable in the receptor fluid (27, 32).

In the present study skin absorption of retinol was limited to between 0.28 and 0.80% of the applied dose. These results are in accordance with those of Jenning et al. (33) who applied a retinol-based nanoemulsion and a SLN suspension ten times less concentrated than in this study. They found a total retinol absorption into the skin of between 0.5 and 0.8% of the applied dose, the exact value depending on the formulation. The total amount of retinol absorbed into the skin is, however, considerably

different from one study to another for retinol dosage formulations varying between 0.1 and 0.5% of retinol. In this study it was found that less than 1% of the applied dose accumulated in the skin while Yourick and Bronaugh (34) found that 10% of the applied dose accumulated in human skin after 24 h and Frelichowska et al. found less than 0.1% accumulation in the skin from o/w emulsions. (27). These results point out the importance of the vehicle on retinol penetration.

In this study o/w emulsions were chosen as vehicles because the major part of topical formulations intended for pharmaceutical or cosmetic uses is based on o/w emulsions. For comparison purpose related to the surfactant effect on the retinol penetration surfactant solutions were also selected.

As previously observed in the literature, surfactants affect retinol penetration into the skin. PEG6C18:1 promoted retinol penetration whatever the formulation and especially so in viable skin. Surfactants have been shown to affect the permeability characteristics of several biological membranes, including skin (14), and for this reason they can enhance the skin penetration of other compounds. Polyethoxylated non-ionic surfactants display penetration enhancement properties (13, 15-17, 35) but at the same time these surfactants can also decrease the permeation of lipophilic drugs into skin due to a decrease in thermodynamic activity when a drug of this type is solubilized in the micelles (35). The hydrophilic-lipophilic balance value (HLB) is not a good indicator of the enhancing effect of a surfactant and therefore many studies have been focused on the influence of the alkyl chain length of the hydrophobic portion of non-ionic surfactants attached to a polar head group in the potency of surfactants as penetration enhancers (17, 36, 37) with a particular enhancing effect for the C12 alkyl chain being observed. A medium length alkyl chain surfactant (e.g. C12) may penetrate the lipid bilayers more easily, because of its proper aqueous solubility and higher critical micellar concentration than a longer alkyl chain surfactant (e.g. C18). However in this study the C12 chain had almost the same effect as a C18:1 chain but the C18 oleic chain is known to exert a strong enhancer effect. Concerning longer alkyl chain lengths, it has been demonstrated earlier that for penetration purposes enhancers containing unsaturated alkyl chains such as C18 appear to have near optimum penetration properties.

The effect of a polar head group of a surfactant is not as clear and in particular in the way in which they influence the activity of surfactants as enhancers. Recently positive effects of polysorbates with short polar head groups on methanol penetration of skin have been reported by Cappel and Kreuter (35). They observed an enhancement effect for PEG-4 sorbitan monolaurate and PEG-5 sorbitan monooleate on methanol penetration. These researchers suggested that surfactants insoluble in water have a significant effect on the leaving tendency of the hydrophilic compound as a result of a higher thermodynamic activity and a modification of the vehicle/*SC* partition coefficient. Moreover, these short surfactants have been shown to affect the barrier properties of skin to a greater extent than do their hydrophilic counterparts. In this study it was noticed that there was a stronger enhancement effect for a PEG6 polar head group compared to a PEG20 polar head group. Park et al. found a similar tendency when studying the influence of polyoxyethylene (POE) alkyl ethers on the permeation of ibuprofen through rat skin. The enhancers containing an ethylene oxide (EO) - chain length of 2-5, an HLB value of 7-9 and a C16-18 alkyl chain length appear to be very effective promoters for the skin permeation of such a drug.

For one particular surfactant (PEG6C18:1) the oily surfactant solution significantly promoted retinol penetration in comparison with a PEG6C18:1 emulsion of the o/w type. PEG6C18:1 also promoted dodecane penetration into the epidermis as evidenced by Figure 4. The impact of surfactant on oil transport was reported by Mélot et al. (11) whose work showed similar enhancement effects. They found a significant effect for Triton X100 and oleic acid on the penetration of Myritol®318 (medium chain triglycerides). They reported oleic acid as a lipid fluidizer and Triton X100 as a lipid extractor but did not relate the observed enhancement effects directly to these two functions. Apart from the role of PEG6C18:1 on retinol penetration, the results of this study suggest a strong effect of the oil on the lipid barrier as shown by the S_{lat} modification.

The results reported in Table IV and illustrated

in Figure 6 show clearly the influence of pure dodecane on untreated skin (S_{lat} = 0.328±0.028) compared with a water treated skin (S_{lat} = 0.575±0.008). Pure dodecane induced the lowest lateral interaction parameter, S_{lat}, indicating the most liquid crystalline lipid conformation in the *SC*. It is noteworthy that this had no influence on the retinol quantity accumulated in the *SC* where the lipid barrier lies. All surfactant solutions showed a similar retinol quantity in the *SC* (~0.31 %/cm2/24 h). The retinol solution in dodecane associated with the most fluid lipid barrier resulted in the lowest retinol quantity in the *SC* (0.05 %/cm2/24 h). However the modified S_{lat} correlated directly to the penetrated retinol amounts in the deeper skin layers. Dodecane showed the second highest retinol quantity in the dermis and epidermis after 24 h (0.32±0.04 %/cm^2/24 h). The highest quantity (0.45±0.00 %/cm^2/24 h) was obtained from PEG6C18:1 surfactant solution in dodecane which gave a S_{lat} of 0.475±0.022. From pure dodecane solution, retinol penetration into epidermis and dermis was smaller than from the PEG6 surfactant solution because of two conflicting effects: while the dodecane affected the lipid barrier, at the same time the surfactant (PEG6C18:1) influenced the partition coefficient between retinol and skin. This effect of the surfactant was missing in the retinol solution prepared with pure dodecane; this may explain why using a skin with the lowest S_{lat} did not result in the highest penetration rate. The lipid fluidizer impact of dodecane on a lipid barrier is well known and related to its skin irritation properties (38), which could explain the 'brutal' penetration enhancement of a dodecane surfactant solution when compared with an aqueous surfactant solution. This hypothesis is reinforced by the S_{lat} value calculated for the PEG6C18:1 o/w emulsion which was not significantly different from the untreated skin or water treated skin (Table IV and Figure 7). In practice, in emulsions, dodecane is always in the disperse phase and the observed differences cannot be assigned to a modification of the lipid barrier but is, more probably, linked to a surfactant effect. The influence of the surfactant on the retinol partition coefficient between the formulation and the skin might explain the higher penetration in epidermis and dermis using PEG6C18:1. To summarize, the particular behavior of PEG6C18:1 appears to be related to its oil solubility and its formulation in dodecane on the one hand, and to its short polar head group on the other.

The hydrophilic surfactants were formulated in aqueous or o/w vehicles. Surfactant solutions also promoted the penetration of retinol but mostly into the *SC*. Hydrophilic surfactants with long polar head groups did not have a similar enhancement effect to that observed with the shorter chain esters as demonstrated earlier by Cappel et al. Additionally no relationship between S_{lat} and the different retinol penetration behaviors was observed with these hydrophilic surfactants (Table IV, Figure 6 and Figure 7).

Only the surfactant solution of PEG20C12 had a significant influence on the lipid barrier with S_{lat} = 0.720±0.025 compared to untreated skin (S_{lat} = 0.610±0.0191) or water treated skin (S_{lat} = 0.575±0.008) (Figure 6). Such an increase in the S_{lat} value corresponds to a solidifying of the lipids. This solidifying effect on the lipid barrier did not appear to have any influence on the retinol penetration into the epidermis and dermis.

The results appear not to be related specifically to the oil or to a change in the S_{lat} value. They appear, instead, to result from a different partition coefficient between the formulation and the skin and, in particular, to the *SC*. In fact it seems that this partition modification can have such a large effect that the quantity of retinol in the *SC* was very similar to that from an oily surfactant solution with a S_{lat} of 0.495 and from an aqueous surfactant solution with a S_{lat} of 0.720.

Conclusion

In this research project the possibility of tracking the main components of two different formulation types, a surfactant solution and an o/w emulsion has been demonstrated. The influence of these components on the penetration behavior of retinol, chosen as a model active substance, has also been studied. The work has shown the necessity for studying the impact of all formulation components for a complete understanding of the penetration behavior of a chosen active substance. The penetration behavior can be influenced by the partition existing between the formulation and the skin (quantified as the partition coefficient) and by modification of the lipid barrier. In this study the combination of these two factors has been shown for each formulation type. Lipid organization was studied through the S_{lat} parameter, which decreases when lipid

fluidization occurs. It has been shown that when the S_{lat} value is low (less than 0.55 in this study), it is possible to link the decrease in the value of this parameter with an enhancement of retinol penetration into the hydrophilic parts of the skin. On the contrary, if the value of S_{lat} is high (~0.55 in this study), a change in value of this parameter is indicative of a change in lipid structure, which then appears to have less influence on penetration behavior. In this latter case, the suggested mechanism for explaining the change in penetration behavior is a change in the partition existing between the formulation and skin retinol (quantified as the partition coefficient) rather than lipid structure influence. Results obtained with the oily soluble surfactant PEG6C18:1 confirmed the influence that a short polar head group has on penetration enhancement. This enhancement was also reinforced by the oil used to dissolve the surfactant, which showed itself as a fluidization effect of the skin barrier.

These fundamental results were only possible through the use of CRM and very simple formulations. Using these techniques the study provided some explanations about the impact of each emulsion component on penetration behavior based on measured results and proof theoretical hypotheses.

Acknowledgments

We thank Gattefossé SAS for their financial support for this work and Robin Hillman for insightful discussion and editing of the manuscript.

Notations

aq	aqueous
BHT	Butylhydroxytoluene
Brij®98	Polyoxyethylene (20) oleyl ether
CRM	Confocal Raman Microscopy
D	Dermis
E	Epidermis
FWHM	Full width half maximum
HLB	Hydrophilic-lipophilic balance parameter
HPLC	High performance liquid chromatography
Myritol®318	Caprylic/Capric Triglyceride
PEG	Polyethyleneglycol
POE	Polyoxyethylene
Rpm	Revolutions per minute
SC	*Stratum corneum*
SD	Standard deviation
SEM	Standard error of the mean
S_{lat}	Lateral interaction parameter

References

1. M. Förster, M.-A. Bolzinger, H. Fessi, and S. Briançon. Topical delivery of cosmetics and drugs. Molecular aspects of percutaneous absorption and delivery. Eur J Dermatol. 19:309-323 (2009).
2. R. Potts and R. Guy. Predicting Skin Permeability. Pharm Res. 9:663-669 (1992).
3. R.H. Guy and J. Hadgraft. Physicochemical aspects of percutaneous penetration and its enhancement. Pharm Res. 5:753-758 (1988).
4. J. Hadgraft and M.E. Lane. Skin permeation: the years of enlightenment. Int J Pharm. 305:2-12 (2005).
5. D. Kessner, A. Ruettinger, M.A. Kiselev, S. Wartewig, and R.H.H. Neubert. Properties of ceramides and their impact on the stratum corneum structure. Part 2: stratum corneum lipid model systems. Skin Pharmacol. 21:58-74 (2008).
6. A.L. Bunge, R.L. Cleek, and B.E. Vecchia. A new method for estimating dermal absorption from chemical exposure. 3. Compared with steady-state methods for prediction and data analysis. Pharm Res. 12:972-982 (1995).
7. A.L. Bunge and R.L. Cleek. A new method for estimating dermal absorption from chemical exposure: 2. Effect of molecular weight and octanol-water partitioning. Pharm Res. 12:88-95 (1995).
8. A. Otto, J.du Plessis, and J.W. Wiechers. Formulation effects of topical emulsions on transdermal and dermal delivery. Int J Cosmet Sci. 31:1-19 (2009).
9. S. Grégoire, C. Ribaud, F. Benech, J.R. Meunier, A. Garrigues-Mazert, and R.H. Guy. Prediction of chemical absorption into and through the skin from cosmetic and dermatological formulations. Br J Dermatol. 160:80-91 (2009).
10. A.C. Williams and B.W. Barry. Penetration enhancers. Adv Drug Deliv Rev. 56:603-618 (2004).
11. M. Mélot, P.D.A. Pudney, A.-M. Williamson, P.J. Caspers, A. Van Der Pol, and G.J. Puppels. Studying the effectiveness of penetration enhancers to deliver retinol through the stratum cornum by in vivo confocal Raman spectroscopy. J Control Release. 138:32-39 (2009).

12. P.D.A. Pudney, M. Mélot, P.J. Caspers, A. Van Der Pol, and G.J. Puppels. An in vivo confocal Raman study of the delivery of trans retinol to the skin. Appl Spectrosc. 61:804-811 (2007).
13. A. López, F. Llinares, C. Cortell, and M. Herráez. Comparative enhancer effects of Span® 20 with Tween® 20 and Azone® on the in vitro percutaneous penetration of compounds with different lipophilicities. Int J Pharm:133-140 (2000).
14. A.T. Florence. Surfactant interaction with biomembranes and drug absorption. Pure Appl Chem. 53:2057-2068 (1981).
15. E.S. Park, S.Y. Chang, M. Hahn, and S.C. Chi. Enhancing effect of polyoxyethylene alkyl ethers on the skin permeation of ibuprofen. Int J Pharm. 209:109-119 (2000).
16. K. Ichikawa, I. Ohata, M. Mitomi, S. Kawamura, H. Maeno, and H. Kawata. Rectal absorption of insulin suppositories in rabbits. J Pharm Pharmacol. 32:314-318 (1980).
17. S. Guarini and W. Ferrari. Structural restriction in bile acids and non-ionic detergents for promotion of heparin absorption from rat gastro-intestinal tract. Arch Int Pharmacodyn Ther. 271:4-10 (1984).
18. B.P. Gaber and W.L. Peticolas. On the quantitative interpretation of biomembrane structure by Raman spectroscopy. Biochim Biophys Acta. 465:260-274 (1977).
19. A. Tfayli, E. Guillard, M. Manfait, and A. Baillet-Guffroy. Thermal dependence of Raman descriptors of ceramides. Part I: effect of double bonds in hydrocarbon chains. Anal Bioanal Chem. 397:1281-1296 (2010).
20. C. Antille, C. Tran, O. Sorg, and J. Saurat. Penetration and metabolism of topical retinoids in ex vivo organ-cultured full-thickness human skin explants. Skin Pharmacol:124-128 (2004).
21. S.B. Kurlandsky, E.A. Duell, S. Kang, J.J. Voorhees, and G.J. Fisher. Auto-regulation of retinoic acid biosynthesis through regulation of retinol esterification in human keratinocytes. J Biol Chem. 271:15346-15352 (1996).
22. T.C. Roos, F.K. Jugert, H.F. Merk, and D.R. Bickers. Retinoid metabolism in the skin. Pharmacol Rev. 50:315-333 (1998).
23. OECD. Guidance Document for the conduct of skin absorption studies. OECD Series on testing and assessment:31 (2004).
24. E.Z. Szuts and F.I. Harosi. Solubility of retinoids in water. Arch Biochem Biophys. 287:297-304 (1991).
25. W.C. Griffin. Calculation of HLB values of non-ionic surfactants. J Soc Cosmet Chem. 5:249-256 (1954).
26. L. Montenegro, J. Ademola, F. Bonina, and H. Maibach. Effect of application time of betamethasone-17-valerate 0.1% cream on skin blanching and stratum corneum drug concentration. Int J Pharm. 140:51-60 (1996).
27. J. Frelichowska, M.-A. Bolzinger, J. Pelletier, J.-P. Valour, and Y. Chevalier. Topical delivery of lipophilic drugs from o/w Pickering emulsions. Int J Pharm. 371:56-63 (2009).
28. L. Chrit, C. Hadjur, S. Morel, G. Sockalingum, G. Lebourdon, F. Leroy, and M. Manfait. In vivo chemical investigation of human skin using a confocal Raman fiber optic microprobe. J Biomed Opt. 10:044007 (2005).
29. P.J. Caspers, G.W. Lucassen, E.A. Carter, H.A. Bruining, and G.J. Puppels. In vivo confocal Raman microspectroscopy of the skin: noninvasive determination of molecular concentration profiles. J Invest Dermatol. 116:434-442 (2001).
30. T. Loftsson and D. Hreinsdóttir. Determination of aqueous solubility by heating and equilibration: a technical note. AAPS PharmSciTech. 7:E1-E4 (2006).
31. H.P. Gollnick and U. Dümmler. Retinoids. Clin Dermatol. 15:799-810 (1997).
32. V. Jenning, M. Schäfer-Korting, and S. Gohla. Vitamin A-loaded solid lipid nanoparticles for topical use: drug release properties. J Control Release. 66:115-126 (2000).
33. V. Jenning and S.H. Gohla. Encapsulation of retinoids in solid lipid nanoparticles (SLN). J Microencapsul. 18:149-158 (2001).
34. J.J. Yourick, C.T. Jung, and R.L. Bronaugh. In vitro and in vivo percutaneous absorption of retinol from cosmetic formulations: significance of the skin reservoir and prediction of systemic absorption. Toxicol Appl Pharmacol. 231:117-121 (2008).
35. M.J. Cappel and J. Kreuter. Effect of nonionic surfactants on transdermal drug delivery: I. Polysorbates. Int J Pharm:143-153 (1991).
36. B.Y. Zaslavsky, N.N. Ossipov, V.S. Krivich, L.P. Baholdina, and S.V. Rogozhin. Action of surface-active substances on biological membranes. II. Hemolytic activity of nonionic surfactants. Biochim Biophys Acta. 507:1-7 (1978).
37. K.A. Walters, M. Walker, and O. Olejnik. Non-ionic surfactant effects on hairless mouse skin permeability characteristics. J Pharm

Pharmacol. 40:525-529 (1988).
38. R.J. Babu, A. Chatterjee, and M. Singh. Assessment of skin irritation and molecular responses in rat skin exposed to nonane, dodecane and tetradecane. Toxicol Lett. 153:255-266 (2004).

Chapitre 6 L'influence de la chaîne carbonée des tensioactifs PEG20 esters sur la pénétration d'un actif des émulsions simples

La compréhension de l'influence des composants d'une formulation sur la pénétration percutanée est indispensable pour pouvoir développer des formulations efficaces. Dans ce chapitre, la pénétration des émulsions simples est testée. Les émulsions simples contiennent seulement un actif, une huile, de l'eau et un tensioactif pour les stabiliser. Divers tensioactifs et huile ont été testés afin d'évaluer l'influence de la longueur de la chaine carbonée du tensioactif et de la polarité de l'huile. Le choix des tensioactifs et des huiles est lié à des formulations commerciales. Les huiles utilisées sont le Cocoate BG® (Butylene glycol cocoate) à 20 %, le MOD (Octyldodecyl Myristate) à 20 % et la paraffine liquide à 20 et 50 % selon la stabilité. Les tensioactifs sont du type non-ionique, esters de polyéthylène glycol avec une chaine carbonée en C8, C12, C18 et C18 :1, ce dernier ayant une liaison insaturée au 9ème atome de carbone. Les tensioactifs ont été utilisés à 3 % (en majorité) ou 6 % selon la stabilité de la formulation. L'actif principal de cette étude est la caféine (1,5 %), un actif hydrosoluble. Le rétinol est utilisé dans un deuxième temps à 0,5 % pour vérifier si le comportement observé avec la caféine, actif hydrophile localisé dans la phase externe de l'émulsion, est retrouvé avec un actif lipophile situé dans la phase dispersée de l'émulsion.

Si l'on considère la quantité de caféine dans le liquide récepteur à 24 h, plusieurs points peuvent être soulignés. Tout d'abord on constate une diminution de la pénétration de la caféine depuis les solutions de tensioactifs en comparaison à la solution aqueuse. La solution de tensioactif en C12 en particulier limite la pénétration de façon significative par rapport à la solution et par rapport aux autres tensioactifs. L'augmentation de la longueur de la chaine carbonée provoque une augmentation de la pénétration de la caféine. Cette tendance a été montrée dans plusieurs études utilisant des tensioactifs avec les mêmes chaines carbonées et des PEG9, PEG10 [8] et PEG20 [9].

Concernant les émulsions, une diminution de la pénétration de la caféine est également observée par rapport à la solution avec un effet couplé de l'huile et du tensioactif. Seules les émulsions stabilisées par les tensioactifs en C18 et C18 :1 montrent un effet promoteur de la pénétration, qui reste cependant plus faible qu'à partir de la solution. La chaine carbonée ayant une insaturation augmente la pénétration, cela a déjà été observé lors de l'étude précédente avec le rétinol et le dodécane et dans la littérature [10,11].

Cependant, avec un actif lipophile, le comportement et la pénétration sont modifiés. Toutes les solutions de tensioactifs dans l'huile montrent une augmentation de la pénétration du rétinol dans la peau (*stratum corneum*, épiderme, derme) par rapport à l'huile seule. Une influence très forte du tensioactif PEG20C18 en solution est observée. Ce dernier augmente significativement la pénétration du rétinol (facteur ~20) par rapport aux formulations contient PEG20C12 et C18 :1. Les PEG20C12 et PEG20C18 :1 conduisent à une pénétration du même ordre de grandeur, la quantité retrouvée dans la peau est 5 fois supérieure à celle obtenue avec la solution mais 4 fois inférieure à celle obtenue avec le PEG20C18.

Lorsque le rétinol est formulé en émulsion, la pénétration dans la peau est similaire pour les 3 formulations et la quantité retrouvée est proche de celle obtenue avec les solutions de PEG20C12 et C18 :1. En revanche une distribution différente du rétinol dans les couches de la peau est observée, les émulsions favorisent le passage dans les couches viables.

Les deux actifs étudiés présentant des propriétés physicochimiques différentes, leur pénétration dans la peau l'est également. Avec la caféine, nous nous sommes intéressés à la perméation et aux quantités retrouvées dans le liquide récepteur à 24 h, alors que pour le rétinol, ce sont les quantités retrouvées dans les couches de la peau qui ont été considérées, le caractère lipophile du rétinol limitant la pénétration, il n'est pas retrouvé dans le liquide récepteur. Par ailleurs, les quantités retrouvées dans le liquide récepteur ou dans la peau pour le rétinol, exprimées en pourcentage de la dose appliquées, sont largement inférieures pour le rétinol. Le comportement des deux actifs peut cependant être comparé en considérant

les formulations à base de Butylene glycol cocoate comme huile. Il apparaît premièrement que l'ajout d'un tensioactif dans une solution aqueuse de caféine diminue la quantité de caféine pénétrée dans la peau, contrairement à ce qui est obtenu avec le rétinol. Ajouter un tensioactif dans une solution huileuse de rétinol augmente de manière significative la quantité d'actif pénétrée dans le *stratum corneum*, en particulier avec le tensioactif PEG20C18.

Si l'on considère les émulsions, les 3 tensioactifs n'induisent pas de différence significative pour la pénétration du rétinol, qui reste cependant plus importante depuis les émulsions par rapport à la solution huileuse. L'effet promoteur des tensioactifs stabilisant les gouttelettes de rétinol dans l'émulsion est ici mis en avant. Avec la caféine, la pénétration depuis les émulsions est plus faible qu'avec la solution aqueuse, sauf l'huile MOD avec comme tensioactif le PEG20C18 :1.

L'augmentation de la pénétration avec certains tensioactifs est très souvent expliquée par l'interaction du tensioactif avec les régions intercellulaires du *stratum corneum,* qui augmentent la fluidification et solubilisent ou extraient des composants lipidiques de la barrière de la peau.

Ces hypothèses peuvent maintenant être vérifiées par le MCR. Pour compléter les études de ce chapitre et pour pouvoir donner des explications basées sur des résultats expérimentaux, il faut vérifier l'influence des formulations utilisées sur le paramètre d'interaction latérale des lipides. Les huiles utilisées n'ont pas d'influence sur la couche lipidique comme c'était le cas pour le dodécane. La question qui reste à élucider est si les tensioactifs en solution dans ces trois huiles ont un effet sur la couche lipidique.

Les faits marquants :

- Les tensioactifs en solution aqueuse diminuent la pénétration de la caféine par rapport à une solution aqueuse.

- Effet promoteur de la pénétration du rétinol des tensioactifs en solution dans le Butylene glycol cocoate, en particulier PEG20C18.

- En émulsion, la pénétration de la caféine augmente avec l'augmentation de la longueur de chaine carbonée. Elle reste inférieure à celle de la solution.

- En émulsion (Butylène glycol cocoate), la pénétration du rétinol est supérieure à celle obtenue avec la solution huileuse. Il n'y a pas de différence significative entre les tensioactifs.

Förster et al. Influence of the carbon chain lenght in PEG20 ester surfactants on the pénétration behaviour of a model active in simple formulations. En rédaction

Influence of the carbon chain length in PEG20 ester surfactants on the penetration behaviour of a model active in simple formulations

Matthias, Förster [1, 2, 3]; Marie-Alexandrine, Bolzinger [2, 3]; Jocelyne Pelletier [2, 3]; Gilles Montagnac [4]; Stephanie Briançon [2, 3]

[1] Gattefossé SAS, St Priest, France

[2] Université de Lyon F-69008, Lyon, France; Université Lyon 1, Institut des Sciences Pharmaceutiques et Biologiques, Laboratoire de Dermopharmacie et Cosmétologie, F-69008, Lyon, France;

[3] Laboratoire d'Automatique et de Génie des Procédés (LAGEP), UMR CNRS 5007, F-69622, Villeurbanne, France

[4] Université de Lyon F 69007, Lyon, France; Université Lyon 1, Laboratoire des Sciences de la Terre UMR 5570 CNRS, ENS de Lyon, Lyon, France

Key words: Confocal Raman microspectroscopy, Polyethyleneglycol ester, Retinol, Caffeine, Penetration, Franz diffusion cells

In the modern dermatology and more detailed in the modern medical cosmetology it is well known that the formulation intended for topical skin delivery influence the penetration quality. The delivery efficacy is always based on the penetration efficacy of actives from the formulation. This formulation based increase in penetration can be achieved by two approaches: first the partition of the active from the formulation to the skin (i.e. via transport vehicles) and second the modification of the skin barrier using chemical penetration enhancer and/or lipid disruption/fluidization. The transport of drugs or cosmetic actives that are topically applied can be studied using *in vitro* diffusion studies such as the diffusion Franz cell method ((1)). Therefore for any new drug preparation it is now possible to determine *in vitro* whether the pharmaceutically active ingredient is able to penetrate the skin "barrier". *In vitro* studies also offer an interesting alternative when optimizing the composition of a formulation to achieve the required drug uptake across the skin. Several authors have set models to describe transport properties of solutes through the skin. As example Potts and Guy (2) developed an equation correlating skin permeability to solute molecular weight and octanol/water partition coefficient. Later, models have been developed to increase fit of the data taking in consideration new parameters such as hydrogen bonding, melting point, and interactions between the lipid chains and the solute (3) (4) (5-7) or pathways for transdermal solution diffusion (8) (9-11). However dermatological products are rarely simple. The main ingredients in a cosmetic emulsion are water, oil and surfactant but especially in commercial formulations a lot of other ingredients like fragrances or thickener are used to increase the formulation stability, change the aspect of the product or influence its sensory properties. These ingredients can have an influence on the penetration behaviour of the drug. Williams has written a review about general absorption promoters and their mechanism (12). This paper shows that it is very difficult to compare different studies in this topic because from one study to another there are often a lot of formulation parameters that changed. Until now studies that attempt to predict skin absorption from complex formulations were little scarce and obviously this is a complicated task (1, 13-16).

For avoiding side effects of additional formulation ingredients and to guaranty a study of each emulsion component this work used simple oil in water emulsions and their corresponding surfactant solutions. This approach allowed changing only one parameter at the time. Two different actives, caffeine, a hydro soluble active and retinol a liposoluble active were used. These two ingredients are standard actives used in skin penetration studies. Caffeine (logP=-0.07) is widely used because it permeates well in the skin related to its low logP

value and moreover it is not metabolized in the skin (17-19). Caffeine is commonly used in cosmetic products due to its slimming effect. However, the active site of caffeine is the adipocytes located in the hypodermis. It has to reach this skin layer to be efficient. (20-22). Retinol is highly lipophilic (logP=7.62 (23) (24)) and tends to accumulate in the epidermis (25) (26) (18) (27). This drug is used in dermatological products as an ointment intended for skin repair. In cosmetic products retinol is known to promote keratinocyte proliferation and to induce epidermal thickening in photo-damaged skin through its biologically active compound: retinoic acid (28) (29).

Surfactants are one of the most important groups of adjuvants in pharmaceutical or cosmetic preparations. They are necessary to stabilize emulsions and can be classified in ionic and non-ionic ones. This paper will compare non-ionic surfactants (ester of polyethyleneglycols, PEG) with different hydrophilic-lipophilic-balance (HLB) values. The HLB can be modified by changing the repeating PEG unit and/or the carbon chain length and their saturation degree. The literature reports penetration modification effects by PEG ethers. Two principal surfactant properties influence the skin penetration of an active: first the carbon chain length and the length of the PEG, second the presence of an insaturation in the carbon chain and its conformation (cis/trans) (30-34).

In this work firstly the kinetic penetration of caffeine into the skin from simple oil in water o/w emulsions varying the oil (Butylene glycol Cocoate or BGC, Octyldodecyl Myristate or ODM and liquid paraffin) was measured using Franz cells diffusion method. In these formulations caffeine was mainly dissolved in the continuous phase. The oils differ in their polarity described by the interfacial tension values ranging from 50 mN/m for the liquid paraffin to less than 10 mN/m for BGC by passing through 20 mN/m for ODM. Secondly the penetration of retinol entrapped in the core of the oil droplets was investigated using o/w emulsions using BCG as oily phase and surfactant solutions. As retinol does not reach the receptor fluid after 24 h under the applied conditions skin absorption was evaluated in each skin layer.

Even in 1959, Higuchi explained that surfactants possess a particular affinity for membranous structures. As a result a nonionic surfactant can possibly emulsify the sebum, enhance the thermodynamic affinity of drugs or change the diffusion constant and activity coefficient of drugs, all of which would permit easier penetration of the drugs or active substances into the cells (35). Therefore it can be concluded that ultrastructural modifications of the *stratum corneum* caused by enhancer and surfactants may play a major role in percutaneous absorption.

Walters et al. explained the observed enhancement effect of these surfactants by a penetration of the surfactant into the intercellular regions of the *stratum corneum*, which increase fluidity and eventually solubilise and extract lipid components. (36, 37).

For these reasons this study will secondly investigate the impact of the formulation on the lipid barrier by a non-invasive method, the confocal Raman microspectroscopy (CRM).

This new technique allows considering in the same time the ingredients and the drug penetration but also allows evaluating the effect of formulation ingredients on the stratum corneum lipid bilayers arrangement. Skin perturbation of lipid bilayers may explain skin enhancement (38) (39) (12) and should be examined carefully when optimizing a formulation (40, 41). The fluidizing action of surfactants on intercellular lipids was assessed by CRM measuring the degree of alkyl chain order. The extent of alkyl chain order was obtained from the ratio $\nu_{asym}CH_2/\nu_{sym}CH_2$, which is a measurement of the relative population of trans and gauche conformers and of the degree of order of the alkyl chain. (42-44). The 2880 cm^{-1} is sensitive to intra- and interchain interactions. The integrated intensity and peak height of the band decrease as intramolecular chain disorder (trans-gauche C-C bond isomerisation) increases. About 50% of the relative intensity of this band is influenced by trans-gauche rotamer content. Lateral packing interactions between chains contribute to the other 50% of the intensity of the 2880 cm^{-1} band; less interactions resulting in lower intensity. Except for transitions in crystal packing, there is relatively little change observed in the 2850 cm^{-1} band in lipid transitions. Therefore, the peak height ratio I_{2880}/I_{2850} is used to monitor the change in the peak height of the 2880 cm^{-1} band.

In this paper the penetration of caffeine from three different o/w emulsions and surfactant solutions will be compared. In the emulsions the hydrosoluble caffeine is located in the continuous phase. Retinol is a lipophilic active and in oil in water emulsions located in the disperse phase. To compare the different penetration behavior of a hydrophilic and lipophilic active the retinol penetration of the same oil in water emulsion (BGC) will be measured. Caffeine, which penetrates into the receptor fluid the permeation and the flux will be measured. For the retinol, which does not penetrate into the receptor fluid, the skin distribution, quantity of penetrated retinol in the *stratum corneum*, epidermis and dermis, will be measured. The influence of these formulations on the skin barrier, the *stratum corneum* lipid layer, will be analyzed using CRM.

Methodology

Materials

Caffeine anhydrous (HPLC grade) was purchased from Carlo-Erba (France), Paraffin liquid with a surface tension of 50mN/m from Cooper (France), BGC (Butylene glycol cocoate) with a surface tension <10mN/m and ODM (Octyldodecyl Myristate) with a surface tension of 20mN/m from Gattefossé (France). *All-trans* Retinol and n-dodecane were purchased from Sigma-Aldrich (Saint Quentin Fallavier, France), Butylhydroxytoluene (BHT) and α-tocopherol acetate were a kind gift from Jan-Dekker (Saint Germain en Laye, France) and four different polyethyleneglycol esters (PEG20) with the carbon chain length of C8 (HLB=18.1), C12 (HLB=17.1), C18 (HLB=15.9) and C18:1 (HLB=16) were synthesized by Gattefossé SAS (Saint Priest, France) with minimum 70 mass-% of monoesters. The HLB values were calculated according to the Griffin's method (45). Oleth-20 was a gift from Croda (Trappes, France), analytical grade methanol was purchased from Carlo Erba (Milan, Italy). Deionized water of 16 $M\Omega.cm^{-1}$ resistivity was used throughout the work.

Full-thickness pig skin (mean thickness ± SEM = 0.84 ± 0.02 mm) (Laboratoire de Physiologie, Université Claude Bernard Lyon 1, France) was used in the skin absorption experiments. The flank skins of 3 donor animals were washed and excised, the subcutaneous fatty tissue was carefully removed and the skin pieces were stored flat at -20 C until use but not longer than 4 months. The skin is considered as dead and consequently no metabolism of retinol may occur during skin absorption study as we know that retinol is converted in vivo mainly to retinyl esters but also in retinal or retinoic acid in a less extent (25, 46) (47, 48) (29). The thickness of each skin piece was measured with a micrometer (Mitutoyo). TransEpidermal Water Loss (TEWL) was measured using a Tewameter®TM300 from Courage and Khazaka (Cologne, Germany). The measurements were performed in triplicate on skin pieces just before performing the skin absorption studies. The skin samples with TEWL value higher than 15 $g.m^{-2}\ h^{-1}$ were discarded (49).

Formulations

Caffeine formulations

The compositions and quantities of the surfactant solutions and emulsions used for skin absorption studies are presented in Table 1. The 100% are filled up with deionised water. The used Caffeine concentration is with 1.5% in water around the saturation concentration of Caffeine at room temperature (2%). In the formulations (surfactant solutions and emulsions) the caffeine concentration is lower (~1.44 and ~1.15%). Using higher Caffeine concentration in the formulations provoked a phase separation and crystallisation of Caffeine. It can be assumed that the used caffeine concentrations are near the saturation concentration and the thermodynamic activity is similar in all used formulations.

Surfactant solutions

Each surfactant was diluted in an aqueous caffeine solution by heating the suspension under continuous stirring to 70°C for 5 min then cooling it down to room temperature.

Emulsions

Four o/w emulsions and four surfactant solutions were prepared with four surfactants differing by their PEG Chain or Alkyl chain length: PEG20C8, PEG20C12, PEG20C18 and PEG20C18:1.

Oil	Oil conc (w/w)	Surfactant	Surfactant conc (w/w)	Caffeine (w/w)	Water conc (w/w)	Size / Span	Viscosity (mPa.s)
Caffeine	-	-	-	1.49%	98.51%	-	-
Caffeine	-	PEG20C8	3.24%	1.44%	95.32%	-	-
Caffeine	-	PEG20C12	3.15%	1.44%	95.41%	-	-
Caffeine	-	PEG20C18	3.34%	1.44%	95.60%	-	-
Caffeine	-	PEG20C18:1	3.09%	1.44%	95.47%	-	-
BGC	20.02%	PEG20C12	3.00%	1.15%	75.83%	1798±1nm / 1.56±0.00	14
BGC	20.00%	PEG20C18	3.00%	1.15%	75.85%	1115±28nm / 2.20±0.02	82
BGC	19.99%	PEG20C18:1	3.02%	1.15%	75.84%	2727±1nm / 1.47±0.05	13
ODM	20.01%	PEG20C8	6.00%	1.10%	72.89%	2481±2µm / 2.34±0.00	13
ODM	20.01%	PEG20C12	5.99%	1.10%	72.90%	2692±2nm / 2.56±0.00	16
ODM	20.00%	PEG20C18	3.02%	1.15%	75.83%	3379±3nm / 3.98±0.02	13
ODM	20.00%	PEG20C18:1	6.01%	1.10%	72.89%	3121±4nm / 3.17±0.01	20
Liquid paraffin	20.01%	PEG20C12	6.01%	1.10%	72.88%	6088±183nm / 2.54±0.10	18
Liquid paraffin	50.00%	PEG20C18:1	6.00%	0.66%	43.34%	2638±1nm / 1.44±0.00	66

Table 1: Composition of caffeine containing solutions, surfactant solutions and emulsions with corresponding physical characterisations (±SD). The emulsion compositions used for retinol and caffeine are highlighted in gray.

The aqueous (caffeine solution) and oil phases (surfactant and oil) were heated up to 70°C. The emulsion was prepared by slow addition of the internal phase (oily) to the external phase under continuous stirring with an UltraTurrax® (Germany) at 12,500 rpm during 3 min. The emulsion was thereafter stirred with a TurboTest® (Rayneri/VMI, Montaigu, France) at 1000 rpm and maintained at 500 rpm during further 15 min until the temperature reached 25°C.

The o/w type of the emulsions was checked by the electrical resistance measurements. The electrical resistance was measured with a DT-830 B conductivity meter) and very high (<2000 kΩ.cm) which is equal with water, measured at same conditions, showing that water is the continuous phase.

Retinol formulations

Retinol saturation concentration was measured with 15.98±4.54 mg/g (±SD) in BGC containing 0.5% of BHT. Its water saturation concentration is 0.06 µM at pH 7.3 (50).

All retinol solutions and emulsions contained 0.5 mass-% of BHT to avoid the retinol degradation.

Three o/w emulsions and three surfactant solutions were prepared with three surfactants differing by their PEG Chain or Alkyl chain length: PEG20C12, PEG20C18 and PEG20C18:1. The oil/aqueous phase's ratio for emulsions was adapted for stability purposes. The emulsions formulated with BGC had the same quantitative composition for the two active substances studied.

Oil	Oil conc (w/w)	Surfactant	Surfactant conc (w/w)	Retinol (w/w)	Water conc (w/w)	Size / Span	Viscosity (mPa.s)
BGC	98.84%	-	-	0.59%	-	-	-
BGC	96.02%	PEG20C12	2.96%	0.50%	-	-	-
BGC	95.95%	PEG20C18	3.02%	0.52%	-	-	-
BGC	91.44%	PEG20C18:1	2.98%	0.50%	-	-	-
BGC	19.94%	PEG20C12	3.04%	0.50%	76.52%	1444±3nm / 1.58±0.00	97
BGC	20.00%	PEG20C18	3.05%	0.47%	75.98%	2417±57nm / 1.67±0.43	87
BGC	20.18%	PEG20C18:1	3.10%	0.49%	75.73%	1414±405nm / 0.84±0.17	90

Table II: Composition of retinol containing solutions, surfactant solutions and emulsions with corresponding physical characterisations (±SD). The emulsion compositions used for retinol and caffeine are highlighted in gray.

The surfactant solutions were prepared in water and contained retinol as dispersed phase similarly to emulsions. The compositions of the formulations are shown in details Table II

To prepare the emulsions, the oil and aqueous phases were mixed together with an UltraTurrax® device (Ika®T25 Germany) working at 9000 rpm for 2-5 min and then at 12000 rpm for 12 min and lastly to 9000rpm for 20 min at room temperature. Surfactant solutions were prepared by mixing the components together using an ultrasonic bath for 15 min. The stability of retinol in formulations was investigated for 48 h at 20°C. All formulations were used for skin permeation studies immediately after preparation.

Physicochemical characterisations

Emulsions droplet size distributions were measured by small angle light scattering using a MasterSizer® 2000 (Malvern, UK). The refractive indices used for the "optical model" were 1.332 for water and 1.460 for the emulsion droplets. The measurements were performed in triplicate.

The viscosity of emulsions was measured at 20°C using a Couette rheometer TV-e 05 (Lamy, France) equipped with a mobile system MS-BV 100 rotating at 600 rpm.

In vitro penetration studies

The thawed skin was mounted in two-chamber glass diffusion cells. The effective penetration area was 2.54 cm^2. The study was carried out, for retinol containing formulation in occlusive conditions, for 24 h in static Franz cells. 1 ml (corresponding ~0.7g for all emulsions and the oily surfactant solutions and 1g for the aqueous surfactant solutions) of freshly prepared formulations were spread uniformly on the skin surface in the donor compartment of diffusion cells. The experiment was repeated six times for each formulation (n = 6).

Caffeine formulation

The receptor compartment contained 14 ml of 0,01M PBS pH 7,2 (Sigma). Caffeine solubility in the receptor fluid was 20 mg/g at room temperature. 1 ml of sample was applied on the skin surface and the donor chamber was closed to avoid evaporation this sink conditions also called infinite dose could be assumed according to the OECD guidelines (49).

The cells were placed in a water bath at 37°C providing a skin surface temperature of 32°C because of heat loss. The skin was equilibrated with the receptor fluid for 1.5 h before applying the formulations.

UV-spectroscopy analysis of caffeine content

The receptor phase was continuously pumped in a UV Spectrometer and every 15 min the absorption was measured at a wavelength of 271 nm. For quantification a calibration curve from 0 µg/ml to 411.4 µg/ml with 11 different points and an equation of $y=0.009x+0.0362$ and a $R^2=0.999$ was used. The replication for each experiment was $n \geq 6$. The lower detection limit was 0,422 µg/ml.

Data analysis Caffeine

The cumulated quantity of caffeine ($g.cm^{-2}$) permeating through the skin was plotted against time. The steady-state flux (JSS) was estimated from the slope of the linear part of the

permeation profile ($R^2 \geq 0.99$). The standard error of the mean (SEM) of $n \geq 6$ samples was calculated. Statistical analysis was performed using the Student's t-test and the differences were considered significant when $p \leq 0.05$.

Retinol formulations

The volume of the receiver chamber was 11 ml. The retinol solubility in the receptor fluid was 45 mg/g. The receiver solution was composed of a phosphate buffer at pH 7.4 containing 1.5% Brij®98 (Oleth-20) and 0.1% BHT. Brij®98 and BHT were dissolved in the buffer solution at 60°C; the solution was filtered after cooling.

At the end of the study the receptor fluid was removed, filtered and analyzed by HPLC. The formulation in the donor compartment was collected in a vial. The remaining formulation was absorbed by 2 filter papers, which were also collected in a vial. Then the skin samples were separated into *stratum corneum*, epidermis and dermis. The *stratum corneum* was separated by the cyanoacrylate skin surface biopsy method. We showed in a previous work (study under publication) that this method was the most adequate to remove the entire *stratum corneum*. For this procedure a microscope slide (76 x 26 mm; Roth, Karlsruhe, Germany) was coated with cyanoacrylate resin (Loctite® Super Glue-3 from Henkel, France) on the *stratum corneum* for a defined polymerization time of 15 min. Removing the slide detached the *stratum corneum* (51). The viable epidermis was separated from the dermis by heat treatment in water at 60°C for 45 s. After separation, the epidermis and dermis were cut into pieces with a scalpel. Retinol was extracted, and samples were filtered and analyzed by HPLC. Methanol with 0.5 wt% α-tocopherol acetate was used for extraction of retinol. Skin samples and biopsy slides were immersed in extracting medium under agitation for 90 min in order to achieve full extraction. All experiments were undertaken in the dark to avoid degradation of retinol under light exposure (18).

HPLC analysis of retinol content

The samples were analyzed for retinol content using liquid chromatography with a reverse phase column. The HPLC set up from Waters (St Quentin en Yvelines, France) was composed of a Waters 717 injector, a Waters 600 pump, a reverse phase column XTerra®MS C18 (3.9 mm × 150 mm, 5 µm) and a Waters 2996 photodiodearray UV detector working at 325 nm wavelength. The elution with methanol/water (85:15) solvent at 1 ml/min flow rate and 25°C gave a retention time of 8.8 min for retinol. Injection volume was 20 µL. The calibration curve for quantitative analysis was linear up to 84.73 µg/g and the detection limit for retinol was 491 pg.

HPLC quantitative data analysis

The mean and standard error of the mean (SEM) of n = 6 determinations were calculated. Statistical comparisons were made using the Student's t-test (two-sample assuming different variances) with the level of significance at $p \leq 0.05$.

Confocal Raman microscope studies

The experimental device included a Raman spectrograph (LabRam HR800, Horiba Jobin Yvon) and a confocal microscope probe (BXFM Olympus). The objective used in this experiment was a long working distance 50x of magnitude (Mitutoyo) with a numerical aperture of 0.42, operating in air. The excitation source was a green 514.5 nm argon ion laser (Spectra Physics), delivering about 10 mW CW (continuous wave) at sample level. The spectrograph was equipped with an air-cooled CCD detector (Synapse, Horiba Jobin Yvon), and a 600-gr/mm grating, which allows the covering of the large spectral range from 200 to 3900 cm^{-1} in three shot acquisitions with a spectral resolution of about 4 cm^{-1}, which is conserved at deeper regions. The acquisition time was about 5 s, which enabled to perform rapid measurements at the surface as well as in deeper layers. The surface of the skin was not covered with a window to avoid interferences of Raman features generated by the window material itself in contact with the skin, but also to limit the refraction index effects induced by an additional interface, which might affect the spatial and namely axial resolution as discussed by Chrit (52). Data reproducibility was experimentally checked by recording ten successive spectra at the skin surface, showing very slight spectral features and intensity variations of less than 3%. The axial resolution, which was a critical achievement for our measurements, was determined by plotting the intensity of the Raman peak associated to the Si-Si vibrational mode of silicon at 520 cm^{-1} against

the position of the laser focus. The axial resolution was inferred from the full width at half maximum (FWHM) of this response curve with about 5.6 µm with a confocal opening aperture of 200 µm.

Data analysis

To get rid of the intrinsic skin fluorescence a linear baseline was subtracted. Due to the loss of light from an increase in scattering when deeper probing in the sample, the signal get weaker (41). To be able to compare the intensity of bands in the region 2600 - 3900 cm^{-1} and 1500 - 300 cm^{-1} spectra were equalized for the 2940 cm^{-1} and 1450 cm^{-1} band intensity respectively. The band at 2940 cm^{-1} corresponds to the protein C-H_3 symmetric stretching band, and 1450 cm^{-1} corresponds to the δCH_2 scissoring bands of proteins in the *stratum corneum*.

The ratio I_{2880}/I_{2850} reflects the lateral packing of lipids. The 2880 cm^{-1} band is sensitive to both intra-chain and inter-chain interactions. The integrated intensity and the peak height of the band decrease as intramolecular chain disorder (trans-gauche C-C bond isomerization) increases.

To calculate this ratio the intensities at 2850 cm^{-1} and 2880 cm^{-1} were measured. Each skin sample was measured along the *SC* at 0, 4, 6 and 8 µm and the mean was taken as the Ratio I_{2880}/I_{2850} for the skin sample.

Results and Discussion

Caffeine penetration

The penetration quality depends on two main effects (53): firstly the partition of the active between the formulation and the skin (i.e. via vehicles) and, secondly, the modification of the skin barrier by using penetration enhancers which might modify the lipid structure of the skin (termed skin barrier disruption or skin lipids fluidization). These effects can be provoked by all formulation components specially the oil and the surfactant.

In the present study PEG esters were selected because they are widely used to formulate cosmetic emulsions but surprisingly their effects on skin absorption of drugs were scarcely studied in the literature conversely to PEG ethers or sorbitan derivatives. Enhancement by nonionic surfactant is a complicated task. Depending on the polarity of the drug entrapped in micelles or not, different enhancer effects of surfactant related to their chemical structures have been observed in the literature. For instance, Cappel and Kreuter (54) studied the skin absorption of methanol and octanol from saline solutions containing various concentrations of polysorbates. Depending on the alcohol polarity and the PEG or alkyl chain length of the surfactants various behaviors were observed. Guarini et al. (31) noticed an enhancing effect of polyoxyethylene ether with C16 and C18 alkyl chain length on heparin

Oil	Oil conc (w/w)	Surfactant	Surfactant conc (w/w)	% of applied quantity/24h	Flux [µg.cm^{-2}.h^{-1}]
Caffeine				36.90±3.30	91.01±7.29
Caffeine		PEG20C8	3.24%	25.20±3.87	60.10±8.63
Caffeine		PEG20C12	3.15%	10.31±0.90	25.81±1.76
Caffeine		PEG20C18	3.34%	19.70±2.23	48.76±4.96
Caffeine		PEG20C18:1	3.09%	27.48±4.37	64.77±9.72
BGC	20.02%	PEG20C12	3.00%	31.49±3.44	60.66±6.28
BGC	20.00%	PEG20C18	3.00%	21.21±2.55	42.56±4.44
BGC	19.99%	PEG20C18:1	3.02%	30.55±3.20	58.97±5.62
ODM	20.01%	PEG20C8	6.00%	15.90±2.23	29.89±3.68
ODM	20.01%	PEG20C12	5.99%	27.05±4.45	50.20±7.51
ODM	20.00%	PEG20C18	3.02%	39.71±3.79	75.37±6.70
ODM	20.00%	PEG20C18:1	6.01%	63.68±6.94	117.52±11.74
Liquid paraffin	20.01%	PEG20C12	6.01%	15.07±1.88	28.72±3.01
Liquid paraffin	50.00%	PEG20C18:1	6.00%	27.74±4.37	31.48±4.44

Table III: Caffeine penetration results from an aqueous solutions, aqueous surfactant solutions and oil in water emulsions with three different oils after 24h (SEM).

penetration by the oral route while Ichikawa (30) noticed that insulin was preferentially absorbed using polyoxyethylene ether with a C12 chain. Florence (55) noticed that the C12 chain has an intermediate solubility between oil and water. A medium alkyl chain length surfactant may penetrate the lipid bilayer easily, because of its proper aqueous solubility and higher critical micelle concentration than a longer alkyl chain surfactant. The hydrophilic–lipophilic balance (HLB) alone does not seem a reliable predictor of the absorption enhancing capability, but the size and shape of both the alkyl chain and the polar group (e.g. POE) influence absorption-enhancing ability (32).

Therefore the study was conducted using two actives the first one caffeine was dispersed in the continuous phase of the emulsion and the second one retinol was entrapped in the micelles of the surfactant or in the droplets of emulsion.

Influence of surfactant

Comparing the caffeine penetration from surfactant solutions with the penetration from an aqueous caffeine solution showed that the penetration of the latter one was surprisingly significantly higher (Fig 1a).

These results are in accordance with those of Cappel and Kreuter who studied the penetration of methanol through hairless mouse skin. Polysorbate 20, 21, 80 and 81 at a concentration around 3 % did not influence methanol penetration but had no particular retarding effect. A significant retarding effect on skin absorption was obtained when they used octanol instead of methanol (54).

Sarpotard and Zatz (56) studied the influence of polysorbate 20 and 60 on lidocaine penetration through hairless mouse skin in vitro. They showed that in a solution containing 40 % propylene glycol, the addition of either surfactant results in a decrease in the lidocaine penetration rate, the magnitude of which depends on the surfactant concentration. They explained that by micellar solubilization of lidocaine, which lowers its activity in the vehicle.

Among the surfactant solutions only a significant difference between the PEG20C12 and the others could be observed. A particular effect of PEG surfactant with C12 chain length was also observed in other studies. Guarini who studied the oral absorption of heparine using non-ionic ether surfactants, found the lowest penetration with the oleyl derivative and even less with lauryl derivatives compared to cetyl or stearyl polyoxyethylene ethers. A two times less absorption was observed with PEG10C12 compared to PEG10C16 and PEG10C18 and the lowest absorption rate was even observed with PEG9C12 compared to the other tested surfactants (PEG10C12, PEG10C18, PEG10C18:1) (31).

Adding a very polar oil (BGC) to the surfactant solution, for obtaining an emulsion, did not influence caffeine transport through the skin, which was always lower than from the aqueous solution. No significant influence of the surfactants on the caffeine penetration behavior could be measured (Fig 1b). Only the PEG20C18 stabilized emulsion showed a significant lower penetration than the other two emulsions. Compared to the aqueous solution the emulsion dosage form caused a significant retarding effect of caffeine penetration.

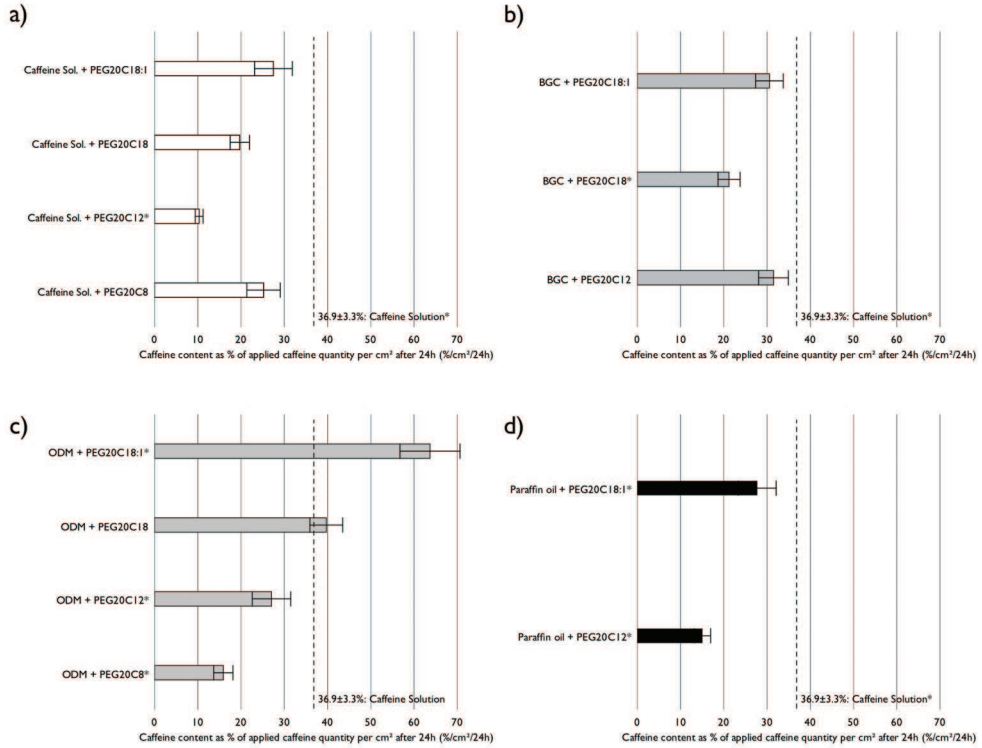

Figure 1: Caffeine content in the receptor fluid given in percentage of applied caffeine quantity per cm2 after a 24h exposition with a) the four different surfactant solutions using PEG20C8, PEG20C12, PEG20C18 and PEG20C18:1; b) stable oil in water emulsions with the oil BGC; c) stable oil in water emulsions with the oil ODM; d) stable oil in water emulsions with the oil Paraffin The error bars represent the SEM (n=6) and columns marked with a * represent a significant difference ($p \leq 0.05$) to the other ones. The result obtained with caffeine solution is indicated on each graph by a dotted line.

For the ODM emulsions a significant trend of an increasing caffeine penetration provoked by the surfactants can be observed. Caffeine penetration seems correlated to the increase of the surfactant carbon chain length. PEG20C8 and C12 emulsions still showed the retarding effect but using the PEG20C18 and C18:1 the penetration of caffeine became greater than the aqueous caffeine solution (Fig 1c).

Park et al evaluated in vitro on rat skin the penetration of ibuprofen from aqueous surfactant solutions with a surfactant concentration of 15% w/w. They tested several polyoxyethylene alkyl ethers ranging from C12-C18:1. For PEG20C16 they found the same penetration rate than for their control aqueous solution. When they used PEG20C18 the penetration rate increased by a factor two. Conversely to the results of the present study, an unsaturation in the carbon chain length had no effect. The penetration rate with PEG20C18:1 was not significantly different to the rate obtained using PEG20C18 (32). This result was also observed by Sarpotdar and Zatz (57) with hydrocortisone an apolar drug from polysorbate solution. They investigated the influence of polysorbates 20, 40, 60 and 80 on hydrocortisone penetration in vitro. All vehicles tested contained water and varying concentrations of propylene glycol. Skin penetration was significantly enhanced from vehicles containing both propylene glycol and one of the polysorbates mentioned above. The hydrocortisone penetration rate increased as the fatty acid chain length of the surfactant grew from 12 to 18 carbon atoms (polysorbate 20 to 60). There was no effect on hydrocortisone penetration due to unsaturation of the surfactant fatty acid chain (polysorbate 60 vs polysorbate 80).

Park et al. didn't observe a retarding effect with PEG20 surfactants but they didn't evaluate smaller carbon chain length than C16 and they studied a very poorly soluble drug, ibuprofen with a water solubility of 0.11 mg/ml at 32°C entrapped in the core of micelles when surfactants were added. For stability purpose, in the present study the percentage of surfactant was 6% with PEG20C18:1 instead of 3 % for the emulsion formulated with PEG20C18 and could also participate to the enhanced flux noticed for that surfactant (117.52 ± 11.74 $\mu g.cm^{-2}h^{-1}$). This

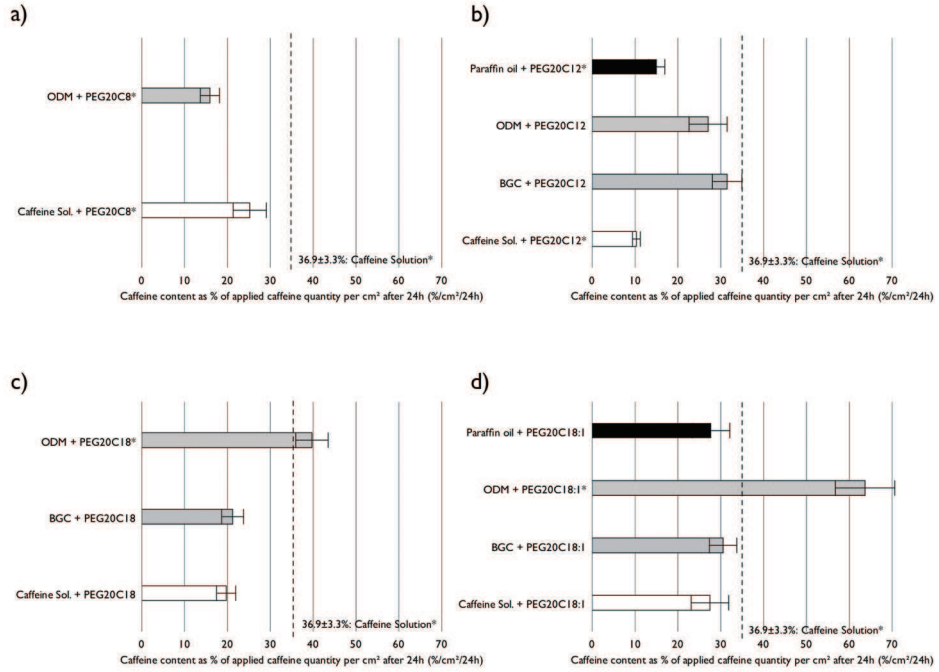

Figure 2: Caffeine content given in percentage of applied retinol quantity per cm2 in the receptor fluid after 24h exposition with a) the four different surfactant solutions using PEG20C8, PEG20C12, PEG20C18 and PEG20C18:1 including the aqueous caffeine solution as control; b) stable oil in water emulsions with the oil BGC; c) stable oil in water emulsions with the oil ODM; d) stable oil in water emulsions with the oil Paraffin The error bars represent the SEM (n=6) and columns marked with a * represent a significant difference ($p \leq 0.05$) to the other ones.

hypothesis shouldn't be excluded even if Cappel and Kreuter didn't notice for polysorbate 80 using methanol a concentration effect of the surfactant on methanol absorption.

Using the paraffin oil, only 2 emulsions were stable enough for skin absorption study. The penetrated caffeine was similar to the surfactant solutions and the trend of higher carbon chain length provoking more caffeine penetration could be observed (Figure 1d).

Influence of oil

For remembering the comparison between the aqueous caffeine solution and the aqueous surfactant solutions showed that all surfactants slowed down caffeine absorption (Fig 1a). Only the addition of oil and the use of emulsions modified caffeine absorption and the results showed a certain enhancement effect depending on the oil and surfactant.

For PEG20C8 no comparison could be done between the different oils because only the ODM oil allowed formulating a stable emulsion. For this oil the retarding effect is very high and the emulsion showed even a lower caffeine penetration than the corresponding surfactant solution. This result is interesting because if on the contrary the PEG chain is decreased and the carbon chain length increased enhancing effect could be expected as observed by Cappel and Kreuter with polysorbate 21 and 81 on methanol absorption.

By increasing the carbon chain length of the surfactant to PEG20C12 an enhancement effect compared to the surfactant solution could be observed for all investigated oils. But compared to the caffeine solution the penetrated caffeine from these emulsions was still lower.

With the PEG20C18 the penetration enhancement depends on the used oil. BGC with a tension surface of <10mN/m did not show a significant enhancement but ODM with a surface tension of 20mN/m showed a clear penetration enhancement compared to the aqueous surfactant solution. Compared to the aqueous caffeine solution the penetrated caffeine quantity were not significantly different.

Savic et al (58) studied the bioavailability of hydrocortisone from three formulations based on cetearyl glucoside and cetearyl alcohol in vivo

and in vitro. The three formulations contained oils of different polarity (medium chain triglycerides: MG, isopropyl myristate: IPM and light liquid paraffin: LP), respectively. In vitro permeation was followed through the artificial skin constructs (ASC). The samples with MG and IPM, with close values of indexes of oil polarity (21.3 and 24.2 mN/m, respectively) had shown comparable fluxes and permeation coefficients. They were significant higher than for non-polar LP. In this work the complexity of the oil properties (IPM) involving the penetration is discussed. IPM improves hydrocortisone solubility and partitioning into the skin. Despite that IPM can lead to a denser packaging of the *stratum corneum* lipid layers, this decreasing the active permeation rate. Savic proposed to check that actually happened in the skin regarding the effect of different vehicles on the hydrocortisone permeation.

Using a surfactant with an unsaturated carbon chain had the highest enhancement effect on caffeine penetration for the paraffin oil and ODM oil. ODM emulsion showed even two times more penetrated caffeine in skin than the aqueous caffeine solution. The role of the unsaturation on skin absorption is under debate in the literature. Aungst et al., who studied in vitro naloxone penetration on human skin and Cooper who studied in vitro salicylic acid penetration in human skin, found an enhancement effect by unsaturated carbon chain length (33, 34). Comparing the penetration rate of PEG20C18 and C18:1 stabilized emulsions these observations could be affirmed for the BGC oil and ODM oil. For the liquid paraffin the PEG20C18 emulsion was not stable.

Walters et al. found out that surfactants with a linear alkyl chain length greater than C8 and an ethylene oxide chain length of less than PEG14 caused significant increase in the flux of methyl nicotinate in mouse skin (37). The best enhancement effect on methyl nicotinate penetration was achieved with PEG10C12. The major reason for this enhancement effect was due to a penetration of the surfactant into the intercellular regions of the *stratum corneum*, which increase fluidity and eventually solubilize and extract lipid components. This surfactant role on the skin barrier was also suggested by Cappel and Kreuter for Tween 21 (Polyoxyethylene 4 sorbitan monolaurate) and Tween 81 (Polyoxyethylene 5 sorbitan monooleate).

In previous studies we showed that with the confocal Raman microspectroscopy it is possible to measure the formulation impact on the lipid layer in the *stratum corneum* from the ratio $\nu_{asym}CH_2/\nu_{sym}CH_2$, R. Table IV shows R of the *stratum corneum* after a 24h treatment of the different oils and surfactant solutions. Compared to untreated skin (R=1.615) no oil or surfactant shows a significant modification of the ratio related to the lipid organization. This will say that the hypothesis of Walters couldn't be proofed and the different penetration behavior cannot be related to a lipid layer organization modification. The reason could be found in a modification of the penetration coefficient and should be studied in the future for a complete understanding of skin penetration enhancement.

Treatment	R	±SEM
BGC	1.583	0.031
Blank	1.615	0.029
ODM	1.557	0.026
Paraffin	1.532	0.036
H2O	1.562	0.012
Surfactant Solutions of:		
BGC+PEG20C12	1.632	0.032
BGC+PEG20C18	1.653	0.028
BGC+PEG20C18:1	1.612	0.007

Table IV: Ratio $\nu_{asym}CH_2/\nu_{sym}CH_2$, of skins treated by different products. The standard error of the mean is given for n=3. No significant ($p \leq 0.5$) difference of R among the different treated skin could be shown.

Retinol penetration

When the hydrosoluble active caffeine was changed against retinol, a lipophilic active, the major formulation organization changed. In the surfactant solutions the active was still in the continuous phase, BGC and also in the surfactant droplets. But in the oil in water emulsions the retinol was located in the oily droplets stabilized by the surfactants because of its low water solubility.

Depot	*SC*	Epidermis (E)	Dermis (D)	Receptor Fluid	E+D	Skin	Total
Retinol solution in BGC; % of applied retinol par cm^2 (%/cm^2/24h)							
101.39 ±0.30	0.01 ±0.00	0.00 ±0.00	0.00 ±0.00	0.00 ±0.00	0.00 0.00	0.01 ±0.00	101.39 ±0.30
Emulsion (o/w) PEG20C12; % of applied retinol par cm^2 (%/cm^2/24h)							
105.42 ±1.56	0.06 ±0.01	0.01 ±0.00	0.01 ±0.00	0.00 ±0.00	0.02 ±0.00	0.08 ±0.01	105.5 ±1.56
Surfactant solution PEG20C12; % of applied retinol par cm^2 (%/cm^2/24h)							
105.44 ±0.71	0.07 ±0.01	0.00 ±0.00	0.00 ±0.00	0.00 ±0.00	0.01 ±0.00	0.07 ±0.01	105.51 ±0.71
Emulsion (o/w) PEG20C18; % of applied retinol par cm^2 (%/cm^2/24h)							
97.04 ±0.47	0.03 ±0.01	0.00 ±0.00	0.01 ±0.00	0.00 ±0.00	0.02 ±0.00	0.05 ±0.01	97.09 ±0.47
Surfactant solution PEG20C18; % of applied retinol par cm^2 (%/cm^2/24h)							
95.36 ±0.92	0.19 ±0.04	0.00 ±0.00	0.01 ±0.00	0.00 ±0.00	0.01 ±0.00	0.21 ±0.04	95.56 0.95
Emulsion (o/w) PEG20C18:1 % of applied retinol par cm^2 (%/cm^2/24h)							
100.93 ±1.14	0.05 ±0.01	0.01 ±0.00	0.02 ±0.00	0.00 ±0.00	0.03 ±0.00	0.08 ±0.01	101.02 ±1.13
Surfactant solution PEG20C18:1; % of applied retinol par cm^2 (%/cm^2/24h)							
102.73 ±0.42	0.08 ±0.02	0.00 ±0.00	0.00 ±0.00	0.00 ±0.00	0.01 ±0.00	0.09 ±0.02	102.82 ±0.43

Table V: Retinol penetration results from BGC, oily surfactant solutions and oil in water emulsions after 24h (SEM).

Using only a retinol BGC solution the penetration rate was with less than 0.01 % of applied quantity after 24h. Conversely to the caffeine surfactant solutions where caffeine was located outside of the micelles, adding a surfactant in this experiment increased the retinol penetration significantly. A discriminating effect of the surfactant could be observed in this case. With the surfactant solutions of PEG20C18:1 and PEG20C12 5 times more retinol penetrated into *stratum corneum* compared to BGC solution but between the two surfactant solutions no significant difference can be observed. With the PEG20C18 surfactant solution the highest retinol penetration was measured. Nearly 4 times more retinol was found in the *stratum corneum* compared to the other two surfactant solutions. Conversely to caffeine formulations the absorbed amounts in this experiment were always higher from the formulations compared to the control solution.

In the hydrophilic parts of the skin, the viable epidermis and dermis, only a small amount of retinol loaded in surfactant solutions penetrated. No retinol was detected in the epidermis and dermis from the BGC retinol solution.

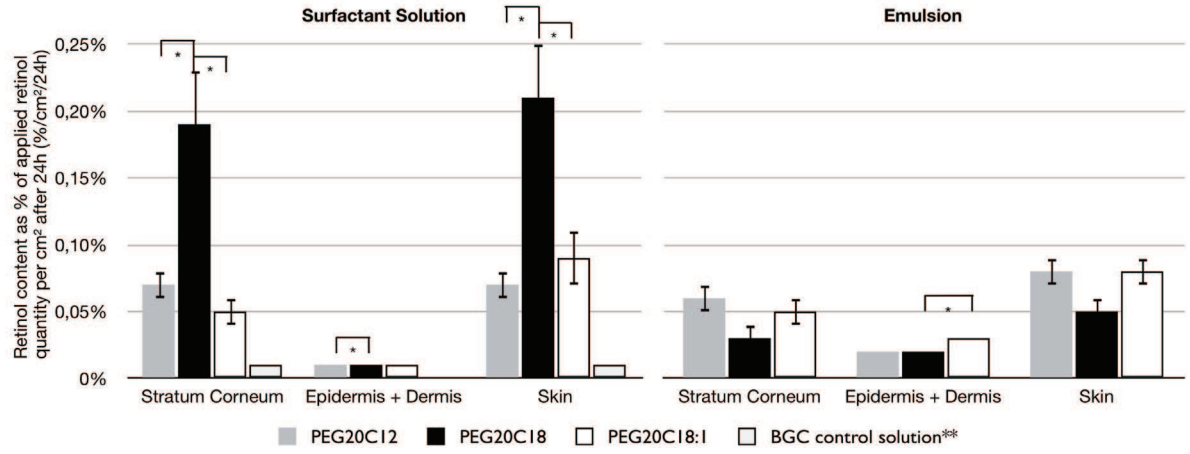

Figure 3: Retinol content given in percentage of applied retinol quantity per cm^2 in different skin compartments (*Stratum corneum* (SC), epidermis + dermis (E+D) and the whole skin (skin) after 24h exposition with the three different surfactant solutions (left) using PEG20C12, PEG20C18 and PEG20C18:1 including the oily BGC control retinol solution and three different emulsions (right) stabilized by the same surfactants. The error bars represent the SEM (n=6) and the content between columns marked with a * represent a significant difference ($p \leq 0.05$); ** penetrated retinol content of the BGC control solution is significant different compared to the surfactant solutions.

Switching to the oil in water emulsion formulations the overall penetration quantity of retinol in the skin was similar. Only the PEG20C18 showed a decrease in penetrated retinol. This is related to a smaller retinol penetration into the *stratum corneum* compared to the surfactant solutions.

No significant difference between the emulsions stabilized with different surfactants could be observed. Nevertheless it can be observed that the retinol penetrated deeper into the skin with the emulsions. In the epidermis and dermis two times and with the PEG20C18:1 even 3 times more retinol was found in these compartments compared to the surfactant solutions.

Overall less retinol was found in the skin with the PEG20C18 surfactant using oil in water emulsions than BGC surfactant solutions. It has to be proofed if these results are related to a modification of the lipid layer organization or if the partition coefficient of the formulations is differently modified. In previous studies using model oil such as dodecane and retinol the same trends were observed with surfactant solutions allowing an enhanced retinol penetration in the whole skin comparatively to emulsions especially in the stratum corneum and also a deeper penetration of retinol in viable skin from emulsions.

Conclusion

This work is the first study, which analyzes simple emulsions, where a modification of the penetration behavior can be related directly to the responsible formulation compositions and where the penetration of a hydrophilic active, caffeine, and a lipophilic active, retinol, from an emulsion with same compositions were compared. First the effects of different carbon chain length in PEG ester surfactants were tested for the caffeine. The effect of the carbon chain length depends on the used oils. In aqueous surfactant solutions a tendency of penetrated caffeine increase with an increase in the carbon chain length of PEG20 esters could be observed. But the overall caffeine penetration with surfactant solutions was smaller than with an aqueous caffeine solution. In emulsions it depended on the used oil. With the BGC no clear tendency could be found. ODM and Paraffin showed the same behaviors than the surfactant solutions. Using the surfactant PEG20C18 or even the PEG20C18:1 the caffeine penetration got even higher than the aqueous caffeine solution, which correlates with studies in the literature. For the retinol penetration no correlation to the carbon chain length could be found. The penetrated retinol quantity from the surfactant solutions was in any skin compartment different using PEG20C12 or PEG20C18. Only the PEG20C18 surfactant solution, compared to the other surfactant solutions, showed a significant higher retinol penetration. In the hydrophilic epidermis and dermis less retinol was found. With the emulsions the penetrated retinol quantity was not different among the different used surfactants. The PEG20C18 stabilized emulsion did not show a significant higher penetration of retinol as in the surfactant solution. The penetrated retinol quantity in the epidermis and dermis was higher with the emulsions than with the surfactant solutions.

The aim of this study was not only to show the effects of surfactants on the penetration behavior but also to explain these enhancement observations. The literature explained enhancement effect of these surfactants with a hypothesis by a penetration of the surfactant into the intercellular regions of the *stratum corneum*, which increase fluidity and eventually solubilize and extract lipid components. This study could proof with the CRM measurements that this is not the case. A modification of the lipid layer in the *stratum corneum* by the pure oils and water or by the used surfactants could not be measured. These results give the conclusion that the penetration modification is related to a penetration coefficient between the formulation and the skin in favor to the latter one. It has also been discussed the reliability of the used method and even mention that further information about a possible lipid modification could be obtained by optimizing the complex method of CRM. However this study had shown the potential of this relative new method and its potential in understanding of topical applied formulation and their delivery process.

Acknowledgments

We thank Gattefossé SAS for the financial support.

References

1. A. Otto, J.d. Plessis, and J.W. Wiechers. Formulation effects of topical emulsions on transdermal and dermal delivery. Int J Cosmet Sci. 31:1-19 (2009).
2. R. Potts and R. Guy. Predicting Skin Permeability. Pharm Res. 9:663-669 (1992).
3. R.H. Guy and J. Hadgraft. Physicochemical aspects of percutaneous penetration and its enhancement. Pharm Res. 5:753-758 (1988).
4. J. Hadgraft and M.E. Lane. Skin permeation: the years of enlightenment. Int J Pharm. 305:2-12 (2005).
5. T. Ghafourian, P. Zandasrar, H. Hamishekar, and A. Nokhodchi. The effect of penetration enhancers on drug delivery through skin: a QSAR study. J Control Release. 99:113-125 (2004).
6. D. Fitzpatrick, J. Corish, and B. Hayes. Modelling skin permeability in risk assessment--the future. Chemosphere. 55:1309-1314 (2004).
7. W.J. Pugh and J. Hadgraft. Epidermal permeability–penetrant structure relationships: 4, QSAR of permeant diffusion across …. Int J Pharm (2000).
8. S. Mitragotri. Modeling skin permeability to hydrophilic and hydrophobic solutes based on four permeation pathways. J Control Release (2003).
9. G. Lian, L. Chen, and L. Han. An evaluation of mathematical models for predicting skin permeability. J Pharm Sci. 97:584-598 (2008).
10. D. Kessner, A. Ruettinger, M.A. Kiselev, S. Wartewig, and R.H.H. Neubert. Properties of ceramides and their impact on the stratum corneum structure. Part 2: stratum corneum lipid model systems. Skin Pharmacol Physiol. 21:58-74 (2008).
11. P. Talreja, N.K. Kleene, W.L. Pickens, T.F. Wang, and G.B. Kasting. Visualization of the lipid barrier and measurement of lipid pathlength in human stratum corneum. AAPS PharmSci. 3:E13 (2001).
12. A.C. Williams and B.W. Barry. Penetration enhancers. Adv Drug Deliv Rev. 56:603-618 (2004).
13. A.L. Bunge, R.L. Cleek, and B.E. Vecchia. A new method for estimating dermal absorption from chemical exposure. 3. Compared with steady-state methods for prediction and data analysis. Pharm Res. 12:972-982 (1995).
14. A.L. Bunge and R.L. Cleek. A new method for estimating dermal absorption from chemical exposure: 2. Effect of molecular weight and octanol-water partitioning. Pharm Res. 12:88-95 (1995).
15. J.W. Wiechers, C.L. Kelley, T.G. Blease, and J.C. Dederen. Formulating for efficacy. Int J Cosmet Sci. 57:191-192 (2006).
16. S. Grégoire, C. Ribaud, F. Benech, J.R. Meunier, A. Garrigues-Mazert, and R.H. Guy. Prediction of chemical absorption into and through the skin from cosmetic and dermatological formulations. Br J Dermatol. 160:80-91 (2009).
17. F.K. Akomeah, T. Nazir, G.P. Martin, and M.B. Brown. Effect of heat on the percutaneous absorption and skin retention of three model penetrants. Eur J Pharm Sci (2004).
18. J. Frelichowska, M.-A. Bolzinger, J. Pelletier, J.-P. Valour, and Y. Chevalier. Topical delivery of lipophilic drugs from o/w Pickering emulsions. Int J Pharm. 371:56-63 (2009).
19. R.L. Bronaugh, R.F. Stewart, and J.E. Storm. Extent of cutaneous metabolism during percutaneous absorption of xenobiotics. Toxicol Appl Pharmacol. 99:534-543 (1989).
20. A.V. Rawlings. Cellulite and its treatment. Int J Cosmet Sci. 28:175-190 (2006).
21. A.B. Rossi and A.L. Vergnanini. Cellulite: a review. J Eur Acad Dermatol Venereol. 14:251-262 (2000).
22. D. Hexsel, C. Orlandi, and D. Zechmeister do Prado. Botanical extracts used in the treatment of cellulite. Dermatol Surg. 31:866-872; discussion 872 (2005).
23. T. Loftsson and D. Hreinsdóttir. Determination of aqueous solubility by heating and equilibration: a technical note. AAPS PharmSciTech. 7:E1-E4 (2006).
24. T. Maugard, B. Rejasse, and M.D. Legoy. Synthesis of water-soluble retinol derivatives by enzymatic method. Biotechnol Prog. 18:424-428 (2002).
25. C. Antille, C. Tran, O. Sorg, and J. Saurat. Penetration and metabolism of topical retinoids in ex vivo organ-cultured full-thickness human skin explants. Skin Pharmacol Physiol:124-128 (2004).
26. C. Antille, C. Tran, O. Sorg, P. Carraux, L. Didierjean, and J.-H. Saurat. Vitamin A exerts a photoprotective action in skin by absorbing ultraviolet B radiation. J Invest Dermatol. 121:1163-1167 (2003).
27. V. Jenning, A. Gysler, M. Schäfer-Korting, and S.H. Gohla. Vitamin A loaded solid lipid nanoparticles for topical use: occlusive

properties and drug targeting to the upper skin. Eur J Pharm Biopharm. 49:211-218 (2000).
28. T. Perlmann. Retinoid metabolism: a balancing act. Nat Genet. 31:7-8 (2002).
29. T.C. Roos, F.K. Jugert, H.F. Merk, and D.R. Bickers. Retinoid metabolism in the skin. Pharmacol Rev. 50:315-333 (1998).
30. K. Ichikawa, I. Ohata, M. Mitomi, S. Kawamura, H. Maeno, and H. Kawata. Rectal absorption of insulin suppositories in rabbits. J Pharm Pharmacol. 32:314-318 (1980).
31. S. Guarini and W. Ferrari. Structural restriction in bile acids and non-ionic detergents for promotion of heparin absorption from rat gastro-intestinal tract. Arch Int Pharmacodyn Ther. 271:4-10 (1984).
32. E.S. Park, S.Y. Chang, M. Hahn, and S.C. Chi. Enhancing effect of polyoxyethylene alkyl ethers on the skin permeation of ibuprofen. Int J Pharm. 209:109-119 (2000).
33. E.R. Cooper. Increased skin permeability for lipophilic molecules. J Pharm Sci. 73:1153-1156 (1984).
34. B.J. Aungst, N.J. Rogers, and E. Shefter. Enhancement of naloxone penetration through human skin in vitro using fatty acids, fatty alcohols, surfactants, sulfoxides and amides. Int J Pharm (1986).
35. C.C. Hwang and A.G. Danti. Percutaneous absorption of flufenamic acid in rabbits: effect of dimethyl sulfoxide and various nonionic surface-active agents. J Pharm Sci. 72:857-860 (1983).
36. K.A. Walters, W. Bialik, and K. Brain. The effects of surfactants on penetration across the skin. Int J Cosmet Sci. 15:260-270 (1993).
37. K.A. Walters, M. Walker, and O. Olejnik. Non-ionic surfactant effects on hairless mouse skin permeability characteristics. J Pharm Pharmacol. 40:525-529 (1988).
38. C.H. Purdon, C.G. Azzi, J. Zhang, E.W. Smith, and H.I. Maibach. Penetration enhancement of transdermal delivery--current permutations and limitations. Crit Rev Ther Drug Carrier Syst. 21:97-132 (2004).
39. P. Karande, A. Jain, K. Ergun, V. Kispersky, and S. Mitragotri. Design principles of chemical penetration enhancers for transdermal drug delivery. Proc Natl Acad Sci USA. 102:4688-4693 (2005).
40. M. Mélot, P.D.A. Pudney, A.-M. Williamson, P.J. Caspers, A. Van Der Pol, and G.J. Puppels. Studying the effectiveness of penetration enhancers to deliver retinol through the stratum cornum by in vivo confocal Raman spectroscopy. J Control Release. 138:32-39 (2009).
41. P.D.A. Pudney, M. Mélot, P.J. Caspers, A. Van Der Pol, and G.J. Puppels. An in vivo confocal Raman study of the delivery of trans-retinol to the skin. Appl Spectrosc. 61:804-811 (2007).
42. B.P. Gaber and W.L. Peticolas. On the quantitative interpretation of biomembrane structure by Raman spectroscopy. Biochim Biophys Acta. 465:260-274 (1977).
43. A. Tfayli, E. Guillard, M. Manfait, and A. Baillet-Guffroy. Thermal dependence of Raman descriptors of ceramides. Part I: effect of double bonds in hydrocarbon chains. Anal Bioanal Chem. 397:1281-1296 (2010).
44. A. Anigbogu, A. Williams, B.W. Barry, and H. Edwards. Fourier transform Raman spectroscopy of interactions between the penetration enhancer dimethyl sulfoxide and human stratum corneum. Int J Pharm. 125:265-282 (1995).
45. W.C. Griffin. Calculation of HLB values of non-ionic surfactants. J Soc Cosmet Chem. 5:249-256 (1954).
46. C. Antille, C. Tran, O. Sorg, and J. Saurat. Topical beta-carotene is converted to retinyl esters in human skin ex vivo and mouse skin in vivo. Exp Dermatol:558-561 (2004).
47. S.B. Kurlandsky, E.A. Duell, S. Kang, J.J. Voorhees, and G.J. Fisher. Auto-regulation of retinoic acid biosynthesis through regulation of retinol esterification in human keratinocytes. J Biol Chem. 271:15346-15352 (1996).
48. S.B. Kurlandsky, J.H. Xiao, E.A. Duell, J.J. Voorhees, and G.J. Fisher. Biological activity of all-trans retinol requires metabolic conversion to all-trans retinoic acid and is mediated through activation of nuclear retinoid receptors in human keratinocytes. J Biol Chem. 269:32821-32827 (1994).
49. OECD. Guidance Document for the conduct of skin absorption studies. OECD Series on testing and assessment:31 (2004).
50. E.Z. Szuts and F.I. Harosi. Solubility of retinoids in water. Arch Biochem Biophys. 287:297-304 (1991).
51. L. Montenegro, J. Ademola, F. Bonina, and H. Maibach. Effect of application time of betamethasone-17-valerate 0.1% cream on skin blanching and stratum corneum drug concentration. Int J Pharm. 140:51-60 (1996).
52. L. Chrit, C. Hadjur, S. Morel, G. Sockalingum, G. Lebourdon, F. Leroy, and M. Manfait. In vivo chemical investigation of human skin using a confocal Raman fiber optic microprobe. J Biomed Opt. 10:0440071-

04400711 (2005).
53. M. Förster, M.-A. Bolzinger, H. Fessi, and S. Briançon. Topical delivery of cosmetics and drugs. Molecular aspects of percutaneous absorption and delivery. Eur J Dermatol. 19:309-323 (2009).
54. M.J. Cappel and J. Kreuter. Effect of nonionic surfactants on transdermal drug delivery: I. Polysorbates. Int J Pharm:143-153 (1991).
55. A.T. Florence. Surfactant interaction with biomembranes and drug absorption. Pure Appl Chem. 53:2057-2068 (1981).
56. P.P. Sarpotdar and J.L. Zatz. Evaluation of penetration enhancement of lidocaine by nonionic surfactants through hairless mouse skin in vitro. J Pharm Sci. 75:176-181 (1986).
57. P.P. Sarpotdar and J.L. Zatz. Percutaneous absorption enhancement by nonionic surfactants. Drug Dev Ind Pharm. 13:15-37 (1987).
58. S. Savić, M. Savić, S. Tamburić, G. Vuleta, S. Vesić, and C.C. Müller-Goymann. An alkylpolyglucoside surfactant as a prospective pharmaceutical excipient for topical formulations: the influence of oil polarity on the colloidal structure and hydrocortisone in vitro/in vivo permeation. Eur J Pharm Sci. 30:441-450 (2007).
59. H.P. Gollnick and U. Dümmler. Retinoids. Clin Dermatol. 15:799-810 (1997).
60. J. Bailly, M. Crettaz, M.H. Schifflers, and J.P. Marty. In vitro metabolism by human skin and fibroblasts of retinol, retinal and retinoic acid. Exp Dermatol. 7:27-34 (1998).
61. V. Jenning, M. Schäfer-Korting, and S. Gohla. Vitamin A-loaded solid lipid nanoparticles for topical use: drug release properties. J Control Release. 66:115-126 (2000).

Partie C Résumé et discussion

Ce projet de thèse est réalisé en collaboration avec l'entreprise Gattefossé SAS à Saint-Priest qui est spécialiste dans la production de matières premières pour l'industrie pharmaceutique et cosmétique. Dans ce contexte, l'entreprise était intéressée par des études de pénétration percutanée des formulations de type émulsion et solution de tensioactifs pour comprendre l'effet des différents tensioactifs non ioniques et des huiles sur la pénétration.

Le transport d'un actif dans la peau est le but principal des produits dermopharmaceutiques et cosmétiques. Une augmentation de la biodisponibilité de la part du véhicule peut avoir deux raisons [104] : premièrement, le partage de l'actif entre la formulation et la peau, en faveur de la peau et, deuxièmement, la modification de la barrière cutanée par des promoteurs chimiques de la pénétration pouvant modifier la structure lipidique de la peau (appelée perturbation de la barrière cutanée ou fluidification des lipides). Le système galénique peut influencer le passage cutané et percutané selon le type d'émulsion (émulsion E/H versus H/E), la taille des gouttelettes, la phase huileuse utilisée, l'émulsifiant mais aussi l'organisation et la nature du tensioactif (micelles, cristaux liquides lyotropiques, HLB) comme expliqué dans la partie 1 de la thèse.

Plusieurs auteurs ont proposé des modèles pour décrire les propriétés de transport des actifs dans la peau. Des corrélations ont pu être établies dans la littérature entre la vitesse de diffusion des actifs matérialisée par le coefficient de perméabilité et certains paramètres inhérents à la molécule d'actif comme sa polarité et sa masse molaire. Ainsi Potts et Guy ont relié ces paramètres de façon empirique à partir de l'étude de séries de molécules de masse moléculaire allant de 18 à 750 g/mol avec un logP entre 3 et 6 (Equation 1-2) [14]. Les formulations utilisées pour cette étude étaient de simples formulations.

Les produits dermopharmaceutiques sont rarement de simples solutions aqueuses et contiennent, en plus, beaucoup d'autres ingrédients, comme des tensioactifs, qui influencent

le transport de l'actif dans la peau. Jusqu'à aujourd'hui, les études examinant l'absorption percutanée des formulations complexes ne sont pas très nombreuses. Ces études sont très compliquées dans leur nature [2-4].

De façon générale, il est très difficile de tracer des conclusions globales de ces études, parce que les formulations sont différentes dans leur composition et dans leurs propriétés physicochimiques.

Grégoire et al. ont essayé d'appliquer ces modèles à des formulations réelles (émulsions H/E). Ils ont pu prévoir la pénétration de seulement 26 % des 101 actifs testés. En considérant que les expériences ont été réalisées dans des conditions stationnaires, même si une dose finie était appliquée, en négligeant les effects du véhicule et en supposant que seule la fraction contenue dans la phase aqueuse est disponible pour la pénétration, le caractère prédictif est amélioré puisque la pénétration de 91 % des actifs peut être correctement prédite par la corrélation (la valeur expérimentale est inférieure d'un facteur 5) [1].

De plus, différents actifs sont utilisés, différentes formulations contrôles et la méthodologie des études biopharmaceutiques, avec le choix du type de membrane, la quantité de formulation déposée dans le compartiment donneur définissant une dose finie ou infinie, la qualité du liquide récepteur et les conditions de l'étude en occlusion ou non conditionnent les résultats.

Le premier objectif de notre travail était de trouver une corrélation entre les propriétés physicochimiques des tensioactifs, des huiles et des actifs et les profils biopharmaceutiques cutanés des actifs.

Dans la littérature, il est par ailleurs extrêmement difficile de déterminer quel composant de la formulation a quel impact sur la pénétration percutanée. Les travaux n'étudient que rarement l'impact de tous les composants des formulations sur le passage d'un actif. C'est la raison pour laquelle l'objectif de cette thèse est resté fixé sur des formulations simples. De ce fait, les formulations type émulsion, contenant un seul tensioactif et une seule phase huileuse

et des solutions de tensioactifs ont été choisies pour étudier la pénétration percutanée d'actifs modèles par des méthodes standards et nous avons respectivement étudié :

- l'effet de différents tensioactifs non ioniques différant par la longueur de leur chaine carbonée lipophile et la longueur de leur chaîne polymérique hydrophile,
- l'effet des huiles différant par leur polarité,
- et la polarité de l'actif.

Des émulsions H/E, des solutions de tensioactifs et des solutions contrôles aqueuses et huileuses, en fonction de la solubilité de l'actif et des tensioactifs ont été choisies. Deux actifs, de solubilité différente, ont de même été choisis : la caféine, plutôt hydrosoluble (logP=-0,07), et le rétinol liposoluble (logP=7,62 [105]). Ce choix a été fait pour pouvoir comparer la pénétration des actifs qui sont localisés dans des phases différentes au sein des émulsions. La caféine hydrosoluble est localisée dans la phase continue de l'émulsion H/E et le rétinol, n'étant pas soluble dans l'eau, est localisé dans les gouttelettes huileuses des émulsions. Trois huiles différentes ont été sélectionnées en fonction de leurs tensions interfaciales respectives afin d'étudier leurs rôles sur la pénétration percutanée. Ces huiles sont la paraffine fluide avec une tension interfaciale de 50 mN/m, le Cocoate BG® (Butylene glycol cocoate) avec une tension interfaciale inférieure à 10 mN/m et le MOD (Octyldodecyl Myristate) avec une tension interfaciale intermédiaire de 20 mN/m. En ce qui concerne les tensioactifs, le groupe des tensioactifs non ioniques a été sélectionné parce que plusieurs produits commerciaux développés par Gattefossé contiennent en grande majorité des esters de polyéthylène glycol. Dans cette thèse, cinq tensioactifs vont être utilisés. Ces tensioactifs diffèrent par leur HLB, la longueur de leur chaine carbonée et le nombre d'unités d'éthylène glycol. Tout d'abord, des PEG20 avec quatre chaines carbonées différentes: une chaine octanoique C8 (HLB=18,1), une chaine laurique C12 (HLB=17,1), une chaine stéarique C18 (HLB=15,9) et une chaine oléique C18:1 (HLB=16), puis finalement un tensioactif avec une plus petite tête hydrophile, le PEG6C18 :1 (HLB=11,3). Il est connu que les tensioactifs influencent la perméabilité des membranes biologiques, dont la peau [44,106] par,

premièrement, une interaction avec les lipides intercellulaires, puis une influence sur le coefficient de partage provoqueé par la longueur de leur chaine carbonée, le nombre d'unités d'éthylène glycol et leurs HLB. Plusieurs publications ont montré que certains éthers alkyliques de PEG amélioraient la délivrance des actifs par voie orale, rectale et cutanée [7-9].

Le premier grand défi était de trouver des formulations simples stabilisées par un seul tensioactif mais stables. Les émulsions stables pendant la durée du test de pénétration contenaient 20 % d'huile, 1,5 % de caféine et des pourcentages de tensioactifs variant entre 3 et 6 %. Les émulsions à base de *caféine* ont été formulées avec les trois phases huileuses précédemment citées et les tensioactifs suivants : PEG20C8, C12, C18 et C18 :1. La quantité de tensioactif ne pouvait pas être identique dans toutes les émulsions pour des raisons de stabilité. Après avoir sélectionné ces formulations, de composition la plus proche possible en terme de rapport huile/eau et quantité de tensioactifs, la pénétration de la caféine dans la peau de porc a été mesurée *in vitro* sur des cellules à flux continu, les solutions de tensioactifs correspondantes ont été utilisées comme contrôle et une solution de caféine en comparaison.

Les résultats ont montré que les solutions de tensioactifs ont significativement diminué la quantité de caféine ayant pénétrée (entre 10 et 25 % de la quantité appliquée après 24 h) par rapport à la solution aqueuse de caféine (36,90 ± 3,30 % de la quantité appliquée après 24 h). Le même effet a été constaté pour toutes les émulsions stabilisées par les tensioactifs avec une chaine carbonée inférieure à C18, le choix de l'huile restant un paramètre peu influent. Seules les émulsions formulées avec l'octyldodecyl myristate et stabilisées avec le PEG20C18 et C18:1 ont montré une pénétration de caféine similaire (C18 : 39,71 ± 3,79 % de la quantité appliquée après 24 h) ou plus importante (C18:1 : 63,68 ± 6,94 % de la quantité appliquée après 24h) que la solution aqueuse de caféine. Ces résultats sont en accord avec les résultats trouvés dans la littérature. Park et *al.* [9] ont réalisé des tests *in vitro* sur la peau de rat pour évaluer la pénétration de l'ibuprofène, en utilisant des solutions de tensioactif avec une concentration de 15 % m/m de tensioactif. Ils ont testé l'effet de

plusieurs polyethylène alkyl éther (C12-C18 :1) et ont constaté une augmentation de la pénétration de l'ibuprofène à partir d'une chaine carbonée en C 16. Cette tendance correspond aux résultats trouvés dans ce travail : l'augmentation de la longueur de la chaine carbonée du tensioactif augmente la quantité de caféine qui pénètre dans la peau. Le rôle favorable de l'insaturation de la chaine carbonée sur l'augmentation de la pénétration de l'actif dans la peau est démontré avec les émulsions formulées avec le Butylene glycol cocoate (C18 : 21,21 ± 2,55 et C18 :1 : 30,55 ± 3,20 % de la quantité appliquée après 24h) et l'Octyldodecyl Myristate (C18 : 39,71 ± 3,79 et C18 :1 : 63,68 ± 6,94 % de la quantité appliquée après 24 h). Nos résultats sont en accord avec des études publiées dans la littérature : ainsi Aungst et *al.* ont étudié la pénétration de la naloxone *in vitro* sur la peau humaine tandis que Cooper a étudié *in vitro* la pénétration de l'acide salicylique sur peau humaine. Ces deux auteurs ont réalisé leurs études en utilisant des véhicules de propylène glycol avec des adjuvants différents par leur longueur de chaine carbonée et présentant une insaturation ou pas. Ils ont constaté une augmentation de la pénétration des actifs utilisés avec des chaines carbonées insaturées [10,11]

La question qui se pose est comment la pénétration d'un actif lipophile se comporte dans ces mêmes formulations. La caféine est hydrophile et donc se localise dans la phase continue des solutions de tensioactif et des émulsions huile dans eau. Par contre, un actif lipophile, comme le rétinol, se localise dans notre étude dans les gouttelettes des émulsions et est « encapsulé » par des tensioactifs dans les solutions de tensioactifs.

L'étude de la pénétration du rétinol depuis les mêmes formulations que celles de caféine n'a pas été possible hormis dans le cas de l'émulsion formulée avec le Butylene glycol cocoate. Ainsi les tensioactifs testés sont le PEG20 C12, le PEG20 C18 et le PEG20C18 :1. La méthode utilisée est celle des cellules de diffusion de Franz en mode statique. Les émulsions sont comparées avec les solutions aqueuses de tensioactifs correspondantes. Une solution de rétinol dans le butylene glycol cocoate a servi de solution contrôle. Le premier résultat est que le rétinol ne pénètre pas dans le liquide récepteur après 24 h. Ce résultat était attendu parce

que le rétinol après 24 h pénètre très peu dans la peau à cause de son caractère lipophile [76] [107] [108] [109]. Cela justifie le choix d'une cellule de diffusion statique et le démontage complet de la cellule afin de quantifier dans chaque compartiment la quantité de rétinol qui s'y localise. La quantité de rétinol ayant pénétré depuis la solution contrôle est très faible, après 24 h, avec moins de 0,01 % de la quantité appliquée retrouvée dans la peau. Cette quantité est totalement localisée dans le stratum corneum. En ajoutant du tensioactif, et en plaçant cette fois le rétinol aussi en phase dispersée, la pénétration du rétinol dans le *stratum corneum* augmente significativement d'un facteur 5 avec le PEG20C18 :1 et le PEG20C12. Le PEG20C18 provoque même une augmentation de la pénétration du rétinol d'un facteur 4 par rapport aux deux autres tensioactifs. Dans les parties viables de la peau, la pénétration de rétinol provenant des solutions de tensioactifs n'est pas significative. La quantité de rétinol qui pénètre depuis les émulsions H/E est comparable avec la quantité pénétrée depuis les solutions de tensioactifs. Seule la solution avec le tensioactif PEG20C18 montre une quantité de rétinol plus faible depuis les émulsions (facteur de 4). Aucune différence significative entre les émulsions contenant des tensioactifs différents ne peut être observée. Par contre le rétinol des émulsions pénètre plus profondément et se retrouve préférentiellement localisé dans les parties hydrophiles de la peau.

En comparant la pénétration du rétinol avec celle de la caféine dans les formulations avec le Butylene glycol cocoate, on constate que, premièrement, ajouter un tensioactif dans une solution aqueuse de caféine diminue la quantité de caféine qui pénètre dans la peau, au contraire du rétinol. Ajouter un tensioactif dans une solution huileuse de rétinol augmente significativement la quantité d'actif qui pénètre dans le *stratum corneum*. La pénétration la plus importante est retrouvée avec le tensioactif PEG20C18. Dans les émulsions, la différence de quantité absorbée parmi les différents tensioactifs utilisés n'est pas significative pour le rétinol, mais la quantité de rétinol absorbée est plus importante depuis les émulsions que depuis la solution huileuse, ce qui prouve l'effet promoteur des tensioactifs. Pour la caféine, la pénétration reste plus modérée qu'avec la solution aqueuse. En revanche de façon

logique, le caractère très lipophile du rétinol privilégie son accumulation en surface au contraire de la caféine plus amphiphile.

Le rétinol est un actif qui a tendance à s'accumuler dans l'épiderme [76,110]. Pour pouvoir étudier la pénétration percutanée du rétinol après 24 h, la concentration du rétinol dans les différentes couches de la peau a été quantifiée. Cela passe par le choix d'une méthode de séparation de la couche lipophile de la peau, le *stratum corneum*, des couches hydrophiles, épiderme et derme, qui doit être suffisamment précise. Pour cette séparation, il existe plusieurs méthodes établies [94,101,102]. Une des méthodes les plus utilisées est la méthode du tape stripping. Cette méthode d'arrachage par un adhésif est simple et minimalement invasive. Elle peut donc être aussi bien utilisée pour étudier *in vivo* [111-114] que *in vitro* [52,76,77,115-118], l'accumulation d'un actif dans le *stratum corneum* après l'application topique sur explants de peaux humaines, dans les études de pénétration cutanée [116,118,119] ou animales [115,120-122].

La méthode du tape stripping est remise en cause depuis les années 50 par Hunter [95] qui a remarqué une influence de la direction dans laquelle le scotch est arraché sur le nombre des strips nécessaires pour la séparation. Weerheim et Ponec [123] montrent que le nombre moyen nécessaire pour une élimination complète du stratum corneum *in vivo* peut être 18-20. La quantité de stratum corneum enlevée par une seule bande adhésive dépend de plusieurs facteur extrinsèques comme le type de la bande adhésive [124], la force d'arrachement [125], la durée de l'application d'une pression sur la peau [126] et la nature de la substance appliquée [127]. De plus plusieurs paramètres intrinsèques comme le site anatomique [119], l'âge [114] et la saison [128] influencent la quantité de stratum corneum enlevé avec chaque bande adhésive.

Ces observations montrent que la détermination d'un protocole standard est indispensable. Pour pouvoir obtenir la quantité de rétinol dans le *stratum corneum* la séparation doit être complète et précise. En effet les résultats observés montrent des différences étroites entre les formes galéniques quant au passage du rétinol et donc la quantification se doit d'être précise.

Une étude préliminaire sur la méthodologie d'arrachage du stratum corneum a été menée. Deux méthodes supplémentaires au traitement par la méthode du tape stripping ont été étudiées : un traitement enzymatique de la peau à la trypsine et la biopsie utilisant de la colle cyanoacrylate. Ces méthodes ont été comparées par rapport à leur qualité de séparation du *stratum corneum* de l'épiderme. Pour la méthode du tape stripping les résultats ont montré que, premièrement, la quantité de *stratum corneum* enlevée par chaque bande adhésive n'était pas constante. Les 9 premiers strips permettent d'enlever 50% du *stratum corneum* et après 28 strips, il reste encore 20 % du *stratum corneum* sur la peau. Deuxièmement, la séparation du *stratum corneum* sur la totalité de la surface n'est pas homogène. Il existe des zones sur la peau qui conservent une épaisseur de *stratum corneum* tandis que d'autres sont parfaitement exemptes de stratum corneum. Dans les résultats de la littérature, il est prouvé que l'élimination totale du *stratum corneum* est difficile avec cette méthode et demande l'application de beaucoup de strips (50-80) [96,129].

Une méthode alternative pour obtenir la séparation complète du *stratum corneum* est le traitement par l'enzyme trypsine.

Cette méthode a été discutée dans les années 60 par Kligmann *et al.* [101]. Cette méthode est pratiquée couramment et appliquée pour des objectifs divers (études mécaniques sur le *stratum corneum*, études sur l'organisation des lipides de *stratum corneum*) [130-132], ainsi que pour quantifier la quantité d'actif dans des études de pénétration percutanée [133,134]. Les études montrent que cette méthode enlève le *stratum corneum* d'une manière homogène et totale sur toute la surface. Avec la trypsinisation, il est possible de récupérer la totalité du *stratum corneum* en un seul feuillet, ce qui est important dans les examens mécaniques et thermiques du *stratum corneum* [130,131]. Pour des études quantitatives de la concentration d'actif dans le *stratum corneum*, cette méthode est une bonne alternative au tape stripping parce que le *stratum corneum* est complètement et proprement éliminé. Cependant, avec cette méthode, un screening axial dans le *stratum corneum* n'est pas possible et, par ailleurs, cette méthode utilise une solution aqueuse de trypsine. Pour la quantification d'un actif

hydrosoluble, cette méthode peut entraîner des incertitudes dans la mesure où l'actif peut être extrait de la peau par la solution de trypsine. Enfin, cette méthode ne peut pas être utilisée dans des études *in vivo*. Cependant, dans le cas de notre thèse, ces contraintes n'ont pas un rôle important.

La méthode d'élimination par biopsie utilisant de la colle cyanoacrylate a été présentée en 1971 par Marks et Dawber [102]. C'est une méthode établie pour observer la couche cornée après obtention d'une couche fine de *stratum corneum* avec une colle cyanoacrylique. Cette méthode est utilisée pour quantifier la teneur en substance active du *stratum corneum* [97,135] et pour étudier les lipides du *stratum corneum* par des méthodes thermiques ou quantitatives [136-138]. Cette méthode est rapide et facile à standardiser. De plus, elle ne fait pas intervenir une phase aqueuse comme c'est le cas avec la trypsinisation. D'après les études de cette thèse, la qualité d'élimination du *stratum corneum* avec la colle cyanoacrylique est similaire à celle obtenue après la trypsinisation. Par contre, le *stratum corneum* est collé sur une lame de microscope et donc des études mécaniques sur le *stratum corneum,* possibles lors de l'utilisation de la méthode de trypsinisation, ne peuvent pas être réalisées. De même, il n'est pas possible de réaliser un screening axial en profondeur dans la peau. Elle reste cependant une méthode rapide pour toutes les études de quantification de substances dans le *stratum corneum*, pouvant être extraites du feuillet collé sur la lame du microscope. Dans cette thèse, cette méthode a été choisie avec la mise au point d'un protocole d'extraction du rétinol du *stratum corneum* récupéré sur la lame du microscope.

Connaître la distribution du rétinol dans le *stratum corneum* n'est pas important pour étudier l'effet des tensioactifs ou des huiles sur la pénétration. Le paramètre le plus important est de savoir la quantité d'actif présente dans la totalité du *stratum corneum*, de l'épiderme et du derme. Pour cette raison, la méthode du tape stripping n'a pas été choisie. Entre la trypsinisation et la biopsie par la colle cyanoacrylique, la méthode sans solvant a été favorisée, aussi la méthode choisie pour évaluer la quantité de rétinol dans le *stratum corneum* est la méthode d'arrachage par la colle cyanoacrylique.

Cette méthode d'arrachage associée à l'analyse quantitative par CLHP permet d'étudier quantitativement l'influence des composants des formulations sur la pénétration percutanée des actifs. Pour pouvoir quantifier un actif dans le *stratum corneum* collé sur la lame de microscope avec le colle cyanoacrylique, il faut bien évidement définir un solvant d'extraction adapté. Dans cette thèse, le méthanol avec 0,5 % α-tocopherol acetate a permis d'extraire le rétinol à 100 % de la peau après deux extractions successives. Cependant, ces résultats ne déterminent pas si la pénétration est modifiée à cause d'une modification de la couche lipidique ou / et d'une modification du coefficient de partage de l'actif entre la formulation et la peau.

La MCR nous permet de répondre à cette question. Cette nouvelle technique permet la considération simultanée des ingrédients et de l'actif de la formulation et, en plus, permet d'évaluer l'effet des ingrédients des formulations sur l'organisation de la couche lipidique du *stratum corneum*. La perturbation de la couche lipidique peut expliquer un effet promoteur [6] et doit faire l'objet d'une attention particulière pour optimiser des formulations [58,59]. La fluidification des lipides intracellulaires provoquée par les ingrédients de la formulation a été étudiée par MCR. L'ordre des chaînes alkyles des lipides est obtenue par le paramètre latéral d'interaction, S_{lat} décrit par Gaber [65,139,140]. S_{lat} permet d'estimer l'organisation de la chaine alkyle et le degré d'interaction latérale.

Donc, la méthode classique en cellule de Franz avec quantification de la quantité d'actif dans tous les comportements cutanés a été couplée à la MCR qui permet d'obtenir un suivi qualitatif des ingrédients et de l'actif dans le *stratum corneum* et le début de l'épiderme.

Dans un premier temps, cette nouvelle méthode devait être mise au point. Pour pouvoir suivre tous les ingrédients des formulations dans la peau, chaque ingrédient suivi doit avoir un pic caractéristique dans le spectre Raman. Pour cette raison, le dodécane, qui est commercialisé sous forme deuterée, a été utilisé dans un premier temps. La liaison C-D n'est pas présente dans la peau et il est donc possible de faire la distinction entre le C-H des protéines de la

peau et celui du dodécane. L'eau des formulations est remplacée par de l'eau deuterée. Le rétinol a déjà un pic caractéristique à 1585 cm^{-1}.

Des émulsions H/E à 0,5 % de rétinol stabilisées avec 7 % de PEG6C18 :1, PEG20C12, PEG20C18 et PEG20C18 :1 dans 50% dodécane et leurs solutions de tensioactifs correspondantes ont été étudiées. La plus grande quantité de rétinol qui pénètre provient de la solution de tensioactif fabriquée avec le PEG6C18:1 (0,75 ± 0,06 % de la quantité appliquée après 24 h). Avec la MCR, un grand pouvoir de fluidification des lipides a été mesuré pour le dodécane (S_{lat}=0,33 comparé avec 0,61 de la peau non traitée). Cet effet est très certainement relié à ses propriétés irritantes [141] qui permettent aussi d'expliquer la relative « grande »quantité de rétinol pénétrant à partir de la solution de rétinol dans du dodécane (0,37 ± 0,04 % de la quantité appliquée après 24 h) et de la solution de tensioactif de PEG6C18:1. La pénétration du rétinol est même plus importante avec la solution de tensioactif (S_{lat}=0,47) qu'avec la solution pure de dodécane, même si la fluidification des lipides est déjà assurée avec la solution pure. Cette solution de tensioactif PEG6C18:1 est un exemple de formulation modifiant l'organisation de la couche lipidique et, en même temps, favorisant le coefficient de partage de l'actif en faveur de la peau. Même avec les émulsions H/E avec lesquelles aucune modification de l'organisation lipidique par rapport à la peau non traitée n'a pu être mesurée, cette capacité du PEG6C18:1 de modifier le coefficient de partage a pu être démontrée par une pénétration plus importante (PEG20C18 :1 0,28 ± 0,02 et PEH6C18 :1 0,51 ± 0,03 % de la quantité appliquée après 24 h). Entre les autres solutions aqueuses de tensioactif et les émulsions correspondantes, stabilisées par les PEG20C12 et PEG20C18:1, aucune différence de S_{lat} ni de pénétration de l'actif n'a pu être mesurée. Un effet de la chaine carbonée sur la pénétration du rétinol n'a pas pu être montré, comme c'était le cas pour la caféine dans les formulations avec les huiles MOD, Cocoate BG et paraffine liquide.

Le suivi de l'eau et de l'huile de la formulation dans le *stratum corneum* et l'épiderme a montré une pénétration percutanée des deux ingrédients. Par contre, aucune corrélation n'a

pu être établie entre la pénétration de ces deux ingrédients et une modification de la pénétration du rétinol. Il faut préciser que la pénétration de l'eau et l'huile n'a pas pu être déterminée quantitativement.

Dans le futur, ces formulations modèles avec le dodécane devront s'approcher des formulations de composition proche de celle des produits cosmétiques. Pour cela, le dodécane doit être remplacé par des huiles telles que le Butylene glycol cocoate, l'octyldodecyl Myristate et la Paraffine liquide.

Cela donne les premières formulations qui ont déjà été testées avec l'actif hydrosoluble, la caféine. Au début de ce projet, seulement les mesures cinétiques ont été réalisées et non les études sur l'impact des formulations sur la barrière cutanée parce que la méthode n'était pas encore établie et que nous souhaitions dans un premier temps comparer les flux et les quantités pénétrées dans le liquide récepteur à 24 h, ce qui n'est pas possible avec la MCR.

Le premier point à vérifier est si les huiles cosmétiques utilisées dans cette étude ont un effet sur l'organisation des lipides. Les valeurs de S_{lat} obtenues avec les huiles pures montrent qu'il n'y a pas de modification significative dans l'organisation des lipides cutanés entre les différents huiles, ni par rapport à la peau non traitée ou traitée par l'eau.

Substance	**S_{lat}**	**±SEM**
BGC	0,589	0,0210
Blanc	0,610	0,0191
ODM	0,572	0,0171
Paraffine liq	0,555	0,0240
H_2O	0,575	0,0075

Tableau 6-1 : Paramètre latéral d'interaction (S_{lat}) des peaux traitées avec différents produits. L'erreur standard de la moyenne est donnée pour n=3. Aucune différence significative entre les valeurs de S_{lat} des différents traitements de la peau ne pouvait être montrée.

Ensuite, il fallait vérifier si les tensioactifs, utilisés dans la solution aqueuse de tensioactifs et dans les émulsions H/E, ont un effet sur la couche lipidique pour pouvoir donner une explication à l'augmentation de la pénétration avec l'augmentation de la chaine carbonée des tensioactifs. Walters et *al*. [142,143] ont trouvé que les tensioactifs avec une chaine carbonée plus grande que C8 et une chaine d'oxyde d'éthylène inférieure à PEG14 augmentaient le flux de methyl nicotinate dans la peau de souris. Ils ont montré un flux de methyl nicotinate avec les chaines de tensioactif en C12 plus important. Ces auteurs ont donné comme explication une interaction possible du tensioactif avec la région intercellulaire du *stratum corneum*, qui augmente la fluidification des lipides, solubilise et extrait des composants des lipides. Ces explications peuvent être maintenant vérifiées avec la méthode MCR.

Cette thèse nous a permis d'évaluer une méthode nouvelle et innovante, la MCR, qui est très polyvalente. Avec cette méthode, il est possible de mieux expliquer l'impact d'une formulation sur la pénétration percutanée d'un actif dans la peau. La MCR permet de connaître les ingrédients d'une formulation qui ont un effet sur le coefficient de partage de l'actif entre la formulation et la peau et qui ont un effet sur la barrière lipidique de la peau. Dans un premier temps, cette méthode aide à mieux comprendre l'interaction d'une formulation avec la peau. A l'échelle industrielle, avec cette méthode il est possible de développer des formulations plus efficaces pour promouvoir la pénétration cutanée par une modification simultanée du coefficient de partage et de l'organisation des lipides intracellulaires.

Résumé court

Français

Evaluation de la pénétration cutanée des ingrédients de systèmes dispersés : utilisation combinée des cellules de diffusion et de la microscopie confocale Raman

L'objet de cette thèse est l'étude de la pénétration des actifs cosmétiques dans la peau. Les axes d'investigation principaux ont concerné l'influence des propriétés physicochimiques des actifs et des ingrédients de la formule sur les mécanismes de pénétration. Les actifs cosmétiques choisis sont le rétinol, actif lipophile, et la caféine, actif hydrophile. Les formulations investiguées sont des émulsions de type huile dans eau, comparées aux solutions de tensioactifs correspondantes. Trois huiles cosmétiques ont été utilisées: Butylène glycol de cocoate, Octyldodecyl myristate et la Paraffine liquide, stabilisées en émulsion avec des tensioactifs ester de polyéthylène glycol (PEG20 et PEG6) possédant des longueurs de chaîne carbonées variables (C8, C12, C18 et C18:1). La pénétration percutanée a été mesurée quantitativement en utilisant la méthode des cellules de diffusion de Franz en fonctionnement statique et dynamique et qualitativement par la microscopie confocale Raman. Avec cette combinaison de techniques analytiques, il est possible, de mesurer la pénétration et d'évaluer l'impact de chaque composant de la formulation sur la pénétration cutanée d'un actif. Une corrélation a pu être établie entre l'effet fluidifiant d'une huile et l'augmentation de la pénétration du rétinol. Par ailleurs les tensioactifs, même s'ils ont montré un effet moindre en terme de fluidification conduisent également à une augmentation de la pénétration en raison d'une variation du coefficient de partage de l'actif entre la formule et la peau. Concernant la caféine, l'influence de la structure des tensioactifs et en particulier de la longueur de chaîne carbonée a été mise en évidence.

Anglais

Percutaneous penetraration evaluation of disperse systeme ingredients via a combination of diffusion cells and onfocal Raman micospectroscoy

The purpose of this thesis is to study the penetration of cosmetics actives into the skin. The main lines of investigation concerned the influence of actives and formulation components physicochemical properties on the penetration mechanisms. The selected cosmetic actives are retinol, lipophilic, and caffeine, hydrophilic. The investigated formulations are oil in water emulsions, compared to their corresponding surfactant solutions. Three cosmetic oils were used: Butylene glycol cocoate, Octyldodecyl myristate and liquid paraffin. Emulsions are stabilized with polyethylene glycol ester surfactants (PEG20 and PEG6) having variable carbon chain lengths (C8, C12, C18 and C18: 1). Percutaneous penetration was measured quantitatively using Franz diffusion cells in a static and dynamic way and qualitatively by confocal Raman microscopy. With this combination of analytical techniques, it is possible to measure the penetration and evaluate the impact of each formulation component on skin penetration of an active. A correlation could be established between the fluidizing effect of an oil and the increase in retinol penetration. Moreover, the surfactants, although they showed less effect in terms of fluidizing also lead to an increase in penetration due to a variation of the active partition coefficient between the formula and the skin. Regarding caffeine, the influence of the surfactant structure and in particular the carbon chain length has been pointed out.

Partie D Références

1 Grégoire S, Ribaud C, Benech F *et al.* Prediction of chemical absorption into and through the skin from cosmetic and dermatological formulations. *Br J Dermatol* 2009; **160**: 80-91.

2 Bunge AL, Cleek RL, Vecchia BE. A new method for estimating dermal absorption from chemical exposure. 3. Compared with steady-state methods for prediction and data analysis. *Pharm Res* 1995; **12**: 972-82.

3 Bunge AL, Cleek RL. A new method for estimating dermal absorption from chemical exposure: 2. Effect of molecular weight and octanol-water partitioning. *Pharm Res* 1995; **12**: 88-95.

4 Otto A, Plessis Jd, Wiechers JW. Formulation effects of topical emulsions on transdermal and dermal delivery. *Int J Cosmet Sci* 2009; **31**: 1-19.

5 Darlenski R, Sassning S, Tsankov N *et al.* Non-invasive in vivo methods for investigation of the skin barrier physical properties. *Eur J Pharm Biopharm* 2009; **72**: 295-303.

6 Williams AC, Barry BW. Penetration enhancers. *Adv Drug Deliv Rev* 2004; **56**: 603-18.

7 Ichikawa K, Ohata I, Mitomi M *et al.* Rectal absorption of insulin suppositories in rabbits. *J Pharm Pharmacol* 1980; **32**: 314-8.

8 Guarini S, Ferrari W. Structural restriction in bile acids and non-ionic detergents for promotion of heparin absorption from rat gastro-intestinal tract. *Arch Int Pharmacodyn Ther* 1984; **271**: 4-10.

9 Park ES, Chang SY, Hahn M *et al.* Enhancing effect of polyoxyethylene alkyl ethers on the skin permeation of ibuprofen. *Int J Pharm* 2000; **209**: 109-19.

10 Cooper ER. Increased skin permeability for lipophilic molecules. *J Pharm Sci* 1984; **73**: 1153-6.

11 Aungst BJ, Rogers NJ, Shefter E. Enhancement of naloxone penetration through human skin in vitro using fatty acids, fatty alcohols, surfactants, sulfoxides and amides. *Int J Pharm* 1986.

12 Windsor T, Burch GE. Rate of insensible perspiration (diffusion of water) locally through living and through dead human skin. *Arch Intern Med* 1944; **74**: 428–44.

13 Simonetti O, Hoogstraate AJ, Bialik W *et al.* Visualization of diffusion pathways across the stratum corneum of native and in-vitro-reconstructed epidermis by confocal laser scanning microscopy. *Arch Dermatol Res* 1995; **287**: 465-73.

14 Potts R, Guy R. Predicting Skin Permeability. *Pharm Res* 1992; **9**: 663-9.

15 Yamashita F, Hashida M. Mechanistic and empirical modeling of skin permeation of drugs. *Adv Drug Deliv Rev* 2003; **55**: 1185-99.

16 Swartzendruber DC. Studies of epidermal lipids using electron microscopy. *Semin Dermatol* 1992; **11**: 157-61.

17 Boncheva M, Damien F, Normand V. Molecular organization of the lipid matrix in intact Stratum corneum using ATR-FTIR spectroscopy. *Biochim Biophys Acta* 2008; **1778**: 1344-55.

18 Bouwstra JA, Ponec M. The skin barrier in healthy and diseased state. *Biochim Biophys Acta* 2006; **1758**: 2080-95.

19 Rodríguez G, Barbosa-Barros L, Rubio L *et al.* Conformational changes in stratum corneum lipids by effect of bicellar systems. *Langmuir* 2009; **25**: 10595-603.
20 Forslind B. A domain mosaic model of the skin barrier. *Acta Derm Venereol* 1994; **74**: 1-6.
21 Bouwstra JA, Honeywell-Nguyen PL, Gooris GS *et al.* Structure of the skin barrier and its modulation by vesicular formulations. *Prog Lipid Res* 2003; **42**: 1-36.
22 Bouwstra JA, Dubbelaar FE, Gooris GS *et al.* The lipid organisation in the skin barrier. *Acta Derm Venereol Suppl (Stockh)* 2000; **208**: 23-30.
23 Kessner D, Ruettinger A, Kiselev MA *et al.* Properties of ceramides and their impact on the stratum corneum structure. Part 2: stratum corneum lipid model systems. *Skin Pharmacol Physiol* 2008; **21**: 58-74.
24 Norlén L. Skin barrier structure and function: the single gel phase model. *J Invest Dermatol* 2001; **117**: 830-6.
25 McIntosh TJ. Organization of skin stratum corneum extracellular lamellae: diffraction evidence for asymmetric distribution of cholesterol. *Biophys J* 2003; **85**: 1675-81.
26 Marti-Mestres G, Mestres JP, Bres J *et al.* The "in vitro" percutaneous penetration of three antioxidant compounds. *Int J Pharm* 2007; **331**: 139-44.
27 Moss GP, Dearden JC, Patel H *et al.* Quantitative structure-permeability relationships (QSPRs) for percutaneous absorption. *Toxicol In Vitro* 2002; **16**: 299-317.
28 Geinoz S, Guy RH, Testa B *et al.* Quantitative structure-permeation relationships (QSPeRs) to predict skin permeation: a critical evaluation. *Pharm Res* 2004; **21**: 83-92.
29 Crank J. The Mathematics of Diffusion. *Oxford University Press,* 1979: 1-414.
30 Bos J, Meinardi M. The 500 Dalton rule for the skin penetration of chemical compounds and drugs. *Exp Dermatol* 2000; **9**: 165-9.
31 Behl CR, Flynn GL, Kurihara T *et al.* Hydration and percutaneous absorption: I. Influence of hydration on alkanol permeation through hairless mouse skin. *J Invest Dermatol* 1980; **75**: 346-52.
32 McKenzie AW, Stoughton RB. Methods for comparing percutaneous absorption of steroids. *Arch Dermatol* 1966; **86**: 608–10.
33 Scheuplein RJ, Blank IH. Permeability of the skin. *Physiol Rev* 1971; **51**: 702-47.
34 Agner T, Serup J. Time course of occlusive effects on skin evaluated by measurement of transepidermal water loss (TEWL). Including patch tests with sodium lauryl sulphate and water. *Contact Derm* 1993; **28**: 6-9.
35 Yamane MA, Williams AC, Barry BW. Terpene penetration enhancers in propylene glycol/water co-solvent systems: effectiveness and mechanism of action. *J Pharm Pharmacol* 1995; **47**: 978-89.
36 Francoeur ML, Golden GM, Potts RO. Oleic acid: its effects on stratum corneum in relation to (trans)dermal drug delivery. *Pharm Res* 1990; **7**: 621-7.
37 Rehfeld SJ, Plachy WZ, Hou SY *et al.* Localization of lipid microdomains and thermal phenomena in murine stratum corneum and isolated membrane complexes: an electron spin resonance study. *J Invest Dermatol* 1990; **95**: 217-23.

38 Cornwell P, Barry BW, Bouwstra JA *et al.* Modes of action of terpene penetration enhancers in human skin; differential scanning calorimetry, small-angle X-ray diffraction and enhancer uptake studies. *Int J Pharm* 1996; **127**: 9-26.
39 Ogiso T, Iwaki M, Bechako K *et al.* Enhancement of percutaneous absorption by laurocapram. *J Pharm Sci* 1992; **81**: 762-7.
40 Ongpipattanakul B, Burnette RR, Potts RO *et al.* Evidence that oleic acid exists in a separate phase within stratum corneum lipids. *Pharm Res* 1991; **8**: 350-4.
41 Anigbogu A, Williams A, Barry BW *et al.* Fourier transform Raman spectroscopy of interactions between the penetration enhancer dimethyl sulfoxide and human stratum corneum. *Int J Pharm* 1995; **125**: 265-82.
42 Bouwstra JA, Peschier LJC, BRUSSEE J *et al.* Effect of N-alkyl-azocycloheptan-2-ones including azone on the thermal behaviour of human stratum corneum. *Int J Pharm* 1989; **52**: 47-54.
43 Bouwstra JA, Gooris GS, van der Spek JA *et al.* Structural investigations of human stratum corneum by small-angle X-ray scattering. *J Invest Dermatol* 1991; **97**: 1005-12.
44 López A, Llinares F, Cortell C *et al.* Comparative enhancer effects of Span® 20 with Tween® 20 and Azone® on the in vitro percutaneous penetration of compounds with different lipophilicities. *Int J Pharm* 2000: 133-40.
45 Sloan KB, Wasdo S. Designing for topical delivery: prodrugs can make the difference. *Med Res Rev* 2003; **23**: 763-93.
46 Loftsson T, Brewster ME. Pharmaceutical applications of cyclodextrins. 1. Drug solubilization and stabilization. *J Pharm Sci* 1996; **85**: 1017-25.
47 Scalia S, Villani S, Casolari A. Inclusion complexation of the sunscreen agent 2-ethylhexyl-p-dimethylaminobenzoate with hydroxypropyl-beta-cyclodextrin: effect on photostability. *J Pharm Pharmacol* 1999; **51**: 1367-74.
48 Del Valle E. Cyclodextrins and their uses: a review. *Process Biochemistry* 2004; **39**: 1033-46.
49 Danielsson I, Lindman B. The definition of microemulsion. *Colloids Surf* 1981; **3**: 391-2.
50 Trotta M, Gasco MR, Caputo O *et al.* Transcutaneous diffusion of hematoporphyrin in photodynamic therapy - in-vitro release from microemulsions. *Stp Pharma Sci* 1994; **4**: 150-4.
51 Kreilgaard M, Pedersen EJ, Jaroszewski JW. NMR characterisation and transdermal drug delivery potential of microemulsion systems. *J Control Release* 2000; **69**: 421-33.
52 Bolzinger M-A, Briançon S, Pelletier J *et al.* Percutaneous release of caffeine from microemulsion, emulsion and gel dosage forms. *Eur J Pharm Biopharm* 2008; **68**: 446-51.
53 Vankeirsbilck T, Vercauteren A, Baeyens W *et al.* Applications of Raman spectroscopy in pharmaceutical analysis. *Trends Analyt Chem* 2002; **21**: 869-77.
54 Chrit L, Bastien P, Sockalingum GD *et al.* An in vivo Randomized Study of Human Skin Moisturization by a New Confocal Raman Fiber-Optic Microprobe: Assessment of a Glycerol-Based Hydration Cream. *Skin Pharmacol Physiol* 2006; **19**: 207-15.

55 Crowther JM, Sieg A, Blenkiron P *et al.* Measuring the effects of topical moisturizers on changes in stratum corneum thickness, water gradients and hydration in vivo. *Br J Dermatol* 2008; **159**: 567-77.
56 Egawa M, Kajikawa T. Changes in the depth profile of water in the stratum corneum treated with water. *Skin Res Technol* 2009; **15**: 242-9.
57 Wu J, Polefka TG. Confocal Raman microspectroscopy of stratum corneum: a pre-clinical validation study. *Int J Cosmet Sci* 2008; **30**: 47-56.
58 Pudney PDA, Mélot M, Caspers PJ *et al.* An in vivo confocal Raman study of the delivery of trans-retinol to the skin. *Appl Spectrosc* 2007; **61**: 804-11.
59 Mélot M, Pudney PDA, Williamson A-M *et al.* Studying the effectiveness of penetration enhancers to deliver retinol through the stratum cornum by in vivo confocal Raman spectroscopy. *J Control Release* 2009; **138**: 32-9.
60 Egawa M, Hirao T, Takahashi M. In vivo estimation of stratum corneum thickness from water concentration profiles obtained with Raman spectroscopy. *Acta Derm Venereol* 2007; **87**: 4-8.
61 Bielfeldt S, Schoder V, Ely U *et al.* Assessment of Human Stratum Corneum Thickness and its Barrier Properties by In-Vivo Confocal Raman Spectroscopy. *IFSCC Magazine* 2009; **1**: 9-15.
62 Zhang G, Moore DJ, Flach CR *et al.* Vibrational microscopy and imaging of skin: from single cells to intact tissue. *Anal Bioanal Chem* 2007; **387**: 1591-9.
63 Chrit L, Hadjur C, Morel S *et al.* In vivo chemical investigation of human skin using a confocal Raman fiber optic microprobe. *J Biomed Opt* 2005; **10**: 0440071-04400711.
64 Xiao C, Flach CR, Marcott C *et al.* Uncertainties in depth determination and comparison of multivariate with univariate analysis in confocal Raman studies of a laminated polymer and skin. *Appl Spectrosc* 2004; **58**: 382-9.
65 Gaber BP, Peticolas WL. On the quantitative interpretation of biomembrane structure by Raman spectroscopy. *Biochim Biophys Acta* 1977; **465**: 260-74.
66 Failloux N, Baron M-H, Abdul-Malak N *et al.* Contribution of encapsulation on the biodisponibility of retinol. *Int J Cosmet Sci* 2004; **26**: 71-7.
67 Failloux N, Bonnet I, Perrier E. Effects of light, oxygen and concentration on vitamin A1. *J Raman Spectrosc* 2004; **2**: 140-7.
68 Baranska M, Proniewicz L. Raman mapping of caffeine alkaloid. *Vib Spectrosc* 2008: 153-7.
69 Edwards H, Farwell D, Oliveira L *et al.* FT-Raman spectroscopic studies of guarana and some extracts. *Anal Chim Acta* 2005: 177-86.
70 Caspers PJ, Williams AC, Carter EA *et al.* Monitoring the penetration enhancer dimethyl sulfoxide in human stratum corneum in vivo by confocal Raman spectroscopy. *Pharm Res* 2002; **19**: 1577-80.
71 Tfayli A, Piot O, Pitre F *et al.* Follow-up of drug permeation through excised human skin with confocal Raman microspectroscopy. *Eur Biophys J* 2007; **36**: 1049-58.
72 Xiao C, Moore DJ, Rerek ME *et al.* Feasibility of tracking phospholipid permeation into skin using infrared and Raman microscopic imaging. *J Invest Dermatol* 2005; **124**: 622-32.
73 Xiao C, Moore D, Flach C *et al.* Permeation of dimyristoylphosphatidylcholine into skin-Structural and spatial information from IR and Raman microscopic imaging. *Vib Spectrosc* 2005; **38**: 151-8.

74 Caspers P, Lucassen G, Bruining H *et al.* Automated depth-scanning confocal Raman microspectrometer for rapid in vivo determination of water concentration profiles in human skin. *J Raman Spectrosc* 2000; **31**: 813-8.
75 Caspers PJ, Lucassen GW, Carter EA *et al.* In vivo confocal Raman microspectroscopy of the skin: noninvasive determination of molecular concentration profiles. *J Invest Dermatol* 2001; **116**: 434-42.
76 Frelichowska J, Bolzinger M-A, Pelletier J *et al.* Topical delivery of lipophilic drugs from o/w Pickering emulsions. *Int J Pharm* 2009; **371**: 56-63.
77 Frelichowska J, Bolzinger M-A, Valour J-P *et al.* Pickering w/o emulsions: drug release and topical delivery. *Int J Pharm* 2009; **368**: 7-15.
78 Franz T. Percutaneous absorption. On the relevance of in vitro data. *J Invest Dermatol* 1975; **64**: 190-5.
79 OECD. Skin Absorption: in vitro Method. *OECD Guideline for the testing of chemicals* 2004: 1-8.
80 Bronaugh RL, Stewart RF. Methods for in vitro percutaneous absorption studies IV: The flow-through diffusion cell. *J Pharm Sci* 1985; **74**: 64-7.
81 Crutcher W, Maibach HI. The effect of perfusion rate on in vitro percutaneous penetration. *J Invest Dermatol* 1969; **53**: 264-9.
82 Córdoba-Díaz M, Nova M, Elorza B *et al.* Validation protocol of an automated in-line flow-through diffusion equipment for in vitro permeation studies. *J Control Release* 2000; **69**: 357-67.
83 Shimadzu. Test de linéarité sur UV-1800. *Rapport de la mésure* 2008: 1.
84 Izquierdo P, Wiechers JW, Escribano E *et al.* A study on the influence of emulsion droplet size on the skin penetration of tetracaine. *Skin Pharmacol Physiol* 2007; **20**: 263-70.
85 Clément P, Laugel C, Marty JP. In vitro release of caffeine from concentrated W/O emulsions: effect of formulation parameters. *Int J Pharm* 2000; **207**: 7-20.
86 Baldwin K, Batchelder D. Confocal Raman microspectroscopy through a planar interface. *Appl Spectrosc* 2001; **55**: 517-24.
87 Bruneel J, Lassegues J, Sourisseau C. In-depth analyses by confocal Raman microspectrometry: experimental features and modeling of the refraction effects. *J Raman Spectrosc* 2002; **33**: 815-28.
88 Everall N. Confocal Raman microscopy: Why the depth resolution and spatial accuracy can be much worse than you think. *Appl Spectrosc* 2000; **54**: 1515-20.
89 Everall N. Modeling and measuring the effect of refraction on the depth resolution of confocal Raman microscopy. *Appl Spectrosc* 2000; **54**: 773-82.
90 Everall N. Depth profining with confocal Raman microscopy, part I. *Spectroscopy* 2004; **19**: 22-7.
91 Everall N. Depth profiling with confocal Raman microscopy, part II. *Spectroscopy* 2004; **19**: 16-25.
92 Gotter B, Faubel W, Neubert RHH. Optical methods for measurements of skin penetration. *Skin Pharmacol Physiol* 2008; **21**: 156-65.
93 Gotter B, Faubel W, Neubert RHH. FTIR microscopy and confocal Raman microscopy for studying lateral drug diffusion from a semisolid formulation. *Eur J Pharm Biopharm* 2010; **74**: 14-20.

94 Wolf J. Die innere Struktur der Zellen des Stratum desquamans der menschlichen Epidermis. *Zeitschrift für Mikroskopisch Anatomische Forschung* 1939; **46**: 170-202.
95 Hunter R, Pinkus H, Stelle CH. Examination of the epidermis by the strip method. III. The number of keratin cells in the human epidermis. *J Invest Dermatol* 1956; **27**: 31-4.
96 Lademann J, Jacobi U, Surber C *et al.* The tape stripping procedure--evaluation of some critical parameters. *Eur J Pharm Biopharm* 2009; **72**: 317-23.
97 Teichmann A, Jacobi U, Ossadnik M *et al.* Differential stripping: determination of the amount of topically applied substances penetrated into the hair follicles. *J Invest Dermatol* 2005; **125**: 264-9.
98 Herkenne C, Alberti I, Naik A *et al.* In vivo methods for the assessment of topical drug bioavailability. *Pharm Res* 2008; **25**: 87-103.
99 Pinkus H. Examination of the epidermis by the strip method of removing horny layers. 1. Observations on thickness of the horny layer, and on mitotic activity after stripping. *J Invest Dermatol* 1951; **16**: 383-6.
100 Lorincz AL, Usar MC. Skin desquamating machine; a tool useful in dermatologic research. *J Invest Dermatol* 1957; **28**: 275-82.
101 Kligman AM, Christophers E. Preparation of isolated scheets of human stratum corneum. *Arch Dermatol* 1963; **88**: 702-5.
102 Marks R, Dawber RP. Skin surface biopsy: an improved technique for the examination of the horny layer. *Br J Dermatol* 1971; **84**: 117-23.
103 Anderson RL, Cassidy JM. Variations in physical dimensions and chemical composition of human stratum corneum. *J Invest Dermatol* 1973; **61**: 30-2.
104 Förster M, Bolzinger M-A, Fessi H *et al.* Topical delivery of cosmetics and drugs. Molecular aspects of percutaneous absorption and delivery. *Eur J Dermatol* 2009; **19**: 309-23.
105 Loftsson T, Hreinsdóttir D. Determination of aqueous solubility by heating and equilibration: a technical note. *AAPS PharmSciTech* 2006; **7**: E1-E4.
106 Florence AT. Surfactant interaction with biomembranes and drug absorption. *Pure Appl Chem* 1981; **53**: 2057-68.
107 Bailly J, Crettaz M, Schifflers MH *et al.* In vitro metabolism by human skin and fibroblasts of retinol, retinal and retinoic acid. *Exp Dermatol* 1998; **7**: 27-34.
108 Jenning V, Gysler A, Schäfer-Korting M *et al.* Vitamin A loaded solid lipid nanoparticles for topical use: occlusive properties and drug targeting to the upper skin. *Eur J Pharm Biopharm* 2000; **49**: 211-8.
109 Jenning V, Schäfer-Korting M, Gohla S. Vitamin A-loaded solid lipid nanoparticles for topical use: drug release properties. *J Control Release* 2000; **66**: 115-26.
110 Antille C, Tran C, Sorg O *et al.* Penetration and metabolism of topical retinoids in ex vivo organ-cultured full-thickness human skin explants. *Skin Pharmacol Physiol* 2004: 124-8.
111 Benfeldt E, Serup J. Effect of barrier perturbation on cutaneous penetration of salicylic acid in hairless rats: in vivo pharmacokinetics using microdialysis and non-invasive quantification of barrier function. *Arch Dermatol Res* 1999; **291**: 517-26.
112 Choi MJ, Maibach HI. Topical vaccination of DNA antigens: topical delivery of DNA antigens. *Skin Pharmacol Appl Skin Physiol* 2003; **16**: 271-82.

113 Jacobi U, Meykadeh N, Sterry W *et al.* Effect of the vehicle on the amount of stratum corneum removed by tape stripping. *J Dtsch Dermatol Ges* 2003; **1**: 884-9.
114 Rougier A, Lotte C, Maibach HI. In vivo percutaneous penetration of some organic compounds related to anatomic site in humans: predictive assessment by the stripping method. *J Pharm Sci* 1987; **76**: 451-4.
115 Al Haushey L, Bolzinger MA, Bordes C *et al.* Improvement of a bovine serum albumin microencapsulation process by screening design. *Int J Pharm* 2007; **344**: 16-25.
116 Benech-Kieffer F, Wegrich P, Schwarzenbach R *et al.* Percutaneous absorption of sunscreens in vitro: interspecies comparison, skin models and reproducibility aspects. *Skin Pharmacol Appl Skin Physiol* 2000; **13**: 324-35.
117 Potard G, Laugel C, Schaefer H *et al.* The stripping technique: in vitro absorption and penetration of five UV filters on excised fresh human skin. *Skin Pharmacol Appl Skin Physiol* 2000; **13**: 336-44.
118 Wagner H, Kostka KH, Lehr CM *et al.* Interrelation of permeation and penetration parameters obtained from in vitro experiments with human skin and skin equivalents. *J Control Release* 2001; **75**: 283-95.
119 Schwarb FP, Gabard B, Rufli T *et al.* Percutaneous absorption of salicylic acid in man after topical administration of three different formulations. *Dermatology* 1999; **198**: 44-51.
120 Dupuis D, Rougier A, Roguet R *et al.* In vivo relationship between horny layer reservoir effect and percutaneous absorption in human and rat. *J Invest Dermatol* 1984; **82**: 353-6.
121 Sheth NV, McKeough MB, Spruance SL. Measurement of the stratum corneum drug reservoir to predict the therapeutic efficacy of topical iododeoxyuridine for herpes simplex virus infection. *J Invest Dermatol* 1987; **89**: 598-602.
122 Darmstadt GL, Mao-Qiang M, Chi E *et al.* Impact of topical oils on the skin barrier: possible implications for neonatal health in developing countries. *Acta Paediatr* 2002; **91**: 546-54.
123 Weerheim A, Ponec M. Determination of stratum corneum lipid profile by tape stripping in combination with high-performance thin-layer chromatography. *Arch Dermatol Res* 2001; **293**: 191-9.
124 Jui-Chen T, Weiner N, Flynn G *et al.* Properties of adhesive tapes used for stratum corneum stripping. *Int J Pharm* 1991; **72**: 227-31.
125 Breternitz M, Flach M, Prässler J *et al.* Acute barrier disruption by adhesive tapes is influenced by pressure, time and anatomical location: integrity and cohesion assessed by sequential tape stripping. A randomized, controlled study. *Br J Dermatol* 2007; **156**: 231-40.
126 Reed JT, Ghadially R, Elias PM. Skin type, but neither race nor gender, influence epidermal permeability barrier function. *Arch Dermatol* 1995; **131**: 1134-8.
127 Weigmann H, Lademann J, Meffert H *et al.* Determination of the horny layer profile by tape stripping in combination with optical spectroscopy in the visible range as a prerequisite to quantify percutaneous absorption. *Skin Pharmacol Appl Skin Physiol* 1999; **12**: 34-45.
128 Bommannan D, Potts RO, Guy RH. Examination of stratum corneum barrier function in vivo by infrared spectroscopy. *J Invest Dermatol* 1990; **95**: 403-8.

129 Jacobi U, Weigmann H-J, Ulrich J *et al.* Estimation of the relative stratum corneum amount removed by tape stripping. *Skin Res Technol* 2005; **11**: 91-6.
130 Wu KS, van Osdol WW, Dauskardt RH. Mechanical properties of human stratum corneum: effects of temperature, hydration, and chemical treatment. *Biomaterials* 2006; **27**: 785-95.
131 Van Duzee BF. Thermal analysis of human stratum corneum. *J Invest Dermatol* 1975; **65**: 404-8.
132 Caussin J, Gooris GS, Janssens M *et al.* Lipid organization in human and porcine stratum corneum differs widely, while lipid mixtures with porcine ceramides model human stratum corneum lipid organization very closely. *Biochim Biophys Acta* 2008; **1778**: 1472-82.
133 Downing D, Abraham W, Wegner B *et al.* Partition of sodium dodecyl sulfate into stratum corneum lipid liposomes. *Arch Dermatol Res* 1993; **285**: 151-7.
134 Karande P, Jain A, Arora A *et al.* Synergistic effects of chemical enhancers on skin permeability: a case study of sodium lauroylsarcosinate and sorbitan monolaurate. *Eur J Pharm Sci* 2007; **31**: 1-7.
135 Montenegro L, Ademola J, Bonina F *et al.* Effect of application time of betamethasone-17-valerate 0.1% cream on skin blanching and stratum corneum drug concentration. *Int J Pharm* 1996; **140**: 51-60.
136 Imokawa G, Abe A, Jin K *et al.* Decreased level of ceramides in stratum corneum of atopic dermatitis: an etiologic factor in atopic dry skin? *J Invest Dermatol* 1991; **96**: 523-6.
137 Röpke EM, Augustin W, Gollnick H. Improved method for studying skin lipid samples from cyanoacrylate strips by high-performance thin-layer chromatography. *Skin Pharmacol Physiol* 1996; **9**: 381-7.
138 Silva CL, Nunes SCC, Eusébio MES *et al.* Study of human stratum corneum and extracted lipids by thermomicroscopy and DSC. *Chem Phys Lipids* 2006; **140**: 36-47.
139 Tfayli A, Guillard E, Manfait M *et al.* Thermal dependence of Raman descriptors of ceramides. Part I: effect of double bonds in hydrocarbon chains. *Anal Bioanal Chem* 2010; **397**: 1281-96.
140 Gniadecka M, Faurskov Nielsen O, Christensen DH *et al.* Structure of water, proteins, and lipids in intact human skin, hair, and nail. *J Invest Dermatol* 1998; **110**: 393-8.
141 Babu RJ, Chatterjee A, Singh M. Assessment of skin irritation and molecular responses in rat skin exposed to nonane, dodecane and tetradecane. *Toxicol Lett* 2004; **153**: 255-66.
142 Walters KA, Bialik W, Brain K. The effects of surfactants on penetration across the skin. *Int J Cosmet Sci* 1993; **15**: 260-70.
143 Walters KA, Walker M, Olejnik O. Non-ionic surfactant effects on hairless mouse skin permeability characteristics. *J Pharm Pharmacol* 1988; **40**: 525-9.

Remerciement

Tout d'abord, je tiens à remercier Stéphanie Briançon et Marie-Alexandrine Bolzinger, mes encadreuses à l'Université, pour leur collaboration dans l'élaboration de cette thèse.

Je remercie de même Madame Gilberte Marti-Mestres, Madame Arlette Baillet-Guffroy et Monsieur Philippe Humbert pour avoir accepté le rôle de rapporteur de ce travail de thèse. Bien évidemment, je remercie Monsieur Hatem Fessi pour être le président du jury, cela a été un vrai honneur pour moi.

Je souhaite remercier Monsieur Frédéric Demarne, Directeur de la Recherche de Gattefossé SAS, pour avoir soutenu cette thèse CIFRE et de m'avoir accueilli au sein de l'entreprise, où j'ai eu l'occasion de travailler dans de très bonnes conditions. Egalement, je remercie Monsieur Hatem Fessi pour l'accueil au sein de LAGEP. Monsieur Bruno Reynard et Monsieur Gilles Montagnac du Laboratoire de Sciences de la Terre de l'ENS pour leur excellente collaboration concernant la microscopie confocale Raman Lyon et Madame Marie-Rose Rovere et Madame Odile Damour du Laboratoire des Substituts Cutanés concernant l'imagerie d'histologique.

Et je n'oublie pas de remercier très chaleureusement toutes les personnes que j'ai eu le plaisir de rencontrer au cours de ces années au LAGEP et à Gattefossé. Une pensée très especiale vers Jocelyne Pelletier et Ghislaine Passaro.

En fin, je tiens à remercier profondément ma famille et Aitana pour leur soutien et encouragement.